HARNESSING BIOELECTROCHEMICAL SYSTEMS FOR SUSTAINABLE AGRICULTURE

by

Shuyao Wang

Department of Bioresource Engineering

Faculty of Agricultural and Environmental Sciences

McGill University

Ste-Anne-De-Bellevue, Quebec, Canada

June 2023

A Thesis Submitted to McGill University in partial fulfillment of the requirements for the degree of Doctor of Philosophy

ABSTRACT

Hydroponic agriculture has gained more attention to solving the shortage of soil and food. However, issues including greenhouse gas emission and high energy consumption still exist. Bioelectrochemical system (BES) particularly microbial fuel cell (MFC) has a wide range of applications, such as metal recovery, desalination, biosensoring, etc., due to ability to convert chemical energy into bioelectricity. Therefore, this thesis proposed a hydroponic-plant microbial fuel cell (H-PMFC) system to develop the sustainable agriculture.

Our first study developed a 3D floating air-cathode by dip-drying method. The pore size effect of 3D floating air-cathode was investigated for the first time. According to the several advanced characterizations of the traditional carbon felt cathode, the 3 pores/mm 3D floating air-cathode helped in achiving a maximum power density of 92.58 mW/m^3 during MFC operation and improving the maximum power density (PD_{max}) by 160% due to the smaller pores, rougher surface, and higher surface wettability in comparison with 5 pores/mm 3D floating air-cathode.

Based on the configuration construction of first study, an innovative flow-through H-MFC was built to explore the effect of MFC on hydroponic rice plants. The results showed that integrating MFC technology with hydroponic systems showed the highest PD_{max} of 504.39 mW/m^3 and decrease up to 50% of methane (CH_4) emissions from rice plants in hydroponic systems without any negative influence on biomass production.

Following the contributions of the second research, the third study of this thesis focused on optimizing the performance of H-PMFCs. Iron is vital to plant growth and health as the redox-active metal involved in various biochemical activities. Simultaneously, iron affects the anode biofilm formation and oxygen reduction reaction in MFCs. This work investigated the electrochemical performance, CH_4 emission, and biomass production of H-PMFCs with different concentrations and ratios of Fe^{2+} and Fe^{3+}. The PD_{max} was observed when the Fe^{2+} was 7.5 μM and Fe^{3+} was 15 μM (949.17 mW/m^3) and reduced 65% of CH_4 emissions from H-PMFC. Besides, the addition of iron in H-PMFCs could decrease the emission of CH_4 in two ways: (i) iron electron acceptors directly inhibiting methanogens; (ii) iron electron

acceptor enhances the electricity production ability of MFC to inhibit CH_4 production.

Subsequently, the final study evaluated the possibility of affecting CH_4 emission level, biomass production, and bioelectricity generation from rice H-PMFCs by external resistance (R_{ext}) control. Three H-PMFCs were built based on the above research. Results showed that when R_{ext} = internal resistance (R_{int}), the H-PMFC has the highest biomass yield. When $R_{ext} > R_{int}$ displayed the highest average power density. The PD_{max} was 536.79 mW/m^3 when R_{ext}/R_{int} = 150%. The CH_4 emission exhibits an inverse trend with current production, decreasing with the R_{ext}/R_{int} ratio decrease from 50% to 5%. The highest current with the lowest CH_4 was produced when R_{ext}/R_{int} = 9% (0.14 mA and 453.52 ± 0.28 $g/m^2/h$). Thus, the performance of H-PMFCs can be controlled by changing R_{ext}/R_{int} ratio according to desired actual needs.

The findings presented in our work demonstrate the possibilities of integration of BES with hydroponics, providing the concept of H-PMFC, and provided new ideas for sustainable agriculture.

RÉSUMÉ

L'agriculture hydroponique a attiré plus d'attention pour résoudre le manque de sol et de nourriture. Cependant, des problèmes tels que les émissions de gaz à effet de serre et la forte consommation d'énergie existent toujours. Le système bioélectrochimique (BES), en particulier la pile à combustible microbienne (MFC), a une large gamme d'applications, telles que la récupération des métaux, le dessalement, la biocapture, etc., en raison de sa capacité à convertir l'énergie chimique en bioélectricité. Par conséquent, cette thèse a proposé un système hydroponique de pile à combustible microbienne végétale (H-PMFC) pour développer l'agriculture durable.

Notre première étude a développé une cathode à air flottante 3D par la méthode de séchage par trempage. L'effet de la taille des pores de la cathode à air flottante 3D a été étudié pour la première fois. Selon les nombreuses caractérisations avancées de la cathode traditionnelle en feutre de carbone, la cathode à air flottante 3D à 3 pores/mm a permis d'atteindre une densité de puissance maximale de 92,58 mW/m^3 pendant le fonctionnement du MFC et d'améliorer la densité de puissance maximale (PD_{max}) de 160 % en raison des pores plus petits, de la surface plus rugueuse et de la mouillabilité de surface supérieure par rapport à la cathode à air flottante 3D à 5 pores/mm.

Sur la base de la construction de la configuration de la première étude, un H-MFC à flux continu innovant a été construit pour explorer l'effet du MFC sur les plants de riz hydroponiques. Les résultats ont montré que l'intégration de la technologie MFC aux systèmes hydroponiques a montré le PDmax le plus élevé de 504,39 mW/m^3 et réduit jusqu'à 50 % les émissions de methane (CH_4) des plants de riz dans les systèmes hydroponiques sans aucune influence négative sur la production de biomasse.

Suite aux apports de la deuxième recherche, la troisième étude de cette thèse s'est concentrée sur l'optimisation des performances des H-PMFC. Le fer est vital pour la croissance et la santé des plantes en tant que métal redox-actif impliqué dans diverses activités biochimiques. Simultanément, le fer affecte la formation du biofilm anodique et la réaction de réduction de l'oxygène dans les MFC. Ce travail a étudié les performances

électrochimiques, les émissions de CH_4 et la production de biomasse des H-PMFC avec différentes concentrations et ratios de Fe^{2+} et Fe^{3+}. Le PD_{max} a été observé lorsque le Fe^{2+} était de 7,5 μM et Fe^{3+} était de 15 μM (949,17 mW/m^3) et a réduit de 65 % les émissions de CH_4 du H-PMFC. Par ailleurs, l'ajout de fer dans les H-PMFC pourrait diminuer l'émission de CH_4 de deux manières : (i) les accepteurs d'électrons du fer inhibant directement les méthanogènes ; (ii) l'accepteur d'électrons de fer améliore la capacité de production d'électricité du MFC pour inhiber la production de CH_4.

Par la suite, l'étude finale a évalué la possibilité d'affecter le niveau d'émission de CH_4, la production de biomasse et la production de bioélectricité à partir des H-PMFC de riz par le contrôle résistance externe (R_{ext}). Trois H-PMFC ont été construits sur la base des recherches ci-dessus. Les résultats ont montré que lorsque R_{ext} = résistance interne (R_{int}), le H-PMFC a le rendement de biomasse le plus élevé. Lorsque $R_{ext} > R_{int}$ affichait la densité de puissance moyenne la plus élevée. Le PD_{max} était de 536,79 mW/m^3 lorsque R_{ext}/R_{int} = 150 %. L'émission de CH_4 présente une tendance inverse avec la production actuelle, diminuant avec la diminution du rapport R_{ext}/R_{int} de 50% à 5%. Le courant le plus élevé avec le CH_4 le plus bas a été produit lorsque R_{ext}/R_{int} = 9 % (0,14 mA et 453,52 ± 0,28 $g/m^2/h$). Ainsi, les performances des H-PMFC peuvent être contrôlées en modifiant le rapport R_{ext}/R_{int} en fonction des besoins réels souhaités.

Les résultats présentés dans notre travail démontrent les possibilités d'intégration de BES avec la culture hydroponique, fournissant le concept de H-PMFC, et ont fourni de nouvelles idées pour l'agriculture durable.

ACKNOWLEDGEMENTS

Firstly, I would like to express my gratitude to all those who helped me a lot while writing this thesis. I deeply acknowledged the support of my co-supervisor Professor Vijaya Raghavan and Dr. Ademola Adekunle, for always offering me valuable suggestions in academic studies. They always spent lots of time reading through each draft of my papers and provided me with inspiring advice. With their patient instructions, insightful criticism, and expert guidance, I could finish this research. I appreciate Professor Vijaya Raghava for providing me with the platform to complete all my experiments and allowing me to attend international conferences to open my eyes. Thanks to Dr. Ademola Adekunle for always encouraging me like a big brother, even during the pandemic; he also tried to offer me as much as he could to support my research work.

Secondly, I gratefully acknowledge the financial support the China Scholarship Council (CSC) provided for my four-year stay in Canada.

I should give my hearty thanks to Mr. Yvan Gariépy for all his technical support and guidance in my research work. He was always very patient when answering all my questions, helping me build all my microbial fuel cell setups, and teaching me some French. I would like to thank Dr. Darwin Lyew for introducing me to the whole campus and labs on my first arrived in Canada. I would like to thank all my lab and office mates, who are also my best friends in Canada, including Xin Dong, Suhasini Srinivasan, Sellam Perinban, and Brenda Judith Alvarez Chavez, for their help in my Canadian life and research.

Finally, I am indebted to my beloved family for their loving consideration and great confidence in me through these years.

CONTRIBUTION OF AUTHORS

Shuyao Wang is the principal author of this work which was guided by Dr. Vijaya Raghavan, James McGill Professor, Department of Bioresource Engineering, McGill University, Sainte-Anne-de-Bellevue, Quebec, Canada, and Dr. Ademola Adekunle National Research Council of Canada, Montreal, Quebec, Canada. Chapters V, VI, and VIII were conducted in the Post-Harvest Laboratory of the Bioresource Engineering Department of McGill University. Chapter VII was carried out in Automated Research Greenhouse. The co-author, Mr. Yvan Gariépy, provided technical assistance, reviewed, and improved manuscript writing.

This thesis is comprised of seven chapters. Chapter I summarizes the thesis objectives about hydroponic microbial fuel cells and rice methane emission; Chapter II-IV introduces the background of this research by a general literature review of microbial fuel technology and rice methane emission and control; Chapter V presents a simple dipping-drying method to fabricate a practical and economical 3D floating air-cathodes by using carbon black, ethanol, and PTFE solution. Chapter VI proposes a hydroponic-microbial fuel cell agriculture system to investigate the possibility of reducing methane emissions from rice plants by hydroponic microbial fuel cells and the influence of hydroponic microbial fuel cells on biomass production from rice plants. Chapter VII shows the effect of iron concentrations and forms on the performance of rice plants' hydroponic microbial fuel cells. Chapter VIII presents the possibility of controlling the performance of hydroponic microbial fuel cells by changing the internal and external resistance ratio. Chapter IX presents the overall conclusions and contributions to the knowledge of this thesis as well as the recommendations for future work.

Details of the papers from this thesis are listed below.

1. **Wang, S.**, Adekunle, A., Tartakovsky, B., & Raghavan, V. (2021). Synthesizing developments in the usage of solid organic matter in microbial fuel cells: A review. *Chemical Engineering Journal Advances*, *8*(100140), 10-1016. (Chapter IV)
2. **Wang, S.**, Adekunle, A., & Raghavan, V. (2022). Exploring the integration of bioelectrochemical systems and hydroponics: Possibilities, challenges, and innovations. *Journal of Cleaner Production*, *366*, 132855. (Chapter III)

3. **Wang, S.**, Gariepy, Y., Adekunle, A., Raghavan, V. (2023). Effective and economical 3D carbon sponge with carbon nanoparticles as floating air-cathode for sustainable electricity production in microbial fuel cells. *Applied Biochemistry and Biotechnology*, 1-20. (Chapter V)
4. **Wang, S.**, Gariepy, Y., Adekunle, A., Raghavan, V. (2023). The role of hydroponic microbial fuel cell in the reduction of methane emission from rice plants. *Electrochimica Acta*, *450*, 142229. (Chapter VI)
5. **Wang, S.**, Gariepy, Y., Adekunle, A., Raghavan, V. (2023). Fe chelates fertilization form and concentration: the influence on bioelectricity and methane production from hydroponic microbial fuel cells. (to be submitted). (Chapter VII)
6. **Wang, S.**, Gariepy, Y., Adekunle, A., Raghavan, V. (2023). External resistance as a potential tool for bioelectricity and methane emission control from rice plants in hydroponic microbial fuel cell. (to be submitted) (Chapter VIII)

Papers presented at conferences:

1. **Wang, S.**, Gariepy, Y., Adekunle, A., Raghavan, V., A novel floating air-cathode for electricity production in hydroponic microbial fuel cells. Canadian Society for Bioengineering/Société Canadienne de Génie Agroalimentaire et de Bioingénierie, Virtual on Zoom, 2022, February 11th.
2. **Wang, S.**, Gariepy, Y., Adekunle, A., Raghavan, V., Influence of flow microbial fuel cell on methane emission from hydroponic cultivation of rice plant. Canadian Society for Bioengineering/Société Canadienne de Génie Agroalimentaire et de Bioingénierie, Prince Edward Island, 2022, July 25th.
3. **Wang, S.**, Gariepy, Y., Adekunle, A., Raghavan, V., Exploring the integration of bioelectrochemical systems and hydroponics: possibilities, challenges, and innovations. People, Montreal, 2023, August 9th.

TABLE OF CONTENTS

LIST OF TABLES

LIST OF FIGURES

LIST OF SYMBOLS

$E_{cathode}$	The potential of cathode
E_{anode}	The potential of anode
E_e	The equilibrium potential of an electrode
E°	The standard potential at pH 0
R	The molar gas constant, 8.314 J/mol/K
n	The number of electrons transferred
F	The Faraday's constant, 96,485 C/mol
Co	the concentration of the oxidized
C_R	The reduced products at the electrode surface
F	The stress of film at break, N
a	Film thickness, mm
b	Film width, mm
ΔL	Elongated length of film
L_0	Original lengths of film
m_1	The initial weight of the cathode sample
m_2	The weight after dipping in the Kimura solution
H	The chamber height, m
M_w	CH_4 mole mass, 16.123×10^{-3} mg
M_v	CH_4 mole volume, 22.41×10^{-3} m^3
T	Temperature, 23 °C
ΔC/Δt	The change in the CH_4 between the initial and final measurement per unit of time (12 h), ppm
R_{anode}	Anode resistance
$R_{cathode}$	Cathode resistance
$R_{electrolyte}$	Electrolyte resistance
$R_{membrane}$	Membrane resistance
$r_{anode/cathode}$	Area-specific resistance of anode/cathode
$S_{anode/cathode}$	Projected areas of anode/cathode
L	Electrode spacing
S_r	Cross-sectional area of the reactor

$C_{electrolyte}$	The concentration of charge transfer electrolyte.
ΔE	The potential between anode and cathode in MFC
E_{anode}	Anode potential
E_{cathde}	Cathode potential
$\overline{\underline{a_{M^{n+}}}}$	The activities of the oxidized M^{n+}
a_M	The activities of the reduced M species
R_{COD}	COD removal rate
V	The liquid volume of the reservoir
ΔCOD	The amount of removed COD within a specified time

LIST OF ABBREVIATIONS

CO_2	Carbon dioxide
N_2O	Nitrous oxide
CH_4	Methane
MFC	Microbial fuel cell
PMFC	Plant microbial fuel cell
EAB	Electrochemically active bacteria
H-PMFC	Hydroponic-PMFC
Fe	Iron
O_2	Oxygen
H_2	Hydrogen
BES	Bioelectrochemical system
MDC	Microbial desalination cell
MES	Microbial electrosythesis cell
EBC	Enzymatic biofuel cell
MRC	Microbial reverse-electrodialysis cell
MSC	Microbial solar cell
MEC	Microbial electrolysis cell
CFS	Continuous flow solution
SS	Static solution
AS	Aeroponic system
NO_x	Nitrogen oxides
SO_2	Sulfur dioxide

GWP	Global warming potential
CW	Constructed wetland
HPLC	High-performance liquid chromatography
GC	Gas chromatography
BOD	Biological oxygen demand
COD	Chemical oxygen demand
SOM-MFCs	Solid organic matter based microbial fuel cells
PD	Power density
SOM	Solid organic matter
WW-MFC	Wastewater based MFC
CW-MFC	Constructed wetland microbial fuel cell
AMFC	Algae microbial fuel cell
BW-MFC	Biowaste microbial fuel cell
SMFC	Soil microbial fuel cell
PEM	Proton exchange membrane
NF/rGO	Nickel foam/graphene
UASB	Upflow anaerobic sludge blanket
NO_x	Nitrogen oxides
SO_2	Sulfur dioxide
GWP	Global warming potential
EC	Electrical conductivity
HPLC	high-performance liquid chromatography
GC	gas chromatography
3D	Three-dimensional
CB	Carbon black

CC	Carbon cloth
CF	Carbon felt
CC-CF-MFC	Carbon cloth anode carbon felt cathode microbial fuel cell
CC-I-MFC	Carbon cloth anode Type-I polyurethane sponge cathode microbial fuel cell
CC-II-MFC	Carbon cloth anode Type-II polyurethane sponge cathode microbial fuel cell
SEM	Scanning electron microscopy
FTIR	Fourier transforms infrared
TGA	Thermogravimetric analysis
WCA	Water contact angle
CV	Cyclic voltammogram
PTFE	Polytetrafluoroethylene
TS	Tensile strength
EB	Elongation at break
P-test	Polarization test
R_{ext}	External resistance
OCV	Open-circuit voltage
R_{int}	Internal resistance
ANOVA	Analysis of variance
ORR	Oxygen reduction reaction
DTG	Derivative thermogravimetric
H-MFC	Hydroponic microbial fuel cell
NPMFC	Hydroponic microbial fuel cell with no plant
PD_{max}	Highest power density
GHG	Greenhouse gas
OC	Open circuit

CC	Close circuit

CHAPTER I

GENERAL INTRODUCTION

1.1. MOTIVATIONS

Agriculture is one of the key economic sectors and is responsible for both food and nutritional security. As the global population is projected to rise to 9 billion by 2025 [1], food production must double to meet food demands. However, agriculture impacts directly/indirectly towards global climate change by greenhouse gas emissions, which account for 10-20% of total global anthropogenic greenhouse emissions on a 100-year time horizon. The non-carbon dioxide (CO_2) gases - nitrous oxide (N_2O) and methane (CH_4) comprise a large share of agricultural emissions with relative global warming potentials of 34 and 298 times higher than CO_2 [2]. Rice (Oryza sativa) is grown in 114 countries over a total land of around 153 Mha, which covers 11% of the world's arable land and is considered the second biggest (745 Tg in 2013) cereal crop produced in the world [3]. However, rice cultivation is a considerable threat to sustainable agriculture. The global warming potential of rice crop is 467% and 169% compared to wheat and maize, respectively [4]. Rice cultivation is a primary source of vital and long-lasting greenhouse gases - CH_4 and N_2O. Around 30% and 11% of global agricultural CH_4 and N_2O are emitted from rice fields [5].

Rice paddy releases some amounts of N_2O due to the anaerobic conditions of the soil, but it mainly leads to CH_4 emission [6]. Considering natural emissions, wetlands and rice agriculture combined amount to 32-47 % of total CH_4 emissions [7]. Besides, the CH_4 emission has increased due to the rapid increase in fertilizer application and rice production over the last 70 years. It is projected that up to 2030, emissions of CH_4 and N_2O may increase by 35-60% [3]. However, rice production needs to be increased by 40% by 2030 to meet rising demand from the ever-growing population [3], which will cause more serious environmental problems. Furthermore, to improve rice production, the increased application of inorganic fertilizer is needed, which may also boost the emissions of CH_4 from rice paddy

[8]. Thus, it is urgent to find a way to combine increased grain production and decreased CH_4 gas emissions.

Until now, several management methods have been practiced for decreasing CH_4 emission from paddy rice; they are mainly classified into three categories: (i) selecting suitable cultivars and cover crops; (ii) adjusting irrigation patterns, tillage practices, copping regime, and uses of appropriate irrigation rate; (iii) managing organic additives. These methods could reduce CH_4 emissions to a certain extent. However, these methods need higher investment costs, such as labor and specific machine costs. They require a lot of time to manage specific organic additives. Moreover, it cannot control the amount of CH_4 emissions from rice paddies. Therefore, finding a new way to simultaneously achieve control and decrease CH_4 emission from rice paddy fields is essential.

Recently, microbial fuel cell (MFC) as one of the most potential alternative renewable energy technology of bioelectrochemical system (BES) attracted the attention of many researchers, which capitalizes on the ability of certain electroactive microorganisms to transfer electrons from a source of organic carbon to a solid electrode, thus facilitating the production of renewable electricity [9-11].

The aerenchyma of plants (90%) is one of the main pathways of gas exchange with the rhizosphere under waterlogged conditions [12, 13]. Therefore, a promising route for mitigating CH_4 emissions is to prevent the formation of CH_4 in the rhizosphere. The rhizodeposition is the process of organic material transport from the plant roots to the rhizosphere (around the roots and about 4 mm from the root surface [14]). During the growth and development of the plants, the organic matter enters the support matrix as rhizodeposition, which consists of exudates (sugars, organic acids), secretions (polymeric carbohydrates and enzymes), lysates (dead plant cell materials) and gases (ethylene and CO_2) [15, 16]. They are explicitly excreted by the roots and oxidized electrochemically by active microorganisms (naturally present in an anode) to yield bioelectricity. Hence, there has been growing interest in incorporating plants with MFC for bioenergy production in the past ten years (about 21.77%, according to Scopus). Plant microbial fuel cell (PMFC) is a derived technology of MFC, which converts solar energy into bioelectricity indirectly via the electrochemically active bacteria (EAB) at the rhizosphere region of their roots [17, 18]. PMFC can be seen as a

type of biosystem, having two structures, viz., biocontrol and bioprocess. In the biocontrol structure, plants convert sunlight into voltage by photosynthetic processes. In the bioprocess structure, the microbial community uses exudates to produce electricity via microbial metabolism [18]. Therefore, due to the photosynthetic processes, PMFCs make bioelectricity without the artificial addition of extra organic matter or nutrients [19]. PMFC was first reported in 2008, which could produce a current of up to 120 mA/m^2 [16]. This current value is well within the same order of magnitude as CH_4 emission from the paddy field. Thus, it has been hypothesized that the current produced by PMFC metabolism can mitigate rice paddy/waterlogged wetlands' emission of CH_4 [16, 20].

1.2. PROBLEM DEFINITION

With more water, food, and living habitat needed for agricultural cultivation, emerging environmental problems, e.g., forest loss, greenhouse gas emission, climate change, fragmentation, etc., can be expected [21]. Soil, the most favorable and available support matrix in agriculture, will be particularly affected due to increased erosion, compaction, and soil degradation, all leading to the topographical conditions affecting agricultural productivity. Recently, hydroponic agriculture has been gaining popularity as the promise of growing terrestrial plants by solely exposing their roots exposed to a nutritious liquid. According to Barbosa et al. [22], the land requirements of the hydroponic systems can be ten times less, and the yields can be over 11 times greater than traditional agriculture. Thus, the hydroponic method removes the reliance on the soil as a growth medium [23].

Studies have proved that with the help of PMFC, CH_4 can be reduced by up to 50% from rice paddy [24, 25]. However, they only tested the CH_4 sampling from portable containers [24, 26]; only two directly measured CH_4 gas from rice plants [27, 28]. Further, until now, no research has reported the influence of continuous flow hydroponic-PMFC (H-PMFC) on the CH_4 emission from rice plants. The constant flow system has several advantages such as (i) the maximum productivity by optimizing the composition medium; (ii) controlling the secondary metabolites; (iii) the process leading to reproducible results and reliable data, (iv) achieving high productivity per unit, (v) promising the nutrition supply, etc. [29].

Therefore, our work is based on the hypothesis that the BES is a potential technology to dynamically control CH_4 emissions in sustainable agriculture and investigate the effects of H-PMFC systems on biomass production, CH_4 emissions, and electricity generation during rice plants' growth.

1.3. RESEARCH OBJECTIVES

The global objective of the proposed studies is to design, develop, and optimize the H-PMFC system and to assess the influence of H-PMFC on rice biomass production, CH_4 emissions, and bioelectricity generation.

1.4. SPECIFIC OBJECTIVES

- Explore the most cost-effective and high-efficiency electrode materials for MFC.
- Explore the background level of CH_4 emission in a rice cultivation hydroponic system; characterize plant health. Compare the hydroponic system and characterized parameters to a rice paddy microcosm.
- Explore how the rice H-PMFC system affects CH_4 emissions, plant biomass production, and electricity generation.
- Explore the effect of iron (Fe) fertilization concentration on CH_4 emissions, plant biomass production, and electricity generation in H-PMFC systems.
- Explore the effect of different forms of Fe ions on plant biomass production and electricity generation in MFC-integrated hydroponic systems.
- Develop an H-PMFC system to control CH_4 emissions from rice plants.

1.5. ORGANIZATION OF THE THESIS

This Chapter I summarizes the thesis background about CH_4 emissions from rice plants, the problems of hydroponic cultivation systems, and objectives for designing the H-PMFC for rice plant cultivation. Chapter II-IV introduces the background of this research by a general literature review of microbial fuel technology and rice methane emission and control; Chapter V presents a simple dip-drying method to fabricate a practical and economical 3D floating

air-cathodes by using carbon black, ethanol, and PTFE solution; Chapter VI proposes a hydroponic-microbial fuel cell agriculture system to investigate the possibility of reducing methane emissions from rice plants by hydroponic microbial fuel cells and the influence of hydroponic microbial fuel cells on biomass production from rice plants. Chapter VII shows the effect of iron concentrations and forms on the performance of rice plants' hydroponic microbial fuel cells. Chapter VIII presents the possibility of controlling the performance of hydroponic microbial fuel cells by changing the internal and external resistance ratio. Chapter IX presents the overall conclusions and contributions to the knowledge of this thesis as well as the recommendations for future work.

CHAPTER II

LITERATURE REVIEW-PART 1

2.1. THE GAS EMISSION FROM RICE FIELD

Global warming is one of the most prominent challenges in the present era. The temperature of the earth is governed by various components, such as ozone, water vapor, and gases (oxygen (O_2), CO_2, N_2O, etc.), which absorb heat, causing a concomitant increase in atmospheric temperatures with consequences of disasters (e.g., hurricanes, floods, drought, etc.) [30, 31]. Among all these compositions, the growth of greenhouse gases in the atmosphere results in global warming. Greenhouse gases cause the widely known phenomenon "greenhouse effect". Due to the enhanced greenhouse effect, the global mean annual temperature has increased. The projected rise in the temperature by the end of the 21st century is estimated at 1.1~6.4 °C [30]. Some researchers predicted that greenhouse emissions may increase by 35-60% by the end of 2030 [32]. Globally, CO_2 (60%), CH_4 (15%), and N_2O (5%) are the main contributors to the anthropogenic component [33]. For the total anthropogenic emissions, CH_4 and N_2O are the significant contributors to greenhouse gases owing to their origin identified in the agricultural sector. Compared to CO_2, CH_4 and N_2O have 298 and 25 times more global warming potential [30].

Agriculture is one of the key economic sectors and is responsible for both food and nutritional security. However, the growth rate of the global human population is 1.1% per year or around 83 million annually [34], which makes humans rely more on optimizing land area and conserving biodiversity. According to FAO, a projected net increase in the arable area of 120 million ha (12%) will be happening in developing countries from 1977 to 2030 (from 956 to 1076 million ha) [35]. However, agriculture impacts directly/indirectly towards the global climate by emitting greenhouse gases. Agriculture greenhouse gas emissions account for 10-20% of global anthropogenic greenhouse emissions [36]. In order to ensure food security and protect the environment and natural resources, controlling greenhouse gas

emissions is a dire necessity [37, 38].

2.2. METHANE EMISSION FROM RICE PADDY

CH_4 is the main hydrocarbon present in the atmosphere. The average concentration of CH_4 is 1.7 ppm. About 70-80% of CH_4 in the atmosphere is from biological origin. It is produced in anoxic environments, such as submerged soils, by methanogenic bacteria during the anaerobic digestion of organic matter. CH_4 escapes to the atmosphere through bubbling, diffusion, and via rice stems (**Figure 2.1.**). Therefore, flooded rice fields are the major sources of CH_4 emission, which contribute to about 30% of global agricultural CH_4 [5]. Sass [39] concluded a CH_4 emission of 25-54 Tg/yr from a total rice area of 147.5 million ha, and China is the most important region with 13-17 Tg from 32.2 million ha. In the rice field, CH_4 is emitted mainly by the decomposition of organic materials in the anoxic flooded rice cultures by transport, production, and oxidation [40]. Due to the economic importance and high potential for the CH_4 source, the rice fields have been the most studied methanogenic ecosystems. Further, because methanogenesis and methanotrophic are very active and all modes of CH_4 transfer occur in rice fields, rice fields are also the most suitable model to study CH_4 [40].

Under the low sulfate and nitrate concentrations and anaerobic environment, the complete mineralization of organic matter by the methanogenic fermentation, which generates CH_4 and CO_2 as follows:

$$C_6H_{12}O_6 \rightarrow 3CO_2 + 3CH_4 \qquad 2.1$$

Where four populations of microorganisms are required, which could degrade complex molecules into simpler compounds: (i) hydrolysis of biological polymers into monomers through a hydrolytic microflora that can be either aerobic/facultatively or strictly anaerobic (amino acids, fatty acids, glucose); (ii) acidogenesis from monomeric compounds as well as intermediary compounds formed during fermentation through a fermentative microflora that can be facultatively/strictly anaerobic (volatile fatty acids, organic acids, alcohols, hydrogen (H_2), CO_2); (iii) acetogenesis from the previous metabolites though the syntrophic/homoacetogenic microflora; (iv) methanogenesis from the simple compounds that

can be used by methanogens [40]. In the rice field, the H_2 and CO_2-dependent methanogenesis contributed to about 25-30% of the CH_4 generation [41], driven by the decay and fermentation of root material [41, 42]. Besides, the variations in CH_4 production are primarily attributed to variations in microbial activity, roots, and the development stage of the rice plant [43-45]. Therefore, CH_4 emissions from rice depend on the flooded period, climate, soil type, management, amount, and application method of fertilizers.

Currently, three main strategies have been suggested to prevent CH_4 production from rice fields. (i) Select suitable cultivars and cover crops. However, not all kinds of rice plants are available for farmers or native soil to plant. (ii) Adjust irrigation pattern, tillage practices, cropping regime, and use of appropriate irrigation rate. Also, intermittent draining can be considered, but it is only applied in the area with abundant water. Besides, more specialists and material resources will be required, increasing costs. (iii) Managing organic additives. However, organic additives will cause environmental problems and increase the price.

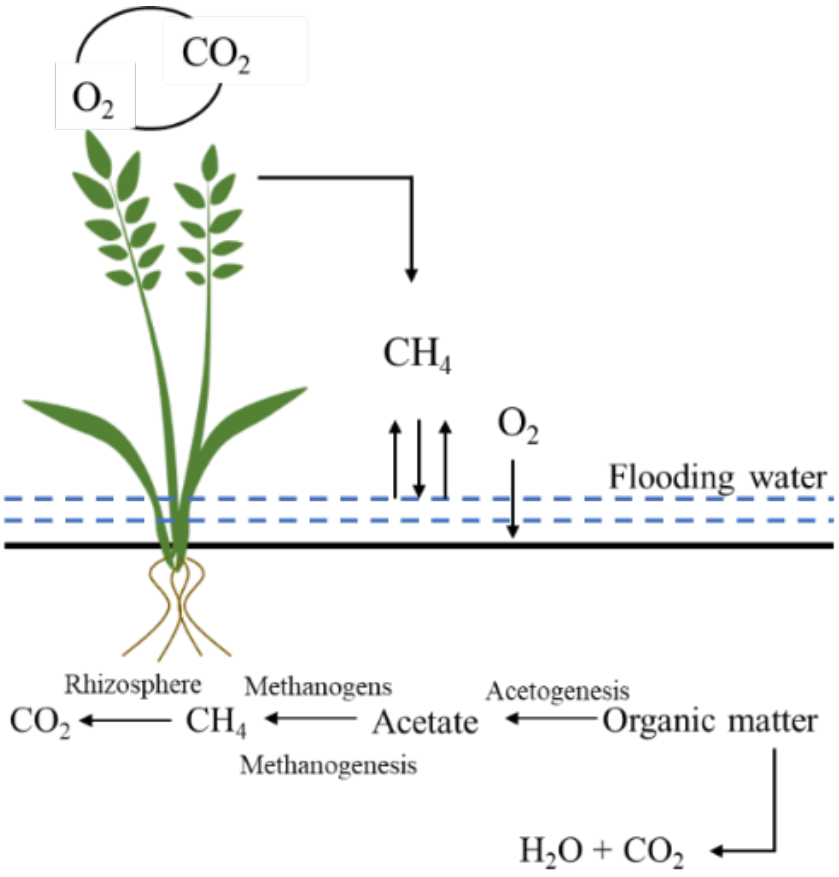

Figure 2.1. The schematic diagram of CH_4 emission from the paddy soil.

CONNECTING TEXT

From the literature review in chapter II, methane emission from rice paddy is a severe problem. As the population continues to grow, so does the demand for land. Therefore, in order to solve the shortage of arable land, hydroponics has attracted more and more attention. Hydroponic is a sustainable agriculture alternative that emphasizes the effectiveness and efficiency of land and time. Recently, several advanced bioelectrochemical systems has been adequately explored in biosensing, metal recovery, polluted sediment, especially wastewater treatments. Plant - bioelectrochemical system is one of bioelectrochemical systems variant that uniquely utilizes the plant-microbe relationship at the rhizosphere area of the plants for bioelectricity generation.

Chapter III systematically i) overviewed the main problems hindering hydroponic agriculture developments; then ii) conceptualized and discussed the potential solutions of the bioelectrochemical systems to resolve the identified issues, and finally iii) provided our perspectives for the future development trends of hydroponic bioelectrochemical systems

CHAPTTER III

LITERATURE REVIEW-PART 2

EXPLORING THE INTEGRATION OF BIOELECTROCHEMICAL SYSTEMS AND HYDROPONICS: POSSIBILITIES, CHALLENGES, AND INNOVATIONS

3.1. ABSTRACT

Hydroponics is a modern cultivation technique that utilizes nutrient solutions instead of soil for crop production. Currently, challenges, such as high cost, high energy consumption, greenhouse gas emission, and significant wastewater generation are drawbacks that limit its scale up. On the other hand, bioelectrochemical systems have emerged as a sustainable technology that resolve some of the aforementioned drawbacks, albeit in other scenarios. Bioelectrochemical systems applications are well documented in desalination, metal recovery, energy generation, contamination remediation, etc. This work conceptualizes the integration of bioelectrochemical systems and hydroponics with a view to improving the efficiency and sustainability of hydroponics. Firstly, a systematic review of the main challenges hindering hydroponic agriculture developments is first carried out to identify possible entry points for the proposed systems integration. Thereafter, a conceptualized point-by-point resolution of the main identified challenges of hydroponic systems through bioelectrochemical systems integration is explored. Furthermore, the feasibility, stability, and scalability of the conceptualized hydroponic-bioelectrochemical integrated systems are discussed.

Keywords: bioelectrochemical systems, hydroponic technology, sustainable hydroponic agriculture, clear energy production

3.2. INTRODUCTION

The growth rate of the global human population is 1.1% or around 83 million annually [34], making the optimization of land area and the conservation of biodiversity more challenging. According to FAO [35], a projected net increase in the arable area of 120 million ha (12%) will happen in developing countries by 2030 (from 956 to 1076 million ha). With more water, food, and living habitat needed for agricultural cultivation, emerging environmental problems including forest loss, greenhouse gas emission, and climate change implications are to be expected [21]. Besides, problems for human health, agriculture and decreasing crop yields are also to be expected to be affected [46]. Soil, the most favorable and available support matrix in agriculture will be particularly affected due to increased erosion, compaction, degradation, leading to a decline of topographical conditions, etc., all cause limiting agricultural productivity.

In recent times, hydroponic agriculture has gained popularity as the promise of growing terrestrial plants by solely exposing their roots exposed to a nutritious liquid removes the reliance on the soil as a growing medium [23]. It is an environmentally sustainable way to address the water and soil scarcity, improve the productivity of various crops species and help to face the challenges of climate change [47, 48]. Nutrients used in hydroponic systems come from a wide range of sources, such as manure, chemical fertilizers, wastewater, artificial nutrient solutions, etc. [49]. According to Barbosa et al. [22], the land requirements of the hydroponic systems can be ten times less and the yields can be over 11 times greater than traditional agriculture. In addition, when compared with soil cultivation (0.23 kg carbon dioxide (CO_2) equivalent), hydroponic systems have low gas emissions (0.11 kg CO_2 equivalent) [50]. It also has significant potential to save water as water is recycled in hydroponic set originalups [51], and as much as 33% of water was recycled in a hydroponic system used for tomatoes [52]. Other advantages of hydroponic cultivation systems include that they can be grown in urban areas, are not limited by season, efficiently use fertilizers, and the whole cultivation can be controlled [53-58].

The productivity and quality of hydroponic system crops are markedly dependent on the nutrients acquired from the growing solution [59]. It is interesting to note that the root physiological process is affected by both the availability levels of the nutrients in the medium solution and the interactions among the different nutrients [60]. Besides, temperature, pH, allelopathy/autotoxicity phenomenon, etc. all have a huge influence on hydroponic systems. Environmental temperature monitoring, plant health, high initial cost, gas production, high energy consumption, a huge amount of water needed as the solvent, discharge of nutrition wastewater treatment, more quickly speed of disease in solution, etc. are the main challenges associated with hydroponic systems.

Bioelectrochemical systems (BESs) are a group of biotechnologies, which exploit the activities of microorganisms or enzymes to convert chemical energy from waste (e.g. wastewater, polluted soil, sediment, etc.) into sustainable bioelectricity, fuels, or generation of usable by-products [61, 62]. The major types of BES include microbial fuel cell (MFC), microbial desalination cell (MDC), microbial electrosynthesis cell (MES), enzymatic biofuel cell (EBC), microbial reverse-electrodialysis cell (MRC), microbial solar cell (MSC), and microbial electrolysis cell (MEC) [63]. BESs can also be integrated with advanced technologies such as photocatalysts to produce hydrogen [64], or photobioreactors to convert hydrogen to more clean energy and pure water [65]. BESs are used mostly for renewable power generation, wastewater treatment, biosensors, nutrients recovery/removal, etc. [66-68]. In 2008, this technology was first merged with plants to form a hybrid system consisting of biocontrol and bio-process structures, mainly involving the conversion of excess organic matter into bioelectricity by microbes living around the rhizosphere region of the plant [16]. As autotrophs, plants use solar energy to produce biomass with the help of chlorophyll; while 40% of the biomass will be consumed by itself, the remaining part will be exuded to the rhizosphere region [15]. The promising nature of these plants combined with BES means that besides electricity generation, they can also be easily integrated into the existing indoor-based agricultural system without competition with plants [18].

For a period of 5 years (2017-2022), about 668 review articles (Scopus data) reviewed the different aspects of BESs, including wastewater treatment [69-71], valuable products recovery [72, 73], fundamental principles and mechanisms [63, 74, 75], mathematical models for BESs [76], environmental remediation [77, 78], and valuable chemical synthesis (e.g., CO, H_2O_2, etc.) [79, 80]. In addition, some of the previous review articles have outlined the combination of BES with plants and constructed wetland (CWL). For example, Kabutey et al. [81] comprehensively reviewed the fundamental aspects of PMFCs in terms of living plants, supporting matrix, rhizosphere microorganisms, mechanism of substrate conversion, and electron transfer. Maddalwar et al. [82] presented an extensive review of the challenges and commercially feasible associated with PMFC, various factors (e.g., carbon dioxide concentration in air, light intensity, electrode materials, type of plants, etc.), and the possibility of future intervention (e.g., application of biochar and preferable plants). Apollon et al. [83] provided the recent configuration development of PMFC and evaluated the performance of PMFC in different water conditions (including power density, the requirements to generate bioelectricity, as well the bioelectricity measurements and calculations). Wang et al. [84] summarized the wastewater treatment and electricity production mechanism of various CWL-MFCs in terms of microorganisms, electrodes, substrates, and wetland plants. As can be seen, most of the previous review articles are largely focused on the development of BES technologies, the application in industry, or the principle and mechanism of PMFC. As mentioned above, although hydroponics is very important for agricultural production, as far as we know, there is no detailed exploration and discussion of the potential applications of BES for specific problems in hydroponic agriculture. Therefore, different from the exist review papers, our work not only limit to the development of hydroponic agriculture and BES, but also proposed the concept of BES-hydroponic systems.

This article explores the potential for the usage of renewable sustainable BES for resolving several problems with hydroponic agriculture. To date, only one study attempted to combine both systems for domestic wastewater treatment and chemical

removal, achieving 72±2.4% COD, 83±1.1% phosphate, 35±4.2% ammonia removal efficiencies, and the maximum power density of 31.9 mW/m^2 [85]. However, no study has focused on the development of BES or its potential in the hydroponic research field. In this work, we first present an overview of hydroponic agriculture cultivation with the help of bibliometric analysis. Thereafter, we conceptualize how problems identified with traditional hydroponic system cultivation can be solved with BES. The possible characteristics, advantages, and disadvantages of BES in hydroponic systems were also discussed. Based on the in-depth study and analysis of BESs in hydroponic systems, the main problems of BES-hydroponic systems such as the lack of in-depth discussion and mechanism between BESs and hydroponic systems, the monitoring obstacle of the chemicals in hydroponic systems, the risk of over-complicate systems, etc. were reviewed. Various solutions in BES-hydroponic systems include optimizing BES-hydroponic systems, focusing on the mechanism between BES and plant growth, exploring the model systems and more advanced BES systems, as well as the utilizing of decision tree were proposed.

The rest of the paper is structured as follows: Section 2 addresses the problems in hydroponic systems. Section 3 proposes the concept, configuration, and problems advantages of BES-hydroponic systems. Section 4 analyzes the influencing factors, economic analysis, and environmental impact of BES-hydroponic systems. Section 5 discusses the limitations and presents the potential development direction of BES-hydroponic systems. Section 6 concludes this paper.

3.3. The overview view of hydroponic systems

3.3.1. Hydroponic systems

Hydroponic also called soilless cultivation, is a system supplying plants with nutrients (water and minerals) with or without growing medium (e.g., clay, rocks, peat moss, etc.) [86, 87]. The term ‘Hydroponic’ literal translation means water work, which was derived from two Greek words, ‘*hydro*’ and ‘*ponos*’ meaning water and labor, respectively [88]. The timeline of hydroponic agriculture development is shown

in **Figure 3.1.(a)**. There are three main culture technologies in hydroponic cultivation methods, continuous flow solution (CFS) culture, static solution (SS) culture, and aeroponic system (AS) [89]. The main difference, advantages, and disadvantages between these three systems are shown in **Table 3.1.** CFS culture has two main types, nutrient film technique and deep flow technique (**Figure 3.1.(b) & (c)**), and it utilizes a pump to collect circulate and reuse the nutrient solution in the hydroponic system [90]. SS culture has three main types, the root dipping system, the floating system, as well as capillary action system (**Figure 3.1.(d)-(f)**). Unlike CFS culture, the nutrient solution in the SS culture system is not recirculated [90]. AS is an advanced form of hydroponic system, which anchors the roots of plants in the air or mist environment [91] (**Figure 3.1.(g)**). To date, many plants have been successfully grown by hydroponic technology (**Table 3.2**) and the per area yield of the hydroponic greenhouse is more than open agriculture (**Table 3.3**) [92]. Light intensity, temperature, and air humidity are the three key environmental factors to be monitored during hydroponic cultivation. Generally, the level of these factors needs to be carefully maintained as too high or too low could be very detrimental to plant growth. Thus, monitoring and focusing on the law of action of these environmental factors could help hydroponic greenhouse better.

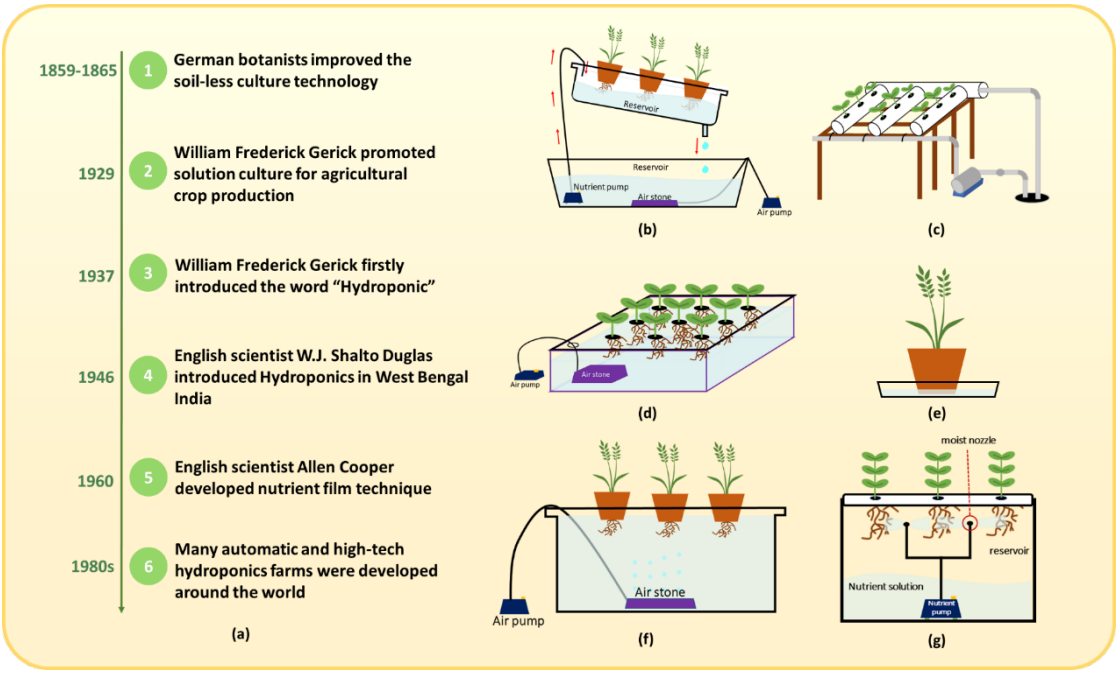

Figure 3.1. (a) The timeline of hydroponic development and diagram of hydroponic structures of continuous flow solution culture (b) nutrient film method; (c) deep flow method hydroponic system; (d) root dipping method; (e) floating method; (f) capillary action method; (g) aeroponic method.

Table 3.1. The classification and characteristics of hydroponic culture technology [89, 90, 93].

Hydroponic culture technology	Branches	Characteristics	Advantages	Disadvantages
Continuous flow solution culture	Nutrient film technique	Nutrient solution is pumped through the tube then flow over the roots of plants, finally drain back to the reservoir.	• automatic control solution feeding • periodically supply a certain amount of nutrient solution • precisely control the amount of delivered nutrient solution • precisely monitor the growth by the targeted supply of nutrient	• high energy consumption. • more greenhouse gas emission • easy to be affected by autotoxicity • sensitive affected by the multi-factors of solutions, such as nutrient components, pH, electrical
	Deep	Nutrient		

Hydroponic culture technology	Branches	Characteristics	Advantages	Disadvantages
	flow technique	solution with 2-3 cm flow through PVC pipes (10 cm diameter), which have some pots and plants in them.	solution • successfully achieve the maximizing water resources by recycling the nutrient solution • easily prevent soil-borne diseases and control insects • independently grow and produce crops, instead of soil type/quality of the cultivated area • achieve vertical farming production which increase the yield of the area unit • achieve continuous production throughout the year	conductivity etc. • special machines for wastewater treatments and monitoring • constant manual management for equipments and data treatments • hard to process wastewater • high cost at large commercial scales • the electricity outages harm for the planted crops
Static solution culture	Root dipping method	Nutrition solution in pots grows continuously, then the bottom of pots (2-3 cm) is submerged into the nutrient solution, and the roots of plants are	• simpler constructure than continuous flow solution culture • easier than continuous flow solution culture to use • more suitable for home use • less cost than continuous flow solution	

Hydroponic culture technology	Branches	Characteristics	Advantages	Disadvantages
		dipped in the nutrient solution	culture • more portable than continuous flow solution culture	
	Floating method	Nutrient solution is put in a shallow container (10 cm deep), plants are grown on a Styrofoam sheet which is floated on the nutrient solution.	• successfully achieve the maximizing water resources by recycling the nutrient solution • easily prevent soil-borne diseases and control insects • higher yield production than soil-borne crops • independently grow and produce crops • achieve vertical farming production • achieve continuous production	
	Capillary action method	Nutrient solution is put in a shallow container with the covering of pots on it. Seedling/seeds are planted in the pots which is filled by inert medium. Nutrient solution in shallow container reaches the		

Hydroponic culture technology	Branches	Characteristics	Advantages	Disadvantages
		inert medium by the capillary action.		
Aeroponic system	--	An advanced form anchors the roots of plants in air or mist environment.	• more easily transplant aeroponic plant, without transplant shock • avoid the disease travel though the nutrient solution • increase aeration of nutrient solution delivers more oxygen to plant roots, stimulating growth and preventing pathogen formation • efficient food production, higher yielding, healthy and fresh food products. • more succeeds in vertical growing arrangements and efficiently use the space • virtually no grow medium used • maximum nutrient absorption by spraying the nutrient rich solution onto the root system • suitable for low leafy	

Hydroponic culture technology	Branches	Characteristics	Advantages	Disadvantages
			vegetables like lettuce, spinach, etc. • can be designed to achieve continuous production throughout the year.	

Table 3.2. Plants grown for hydroponic system [88, 92].

Type of crops	Name of crops		Reference
	Common name	Botanical name	
Cereals	Rice	Oryza sativa	[94]
	Maize	Zea mays	[95]
	Wheat	Triticum aestivum	[96]
	Oat	Avena sativa	[97]
	Soybean	Glycin max	[98]
	Peas	Pisum sativum	[99]
Vegetables	Tomato	Lycopersicon lycopersicum	[100]
	Chilli	Capsicum frutescens	[101]
	Brinjal	Solanum melongena	[102]
	Green bean	Phaseolus vulgaris	[103]
	Bell pepper	Capsicum annum	[104]
	Beet	Beta vulgaris crassa	[105]
	Potato	Solanum tuberosum	[106]
	Swiss chard	Beta vulgaris L.	[107]
	Atriplex	Atriplex patens	[108]
	Cabbage	Brassica oleracea var.	[109]
	Cauliflower	Brassica oleracea	[110]
	Cucumber	Cucumis sativus	[111]
	Onion	Allium cepa	[112]
	Radish	Raphanus sativus	[113]

Type of crops	Name of crops		Reference
	Common name	Botanical name	
Fruits	Spinach	Spinacia oleracea L.	[114]
	Lettuce	Latuca sativa	[100]
	Strawberry	Fragaria ananassa	[115]
	Melons	Cucumis melo	[116]
Fodder crops	Sorghum	Sorghum bicolor	[117]
	Alfalfa	Medicago sativa	[118]
	Barley	Hordeum vulgare	[119]
	Bermuda grass	Cynodon dactylon	[120]
	Carpet grass	Axonopus compressus	[121]
Flower	Marigold	Tagetes patula	[122]
	Roses	Rosa berberifolia	[123]
	Carnations	Dianthus caryophyllus	[124]
	Chrysanthemum	Chrysanthemum indicum	[125]
Condiments	Parsley	Petroselinum crispum	[126]
	Mints	Mentha spicata	[127]
	Sweet basil	Ocimum basilicum	[100]
	Coriander leaves	Coriandrum sativum L.	[128]
	Oregano	Origanum vulgare	[129]
Medicinal crops	Aloe	Aloe vera	[130]
	Coleus	Solenostemon scutellarioides	[131]

Table 3.3. Yield comparisons between hydroponic and open field cultivation [92].

Type of crops	Name of crops	Open agriculture yield (kg per ha)	Hydroponic yield (kg per ha)
Cereals	Maize	1,682.07	8,971.0
	Oat	953.18	3,364.14
	Peas	2,242.76	15,699.32
	Rice	841.03-1,009.25	13,456.56
	Soybean	672.83	1,682.07

	Wheat	672.83	5,606.9
	Beet	10,092.42	22,427.6
	Cabbage	14,577.94	20,184.84
	Cauliflower	11,213.8-16,820.7	33,641.4
	Cucumber	7,849.66	31,398.64
Vegetables	French bean	--	47,097.96
	Lady's finger	5,606.9-8,971.04	21,306.22
	Lettuce	10,092.42	23,548.98
	Potato	17,925.98	156,852.29
	Tomato	11,203.75-22,407.47	403,335.81

3.3.2. Practical obstacles in hydroponic agriculture

Despite the advantages of the hydroponic technology, several shortcomings are existed, such as the requirement of special knowledge, high energy consumption, greenhouse gas emission, and the system must be monitored [132]. These problems are first discussed in detail in this section, thereafter, the possible roles of BES in resolving these problems will be explored.

3.3.2.1. High energy consumption

Hydroponic systems require at least a pump apparatus to support the circulation of nutrient solution and an auxiliary heating system to maintain the optimum temperature inside the greenhouse in cold weather, especially at night [133]. The temperature of the nutrient solution has an inverse relation with dissolved oxygen. When the oxygen level is below 3-4 mg/L, the roots will be inhibited to growth and change to a brown color due to the lack of oxygen [134]. The root uptake and solubility of fertilizers are also get affected by the nutrient solution temperature [134]. Thus, the energy consumption of the hydroponic system is very high, usually 17% higher than traditional land cultivation [50]. Depending on the layout of the structure, the average energy consumption for the hydroponic plant can reach up to the ranges between 14-17 kWh/m^2 [135]. Of this total energy, heat consumption corresponds to 95.3% [136]. In the past, combustion of natural gas, liquefied petroleum, or fossil-fuel-fired heating systems has been used. However, these systems emit greenhouse gases and atmospheric pollutants [133]. Such as in the Midwestern United States,

coal-fired as the main energy source for the hydroponic system causes nitrogen oxides (NO_x), sulfur dioxide (SO_2), heavy metals, particulate matter, as well as one-third of CO_2 in the US [137]. Moreover, due to the system depends on electricity, the power outages will lead to harm to the planted crops [48].

3.3.2.2. Greenhouse gas emission

Greenhouse gases emission (especially CO_2 and methane (CH_4)) is a major problem in hydroponic system cultivation [50, 138]. According to Martinez-Mate et al. [50], the total area of greenhouse gas emissions from the hydroponic system was equivalent to 25,724 kg $CO_{2eq}ha^{-1}year^{-1}$, more than twice as high as the soil cultivation production (11,760 kg $CO_{2eq}ha^{-1}year^{-1}$). The estimates of global CH_4 emission rates from rice fields range from 20 to 100 Tg $year^{-1}$ (1 Tg = 1 million tons) [139]. The CH_4 potential of crops varied from 0.17 to 0.49 m^3 CH_4 kg^{-1} VS_{added} (volatile solids added) and from 25 to 260 m^3 CH_4 t^{-1} ww (tons of wet weight) [140]. In particular, CH_4 with 25 times higher global warming potential (GWP) than CO_2 constitutes a major part of these emissions [141]. Careful attention needs to be paid to the CH_4 emission since hydroponic systems mimic the growing conditions of rice farming - one of the main anthropogenic sources of methane emission (between 9-19%).

In brief, the anoxic environment caused by a waterlogged condition (e.g., in rice fields and hydroponic systems) is conducive to CH_4 production by the anaerobic methanogenic bacteria [142]. These methanogens metabolically reduce organic carbon to produce methane in a process referred to as methanogenesis [143]. Different types of conditions that can be found in the hydroponic system such as neutral pH level, the application of organic manure or fertilizers, as well as roots submergence in deep water increase the population and activities of methanogenic bacteria. Until now, not too many studies reported hydroponic greenhouse gas emissions control technology.

3.3.2.3. Autotoxicity

Autotoxicity is also a major drawback in closed-loop hydroponic cropping

systems, which would reduce the growth and yield of crops. Autotoxicity is a form of allelopathy that happens within plants by the release of a variety of phytotoxic chemicals [144]. Several studies have demonstrated the adverse effect of autotoxicity on plant performance during cultivation in closed hydroponic cropping systems [145]. The influence of autotoxicity becomes more pronounced when crops are cultivated on the same soil for years or grown in recycled hydroponic solutions for several cultures [146]. This condition is caused by toxic exudate accumulation in the media solution due to the continuous recycling of hydroponic nutrient solution [145, 147]. These chemical substances can delay/inhibit germination and/or growth of the plant being cultivated [148, 149]. The chemical substances, without fixed concentration, consist of mainly carbon, although concentrations are not fixed. Altogether, more than 200 various carbon-based molecules have been found as part of root exudates [150]. Several organic acids, such as lactic, vanillic, succinic, salicylic, palmitic, benzoic, etc., have been proved in the reused nutrient solution [145].

Plants' age, species, cultivar, as well as environmental factors decide the exudation profiles [151]. Plants' roots are first affected by phytotoxic chemicals in their rhizosphere, then water and nutrient element uptake are most affected [152]. Until now, the major way to clean the nutrient solution is exclusion or detoxification, such as activated charcoal [153], application of amino acids [149], and electro-degradation, etc. in nutrient solution [154]. However, the activated charcoal and amino acids methods are not sustainable, and probably have some influence on some specific crops, and the amount of them needs to be calculated carefully. Advanced technology such as electro-degradation required more energy consumption, and the cost of the machine is normally high.

3.3.2.4. Nutrient solution related toxicity

The productivity and quality of hydroponic crops are markedly dependent on the extent of plant nutrients uptake from the growing solution medium [155]. Therefore, the fertilizer salts required high solubility and must remain in the solution to be available to the plants [156]. The macro (e.g., N, P, K, Ca, Mg, S, etc.) and micro/trace

(Fe, Mn, B, Cu, Zn, Mo, etc.) elements are the mineral element composition of nutrient solution [157]. Plants can acquire ions at very low concentrations when the nutrient is continuously supplied in solution in the right equilibria conditions [158]. However, a change in these conditions can lead to excessive nutrient acquisition and plant toxicity [159].

The pH and electrical conductivity (EC) of the nutrient solution have paramount importance in the formulation of the hydroponic nutrition solution. In terms of the balance of anions over cations, the changes in the pH depend on the difference in the magnitude of nutrient uptake by the plants [160]. The nutrient composition also determines the EC of the solution. The higher EC impedes the nutrient uptake by increasing the osmotic pressure, while lower EC may severely affect plant health and yield [161, 162]. The optimal pH and EC levels are between 5-7 and 0.8-2.5 dS/m, respectively [145].

Further, the management and control of diseases easily spread through solutions are also major challenges for the hydroponic greenhouse system [163]. For example, a mold infection will spread to all pant in a circulating hydroponic system [164].

3.3.2.5. Wastewater management

Hydroponic wastewater could cause pollution and pose a significant environmental concern to the environment when discharged directly into the environment as it has a high amount of nitrate (N: 150-600 mg/L) and phosphate (P: 30-100 mg/L) [165-167]. Nitrate and phosphate discharge can induce eutrophication in the receiving waters leading to algal blooms, depleting O_2 in the receiving water, and releasing toxins [168]. Besides, nitrate discharge is the origin of the loss of calcium and moving into groundwater (Prystay and Lo 2001). Other characteristics of hydroponic wastewater also include high salinity and low content of organic matter which may be unsuitable for some freshwater inhabitants [169].

The traditional hydroponic wastewater treatment way is recycling the drainage water; however, the efficiency is low between 35-45% [170]. Then, more effective method including ultraviolet treatment, denitrification-based treatment, constructed

wetlands-based treatment, and microalgae-based treatment is developed [156]. Although the wastewater treatment efficiency enhances to >90%, the cost of equipment and labor, and the consumption of energy are also increased. Despite the microalgae-based treatment being the renewable and environmentally friendly way, the follow-up treatment and recovery of algae need further consideration and exploration.

3.3.2.6. High cost

Hydroponics has less impact on the environment than the soil agricultural system which can causes almost all of them are located in the greenhouse [171]. The selection and design of hydroponic greenhouses mainly depend on the environmental factors of the location, climate, and technology development related accessibility. For example, in the cold/hot climatic conditions, the hydroponic system will incur extra costs for heating/cooling the growth environment. There are also minimal design requirements, such as a minimum of 40 large plants or 72 small plants, e.g., banana peppers, bell peppers, lettuce, spinach, etc. [172]. These design costs, other upfront costs (such as pumps, pipes, and tanks, as well as their operation, monitoring, controlling, and maintenance costs increase the cost of hydroponic systems in comparison to conventional cultivation [48, 173, 174]. In addition, high-level skills (e.g., crops' production knowledge, adequate experience, technical skills) are always a requirement for hydroponic systems management which shows a positive correlation with the complexity of the system [175-177].

3.4. HYDROPONIC BIOELECTROCHEMICAL SYSTEM: THE QUEST FOR THE IDEAL SETUP

3.4.1. Bioelectrochemical systems

Bioelectrochemical systems (BESs) also called microbial electrochemical systems, convert chemical energy into electrical energy by employing microbes as catalysts. BES has been employed in various ways (biosensing, renewable energy

production, wastewater treatment, nutrients recovery, etc.) to achieve many goals. Specifically, the common types include: MFC, generating electrical energy via degrading organic matters [178]; MDC, providing desalinated water from seawater/brackish water [179]; MEC, synthesizing value-added chemicals and commodities by a poised biocathode [180]; EBC, relying on purified redox enzymes (e.g., glucose oxidase, laccase, etc.) to achieve electrocatalytic reactions [181]; MRC, capturing energy from salinity gradients between salt and fresh water. With the help of bacterial oxidation of organic matter/oxygen reduction, MRC effectively captures energy, generates hydrogen, or produces chemicals for the carbon dioxide capture from the salinity gradients [182-184]; MSC, utilizing photoautotrophic microorganisms or higher plants to harvest solar energy to generate electricity or chemicals (e.g., hydrogen, methane, ethanol, hydrogen peroxide, etc.) [80, 185, 186]; MEC, generating hydrogen by a microbial electrical supply along with an externally applied voltage [187]. As a result of the versatility of BESs, they can, therefore, be integrated with other technologies, e.g., algal photobioreactors, capacitive deionization, membrane bioreactors, MFC-driven-MEC, etc. in hybrid system configurations to enhance the overall performance (energy consumption/generation, contaminant removal, metal removal/recovery) [188, 189].

3.4.2. Energy savings in hydroponic agriculture

More attention is now being paid to renewable energy sources (wind, solar, biogas, etc.) for the reduction of the energy requirement for greenhouses acclimatization and heating. So far, biogas, solar, and ground source heat pump integration with greenhouse heating systems have been used successfully to support heating energy requirements for greenhouses [190]. However, as natural energy sources like wind and solar etc. are intermittent in nature and not available all the time, searching for a suitable device to store thermal energy becomes another challenge. Energy savings, therefore, could be a more pragmatic approach to reducing energy demand.

MFC, a bioelectrochemical system, is a promising option to achieve energy

savings in hydroponic systems. In principle, the organic matter present in the exudates of hydroponically grown plants can be used for bioelectricity production. The basic working of such a configuration is represented in **Figure 3.2**. Such a configuration for a hydroponic system will be similar to plant microbial fuel cell (PMFC) which has been extensively studied [81]. In PMFCs, 20-40% of carbon-rich biomass produced by the plants can be found in the form of rhizodeposits (sugars, organic acids, polymeric carbohydrates, enzymes, and dead cells) around plant roots. Previous studies have shown that the level of electricity production can match up to traditional biomass electricity generation systems (e.g., 2.8-70 GJ ha^{-1} $year^{-1}$ of energy crops digestion, 27-91 GJ ha^{-1} $year^{-1}$ of biomass combustion) [15, 191].

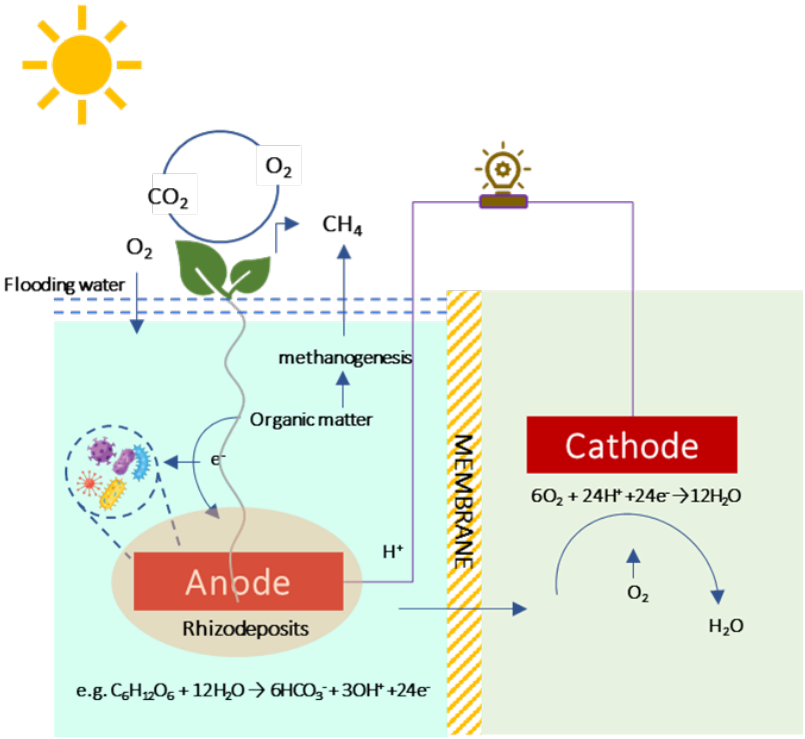

Figure 3.2. Model of a hydroponic microbial fuel cell including the basic principles.

The direct outputs of a single PMFC are primarily at the level of 100-5500 mW/m^2 [192, 193], which generally cannot directly power common electronics. Such as, a single light-emitting diode needs a minimum voltage of 2 V and requires 30 mW, and wireless sensors need a voltage of 3.3 V for temperature, chemical concentration, humidity, and pressure monitoring [194]. Thus, the energy harvesting systems were developed. For example, Yamashita et al. [195] explored an ultra-low-power energy

harvester specially designed for MFCs, which can charge a supercapacitor to 3.3 V, and this value can be utilized in any real-time measurements of humidity, long-range wireless data transmission, gas sensing, and temperature. Prasad and Tripathi [196] utilized a boost converter and a supercapacitor to increase the voltage level of MFC, which charged at a faster rate to the supercapacitor from 2.76 V to 4.5 V in 30 min. When six sediment MFC modules were connected to charge the battery to 100%, the battery could be used for LED bulb lighting (7 W, 230 V, 50 Hz). In addition, capacitor-MFC, charge pump-MFC, boost converter-MFC, and maximum power point tracking-MFC systems are all been proven to efficiently harvest the energy generated by MFC [194]. Based on the above, the renewable sustainable energy recovered from PMFC bioelectricity generation can be used for lighting LED, heating, monitoring, pumping, recycling, and wastewater treatment, vital to the hydroponic system, overall reducing the energy requirements.

3.4.3. Gas emission

As discussed in the previous subsection, under waterlogged conditions, the main pathway of gas exchange with the rhizosphere is through the aerenchyma of plants (90%) leading to the formation of CH_4 [12, 13]. Firstly, plants release available organic compounds for methanogens through root exudates to enhance methane production. Meanwhile, plants deliver oxygen into the rhizosphere and accentuate methane oxidation. More important, plants could serve as a conduit for methane to bypass the aerobic zones and thus strongly increasing methane emission fluxes [197]. Therefore, a promising route for mitigation of CH_4 emission is to prevent the formation or in some cases utilization of formed CH_4 in the rhizosphere area. Electrochemically active microorganisms are founded in BES and can be used in this case as shown in several studies [198-201]. Specifically, it has been shown that a closed circuit PMFC was able to decrease ten times less CH_4 than an open circuit PMFC [202], and in sediment-PMFC, the CH_4 emissions could be reduced by 47% [20] to 50 % [20]. Further, the CH_4 production from constructed wetlands (CW) could also be controlled by operating MFC [198, 203]. All studies confirmed the abundance of

exoelectrogenic bacteria and the correlation of voltage signals with CH_4 emission flux in paddy fields [204-206].

Compared to traditional mitigation strategies (e.g., aeration and microporous aeration, redox potential control, water-level control, and the addition of iron/other chemicals, etc. [207] of CH_4 emission from plants, MFC possesses four main advantages: no chemical/extra energy is involved, decreases the autotoxicity influence by utilizing the rhizodeposition of plants, a certain amount of electrical energy can be harvested, real-time monitoring and real-time control of the CH_4 production. Therefore, MFCs provide a green and sustainable option for CH_4 abatement. **Figure 3.3.(a)** is an illustration of how this can be integrated into hydroponic systems for CH_4 abatement, where the CH_4 emission is controlled by the external resistance and monitored by the electricity production from PMFCs.

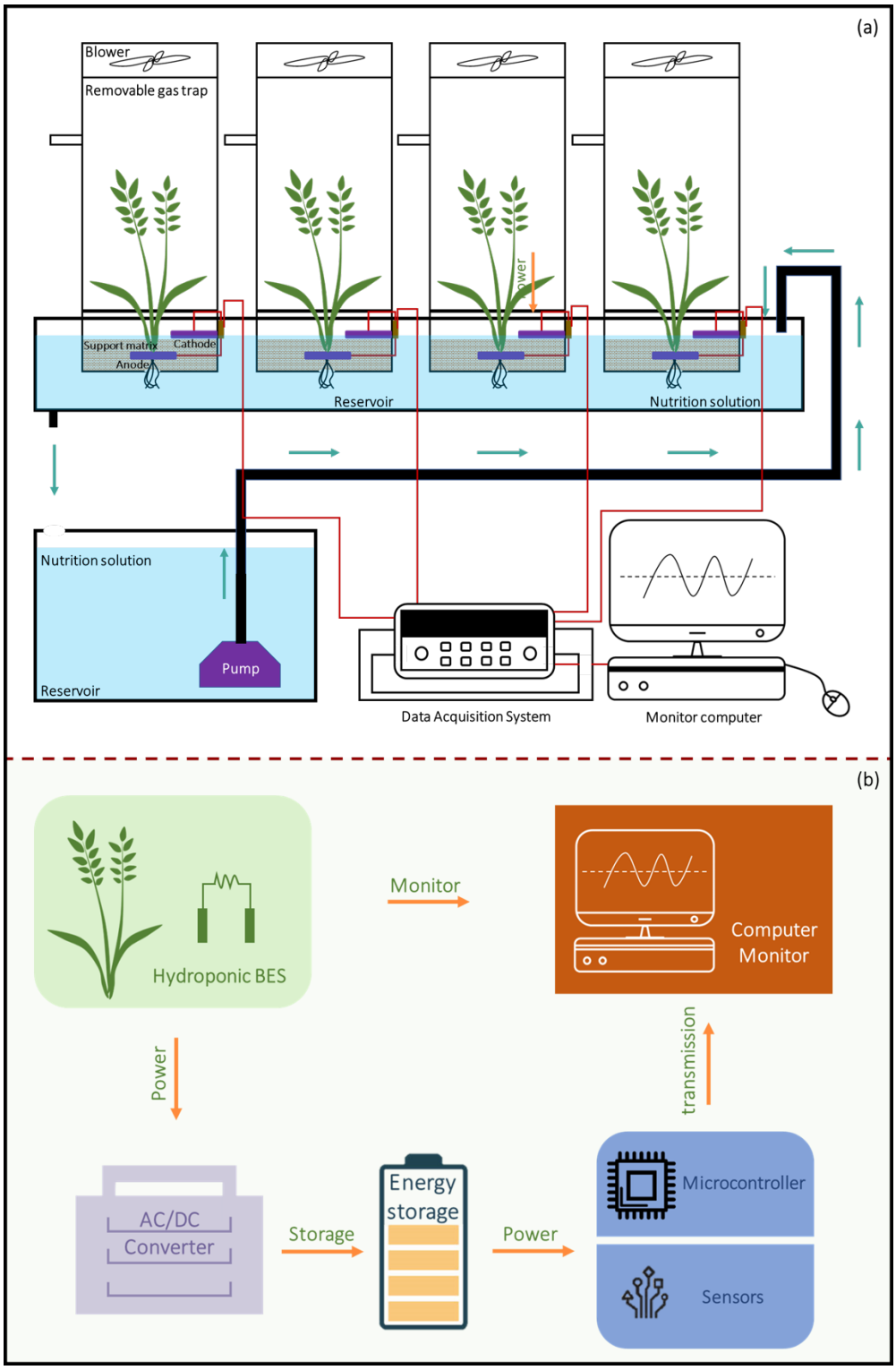

Figure 3.3. (a) The nutrition circulation hydroponic-MFC integrated system for methane control; (b) the block scheme of the hydroponic BES sensor.

3.4.4. Nutrient composition monitoring

Traditional nutrient composition sensors or monitors such as liquid

chromatography, high-performance liquid chromatography (HPLC), and gas chromatography (GC) are time-consuming, tedious, expensive, complex, huge, and not portable. This opens the chance to integrate BES-based biosensors for online monitoring. A conventional biosensor combines biological molecules with a physical transducer to convert the output into an electrical signal [208]. However, compared with traditional biosensors, BES biosensors do not need transducers, time-saving, low cost, maintenance-free, wide applications (from monitoring the anaerobic digestion process to detection of water quality), as well as the fact that they operate for a long time by local resources [209] are all attractive.

Either an MFC or MEC biosensor can be exploited. In an MFC biosensor, the current produced by continuous feeding of a part of the wastewater can be correlated with the nutrient composition. The composition can be measured either in terms of the biological oxygen demand (BOD), chemical oxygen demand (COD), dissolved oxygen, volatile fatty acids, toxicants (e.g., mixed metal, formaldehyde, etc.), as well as water content [210-212]. For example, Nail and Jujjavarapu [213] developed a self-powered and reusable single-chambered cylindrical (MFC) for toxicity detection in water containing heavy metal ions, which showed sensitivity towards the Cu^{2+}, Cr^{6+}, Zn^{2+}, and Ni^{2+} at concentrations above 10 mg/L. Prévoteau et al. [214] successfully designed an O_2 reducing microbial cathode-based MFC sensor for the measurement of Hg^{2+}, Cr^{6+}, and Pb^{2+} in tap water, and the detection limits for these metal ions was a range from 1 mg/L to 10 mg/L. Besides, this research proved that some electro-active microorganisms could survive in fresh tap water for at least 8 months without extra substances. MEC biosensor has a similar working mechanism to MFC, except for an external power supply, which enhances the rate of migration of charged molecules and the consumption of organic molecules [215]. The energy consumption of MEC is very small and can be compensated by the hydrogen produced by MEC. Jin et al. [216] reported a MEC-based biosensor for rapid monitoring of volatile fatty acids. The current density increased with the increase of volatile fatty acids (in a range of 5-100 mM) and vice versa, which indicated good reproducibility of the MEC-based biosensor.

To integrate BES-based biosensors to monitor nutrient composition in real-time, the following criteria must be met, such as calibration, maximum detection range, sensing time, power management, and data transmission steps (**Figure 3.3.(b)**). Four different kinds of MFC/MEC biosensor systems can be envisaged for monitoring changes in the composition of the nutrient solution in the hydroponic systems. Firstly, feed MFC/MEC directly by hydroponic wastewater, then monitor the nutrition/toxicants in wastewater through the voltage fluctuation. Monitoring data can be integrated with wireless infrastructure for remote access using the bioelectricity generated in the monitoring process. Another configuration where no pumping is involved can also be envisaged where the electrodes are integrated into the hydroponic system (**Figure 3.4.(a)**). Besides, a combination of MFC-MEC biosensor systems can be envisaged where the integrated MFC provides the operating voltage for a MEC. Both MFC and MEC could be combined with the hydroponic system (**Figure 3.4.(c)**), or one of them could be used to treat wastewater (**Figure 3.4.(d)**). Finally, a simpler chamber MFC-MEC system from two to one could be explored (**Figure 3.4.(b)**). Initially, MFC-MEC could be run in MFC mode for nutrition solutions monitoring and electricity generation (collected by a capacitor). Then shift to MEC mode for different kinds of nutrition composition monitoring. Earlier studies have shown that there is enough energy from MFCs for achieving an energy-neutral smart sensor that samples and sends data or for operating a MEC [217, 218]. PMFC has also been used to monitor the status of plant health [219]. It should be mentioned that although BES biosensors utilize mixed microbes to detect the components of media solution, specific analyte monitoring can be achieved using engineered strains [220, 221].

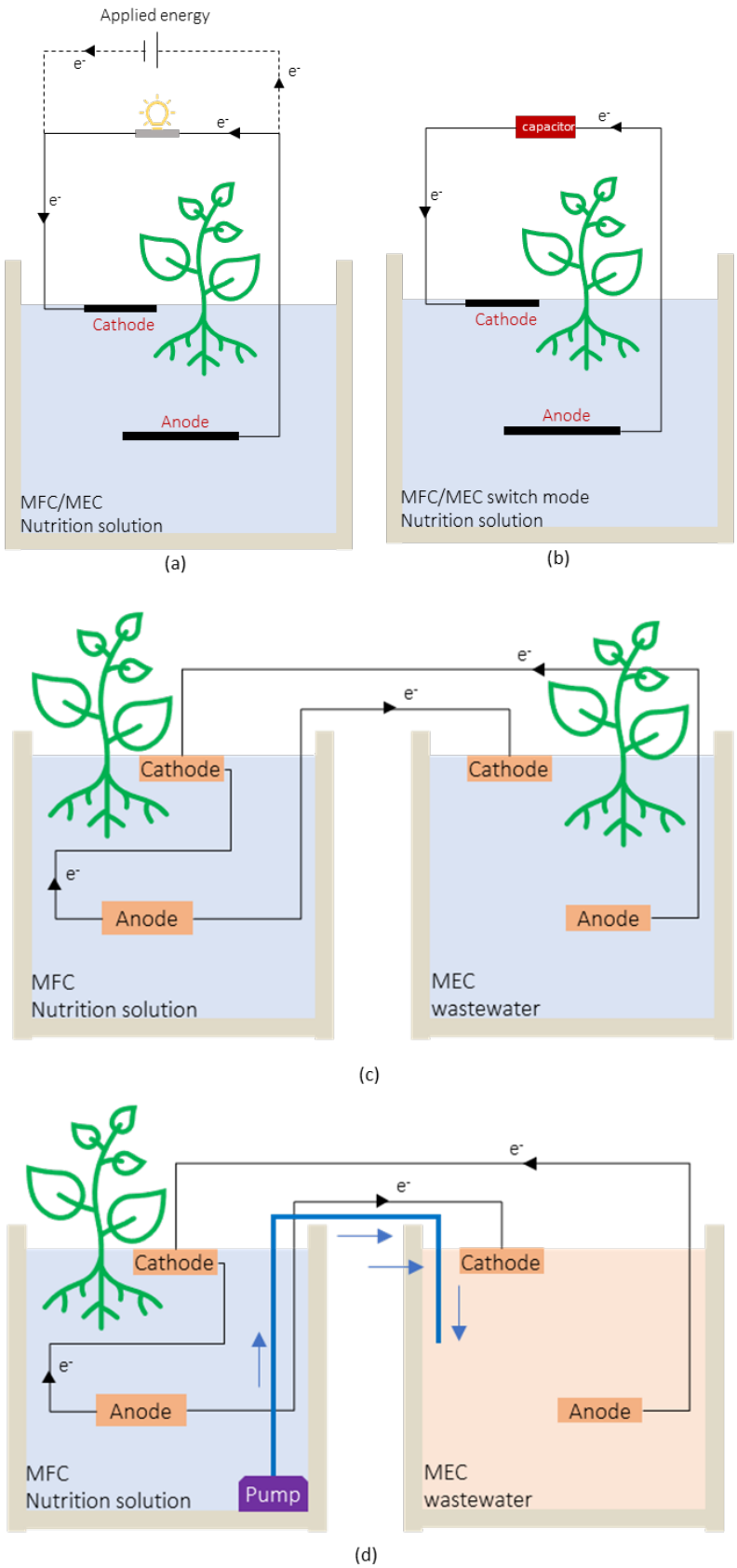

Figure 3.4. Some types of MFC/MEC biosensors that can be used in the hydroponic system, (a) MFC/MEC electrodes are integrated into the hydroponic system; (b)

switch-mode MFC and MEC; (c) MFC driven MEC, both integrated with the hydroponic system; (d) MFC driven MEC, one integrated with a hydroponic system, one process wastewater.

3.4.5. Wastewater treatment/management

The wastewater from the hydroponic system can also be treated by BES. MFC and MEC are the most common BES used for wastewater treatment [222-224]. The configuration of MFC and MEC used in nutrition solution monitoring can also be used in wastewater treatment/management. In addition, the photobioreactors MSC can also be used to process wastewater from hydroponics. Algae residue and dry algae biomass are used as a "solar converter" (substrates) in MSCs for removing nitrogen contaminants from wastewater wastewater [225-227]. Algae are used in these MSCs either at the anode as the substrate for bacteria grown or cathode as the catalyst to provide oxygen [228-230]. Up to a maximum of 99% COD removal efficiency has been recorded in wastewater treatment using algae [231]. In addition to algae, other plants such as saltwater grass, Milano-Nosedo, etc. have been successfully used in MSCs to process wastewater and generate electricity [232, 233]. Another promising wastewater treatment BES technology that could be adapted for treating hydroponic wastewater is MDC. MDCs are the modified form of MFCs powered by the bioenergy generated via the microbial degradation of organic matter [234]. MDC is regarded as a cost-effective approach for simultaneous wastewater treatment and recovery/removal of value-added products/targeted pollutants, such as HCl, H_2, H_2O_2, NaOH, Cu, Pb, Cr, and As, etc. [235], all of which can be found in hydroponic wastewater.

In summary, the following configurations in addition to the common MFC/MEC systems configuration, for hydroponic wastewater are suggested. A hydroponic configuration incorporating a photobioreactor MSC for simultaneous or sequential treatment of the wastewater could be a good option. This algae-based configuration will remove greenhouse gases concurrently, with the potential of the algae use as a fertilizer in later stages. Another configuration where an MDC is incorporated into the circulatory system of the hydroponic system can also be envisaged. Target

contaminants can be removed from the wastewater in real-time and returned to the nutrient reservoir in real-time. This configuration is expected to achieve wastewater treatment and reduce operating costs synchronously. **Figure 3.5.** is a conceptualization of such use of either an MSC or MDC for hydroponic wastewater treatment.

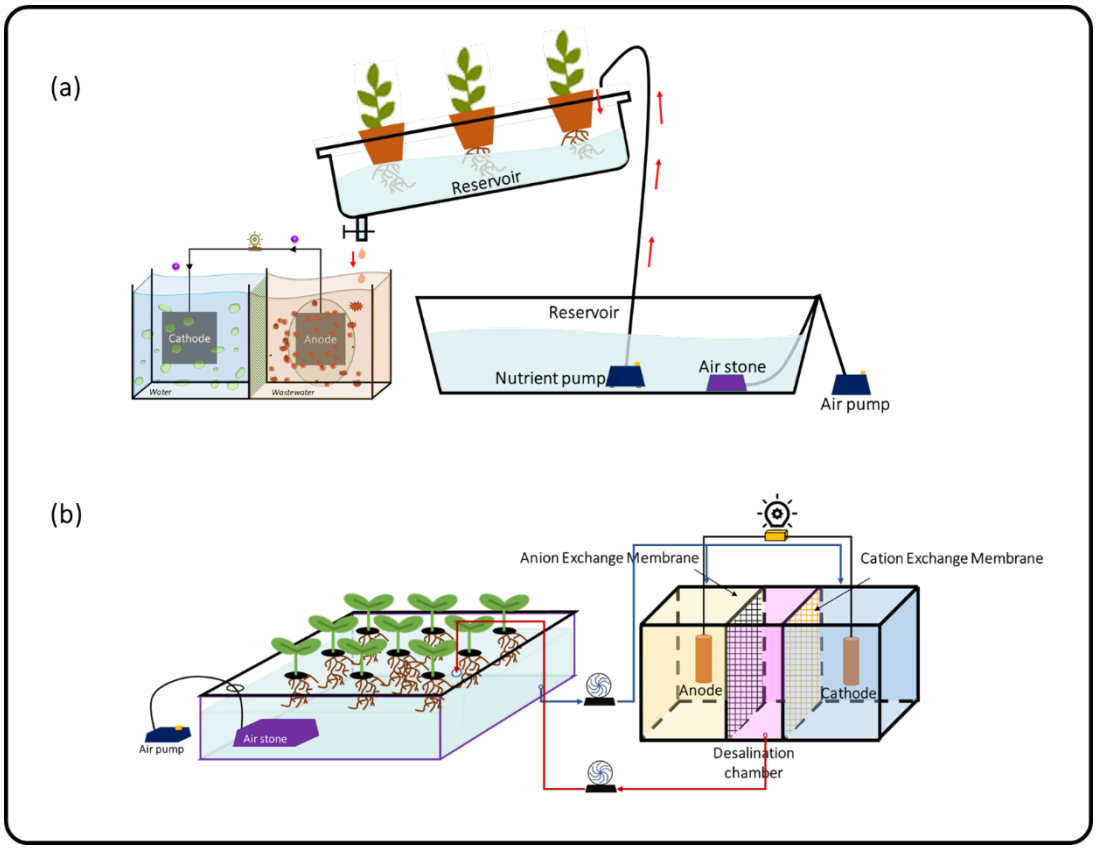

Figure 3.5. Diagram (a) MSC-hydroponic and (b) MDC-hydroponic structures for wastewater treatment.

3.4.6. Other potential advantages

The combination of BES and hydroponic systems is a way that could help to reduce the costs of energy, monitoring, and wastewater treatment of traditional hydroponic agriculture. In comparison with the conventional hydroponic related problems solving technologies, BES is more multifunctional and could solve several problems at a time with one system as shown in **Table 3.4**. Some conventional technologies such as mentioned electro-degradation and ultraviolet treatment could have a negative influence on plant growth, while BES has no related concern.

Furthermore, BES saves more time, which could treat wastewater while plants are growing. Some types of BES not only do not require extra input energy but also could combine with renewable clean nature energy, such as solar energy [81], tidal energy [236], etc., thus, BES is more suitable to use in energy scarcity countries. Besides, the conventional machines are normally big, hard to combine with hydroponic, and need extra space to place. While the basic components of BES are very simple, the scale and size could be adjusted according to various types of hydroponic systems. Interestingly, BES could share some configurations with hydroponic systems, which also could save the overall cost. The price and scale of BES are very flexible, which is decided by the materials and structure of configurations. Thus, the overall price of the hydroponic system can also be revamped.

Table 3.4. The obstacles to hydroponic and innovations of hydroponic-BES technology.

Obstacles in hydroponic	**Bioelectrochemical system**					**Innovations**
	MFC	**MEC**	**MSC**	**MDC**	**Integrated system**	
High energy consumption	√					• Recovering the renewable sustainable energy from BES bioelectricity generation • Reducing the extra energy requirement of hydroponic system, such as lighting LED, heating, monitoring, pumping, recycling, wastewater treatment
Greenhouse gas emission	√					• No chemical/extra energy is involved; • Real-time monitoring of the CH_4 production; • Decreasing the CH_4 production;
Autotoxicity	√	√	√	√	√	• Decreasing the autotoxicity influence by utilizing the rhizodeposition of plants.
Solution toxicity	√	√	√	√	√	• Simple biosensor configuration. BES biosensors not needing transducers and can be

						operate for a long time by local resources; • The wide range of measured composition, such as BOD, COD, dissolved oxygen, volatile fatty acids, toxicants (e.g. mixed metal, and formaldehyde, etc.), as well as water content.
Wastewater	√	√	√	√	√	• Simultaneous achieving wastewater treatment and removal of value-added products/targeted pollutants; • Recovering valuable products in wastewater, such as metals.
High cost	√		√	√		• Reducing the costs of energy, monitoring, and wastewater treatment of traditional hydroponic agriculture; • Recovering the valuable products and reusing treatment wastewater; • flexible price, according to its materials of configuration, thus the overall price of the hydroponic system can also be revamped; • Easy to operate, and free-maintenance.

Moreover, the BES-hydroponic is a good idea for soilless areas, especially outer space. Plants in BES-hydroponic systems will absorb carbon dioxide and stale air, then provide renewed oxygen and energy through the plants' natural growing process. This is important for long-range habitation of both the space stations and other planets [92]. Bioelectricity generated by BES-hydroponics can be used to maintain systems operation as well as provide unobtrusive energy-neutral monitoring to address the needs of future smart agriculture applications.

3.5. Techno-economic analysis

One main advantage of BESs combined with hydroponic systems is their capability to directly extract electric energy from the hydroponic substrate. Unlike the traditional power, electricity generates from BESs is a cleaner and more widely usable

form of energy. Besides, BESs can run well at a wide temperature range [237], therefore, they are more flexible in the hydroponic system. From the environmental sustainability of the hydroponic agricultural point of view, the combination of BESs need to ensure that the crop yield meets the standards of traditional hydroponic cultivation. According to the report of Khudzari et al. [27], the highest shoots and biomass production of PMFCs were similar to soil cultivation plants. Therefore, in theory, BES has no significant effect on crop yield. The major obstacle for BES-hydroponic technology moving into the real world is its suitability for manufacturing, which in turn drives economies of scale. The main cost of BES-hydroponic consists of the initial investment and the operating/maintenance associated costs with materials consumption, chemicals, and energy [238]. Most of the core parts components should be bespoke (e.g., electrodes, ion exchange membrane, BES chambers, etc.) and therefore expensive. Therefore, it is important to identify alternatives that should be inexpensive and widely available. Stoll et al. [239] found that compare with carbon foam ($1995) and hard felt ($220), the cost of a 1m^3 laboratory-scale MFC electrode assembly equipped graphite brush anode could be cheapest ($503) with a capital cost of $9.09. Christwardana et al. [240] demonstrated that the capital cost of Large Yeast MFC is approximately $234.22, which is 2.57 times higher than Small Yeast MFC.

The availability of BES-hydroponic system components (e.g., wiring, membranes, electrodes, resistances, etc.) needs to be explored, in order to assemble and implement the systems on a larger scale. Some materials used in BES-hydroponic systems such as electrodes, substrates, and ion-exchange membranes might have negative environmental impacts. Thus, the viability of the BES technology in a real hydroponic environment under various environmental conditions (e.g., light, temperature, pH, humidity, subtract, etc.) and under operation variables (e.g., light intensity, batch/continuous flow, flow rate, etc.), as well as the overall environmental impacts need to be evaluated.

3.6. Further perspective

Hydroponic agriculture has the potential to supplement agriculture in many areas

worldwide [48], and thinking forward on challenges that may thwart its sustainability is paramount. As shown in Table 3.4, the selection of proper BESs is very important, which relies on several factors and main problems. Under the synergy of BES innovations, the main problems of hydroponics could be solved. The integration proposed in this paper needs further consideration if commercial-scale adaptation is to be realized. Notably, the following non-exhaustive points need to be acknowledged:

- Lack of in-depth discussion on the specific obstacle of hydroponics and solving mechanism of BES. Some researchers reviewed the obstacle of hydroponic agriculture, such as Sambo et al. [60] and Riggio et al. [241], however, they only focus on the traditional methods' mechanism to solve these problems (e.g., nanoparticles, plant growth-promoting rhizobacteria, sensor monitoring). None of them focus on the mechanism of cleaner and sustainable BES technology.
- Lack of the in-depth study of the mechanism between BES and the hydroponic crop yield. Until now, most BES studies mainly focus on the performance of BES electricity production, biosensor, or waste treatment efficiency [242, 243]. Plants in BES are only used as an auxiliary tool to improve the mentioned properties [219, 244]. However, the influence of BES on crop growth (e.g., biomass production, height, root length, etc.) and yield are rarely reported.
- The high cost of hydroponic systems compared with the traditional agricultural is still a challenge that BES integration cannot resolve entirely, such as the initial capital investment and labor cost.
- Monitoring of nutrient composition can only be done on a general basis. Most of the research focused on the enhance the range of detection of BES-based sensors and lowering the detection limit to enhance the sensitivity of the sensor. However, the detection limit of BES sensors is limited by the mass transfer barrier formed by the microbial biofilms and the electrogenic microbes, which leads the BES sensors less sensitive to the exposure of the sensing elements [238, 245]. Besides, when various components in the nutrient solution simultaneously surge, signal interference may occur. Thus, a more precise and specific component monitoring will require a lot more innovation of the BES technologies on their own.

- There is a risk of over-complicate a relatively complex system (when compared to traditional agriculture). With the addition of the BES, the attractiveness of the integration can be challenged. If the technical know-how requirement of a hydroponic system is compounded with that of BES, it is hard to argue for its merits.
- Control might be difficult. BES are microorganisms driven and the complex interaction between these drivers, the chemical composition of the nutrients, and the plants being grown under hydroponic systems is something to be carefully studied. Factors that influence both hydroponic systems (temperatures, humidity, pH, etc.) and BES (plant types, anode/cathode materials, configuration, carbon source substrates, etc.) could create a control nightmare.

To overcome these limitations, new studies could explore optimizing several BES-hydroponic configurations or propositions by:

i. Optimizing BES and hydroponic structural components (e.g., reactor design, electrode modification, electrolyte, substrate choice, catalyst, enzymes coating, external resistance, bacteria species) to improve the efficiency and lower the overall cost. For example, Gajda et al. [246] proved that 250 L MFC module size can generate as low as 0.47 W/m^3 of power density and MFCs stacking could enhance their performance. Besides, the substrate nature has the main influence on BES performance and hydroponic plant growth. From chemical properties aspect, the amount of substrate consumed by bacteria during aerobic or anaerobic respiration affects electron donation rates in BESs and rhizosphere deposition of plants [247].

ii. Paying more attention to studying the mechanism between BES and plants' growth. For example, the relationship between the plant health (e.g., height, greenness, roots length, etc.) and electricity production from the BES; the influence of microbes (e.g., species, quantity, reproductive speed, etc.) in BES on plants' crop production; the influence of greenhouse environmental conditions (e.g., illumination, temperature, humidity, water evaporation rate from the hydroponic system, the circulation speed of nutrient solution, etc.) on BES efficiency (e.g., electricity production, wastewater treatment efficiency, biosensor monitoring accuracy, etc.); the influence of plant growth cycle on BES performance (e.g., energy generation stability, the monitoring

system stability, the flora metabolism, etc.).

iii. Exploring more advanced BES to develop its potential function and improve its precision by combining some existing renewable energy technologies, such as nanophotocatalysis and photocatalytic semiconductor thin films. Nanophotocatalysis is a proficient technology for the reduction of heavy metals to a non-toxic state, which can be used as the photocatalyst in BES [248-250]. The photocatalytic semiconductor thin film materials allow easy incorporation into various devices through changing the properties of materials and reducing the size, which can reduce the cost and improve the efficiency of devices [251], therefore, it can be used as the ion exchange membrane in BES. Or innovation technologies, for example, the hydrogen production technology (pyrolysis, hydrocarbon reforming, plasma technology, etc.) [252], which can improve the hydrogen generation from BES systems and be used as the pretreatment methods to process the substrate of BES systems.

iv. Exploring model systems for BES-hydroponics to optimize the overall system performance. Modeling could simplify the complex BES-hydroponic system and related mechanism into a simpler form for better understanding as well as representation of the whole system. Until now, considerable modeling efforts and experimental validation have been carried out to improve the performance of BESs for practical applications. For example, Buckingham's Pi theorem describes the trend of experimental results by constructing groups of dimensionless variables and can simplify the experimental quantity [247]. Besides, Artificial Neural Networks, Stacked Denoising Auto-Encoder deep learning network, discriminant analysis, and Support Vector Machines techniques [253] could also be used to explore more precise predictive models based on the whole BES-hydroponic systems.

v. Utilizing a decision tree to select suitable BES-hydroponic growing system types is worthy of exploration. For example, if emission is a problem, can this be reduced through this proposed integration? Is wastewater treatment a problem? What are the cost-beneficial advantages of on-site wastewater treatment using this technology? How important is specific monitoring to the growing system in the particular hydroponic system? Figure 3.6. is a decision tree model that can be adapted for

answering these types of questions. Numerous configuration types, carbon sources, and genetic engineering technology can be explored to arrive at the decision to pursue or utilize other methods.

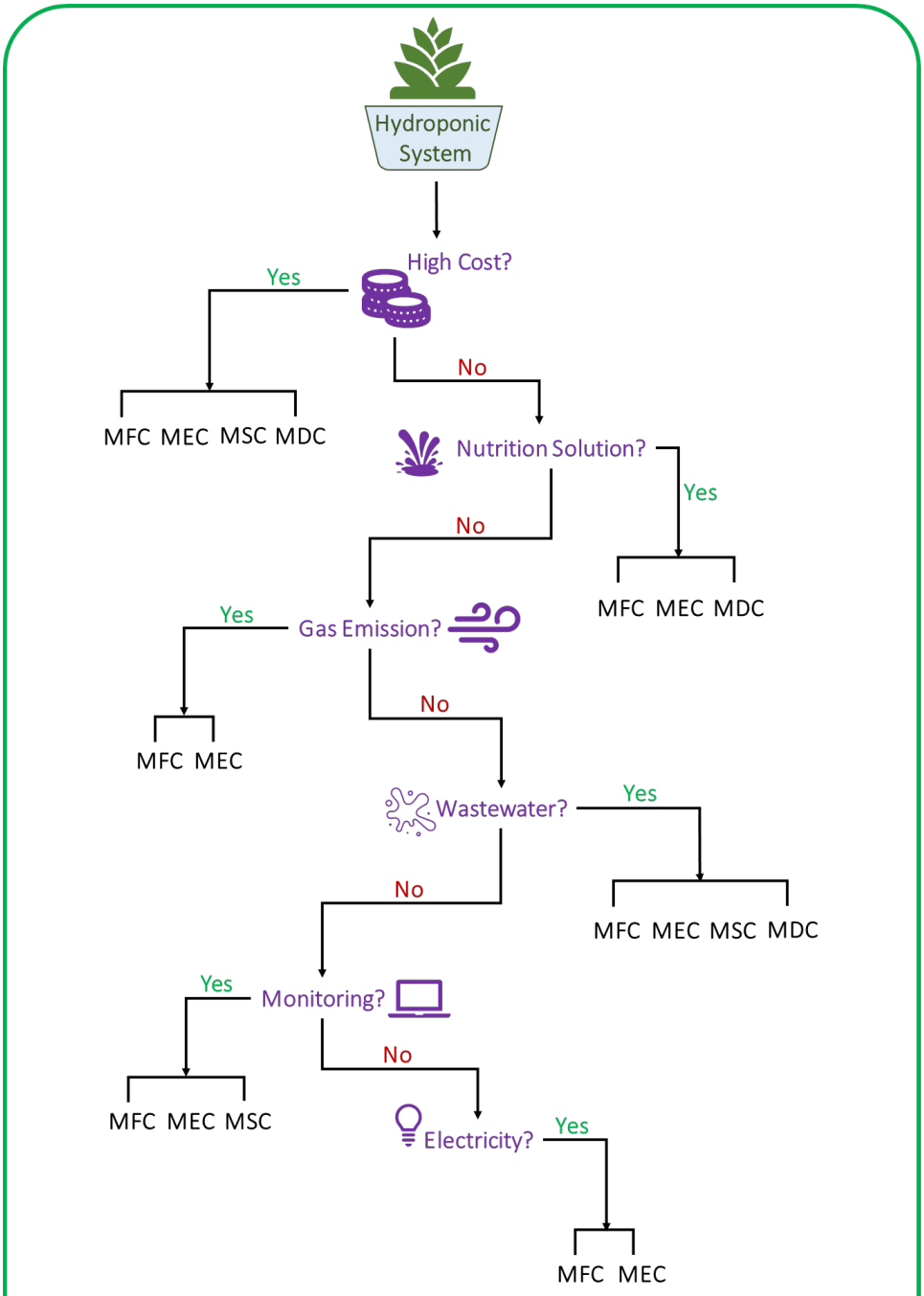

	High cost	Nutrition Solution	Gas Emission	Wastewater	Electricity
MFC	√	√	√	√	√
MEC		√		√	
MSC	√	√		√	
MDC	√	√		√	

Figure 3.6. The decision tree for use of BES in the hydroponic system.

3.7. Conclusion

This paper explores an important concept relating to the integration of BES with hydroponic systems in order to make the latter more sustainable. Although hydroponic systems have a huge potential, it is still plagued by problems such as high cost, high energy consumption, greenhouse gas emission, nutrition solution, wastewater discharge, etc. We have discussed the possibilities for alleviation of these problems through BES, which can be a valid pathway for reducing greenhouse gas emissions (at least 47-50% by PMFC), wastewater treatment (up to a maximum of 99% COD), nutrient problems (biosensor), the high energy providing to hydroponic systems (match up to traditional biomass electricity generation systems). Several configurations are postulated, and a decision tree is developed to aid future research, and for decision-makers to explore. Besides, the BES systems are more multifunctional than the traditional technologies, which could combine with various advanced technologies, save more money, space, and energy, as well be more durable. Another importance of such a system can be important for several areas of environmental concerns as well as application in outer space (or areas with poor soil quality) programs are emphasized. However, for the further commercial application some problems need to be solved, including lack of the in-depth research between the specific obstacle of hydroponic and solving mechanism of BES, the relationship between BES and hydroponic crops yield, the high initial investment, improving the monitoring precision, hard to control, and over-complicate system. Therefore, further research on the suitability and adaptation of BES-hydroponic systems at a large scale is still needed, and a lot of work is needed to develop such efficient, accurate, multifunction, and cost-saving hybrid systems.

CONNECTING TEXT

Chapter III summarized the problems in hydroponic agriculture and the potential utilization of BES to solve these problems.

Chapter IV focuses on microbial fuel cells (MFCs), a promising renewable BES. We summarized the mechanism, standard configuration, the performance, and the categories of the solid substrates (carbon source) used of of soild MFCs. Furthermore, we also introduced the applications of solid MFCs with a detailed, in-depth literature search and bibliographic analysis. Chapter IV also critically analyzed the literature of MFCs to identify gaps for further research and development in future studies.

CHAPTER IV

LITERATURE REVIEW-PART 3

SYNTHESIZING DEVELOPMENTS IN THE USAGE OF SOLID ORGANIC MATTER IN MICROBIAL FUEL CELLS: A REVIEW

4.1 ABSTRATC

Microbial Fuel Cells (MFCs) are a prominent feature in renewable and sustainability literature due to their wide range of potential uses. MFCs have found applications in power production, biosensors, and environmental remediation to mention a few. Importantly, however, one of the factors affecting the transition from laboratory to practical usage is the requirement of ensuring that there is enough organic matter supply to sustain microbial activity. To reduce this energy-intensive and human intervention-dependent requirement, there has been a shift towards solid carbon sources in recent times. These solid carbon sources enable the operation of MFCs autonomously for a long time through the slow release or replenishment of organic matter, characteristics of solids. However, significant progress is not being made due to the uncoordinated and piece-meal information scattered across the existing body of literature. In this work, the substrate categories, electrode materials, reactor configurations, and applications of solid organic matter-based MFCs (SOM-MFCs) have been overviewed comprehensively. We found that although there are a lot of work focused on advancing different aspects or application, one major problem is a lack of contextualization or normalization of results for better planning of future work. Importantly, the present review normalizes and compares the results of different studies using SOM as a substrate in MFCs. Major studies within the identified aspects or application are highlighted while focusing on trends and limitations. Furthermore, to enhance the development of future studies, recommendations for the best approach in future work were made.

Keywords: solid organic matter; microbial fuel cells; carbon source; renewable

energy.

4.2 INTRODUCTION

With the increasing demand for actions to limit climate change, alternative renewable energy research intensifies and spans several areas, comprising biomass, solar, and wind energy [254-256]. A 'Scopus' search with the keyword "renewable energy" indicates an almost 33-fold increase in the number of articles published between 1999 and 2019. Amongst many others, bio-electrochemical systems (BESs) are an emerging set of renewable technologies that appear frequently in the Scopus search. The major categories of BES include microbial fuel cells (MFCs), microbial electrolysis cells (MECs), microbial desalination cells (MDCs), and microbial electrosynthesis systems (MESs). Notably, MFCs are a subset of BES that capitalize on the ability of electroactive microorganisms to transfer electrons from the oxidation of organic carbon to a solid electrode, for the production of electricity [9]. Similar to traditional fuel cells, the distinguishing advantages of MFCs include milder operation requirements (ambient temperature, normal pressure, and neutral pH) and the virtually unlimited range of potential biofuels (sources of biodegradable organic carbon) [257].

In a functional MFC, the most essential components include an anode and a cathode, as well as the carbon source. Several previous studies outline different kinds of electrode configurations, electrode types, as well as the development and testing of new electrode types [258-260]. The carbon source is the most important component because it directly affects the overall composition of the bacterial community in the anode biofilm and the performance of the MFC (power density, coulombic efficiency, etc.) [261, 262]. Over the years, carbon substrates, especially easily degradable compounds like acetate and glucose were commonly used in MFC studies. However, with the realization that pure substrates limit practicality, recent studies have been focusing more on the usage of more unconventional carbon sources typically in the solid or semi-solid form. These solid organic matter (SOM) sources include sewage sludge, biomass, food waste, and soil. The advantages of SOM-MFCs (SOM-MFCs)

include the provision of a stable environment for the anode microorganisms without the need for frequent replacement, steady current output, rich bacterial species, and low energy consumption in substrate transport [263].

In 1911, Potter first reported that bacteria can generate electric current (between bacterial/fungal (yeast)) [264]. Twenty years later, Cohen confirmed the results of Potter and reported a voltage of 35 V and a current of 0.2 mA from a stacked bacterial fuel cell system [265]. After Habermann and Pommer [266] first harvested electrical energy from the biological fuel cell with the coarse clay (buffering properties) as solid substrate, several developments have been reported on different aspects of SOM-MFCs. Of the 845 review articles published on "microbial fuel cell" between 1962 and 2020 (Scopus data), none of these reviews focused on the SOM-MFCs category. Even popular reviews such as Pant et al. [263] and or more recent ones such as Zhang et al. [267] did not comprehensively classify organic substances in detail or properly highlight the solid organic matter category. Thus, there is a lack of synthesis of all the information on SOM-MFCs available in the literature. A category with varying keywords is shown in the mapping of **Figure 4.1**. Subsequently, this review aims to fill the identified gap related to SOM-MFCs by comprehensively reviewing available SOM-MFCs literature. Within each category, we summarize, in order or performance, keystone studies as a reference to guide future studies. We also recommend the next research steps based on the reviewed literature to guide future work.

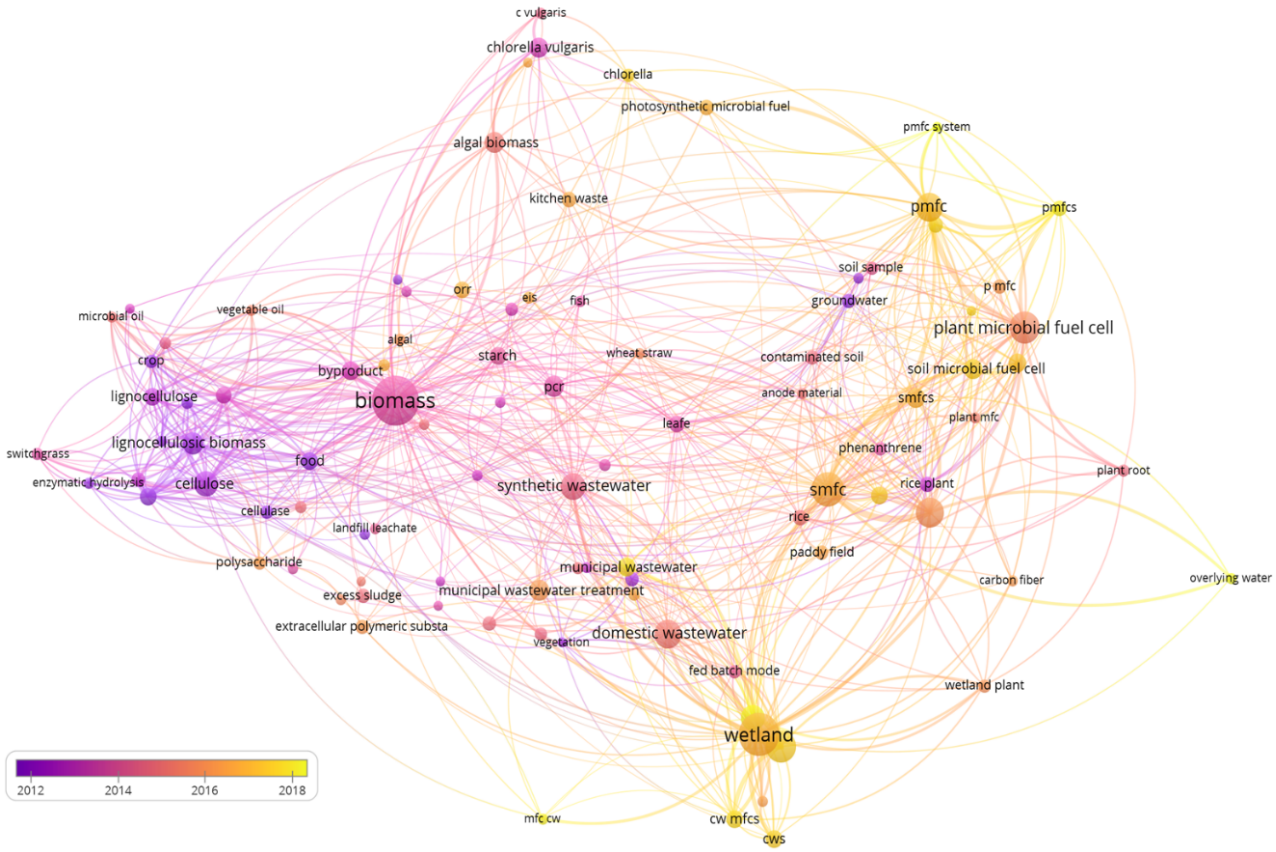

Figure 4.1. The connection between SOM-MFC articles. The data is based on the number of articles mentioning "renewable energy/MFC" in the citation database Scopus in July, 2020.

4.3 METHODOLOGY

This review utilized the bibliometric analysis method to categorize available literature and to access the development progress and challenges, within the SOM-MFC category. A bibliometric analysis is a mechanistic approach, used in several studies to understand the global research trends according to the academic literature database. All data mining for this review was extracted from numerous articles published as of July 30, 2020, from the Scopus database while excluding redundant points. Specifically, literature from 2014 to 2020 containing "microbial*fuel*cell" was performed by utilized query string TITLE-ABS-KEY (microbial AND fuel AND cell) AND (LIMIT-TO (PUBYEAR, 2020) (PUBYEAR, 2019) OR LIMIT-TO (PUBYEAR, 2018) OR LIMIT-TO (PUBYEAR, 2017) OR LIMIT-TO (PUBYEAR,

2016) OR LIMIT-TO (PUBYEAR, 2015) OR LIMIT-TO (PUBYEAR, 2014)). Scopus keywords were then extracted from the article title, abstract, keywords, or main content. To narrow the search of the SOM-MFC category, distinct keywords including “sludge”, “algae”, “lignocellulose”, “waste”, “soil”, “plant” and “wetland” were used by query string e.g. TITLE-ABS-KEY (microbial AND fuel AND cell AND sludge) AND (LIMIT-TO (DOCTYPE, "ar")).

Based on the structure of the articles and information derived from the bibliometric search and analysis, key aspects of SOM-MFC literature were identified for further discussion in this review. Within each of the categories, summary tables of representative peer-reviewed articles are presented. In particular, we carried out normalization of results when needed to enable comparison of data. The discussion is then focused on key studies (based on performance metrics such as power density, coulombic efficiency, or removal efficiency) within each category to highlight multi-perspective insights that future studies may consider. Finally, a synopsis of the microbial population was found in SOM-MFCs is presented.

4.4 DISCUSSION

4.4.1 Trend analysis

By preliminary analysis of Scopus data, we found that from a total of 5562 MFC published articles, studies within the SOM-MFC category account for 30.38% (1690), from 2014 to 2020. As shown in **Figure 4.2.(a)**, annual publications have increased steadily from 2014 to 2017 (SOM-MFC: 181 to 273, MFC: 632 to 921). Then, a slight turning point appeared in 2018, both the number of SOM-MFC and MFC articles were decreased (SOM-MFC: 241, MFC: 864). In 2019, the number of annual publications increased again, which was higher than in 2017 (SOM-MFC: 318 vs 273, MFC: 954 vs 921), until July 2020, the total number of SOM-MFC articles still showing an upward trend (221). **Figure 4.2.(b)** shown the percentage trend of SOM-MFC articles in MFC articles from 2014 to 2020. An upward trend can be seen from

2014 to 2016, while it began to decline from 2017 until the end of 2018. In 2019 and 2020, SOM-MFC publications increased in proportions exceeding the previous five years (33.37% and 33.43%, respectively). It was in 2017 and 2018 that researchers paid more attention to wastewater-based MFC (WW-MFC) than SOM-MFC (2017: 301 vs 273, 2018: 247 vs 241).

For six years, a total of 1690 SOM-MFC articles have been published, and the percentage of MFC with different types of solid carbon source substrates is shown in **Figure 4.2.(c)**. It can be noticed that the number of articles about sludge biomass-based MFC was the highest (30%), followed by natural solid-phase substrates (plant: 27%, wetland: 11%), and agricultural biomass was the lowest (lignocellulose: 2%). The upward trends of plant-based MFC (PMFC) and wetland-based MFC (CW-MFC) were particularly obvious, and the upward trends of algae, biowaste, and soil-based MFC (BW-MFC and SMFC) were slower, while the focus on lignocellulose biomass decreased (**Figure 4.2.(d)**). The surge of PMFCs in recent years could be due to their easy integration with plants which continually provide organic matter for a longer period. PMFC has a wide range of cultivation which includes paddy fields, indoor plants, even green roofs or rooftop gardens, etc. [81]. By extension, all-natural solid-phase substrates have become more attractive to researchers in recent years due to their inherent advantage of ease of operation and maintenance. This is not the case for lignocellulosic materials though, despite its abundance as lignocellulosic biomass, however, they cannot be directly utilized by microorganisms in MFCs [268, 269]. Also, no effective microorganisms for the conversion of pentoses (one of the main components in lignocellulose hydrolysates) have been found [263], leading to a general decline in publication trends.

Based on the trend analysis of the Scopus data, several key aspects of SOM-MFC literature were identified for focus in this review. These include reactor design, electrode components, substrate selection, testing, and their applications in the field.

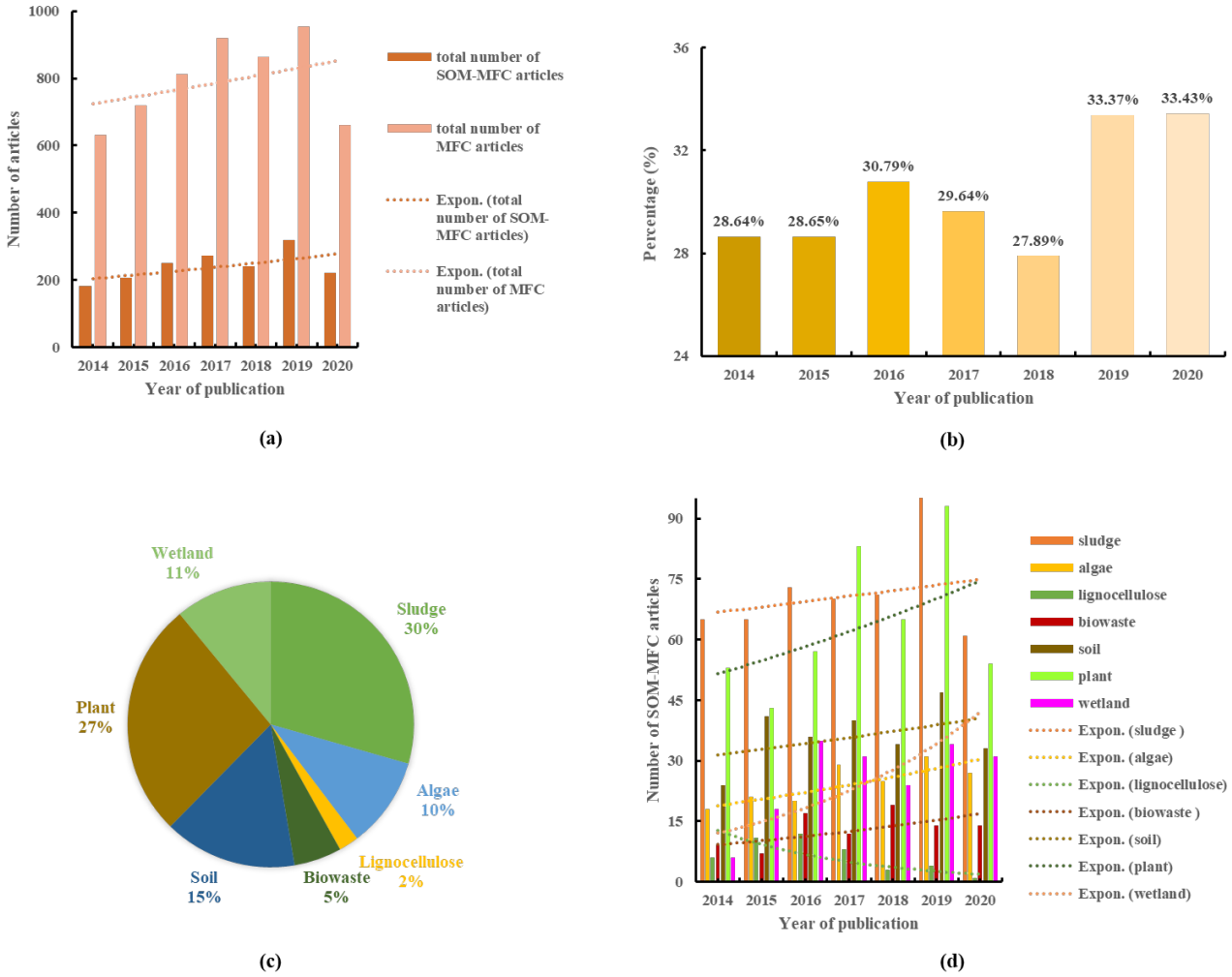

Figure 4.2. In Scopus from 2014 to 2020, the annual and the cumulative number of (a) articles on MFCs and SOM-MFCs; (b) the percentage of SOM-MFC articles in MFC articles; (c) the percentage of different types of SOM-MFCs; (d) the of research articles on different kinds of SOM-MFCs.

4.4.2 Configuration

In MFCs, organic materials are oxidized by electroactive bacteria in the anodic chamber and the electrons transfer from the anode to the cathode due to the difference in electrode potentials, which generates current [10]. In SOM-MFCs, before the electroactive microorganisms can use the SOM carbon source in the anode chamber, the macromolecules in SOM must be hydrolyzed into simple molecules [267]. Typically, SOM transformation to a carbon source suitable for electroactive microorganisms is accomplished by a consortium of hydrolyzing microorganisms in

several sequential steps involving hydrolysis, acidogenesis, and acetogenesis [267].

4.4.2.1 Chamber configurations

Figure 4.3. exhibits some digital photographs of SOM-MFC chamber configurations. There are five major design configurations used for SOM-MFC systems [270]. These configurations can be classified either based on the chamber design or flow organization: single-chambered MFC, two-chambered MFC, upflow MFC, tubular MFC, and stacked MFC. However, single-chambered and two-chambered are two main configurations of SOM-MFC (**Figure 3.4.(a)**).

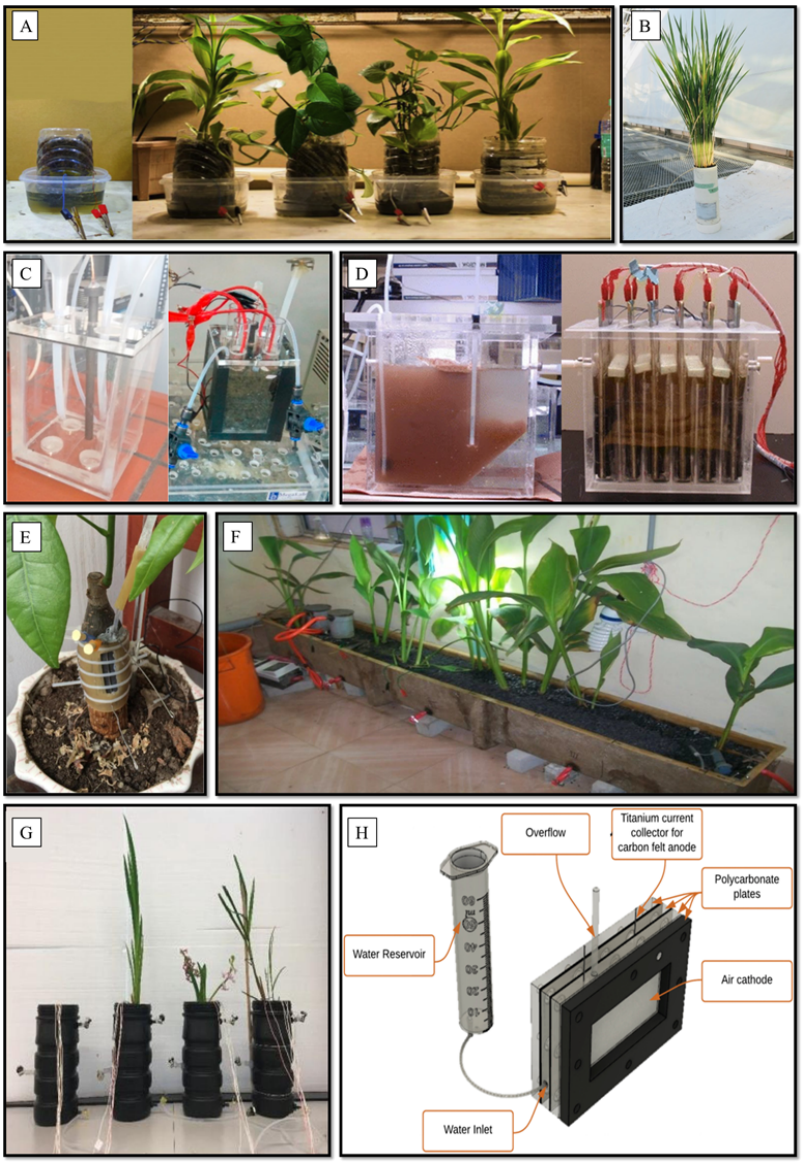

Figure 4.3. Digital photographs of SOM-MFC configurations. A) Experimental setup of PMFC [271]; B) picture of PMFC at the end of the study [27]; C) MFC compact

modular design & perforated cathode tube [272]; D) Setup MFC reactors used in the wastewater treatment experiments [273]; E) A stem-coupled PMFC with *P. macrocarpa* in the experiment [274]; F) Small Pilot-Scale HSSF-CW-MFC installed in the laboratory [275]; G) Schematic diagram of the CW-MFC configuration [276]; H) Schematic diagram of a solid anolyte MFC with an external water reservoir [277].

The cathode of single-chamber SOM-MFC is exposed to air directly, therefore, it uses oxygen as the terminal electron acceptor. The advantages of single-chambered design include low construction cost, membrane-less, low internal resistance, and avoidance of the use of catholyte. As a result, these MFCs often feature high power output [278]. However, it has several limitations: (1) Oxygen diffusion to the anode chamber, which leads to the reduction in coulombic efficiency; (2) Also, the configuration of MFC has a high influence on the distance between anode and cathode, and hence the limited distance between anode and cathode could increase the potential negative effect of oxygen on the activity of the anaerobic bacteria and the risk of the short circuit [279]; (3) Further, for the traditional single-chamber (top cathode, bottom anode), it is hard to change/check the anode electrode at any specific time. Based on the literature reviewed so far, we find that to date, the highest PD obtained in single-chambered SOM-MFC was 2770 ± 30 mW/m^2 by Catal et al. [280] who used lignocellulosic biomass as substrates in an air cathode MFC. Despite, the obvious limitation with lignocellulosic substrates, this performance may be due, in part, to an effective pretreatment process. Besides, smaller anodes were used in single-chamber MFC which could effectively reduce the limitation from the cathodes, and improvethe production of electricity.

In a two-chambered MFC configuration, the anode chamber and cathode chamber are connected by a proton exchange membrane (PEM) [281]. PEM is widely used in two-chambered SOM-MFC to separate the anode and cathode chambers. PEM features such desirable properties as selective permeability, fast transport of cations, and can withstand inactivity without deteriorating in performance [282, 283]. Two-chambered SOM-MFC has been shown to have some advantages over single-chambered designs mainly because it reduces the effect of oxygen diffusion to the

anode [284]. However, due to their complex designs, the cost of two-chambered SOM-MFC is higher than single-chambered ones, while the PD is lower due to the higher internal resistance. To date, the highest PD obtained in double-chambered SOM-MFC was 5500 mW/m^2 by Zafar et al. [285], who utilized petroleum-contaminated soil as the substrate in MFCs. As two-chamber MFC could control anode and cathode chamber in different air conditions, they used a two-chamber structure to maintain anoxic condition in the anode chamber, as well as the air cathode by an aeration pump. With the help of a two-chamber configuration, petroleum-soil can be better fermented under anaerobic conditions to provide a better growth environment for microorganisms, and the air cathode can promote the redox reaction of SOM-MFC, which results in a high PD.

Depending on the substrates, single-chambered SOM-MFCs can also have a semi-open style design as can be seen in the soil and plant MFCs [286], in which the cell does not need to have a strictly anaerobic environment. Also, some multiple-chamber SOM-MFCs have emerged to enhance multifunctionality, including improving electricity generation performance and coulombic efficiency [287].

As the chamber of MFC is the main place where microbes and carbon source substrate redox reaction, and hence its structure, volume, shape, temperature, etc. are very important. It can be seen from the above discussion that the configuration of the SOM-MFC will have a certain impact on its electricity production and overall cost. Therefore, according to the composition and texture of the SOM, it is better to design the optimal chamber structure based on the characteristics of expected results as well as the cost budget. **Figure 4.4.(a)** displays that single-chamber configuration is the most popular in SOM-MFCs, followed by a two-chamber configuration. Although the internal resistance of two-chamber MFC is generally higher, there are still some experiments that prove that two-chamber MFC can also be managed to produce lower resistance. In general, we find that the best configuration in terms of design is single-chamber, not only because of its low price, but it could utilize a wider range of organic substrates as well as the inherent easy way to its operation. Besides, the single-chamber configuration is more economical and practical. With more diverse

forms such as the semi-single chamber, experiments can be more easily adopted to actual production and gaining environmental protection (e.g. CW-MFCs, paddy soil MFCs), and hence it can be recommended for using SOM-MFCs.

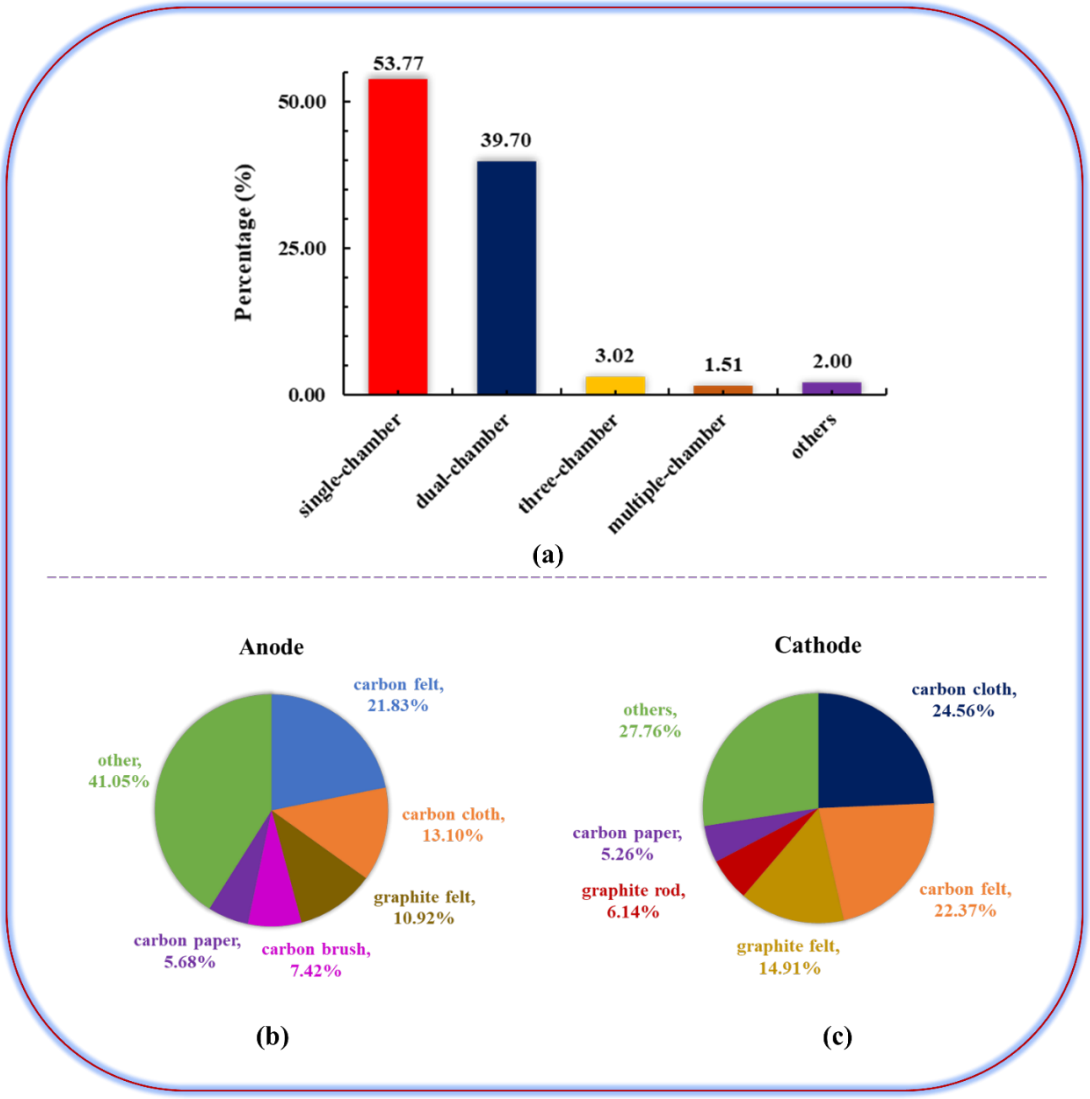

Figure 4.4 (a) SOM-MFC configurations; (b) The anode materials used in SOM-MFC; (c) the cathode materials used in SOM-MFC.

4.4.2.2 Electrode materials

4.4.2.2.1 Anode

The composition, morphology, and surface properties of materials in the anode are important for optimal performance. Considering these properties, in the available literature, the most common anode materials include carbon-cloth, graphite felt,

granular graphite, graphite-rods, carbon-brushes, carbon-paper, carbon-mesh, carbon-felt, nickel foam, and carbon granules (**Figure 4.4.b**). Carbon-cloth, carbon-brushes, and carbon-felt (**Figure 3.5.a-c**) are the most commonly used materials in SOM-MFCs. Carbon-cloth (**Figure 3.5.a**) although expensive has many advantages, including high surface area, relatively high porosity, high electrical conductivity, flexibility, and mechanical strength, etc. [178]. Carbon brushes (**Figure 3.5.b**) have the highest surface area to volume ratio and high electrical conductivity, however, the cost is high. Carbon felt (**Figure 3.5.c**) has high porosity and high electrical conductivity, which is the least expensive [288, 289]. The large pores allow bacteria to access the 3D felt structure and colonize it, forming the biofilm internally and increasing the MFC current.

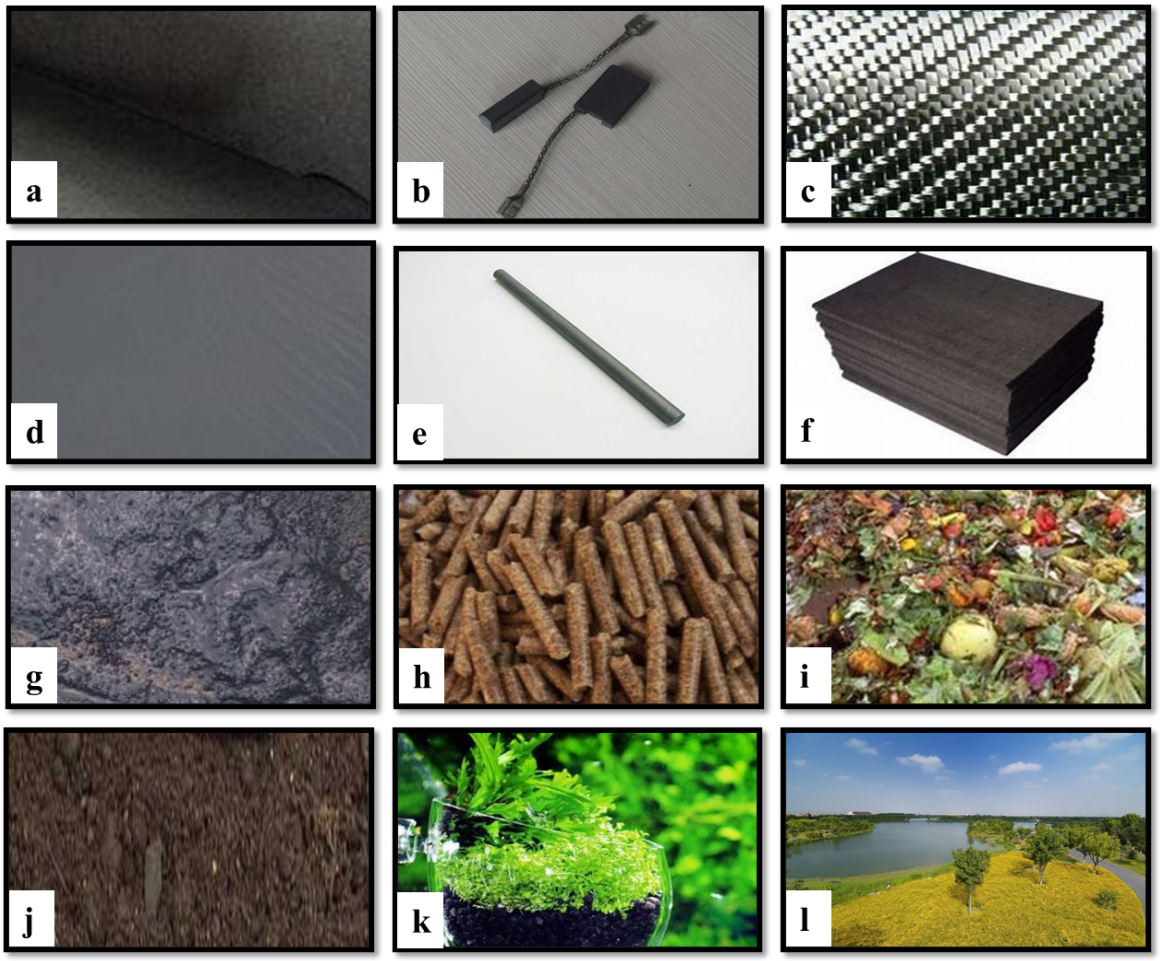

Figure 4.5. Digital photographs of SOM electrode and carbon source substrates materials, a) carbon cloth; b) carbon brush; c) carbon felt; d) carbon paper; e) graphite rod; f) graphite felt; g) sludge; h) biomass; i) biowaste; j) soil; k) plant and l) wetland.

Based on the research of Penteado et al. [290], carbon felt has the best performance in SOM-MFCs with PD of up to 420 mW/m^2, as compared to that of carbon cloth (0.76 mW/m^2) and that of carbon paper with the lowest value of PD (8.37×10^{-6} mW/m^2). The superior performance of carbon felt can be attributed to the roughness and specific area of the electrode which improve the concentration of adhered microbes on the anode electrode (the determining factor for choosing the anode electrode material). Recently, anodic modification is becoming more popular in MFCs, which is crucial in upgrading both interfacial adhesions of bacteria and electron transfer from bacteria to the electrode surface [291]. Zhao et al. [292] obtained more than 2000 mW/m^2 PD from lactate-fed MFCs with nanocomposite anodic materials (graphene oxide and stainless steel-based nanocomposites). Sonawane et al. [293] prepared a conducting polymer-coated stainless-steel wool as a low-cost anode for synthetic wastewater-fed MFCs with a PD value of 2880 mW/m^2. However, most studies on anodic modification of MFCs were driven by liquid carbon source substrates, thus researchers in the SOM-MFCs research field could pay more attention to anodic modification based on the unique characteristics of SOM source substrates, which could be more helpful for the improvement of MFC performance. Besides, anode as the platform for microorganisms to grow, the microbial adhesion ability and carbon source aggregation ability of anode materials should also be considered in anode modification research.

4.4.2.2.2 Cathode materials

The cathode material is also an important factor in MFCs for achieving the highest coulombic efficiency or power production [294]. Air-cathodes, aqueous air-cathodes, and bio-cathodes are three main cathodes in SOM-MFC, however, carbon-based materials are commonly used as cathodes due to their biocompatibility, chemical stability, high conductivity, and low cost related properties. For other materials, catalysts including oxygen reduction catalyst (Pt and Pt/C, etc.), carbon-based catalysts (carbon black, activated carbon, carbon nanofibers/nanotubes), metal-

based catalysts (Fe, Co, Ni, and MnO_x, etc.), metal-carbon hybrids (metal-activated carbon and metal CNTs, etc.) are typically used [295, 296]. Up until now, including carbon cloth, carbon felt, graphite felt, carbon paper, graphite rod, granular graphite, and graphite fiber brush are the most commonly used cathode electrode materials in SOM-MFCs (**Figure 4.5.**).

Carbon paper (**Figure 4.5.d**) is a relatively porous planar carbonaceous material which is not only fragile but also expensive [297]. Also, its performance in SOM-MFCs is limited by the planar surface, as can be seen when an algae-based MFC equipped with carbon paper cathode exhibited a lower PD compared with carbon fiber brush (4.6 mW/m^2 vs 30 mW/m^2) [298]. Graphite granules have a low surface area due to the lack of activation, but a much higher electrical conductivity, and chemical stability [299]. In a representative work carried out by Choi et al. [300] a maximum PD of sludge-based single chamber air-cathode, MFC achieved 370 mW/m^2 with the utilization of graphite rod electrodes (**Figure 4.5.e**). Nevertheless, due to the low porosity and surface area for microorganism attachment, the application of graphite rods is currently limited in MFC design. In particular, when Chaudhuri et al. [301] found out that when the graphite rod was replaced by graphite felt in mediator-less MFCs, the power output was increased threefold, indicating that a larger surface area is necessary for optimizing MFC performance. Graphite felt (**Figure 4.5.f**) is a useful porous 3-D electrode with mechanical flexibility, compressibility, reasonable electrical conductivity, and reasonable cost.

To date, when compared with other biocathode types such as those made from carbon paper, stainless steel, and graphite felt biocathode showed the highest maximum current density and PD of 350 mA/m^2 and 109.5 mW/m^2, respectively [302]. The low catalytic activity of the cathode still limits the performance of all types of MFCs. Also, traditional catalysts use is discouraged due to their unsustainability and high costs. Especially, metal-based electrocatalysts can cause scalability problems for MFC design, while it requires long time operation to generate power during full-scale applications [303, 304]. Therefore, there is a need to explore green renewable carbon materials (e.g. chitosan biopolymers) as cathode/cathode catalysts in SOM-MFCs. In

a recent study, Türker et al. [305] synthesized some smart electrocatalysts by chitosan polymer and magnetic particles, enhancing the PD of MFC 15 times (1298 mW/m^2 vs 87 mW/m^2). It can therefore be postulated that innovating cathode electrode with environment-friendly, low-cost, stable performance catalysts is a research field for SOM-MFC studies in the future.

4.4.3 Substrate categories

In SOM-MFCs, a wide range of substrates, including wastewater, sludge, food waste, can be used as the carbon source. SOMs are generated in various forms, including biomass, biowaste, and soil, etc. The most common category of SOM-MFCs utilizes sewage sludge, biomass, biowaste, and solid substrates. Importantly, compared to MFCs with pure substrates, SOMs have attracted widespread attention due to the stable external environment it provides within an MFC, and the accompanying diverse microbial community, as well as its low costs. Below we summarize the performance, limitations, and further improvements to the categories that were found in the literature.

4.4.3.1 Sludge biomass

Sludge is the semi-solid material produced in biological wastewater treatment processes. It represents up to 2% volume of treated wastewater [306] (Figure 4.5.g). Due to the large volume of sludge produced annually, recycling is often necessary [307]. Therefore, as sludge contains high concentrations of organic materials and microorganisms, it can be used as a source of organic carbon in an MFC [308]. The majority of bacteria in sludge include fermentative bacteria, sulphate reducers, and methanogens (*Methanosarcinaceae* and *Methanosaetaceae*) [309]. MFCs fed inoculum with mixed cultures, therefore, have wider substrate acceptability, can utilize more complex carbon sources, and achieve substantially greater power densities than pure cultures [310]. Also, in addition to microorganisms found in sludge, a large or smaller proportion of inorganic particles, organic fibers, extracellular

polymer substances (EPS, biopolymers, exopolymers), and ions can be found [311-313]. Therefore, due to their wide substrate acceptability inoculum from mixed cultures would be affected by changes in the concentration of the other component of the sludge.

Many sludge types have been tested in MFCs directly, including raw sludge [314], primary sludge [315], digested sludge from anaerobic digesters [316], as well as a mixture of primary sludge with primary effluent [317]. **Table 4.1.** lists all the available studies using sludge as substrate in an MFC, sorting them in order of performance of the maximum power density.

However, as can be seen in **Table 4.1.** despite the number of organic materials in the sludge, the maximum PD obtained from sewage sludge MFC (13.5 μW/m^2~2228 mW/m^2, 563.8±733.05 mW/m^2) is lower than that obtained using easily degradable organics like acetate (4~4590 mW/m^2, 1299.05±1715.95 mW/m^2). Further literature review shows that this is due to the slow hydrolysis of sludge biomass [318]. In reality, sludge biodegradability is typically limited to approximately 50-70% as a significant amount of organic materials in sludge are non-biodegradable [318]. Also, part of the hydrolyzed carbon source can be consumed by methanogenic *Archaea* [319]. Therefore, the complex composition, extremely slow hydrolysis rate, refractory organics in sewage sludge, and the bacteria-influenced pathway of choice are limiting factors. As a result of this, it is recommended, that some form of pretreatment is needed for optimal suitability of sludge in SOM-MFC. Physical, chemical, and biological pretreatment methods that have been explored to increase the dissolved organic concentration of sludge in SOM-MFC include microwave crushing [316], ultrasonication [316, 320], alkali treatment [321], ozonation treatment [314], biocathodes [322], fermentation [323], and aerobic digestion [324]. However, based on our analysis of energy requirement and pollution potential of other methods, for optimal results, biological pre-treatment is the recommended method for sludge biomass pretreatment before usage in SOM-MFCs. Examples of performance improvement based on biological methods are presented in the works of Zhang et al. [323] and Yang et al. [317] where about 90.8% of soluble chemical oxygen demand

(COD) and 82.42% of protein were released from sludge to solution by using the thermophilic bacterium pretreatment at 65 °C and PD increased from 0.87 W/m^2 to 1.03 W/m^2 after the addition of phosphate buffer to sewage sludge in an MFC. Above all, finding green and environmentally friendly pretreatment methods to increase COD release rate, reduce internal resistance, and increase electron transfer rate could be the focus of future SOM-MFC incorporating sewage sludge as the substrate.

Table 4.1. Sludge biomass-based MFCs available in the literature, sorted in order of performance of the maximum power density. **Sodium acetate shown as a comparative baseline*

Inoculum	Substrate	Pretreatment	Anode	Cathode	Density	CE	Reference
Anaerobic sludge	Sodium acetate	Starving aerobic, Aerobic fed, Starving anaerobic processing	Carbon felt	Carbon felt	4590 mW/m^2	12~14%	[325]
Fresh anodic effluent	Sewage sludge	Heating	Graphite plate	Carbon felt	2228 mW/m^2	--	[326]
Anaerobic sludge	Waste activated sludge	Thermal/alkaline pretreatment	Carbon brush	Carbon brush	1.24 W/m^2	4.8%	[327]
Sludge supernatant	Sewage sludge	Fermented	Carbon cloth	Carbon cloth	1120 mW/m^2	33.3±1.5 %	[328]
Anaerobic sludge	Anaerobic sludge	--	Graphite felt	Activated carbon	628.1 mW/m^2	19.5%	[329]
Anaerobic sludge	Effluent, raw primary sludge	--	Graphite fiber brush	Carbon cloth	370 mW/m^2	10.60%	[300]
Anaerobic sludge	Anaerobic sludge and 0.4 g graphene oxide	Cultivated for three months	Round carbon felt	Rectangular cathode carbon	214.09 mW/m^2	--	[330]

Inoculum	Substrate	Pretreatment	Anode	Cathode	Density	CE	Reference
Sediment sludge	Sewage sludge	--	Ti-TiO_2 electrode	Ti-TiO_2 electrode felt	187 mW/m^2	--	[331]
--	Waste activated sludge	Freezing/thawing (F/T) pretreatment	Glassy carbon	Platinum	183 mW/m^2	--	[332]
Anaerobic digestion sludge	Dewatered alum sludge (das)	Inoculated with anaerobic digestion sludge for three weeks	Powder activated carbon modified dewatered alum sludge	Granular graphite	87.9 mW/m^2	1.0~1.1 %	[333]
Sodium acetate	Inactivated waste activated sludge & potato with ratio of 1:2	--	Carbon felt	Carbon felt	4 mW/m^2	31.00%	[334]
Phosphate buffer solution and sodium acetate	Raw potato (5 g) and sterilized waste activated sludge (2.5 g)	The collected sludge was settled for 4 hours and then cultured by addition of glucose in the dark without aeration for one week	Carbon felt	Carbon felt	4 mW/m^2	2.30%	[335]
--	Saline sewage sludge: freshwater-	--	Carbon felt	Carbon felt	40.51±0.4 W/m^3	28.58±0.49%	[336]

Inoculum	Substrate	Pretreatment	Anode	Cathode	Density	CE	Reference
	based wastewater sludge, 1:1v/v						
--	Saline sewage sludge	--	Carbon felt	Carbon felt	34.05±1.22 W/m^3	19.91±1.07%	[336]
Mixed liquor suspended solids	Municipal sewage sludge	--	carbon cloth-graphite	a graphite rod (wrapped by carbon cloth)	27.65 W/m^3	--	[337]
--	Saline sewage sludge: deionized water, 1:1v/v	--	Carbon felt	Carbon felt	12.11±0.08 W/m^3	15.14±1.4%	[336]
--	Sludge	--	Carbon felt with iron	Carbon felt	11.93 W/m^3	--	[338]
Mesophilic anaerobic sludge	Pretreated sludge supernatant	Fenton oxidative	Carbon felt	Carbon felt	8.15 W/m^3	--	[281]
Sludge: acid(H_2SO_4) pretreatment pH of 5.3	Mixed anaerobic sludge	Acid(H_2SO_4) pretreatment pH of 5.3	A single stainless steel mesh	Graphite plates	2187 mW/m^3	4.92±0.09%	[339]
--	Freshwater-based wastewater sludge	--	Carbon felt	Carbon felt	2.03±0.01 W/m^3	2.24±0.16%	[336]

Inoculum	Substrate	Pretreatment	Anode	Cathode	Density	CE	Reference
Sludge	Diluted pretreated sludge products	Heating hydrolysis and fermentation process	Carbon cloth	Graphite carbon plate	1.05 W/m^3	--	[323]
Sludge: ultrasonic processor (120 W, 40kHz)	Mixed anaerobic sludge	Ultrasonic processor (120 W, 40kHz)	A single stainless steel mesh	Graphite plates	556 mW/m^3	2.26±0.18%	[339]
Sludge: heat at 100 °C for 15 min	Mixed anaerobic sludge	Heat at 100 °C for 15 min	A single stainless steel mesh	Graphite plates	454 mW/m^3	2.03±0.08%	[339]
Sludge: aeration using aquarium air pump for 5 min	Mixed anaerobic sludge	Aeration using aquarium air pump for 5 min	A single stainless steel mesh	Graphite plates	304 mW/m^3	1.85±0.07%	[339]
Sludge: acid(H_2SO_4) pretreatment pH of 4.0	Mixed anaerobic sludge	Acid(H_2SO_4) pretreatment pH of 4.0	A single stainless steel mesh	Graphite plates	113 mW/m^3	1.67±0.05%	[339]

4.4.3.2 Algal biomass

Algal biomass features heavily in the analyzed SOM-MFC literature. In the past, algal biomass has been mainly used to produce biofuels, methane, and hydrogen by various physical, chemical, and biological methods [340, 341]. However, due to the high level of proteins (about 30%) and carbohydrates (about 50%), both algae residue produced from water/wastewater treatment processes and dry algae biomass are being used as substrates in MFCs [225, 227].

It is interesting to note that algae can be employed in both anode and cathode chamber applications from **Figure 4.6.(a)&(b) & Table 4.2.** In the anode chamber algae, biomass could be used as the carbon source in MFC [342]. In the cathode chamber, the oxygen produced by algae during the light period can be used as an electron acceptor [342, 343]. This implies that catalysts can be replaced with the usage of algae species as explored in several studies as presented in **Table 4.2.** Recently, integrated systems that combine microalgae growth and energy production at the same time have been developed [344]. This method involves the use of algal biomass in the anodic and growth of algae in the cathodic chambers of MFCs.

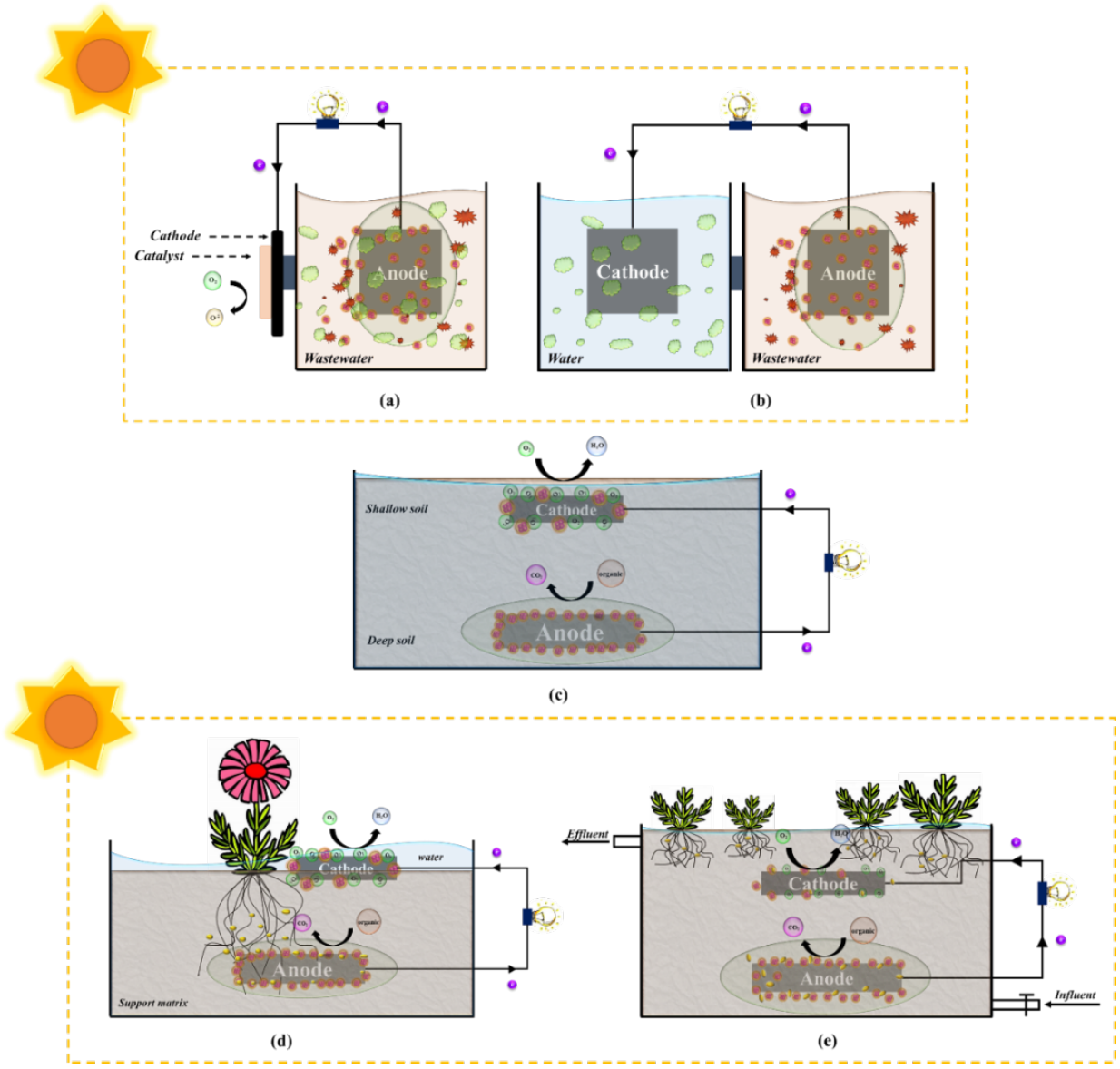

Figure 4.6. Schematic diagram of (a) cathode algae-based MFC; (b) Anode algae-

based MFC; (c) soil-based MFC; (d) plant-based MFC; (e) wetland-based MFC.

Table 4.2. Algae biomass & agricultural biomass-based MFCs available in the literature, sorted in order of performance of the maximum power density.

Biomass Species	Pretreatment	Algae used in anode/cathode	Max PD	Max Current Density	COD Removal	Reference
Lignocellulosic biomass-derived monosaccharides	--	Anode	1240±10-2770±30 mW/m^2	0.76-1.18 mA/cm^2	>80%	[280]
Chlorella regularis	Freeze dry and ultrasonic	Anode	0.86 W/m^2	2.3 A/m^2	52%	[345]
Raw algae	Raw algae combine with acetate	Anode	410 mW/m^2	0.8 A/m^2	86.6%	[346]
Synechococcus sp.	--	Anode	110.92 mW/m^2	5.169 A/m^2	--	[347]
Scenedesmus obliquus	Acid-thermal pretreatment	Anode	102 mW/m^2	276 mA/m^2	74%	[225]
Lignocellulosic raw materials (Banana peel)	Dried at 60°C and ground into 45 µm	Anode	23.75 mW/m^2	0.1928 A/m^2	--	[348]
lignocellulosic biomass (straw)	Crush barley straw into powders	Anode	0.3 mW/m^2	0.3 mA/m^3	--	[349]
Lignocellulosic	Pretreated sugarcane bagasse by Oscillatoria annae	Anode	8.78 W/m^3	20.95 A/m^3	--	[287]
Carbonized *Chlorella pyrenoidosa*	Sonicate	Anode	--	13.44±0.34 A/m^2	--	[350]
Chlorella vulgaris	--	Cathode	1926±21.4 mW/m^2	--	--	[351]
Spirulina platensis	--	Cathode	98 mW/m^2	400 mA/ m^2	60%	[352]
Spirulina platensis	--	Cathode	73.7±4.57 mW/m^2	--	30.15%	[353]
Synechococcus sp.	--	Cathode	41.5±1.2 mW/m^2	--	--	[354]
Chlorella sp. QB-102	--	Cathode	36.4 mW/m^2	--	--	[355]
Chlorella vulgaris	Freeze dry method	Cathode	8.94 mW/m^2	--	63.5%	[356]
Chlorella vulgaris	--	Cathode	5.17 W/m^3	--	--	[357]

Biomass Species	Pretreatment	Algae used in anode/cathode	Max PD	Max Current Density	COD Removal	Reference
Chlorella vulgaris	--	Cathode	3720 mW/m^3	--	--	[358]
Green alga *Golenkinia* sp. SDEC-16	--	Cathode	2.34 W/m^3	--	--	[344]
Chlorella vulgaris FACHB 24	Centrifugation	Cathode	1108.9 mW/m^3	--	--	[359]
Chlorella vulgaris		Cathode	890 mW/m^3	6186 mA/m^3	72 ± 2%	[360]
Chlorella vulgaris	--	Cathode	126 mW/m^3	--	5.47%	[361]
Scenedesmus quadricauda SDEC-8	Centrifugation	In the middle of the chamber	62.93 mW/m^2	--	80.2%	[362]
Chlorella vulgaris	Lipid extracted and stored at 82 °C then crushed	Both anode and cathode	60.07 mW/m^2	--	70.8±4%	[363]
Chlorella sp.	--		54.48 mW/m^2	--	75 ± 5%	[364]
Algae	--	Algae bioreactor connected to cathode	0.63 W/m^3	2.06 A/m^2	--	[228]

Based on the literature review, it can be deduced that the main issue with the usage of algae as a substrate relates to the complexity and strength of its cell wall, leading to a reduced coulombic efficiency suggesting the need for some pretreatment methods. Pretreatment methods such as the freeze-drying method have been shown to increase the maximum PD by as much as 4 times as demonstrated in some studies [365, 366]. Based on our analysis of the available literature, other salient issues relating to the growth time of algae, the difficult extraction process, and system scale-up, are topics that should be considered for research in future work.

4.4.3.3 Agricultural biomass

The most common agricultural biomass found in the SOM-MFC literature is

lignocellulose. Lignocellulose includes cellulose, hemicelluloses, and lignin (more than 80% of the total dry weight), is a cheap and abundant biomass material found around the world, provides a plentiful and renewable resource for fuel and chemicals [367]. Lignocellulosic materials stem from a wide range of agricultural sources, energy crops, industrial waste, and softwood, etc. [368]. However, when it is utilized as the substrate in MFCs, the microbial community of both cellulolytic and exoelectrogenic activities are required [369].

Although lignocellulose-based SOM-MFC performs relatively well (0.3~2770±30 mW/m^2), the power output from lignocellulosic materials is still lower than those obtained from pure substrates. As demonstrated in several studies [368, 370], the low solubility in water or common organic solvents, limit SOM-MFC performance. Here again, pretreatment is recommended to break the structural and chemical complexity of the lignocellulose biomass either through biological, physical, or chemical methods. Based on a review of literature, microbial hydrolysis, however, is the best method for the processing of lignocellulose biomass, as it has the highest rates of hydrolysis and simple operating conditions. Up to 100 times increase in power production was recorded in a system where biological treatment was used [287, 371]. We also find that utilizing an inoculum with hydrolytic and electroactive microbial consortia can increase the performance of lignocellulosic biomass in SOM-MFCs.

4.4.3.4 Biowastes biomass

The biowastes category refers to the various forms of food waste, garden waste, dung, etc., and are generally difficult to dispose [372]. The main components of the majority of these biowastes are cellulose, proteins, fats, starch, lipids, as well as inorganic components [373, 374] making them ideal carbon source substrates for MFCs. Based on the literature review, the best performing biowaste in MFCs are food waste, potato process wastewater, and kitchen food waste. A detailed list of the performance of different types of biowaste as the substrate in SOM-MFCs is

presented in **Table 4.3.** which shows that a wide range of waste could be used in MFCs, especially waste from food. Besides, when biohydrogen fermentation pretreatment of food waste leachate inoculum with heat-treated sludge displayed the highest maximum power density of 1540 mW/m^2 [375].

Unlike previously discussed categories, we find that the main issue with the use of biowastes in SOM-MFCs is their heterogeneity as this can impact hydrolysis dynamics. We see from the literature to overcome these limitations where most studies pretreat biowaste before usage in SOM-MFCs. Notably, the best yield pre-treating methods currently available in the literature are biohydrogen fermentation and ultra-fast hydrolyzation [375, 376]. Choi et al. [375] improved the maximum PD to 1540 mW/m^3 by using biohydrogen fermentation, which is 1.28 times higher than the acidogenic fermentation method (1205 mW/m^3) [377] in batch mode MFCs. Xin et al. [376] estimated about 74,390 tons of dry biofertilizer and 192.5 million kWh electricity could be produced from the food waste of Singapore annually by utilizing the ultra-fast hydrolyzation method for pretreating food waste. Notably, since food wastes are pervasive, it is surprising not to see large-scale applications.

Although different BW-MFCs have been developed, the large-scale application still lags. i) Higher pre-equipment costs and lower environmental awareness make biowaste based MFC difficult to promote; ii) The complex composition of biowaste require more preparatory work, and different treatment methods are needed to pretreat specific biowaste; iii) Low electricity generation with a large span from 16 to 1540 mW/m^2 (**Table 4.3.**). Emerging studies are focusing on the development of a BW-MFCs system with bioanode/biocathode, for economic feasibility and large-scale production of electricity [378, 379]. However, until now no research articles reported the way to process the residues after BW-MFC produces the power, while the residues of BW-MFC could also be a kind of biowaste. Besides, electrode corrosion is also a limited element for the long-term running of BW-MFCs, which should also be considered in future research.

Table 4.3. Biowaste biomass-based MFCs available in the literature are sorted in order of performance of the maximum power density.

Substrate	Inoculum	Pretreatment	Anode	Cathode	Max PD	Reference
Food waste leachate	Heat-treated sludge	Biohydrogen fermentation	Graphite brush	Carbon cloth	1540 mW/m^2	[375]
Food waste	Sludge	--	Carbon felt	Carbon felt	422 mW/m^2	[380]
Food waste	The solution from laboratory-scale Microbial electrolysis cell reactor	Ethanol fermentation	Graphite felt	Carbon black and polytetrafluoroethylene	379.4 mW/m^2	[381]
Food waste	Seed sludge	Enzymatic pretreatment	Carbon brush	Carbon cloth	0.173 W/m^2	[382]
Solid state based canteen waste	--	--	Non-catalyzed graphite plate	Non-catalyzed graphite plate	170.81 mW/m^2	[383]
Potato process wastewater	Anaerobic domestic sludge	--	Plain Toray carbon paper	Single-side Pt-coated electrode paper	88.6 mW/m^2	[384]
Kitchen food waste	Water	--	Carbon fiber	Carbon fiber	60 mW/m^2	[385]
Food waste	Vermicomposted organic matter	--	Carbon cloth	Carbon cloth	50.8 mW/m^2	[386]
Municipal solid waste	Granular sludeg	Pre-hydrolyzed at 120°C and 1 atm for 2 h	Sn/Cu mesh	Stainless steel spring	47.6 mW/m^2	[387]
Shochu waste	Phosphate buffered saline	--	Carbon cloth	Carbon cloth	42.9 mW/m^2	[388]
Bamboo	Water	--	Carbon fiber	Carbon fiber	40 mW/m^2	[385]
Food waste leachate	Cow dung slurry and food industry sludge	--	Carbon rod	Carbon rod	38.39 mW/m^2	[389]
Bakery waste	Anaerobic sludge	Torn into small piece	Carbon paper	Carbon paper	29.96 $mW/^2$	[390]
Household food waste	Anaerobic sludge	Extracted and filtered	Carbon fiber paper	Carbon cloth coated with Pt	29.6 mW/m^2	[391]
Food waste	Slurry	Four wastes mixed together	A brush of high-strength carbon fibers	Graphite/cement with graphite	16-27 mW/m^2	[392]
Waste-leaves litter and canteen based food waste	River sediment	--	Graphene	Graphene	17.74 mW/m^2	[393]
Organic fraction of	--	Shredded and pressed	Graphite plate	Graphite plate	1.98 mW/m^2	[394]

Substrate	Inoculum	Pretreatment	Anode	Cathode	Max PD	Reference
municipal waste					kg	
Food waste	Chlorella vulgaris	Mixed and separate the oil	Graphite	Carbon felt	19151 W/m^3	[379]
Household food waste	Anaerobic digester of the wastewater treatment plant and methanogenic sludge	--	Graphite granules	GORE-TEX cloth	7.7 W/m^3	[395]
Food waste	Anaerobic sludge	Filtered and separate the oil	Carbon cloth	Carbon cloth	5.6 W/m^3	[396]
Cassava waste	--	Fermentation and sonication	Graphite brushes	Custom 5-layer membrane	155 mW/m^3	[397]
Household waste extract	Anaerobic sludge	Fermentation	Graphite granules	GORE-TEX cloth	--	[272]

4.4.3.5 Natural solid-phase substrates

Solid organic substrates from the environment such as soil, plants, and wetland can also be utilized as a fuel in MFCs. Designed, according to the characteristics of the substrates, natural solid-phase substrates are the most sustainable type of MFCs.

4.4.3.5.1 Soil

Some of the most fascinating and interesting microorganisms live in the soil, with approximately between 2,000 and 8.3 million bacterial species per gram of soil [398] (**Figure 4.5.j**). The bacterial population and organic matter content of soil are approximately 10^9 cells/g and 100 mg/g, respectively [399]. All the different types of soil: clay, sandy, silty, peaty, chalky, and loamy have been used in whole or part of a mix in SOM-MFCs and it is the combination of the organic carbon and microbial content in the soil that mostly determines the power output in SOM-MFCs **Figure 4.6.(c)**. However, the power generation of SMFCs is around ten-fold lower than those of liquid-based MFCs (~80 mA/m^2, 1000 Ω vs ~800 mA/m^2, 1000 Ω) [400, 401], which limits their usage as a power source. In general, however, due to the importance of soil remediation, many SMFC studies are focused on the in-situ

bioremediation of refractory organic pollutants. SMFC is used to monitor pollutant toxicity and soil microbial activity, eliminate soil pollutants (phenol, petrol, and oil), and mitigate methane emissions from paddy soil and sediment [402, 403]. A detailed list of SMFCs available in the literature is shown in **Table 4.4.**

Table 4.4. Soil biomass-based MFCs available in the literature sorted in order of performance of the maximum power density.

	Anode	Cathode	Max PD (mW/m^2)	Reference
Petroleum-contaminated soil	Graphite rod	Graphite rod	5500	[192]
Soil	Carbon material	Carbon material	124.16	[404]
Paddy soil	Carbon felt	Carbon felt	123±2.2	[405]
Anaerobic soil	Graphite bars	Graphite bars	89.2	[406]
Topsoil	Carbon cloth	Carbon cloth	77.5	[407]
Sandy soil	Activated carbon	Activated carbon	70.8	[408]
Contaminated soil and anaerobic sludge	Granular activated carbon	Granular activated carbon	65.77	[409]
Mollic Gleysol	3 platinum electrodes	5 platinum electrodes	32	[410]
Saline soil	Carbon meshes	Air cathode	37	[411]
Soil	Graphite felt+bentonite-Fe	Active carbon felt	29.98	[412]
Soil with 3% straw	Circular graphite felt pads	Circular graphite felt pads	25.7	[413]
Cd-Contaminated Soil	Carbon felt	Carbon felt	22.93	[414]
Petroleum hydrocarbon contaminated soil mixed carbon fiber	Graphite rod	Actived carbon air-cathode	17.3	[415]
Soils cotaminated by polycyclic aromatic hydrocarbons	Activated carbon fiber felt	Activated carbon fiber felt	12.1	[416]
Paddy soil	Circular carbon felt	Circular carbon felt	12	[417]
Paddy soil from Changde red clay	Circular carbon felt	Circular carbon felt	10.6±0.9	[418]
Soil with Cd concentrations (98±0.5 mg/kg)	Graphite granules	Carbon felt	7.5	[419]
Vermicompost soil	Carbon cloth	Aluminium	4	[420]
Paddy soils	Carbon felt	Carbon felt	0.14-3.65	[421]

	Anode	Cathode	Max PD (mW/m^2)	Reference
5 cm soil with 3 cm water	Carbon felt	Carbon felt	0.72	[422]
Soil from Jiangsu Province	Carbon felt	Carbon paper	--	[423]
Dry soil	Carbon mesh	Activated carbon	--	[424]
20 mg/kg of metolachlor polluted soils	Carbon fiber cloth	Activated carbon air cathode	--	[425]

Based on the literature review carried out, the major factors that affect the performance of SMFCs in power generation include internal resistances, water content, dissolved oxygen, soil depth, and reactor temperature. Also electrode design or choice affects performance with graphite-based electrode proves to be optimal for SMFCs [412]. The influencing dominating factors, however, during remediation usage include the inherent characteristics of compound (hydrophilicity, polarity, molecular weight, etc.), soil conditions (soil temperature, type, moisture content, pH, salt content, etc.), microbial activity, and species.

As bioremediation usage is more practical, it was determined from the present literature that the following two factors must be critically assessed. (i) The contaminated soil's acidity/alkalinity could deteriorate electrode and catalyst materials performance especially during the long period typical of bioremediation; (ii) the relative abundance of the exoelectrogens in the microbial population since they have a direct relationship with remediation efficiency. Research on the changes of microbial communities during the operation of SMFC such as monitoring functional genes, tracking the dynamic variety of main flora, etc. is recommended.

4.4.3.5.2 Plants

PMFC converts solar energy into bioelectricity indirectly via the electrochemically active bacteria (EAB) at the rhizosphere region of their roots [18]. In general, PMFCs consist of living plants, supporting matrix (**Figure 4.5.k**), conductive anode, and cathode [18, 426]. It also can be seen as a type of biosystem, which has two structures, biocontrol, and bioprocess. In the biocontrol structure, plants convert sunlight into voltage by photosynthetic processes (**Figure 4.6.(d)**). In the bioprocess structure microbial communities use exudates to produce

electricity via microbial metabolism [18]. Therefore, PMFCs produce bioelectricity without the artificial addition of extra organic matter or nutrients due to the photosynthetic processes [19]. Since 2008, when the feasibility of bioelectricity from PMFC was first reported [16, 28], many studies with different plant species in PMFCs have been carried out (**Table 4.5.**).

Photosynthesis, the intensity and quality of light, rhizodeposits production and availability, rhizobia microbial species, growth medium, operation conditions, transport of compounds to the root, the absorption of exudates by bacteria, the reactor configuration, and oxygen reduction are the major parameters observed to influence the performance of PMFCs. Notably, as evident in literature, the rate of photosynthesis, amount of rhizodeposition, and energy recovery are the most important parameters that improve the current and power densities of PMFC. Photosynthetic routes were observed to play an important role in the energy efficiency of PMFCs with C4 plants, which convert CO_2 into 4-carbon compounds, having the best performance, perhaps due to their superior growth rates, photosynthetic efficiency and rhizodeposition. The supporting matrix also plays an important role in PMFCs since this affects the internal resistance between the electrodes and the diffusion of root exudates to the anode. The supporting matrices used so far in PMFCs include soils, paddy, wetland, sediments, etc. Wetlands and CW-MFC, depicted in **Figure 4.5.l & Figure 4.6.(e)**, are one of the most important supporting matrix commonly used for the construction of PMFCs because of their several properties such as water tolerance, presence of aerenchyma tissues, and easy surface to root O_2 transport [427]. Coupling CW to MFCs has several advantages, including methane emission reduction, contaminant removal, and are commonly referred to as the reactors of landscape integration [428-430]. The direction of influent flow and the depth of the wetland are the most critical factors affecting performance [431]. The first CW-MFC was reported by Yadav et al. [432]. Since then, several CW-MFCs designs, including vertical flow subsurface system [433], horizontal subsurface flow system [433], and surface flow system with floating macrophytes [434] have been developed and tested. CW-MFCs have also demonstrated high efficiencies in the elimination of contaminants such as nitrogen and phosphorus [435].

Low PD remains to be the main challenge of PMFCs, therefore, future studies need to focus on performance optimization. This may involve improving MFC design (configuration

and electrode modification), selection of unique plant species with larger rhizodeposits, use of genetic isolation, and engineering technology to modify the EAB strains for more efficient bioelectricity generation. Since PMFC, sediment-based MFC, and CW-MFC have many similarities in principle, so many optimizations and strategies can be replicated in both groups. Furthermore, it was observed that as the reactor volume of the PMFC increased, the power density decreased significantly. Thus, novel methods are needed to improve the ratio of electrode area or decrease the electrode spacing, as well as maintaining the anode environment to improve the power generation efficiency of CW-MFCs. Other suggested optimization strategies include the inclusion of a filter to remove suspended solids to offer the anode a higher ratio of soluble COD, increasing the salinity to achieve a low internal ohmic resistance to improve the electricity generation [436]. It is also recommended that the syntrophic relationship between fermentative and electrophilic bacteria observed in several PMFCs studies be further investigated.

Table 4.5. Plant-based MFCs available in the literature sorted in order of performance of the type of MFCs maximum power density.

Plant Species	Type of PMFC	Substrates	Maximum PD	Anode	Cathode	Operation Period	Reference
Lemna gibba L	PMFC	Anaerobic wetland sediment	1298 mW/m^2	Graphite	Stainless steel mesh	10 Days	[305]
Salt water grass species (*Spartina anglica*)	PMFC	Aerobic wastewater	679 mW/m^2	Three layers graphite felt	Biological oxygen reducing cathode	151 Days	[437]
Canna stuttgart	PMFC	Soil and compost (1:1)	222.54 mW/m^2	Brush	Carbon cloth	30 Days	[438]
Salt marsh grass (*Sporobolasadabicus*)	PMFC	Soil	120 mW/m^2	Graphite	Graphite	8 weeks	[439]
Puccinella distans (weeping alkaligrass)	PMFC	Potting mix	83.7 mW/m^2	Carbon felt	Manganese-based catalyzed carbon	114 Days	[440]
Trigonella foenum-graecum	PMFC	Soil and compost (1:1)	80.26 mW/m^2	Brush	Carbon cloth	30 Days	[438]
Brassica juncea	PMFC	Soil and compost (1:1)	69.32 mW/m^2	Brush	Carbon cloth	30 Days	[438]
Vetiver	PMFC	Manure mixed with soil	68 mW/m^2	Graphite fiber	Graphite wire	4.5 months	[244]
Rice plant (*Oryza sativa* ssp. Indica)	PMFC	Graphite granules and vermiculite	61.72 mW/m^2	Graphite felt with carbon rod	Graphite felt interwoven with carbon rod	100 Days	[24]
Rice plants (*Oryza sativa L.*)	PMFC	Sandy loam soil	41.41 mW/m^2	Carbon felt anode	Manganese-based catalyzed carbon	125 Days	[27]
Milano-Nosedo plant	PMFC	Wastewater	15.5 mW/m^2	Carbon cloth	Carbon cloth	>6 months	[441]
Epipremnum aureum	PMFC	Cow dung and garden soil	15.38 mWm^2	Carbon fiber brush	Carbon fiber cloth	60 Days	[271]
Dracaena braunii	PMFC	Cow dung and garden soil	12.78 mW/m^2	Carbon fiber brush	Carbon fiber cloth	60 Days	[271]
Populus alba	PMFC	Glucose solutions	7.61 mW/m^2	Membrane electrode	Membrane electrode	40 Days	[274]

Plant Species	Type of PMFC	Substrates	Maximum PD	Anode	Cathode	Operation Period	Reference
Rice plant (*Oryza sativa L. var. japonica*)	PMFC	Soil	7.3 mW/m^2	Graphite felt	Polyethylene	53 Days	[442]
Plant	CW-MFC	Anaerobic digestion sludge	87.79 mW/m^2	Powder activate carbon modified dewatered alum sludge	Granular graphite	4 months	[333]
Ipomoea aquatic	CW-MFC	Anaerobic sludge and untrient	55.05 mW/m^2	Granular activated carbon	Carbon cloth, granular activated carbon and stainless mash	70 Days	[443]
Pilot plant	CW-MFC	The effluent of a hydrolytic upflow sludge blanket reactor	36 mW/m^2	Graphite rods	Graphite rods	2.5 years	[444]
Typha latifolia L.	CW-MFC	Activated sludge	25.78 mW/m^2	Graphite	Graphite	90 Days	[445]
Iris pseudacorus	CW-MFC	Dewatered alum sludges	25.14 mW/m^2	Graphite gravel	Graphite gravel	94 Days	[276]
Scirpus validus	CW-MFC	Wastewater	19.5 mW/m^2	Graphite felt	Graphite felt	--	[446]
Iris tectorum	CW-MFC	Mixture of activated sludge and activated carbon with a ratio at 1:1.1	7.432 mW/m^2	Titanium mesh	Titanium mesh	45 Days	[447]
Cyanobacteria_norank	CW-MFC	Activated sludge and cellulose	6.09 mW/m^2	High purity graphite boards	High purity graphite boards	--	[448]
Cannas indica	CW-MFC	Activated sludge	4.21 mW/m^2	Graphite felt	Graphite felt	75 Days	[449]
Typha latifolia	CW-MFC	Gravels	1.58 mW/m^2	Carbon felt	Carbon felt	--	[450]
Common reed (*phragmites australis*)	CW-MFC	Dewatered alum sludge and swine wastewater	0.268 mW/m^2	Granular graphite and graphite rod	Granular graphite and graphite rod	90 Days	[451]
Plant	CW-MFC	Spartina anglica salt marsh	2.9 W/m^3	Graphite felt	Graphite felt	200 Days	[452]

Plant Species	Type of PMFC	Substrates	Maximum PD	Anode	Cathode	Operation Period	Reference
Ipomoea aquatica	CW-MFC	--	0.4964 W/m^3	Stainless-steel wire mesh	Carbon felt	62 Days	[453]
No	CW-MFC	Activated sludge	458.2 mW/m^2	Granular activated carbon	Granular activated carbon	2 Days	[454]
Canna indica	CW-MFC	Mixed anaerobic sludge	258.78 mW/m^3	Carbon felt	Carbon felt	--	[455]
Cyperus alternifolius	CW-MFC	Sodium acetate	0.27 W/m^3	Granular active carbon	Stainless steel wire mesh	3 Days	[198]
Waterweed (*Elodea nuttallii*)	CW-MFC	Mixed culture sludge	184.8±7.5 mW/m^3	Activated carbon	Activated carbon	276 Days	[456]
Eichhornia crassipes	CW-MFC	Wastewater	45.46 ± 3.83 mW/m^3	Activated carbon	Activated carbon	29 Days	[457]
--	CW-MFC	--	30.85 mW/m^3	Graphite rod	Granular graphite	--	[458]
Canna indica	CW-MFC	Synthetic wastewater	11.67 mW/m^3	Graphite gravels	Graphite rod	3 months	[275]
Common reed (*Phragmites australis*)	CW-MFC	Anaerobic sludge	0.15 mW/m^3	Granular activated carbon	Granular activated carbon	3 months	[459]
Phragmites australis	CW-MFC	Municipal wastewater	<0.001 mW/m^3	--	--	6 Months	[460]

4.5 Applications besides bioelectricity production

In general, the common other applications of SOM-MFCs are presented below. Three broad categories: wastewater treatment, remediation, and biosensing were identified in this literature review. Based on an analysis of performance within the context of the application, top studies within each category are presented below.

4.5.1 Wastewater treatment

SOM-MFCs with different types of substrates, as discussed in the previous section, have been employed in the treatment of diverse wastewaters. Cheng et al.[461] used aerobic granular sludge SOM-MFC to treat epoxy reactive diluent wastewater and domestic wastewater. The COD removal and maximum power densities were 77.8% and 63.6%, 408±26 mW/m^2 and 404±4 mW/m^2, respectively. Nguyen et al. [462] treated landfill leachate in algae cathode SOM-MFCs, with a removal efficiency of 97%. Besides, PMFC has been shown to remove up to 100 % COD, 40 % nitrate, and 91% ammonium as shown by Oon et al. [463]. Recent studies utilize multiple anodic chambers to improve the wastewater treatment performance of SOM-MFCs. Yang et al.[344] utilized four photosynthetic MFC units, to achieve a 98 % ammonium removal efficiency.

4.5.2 Remediation

The application of SOM-MFCs in the remediation of contaminated soil has attracted considerable attention in recent times. Yu et al. [416] constructed an SMFC system to remediate polycycle aromatic hydrocarbons polluted soils, with the removal rates of anthracene, phenanthrene, and pyrene at 54.2±2.7%, 42.6±1.9%, and 27.0±2.1%, respectively. Li et al. [464] showed that the remediation performance of SMFC could be improved with an increase in organic matter content, with an increase in total petroleum hydrocarbon degradation rate by 200% in one study. SOM-MFC systems can also be used to remediate heavy metals [465] due to the presence of electrotrophs (microorganisms that can take up electrons directly from the cathode in a microbial electrolysis cell [466]) which contribute to

the heavy metals reduction process [467]. In SMFCs, Habibul et al. [419] reported the removal efficiencies of Cd ad Pb at 31 % and 44.1%, respectively, while Gustave et al. [468] found that the total As concentrations decreased by 53.4%. As noted, the use of SOM-MFCs as a remediation technology is promising, especially with its ability to achieve accelerated decontamination, self-sustained operation, and lower costs.

4.5.3 Biosensing

SOM-MFCs are also used as biosensors for detecting the presence of several compounds [469]. The traditional biosensors are attached to physical transducers to convert their output into an electrical signal, however, MFC biosensors do not need transducers [210]. SOM-MFC biosensors are widely studied for use in monitoring biological oxygen demand (BOD), COD, and toxicants [210-212]. Non-traditional biosensing approaches based on SOM-MFCs are also emerging. Tapia et al. [470] firstly exhibited a low-cost PMFC biosensor to test the relationship between water content and power production of green roofs, which displayed that PMFC biosensor which could be a suitable and more sustainable alternative for monitoring water content in green roofs in semiarid climates. Then in an innovative study in 2018, Yoon et al. [471] built a PMFC technique to monitor plant health, as a facile, cost-effective, and rapid monitoring method, which utilized the reducing action of plant exudates on electrochemically active bacteria (EAB) in the rhizosphere as the basis of the method. Jia et al. [472] explored a hybrid system integrating MFC-based biosensors with upflow anaerobic sludge blanket (UASB) to investigate the internal operation of the UASB reactor, which exhibited a better signal feedback sensitivity and reproducibility when COD concentration changed.

In general, the use of SOM-MFC as biosensors is very limited due to several challenges, including relatively expensive cathode catalysts, the low current generation, and long response time, complex structure and bulkiness, etc.

4.6 MICROBIAL POPULATIONS IN SOM-MFCS

Several populations of microorganisms can be found in different SOM-MFCs, indicating

that a great number of bacterial species can adapt to these types of substrates. Few monoculture strains have been shown to generate PD as high as mixed cultures but mixed communities are the best performing to date leading to PD as high as 6.9 W per m^2 in a study [473]. It can be said that because SOM already contains a rich mixed flora, there is no need for rigorous inoculation. However, inoculation can change the microbial community composition at the anode, although other factors such as cathode types and operational procedures may affect the microbial communities [474]. From the literature reviewed, microorganisms such as *Proteobacteria*, *Bacteroidetes*, *Firmicutes*, *Chloroflex sp.* and *Geobacter* were dominant in SOM-MFCs inoculated with the widely used activated sludge/anaerobic sludge inoculums [267]. **Figure 4.7.** shows the distribution of dominant microbial populations in the papers reviewed in this study. *Bacteroides* and *Proteobacteria* are the two most abundant bacteria, following by *Firmicutes*, *Chloroflex* sp., and *Geobacter*. It is interesting to find that *Bacteroides* and *Proteobacteria* are both Gram-negative bacteria, and most of these microorgrams are anaerobic bacteria or facultative aerobes. Thus, maybe anaerobic pretreatment of SOM-MFC is very helpful for the performance improvement of SOM-MFC.

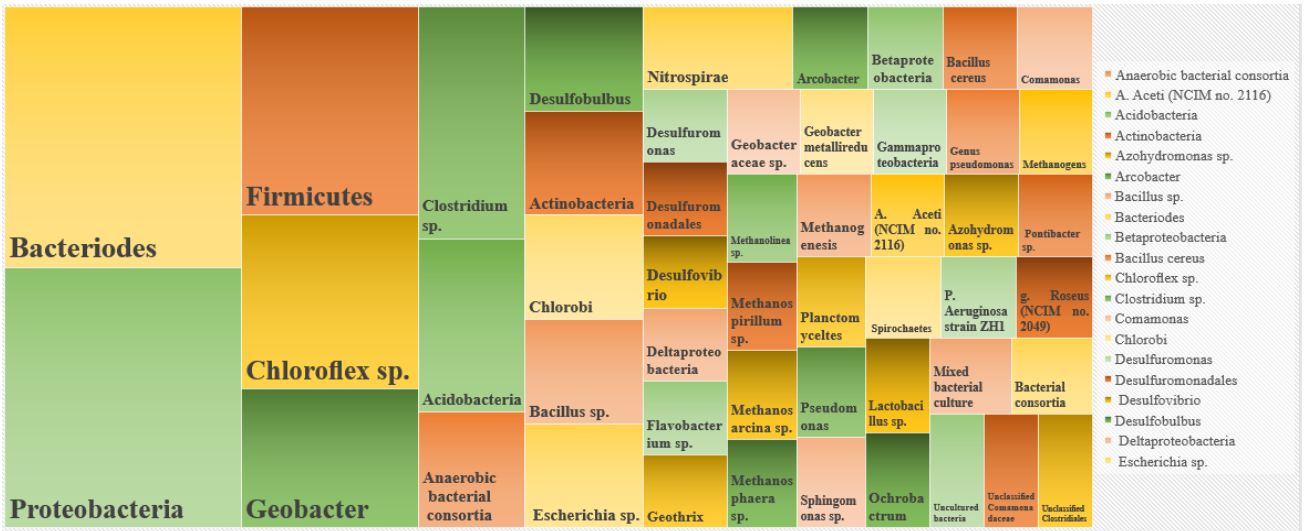

Figure 4.7. The bacterial species in SOM-MFC [281, 287, 323, 326, 328, 334, 335, 381, 388, 418, 425, 461, 475-482].

4.7 CHALLENGES AND FUTURE POTENTIAL OF SOM-MFCS

4.7.1 Challenges and possible solutions

In the development of renewable energy sources, despite the limitations of SOM-MFCs, due to the naturally low carbon source release rate and subsequent slower redox reactions, they still have a key role to play in the realization of the potential contribution of bio-electrochemical systems. This review provided a detailed overview of developments in SOM-MFCs and highlights insightful areas for further research within each category. Most importantly, as pointed out in this review, several limitations are inherent. In summary, the seven main limitations of SOM-MFCs apparent from this review include:

(a) Low coulombic efficiency;

(b) High mass transfer resistance but low mass transfer rate;

(c) High internal resistance;

(d) Low biodegradation/hydrolysis rate of SOM carbon source substrates;

(e) Slow microbial reactions at low temperature;

(f) Potential for biofouling;

(g) High cost of cation exchange membranes;

(k) Lack of uniform normalization parameters to compare different work results.

Based on our analysis of the papers covered in this review, future studies can generally improve the performance of SOM- MFCs by considering:

(a) The design, improvement, and stabilization of the energy harvesting systems in SOM-MFCs are important. Optimization of the choice of electrode materials and MFC design configurations - for example, usage of low cost, high-performance electrodes, catalysts and exchange membranes, larger anodic or stacked compartments;

(b) Development of new and efficient pretreatment methods of SOM carbon source substrates;

(c) Further optimization of SOM-MFC carbon source substrates to improve mass transport. Researchers should especially pay attention to their choice of carbon source substrate (should pretreatment be needed) while exploring several types of carbon source substrates;

(d) A combination with other electrochemical technologies (e.g. MEC, hydrogen-powered

fuel cell) to develop multi-functional and large-scale SOM-MFCs. Beyond laboratory tests, more SOM-MFC studies need to be designed to examine integration with other emerging fields to make the most impact. For example, SOM-MFC integration with other Internet of Things (IoT), Artificial Intelligence tools as well as agriculture especially towards methane reduction are viable approaches that can have an immediate impact;

(e) Genetic engineering of microorganisms found in SOM-MFCs to improve transfer efficiency;

(f) All research articles have their own result parameters, such as voltage density, power density and current density according to unit volume or anode surface. Thus, the absolute power density data and normalized data should be provided in research articles to make readers understand more accurately and make it possible to compare different work.

4.7.2 Future potential and conclusion

Since SOM-MFCs can last for several years due to their slow-release, producing an analog electrical signal without any input of external/additional energy, they can be used in many environments. This effectively means that SOM-MFCs can have multiple practical applications in the future such as powering small electronics as a power supply for a biosensor in the field, as part of a group of more complex and multifunctional SOM-MFC sensors, and a combination with other forms of renewable energy generation, including solar power in highly forested areas. Furthermore, as electroactive microorganisms found in SOM-MFCs utilize the same carbon source substrates used by methanogenic organisms in many cases (particularly in low carbon source substrate concentrations and low temperatures under 20 °C) the rate and production of methane can be regulated by integrating SOM-MFC components. Such an approach could mean infusion with methanogenic digesters (which were already adapted in wide commercial applications) or use in controlling methane emission from plants. SOM-MFC could also be incorporated with methanogenic anaerobic digestion technology to expand its scale, improve its efficiency and application in the future. Innovative ideas such as incorporating disinfectant properties into SOM-MFC that digest household wastes are examples of future applications that may help improve sanitation in

some countries and regions, especially in the developing world.

Overall, based on the findings in this review, it can be concluded that SOM-MFCs are promising avenues for achieving the potential of bio-electrochemical systems, although several optimization efforts, as well as more studies focused on practical utilization, are needed.

CONNECTING TEXT

From the literature review in Chapter II-IV, MFC, as one of the main BES technologies, has the huge potential to combine with hydroponic technology to solve the problems in hydroponic cultivation agriculture. However, rare studies report applying the H-PMFC system in rice CH_4 control field. Besides, for the MFC configuration, the anode and cathode electrodes have a crucial influence on the performance of MFC systems. Especially the cathode reactions have a more severe impact on the MFC performances for bioelectric generation due to the irreversible responses and processes. Also, the cathode accounts for the central part of high cost and low power density problems due to its components' high value and slow oxygen reduction kinetics at a neutral medium. Therefore, it is particularly important to choose suitable electrodes.

In Chapter V, to have the best performance of the H-PMFC system, a continuous flow solution single-chamber MFC with an air-floating cathode was designed. Carbon cloth and carbon felt as anode materials in continuous flow solution single-chamber MFC were evaluated. Furthermore, effective and economical 3D floating air-cathodes were developed using a simple dip-drying method.

CHAPTER V

EFFECTIVE AND ECONOMICAL 3D CARBON SPONGE WITH CARBON NANOPARTICLES AS FLOATING AIR-CATHODE FOR SUSTAINABLE ELECTRICITY PRODUCTION IN MICROBIAL FUEL CELLS

5.1. ABSTRACT

The effective and economical three-dimensional (3D) floating air-cathodes were fabricated by a simple dip-drying method with carbon black (CB), ethanol, and PTFE solution. Pristine Type-I polyurethane sponge (5 pores/mm) and Pristine Type-II polyurethane sponge (3 pores/mm) were used as the support. The deposition of CB on the Pristine Type-I and Pristine Type-II materials was detected by scanning electron microscopy and Fourier transform infrared spectroscopy. The carbon loss rate test exhibited good CB adhesive stability on both air-floating cathodes. Besides, Type-I/CB floating air-cathode displayed 3.7 times higher tensile strength, 10.58 times higher elongation at break, and 3.3 times lower cost than carbon felt. The electricity production ability of carbon cloth (CC) anode with carbon felt (CF), Type-I/CB, and Type-II/CB cathode microbial fuel cells (CC-CF-MFC, CC-I-MFC, and CC-II-MFC) were evaluated. After 130 days, the CC-I-MFC showed a maximum PD of 92.58 mW/m^3, which was 4.6 times higher than the CC-CF-MFC. Compared with Type-II/CB, Type-I/CB cathode improved the maximum power density by 160% due to the smaller pores, rougher surface, and higher surface wettability. Further, CC-I-MFC exhibited the best overall oxidation-reduction performance and chemical oxygen demand removal efficiency. Consequently, Type-I/CB floating air-cathode opens a new opportunity for scaling up simple, inexpensive, and high-performance MFCs for

energy production.

Keywords: Economic cathode; electricity production; microbial fuel cell; three-dimensional floating air-cathode

5.2. INTRODUCTION

Along with the increased human population, industrialization, rapid urbanization, and increasing energy crisis, all have a huge impact on environmental pollution. Therefore, it is necessary to resolve the energy crisis and environmental pollution problems. There are three main energy sources, fossil fuels, nuclear and renewable [483, 484]. Fossil fuels and nuclear are non-renewable sources that harm human health or the environment [485, 486]. Fossil fuels as a traditional energy source have severe influence on human life due to their drastic aftermaths, such as heating pollution, atmospheric pollution (e.g., CO, SO_2, ash, etc.), and global warming [487]. In recent years, interest has grown in using environmentally and economically sustainable renewable energy systems [488, 489]. Extracting energy from organic/inorganic wastes is an alternative potential way to address both energy and environmental issues.

Microbial fuel cells (MFCs) have attracted more researchers these years due to their combustion-less, pollution-free, bioenergy generation with the degradation ability of residual biomass in wastewater [194, 490, 491]. The essential components of a functional MFC include carbon sources, anode, and cathode electrodes. Typically, the anode draws much attention to the exploration and investigation of the exoelectrogenic bacteria that grow in the anode chamber, and the cathode is usually neglected [492]. However, due to the irreversible reactions and processes, cathode reactions severely impact the MFC performances for a bioelectric generation [294]. Besides, the cathode accounts for the central part of high cost and low power density (PD) problems due to the high value of its materials and slow kinetics of oxygen reduction at a neutral medium [493]. The air-cathode is a sustainable advanced design that can substantially decrease operational costs by supplying oxygen through passive air diffusion [494]. One most desirable structures of the cathode material is an open three-dimensional (3D) microporous structure, which enables internal colonization and substrate efficient transportation [495]. The advantages of 3D microporous materials include high specific surface area, stable chemical characteristics, and good biocompatibility [495, 496]. The ideal 3D electrode should have a porous

interconnected framework, a thin layer coating of electroactive materials, and a self-supported structure free of organic binder [497]. Sponge, an inexpensive material, has a typical continuous 3D microporous surface and is virtually no interrupting junctions, which facilitates biofilm attachment and internal microbial growth [498]. Besides, the sponge can be made into any shape to fit the various sizes of MFCs. Therefore, it could be easier to use conductive materials with continuous skin to sponges [495] and has been used as the anode electrode in MFCs [498-500]. In comparison with fixed cathode electrodes, the floating cathode is more flexible to fit various water volumes, e.g., wetland, ocean, hydroponic, greenhouse, etc. Due to the typical structure of a floating cathode, floating MFC has unique advantages in water monitoring. Massaglia et al. [21] reported that the marine floating MFC could work as portable power supply for sensors. Furthermore, the risk of oxygen limitation at the cathode is eliminated with a floating design especially in natural settings where MFCs integration have been explored. This work was designed to contribute to that practical feasibility, hence the design choice. MFCs could benefit from using floating cathodes that have direct contact with air, leading to increased performance [501]. Despite sponge materials being used as electrode materials in MFCs, previous studies only focused on the anode of MFCs. As far as we know, there are few research reports on using sponge materials as cathode electrodes in MFCs [495, 502]. However, the MFC configurations are usually complicated, expensive, and whether the pore size of carbon black coated sponge cathode influences the MFC efficiency has rarely been reported.

Due to the influence of covid-19, it is also hard to get traditional cathode materials online these years. Therefore, in this study, we simplified the cathode fabricate processing. Two kinds of 3D sponges (Type-I and Type-II) based on floating air-cathode without any additional metal catalysts were manufactured using commercial sponges by simple dipping drying methods. To determine the most cost-effective and highest efficient cathode electrode material in MFCs, the influence of the cathode pore size was tested. The 3D floating air-cathodes and traditional electrode carbon felt (CF) were characterized by scanning electron microscopy (SEM), Fourier transforms infrared (FTIR) spectroscopy, thermogravimetric analysis (TGA),

mechanical property analysis, water contact angle (WCA), carbon loss rate, cyclic voltammogram (CV), voltage, PD, as well as chemical oxygen demand (COD).

5.3. MATERIALS AND METHODS

The research was performed for 130 days in the Post-Harvest Engineering Laboratory, McGill University (Sainte-Anne-de-Bellevue, Québec, Canada).

5.3.1 Anode electrode

Carbon cloth anode carbon felt cathode microbial fuel cell (CC-CF-MFC) and carbon felt anode and carbon felt cathode microbial fuel cell (CF-CF-MFC) were designed to choose the best performance of anode electrode material. According to the power density (PD) result in **Figure 5.1.** Before day 40 CF-CF-MFC exhibits higher PD than CC-CF-MFC, however after day 40 CC-CF-MFC shows the higher PD than CF-CF-MFC until day 100. Generally, the rice plant growth cycle is more than 40 days [503]. Thus, we chosen CC as the anode electrode.

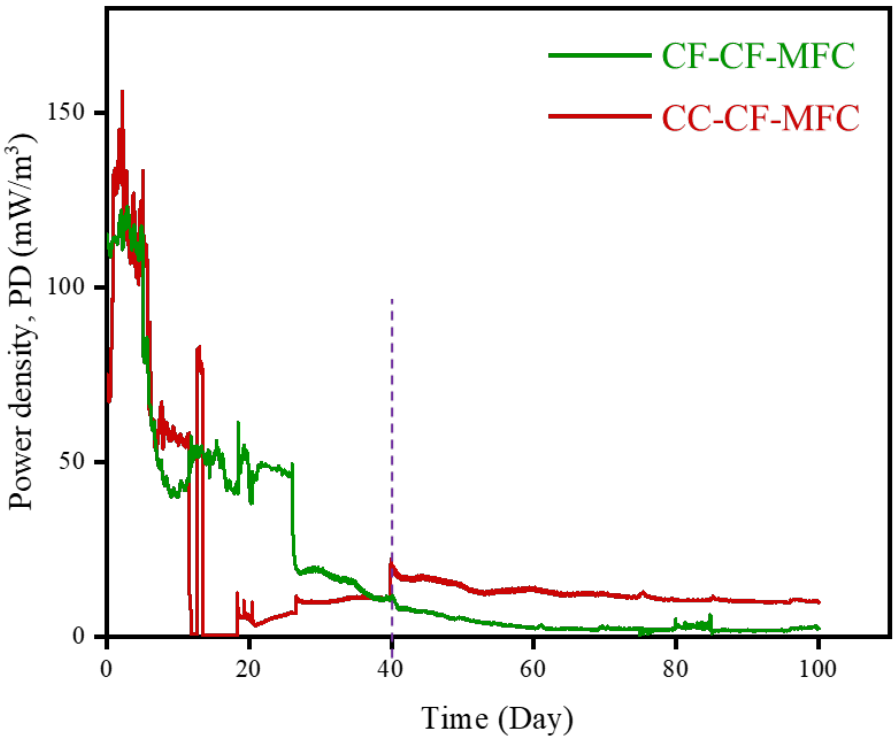

Figure 5.1. Changes in power density in CF-CF-MFC, CC-CF-MFC.

5.3.2 Floating air cathode material fabrication

The processing of the floating air-cathode fabrication is shown in **Figure 5.2.** [495]. The commercially available Type-I blue polyurethane sponge (diameter: 10 cm, projected surface area: 78.54 cm^2, height: 1.0 cm, 5 pores/mm) and commercially available Type-II yellow polyurethane sponge (diameter: 10 cm, projected surface area: 78.54 cm^2, height: 1.0 cm, 3 pores/mm) as the 3D support matrix. Carbon black (CB, Vulcan XC 72R, 50 nm, Fuel Cell Earth Co., Ltd) was used as the conductive layer and catalyst. Polytetrafluoroethylene (PTFE, 60 wt% dispersion in H_2O, Sigma-Aldrich Co., Ltd) was used as the binder. The fabricating process was performed according to the provided protocol with some modifications [504]. Briefly, 0.24 g CB and 1.6 mL PTFE was put into 24 mL ethanol. Subsequently, a uniform CB-PTFE suspension was obtained after 30 min ultrasonication. The sponge matrix was dipped into the suspension solution and dried in the oven under 50 °C several times until the resistance of Type-I/CB and Type-II/CB cathode materials was stable (**Table 5.1.**). The CB of Type-I/CB and Type-II/CB cathode materials was about 80 wt%.

Table 5.1. The resistance changes of floating air-cathodes according to dipping times.

Dipping number	Type-I/CB resistance (Ω)	Type-II/CB resistance (Ω)
1	2000~1400	5000~3000
2	500~300	650~500
3	300~200	500~300
4	150~85	195~180
5	120~85	120~130
6	70~50	110~100
7	70~40	100~85
8	56~40	73~60
9	49~32	65~50
10	47~30	60~50

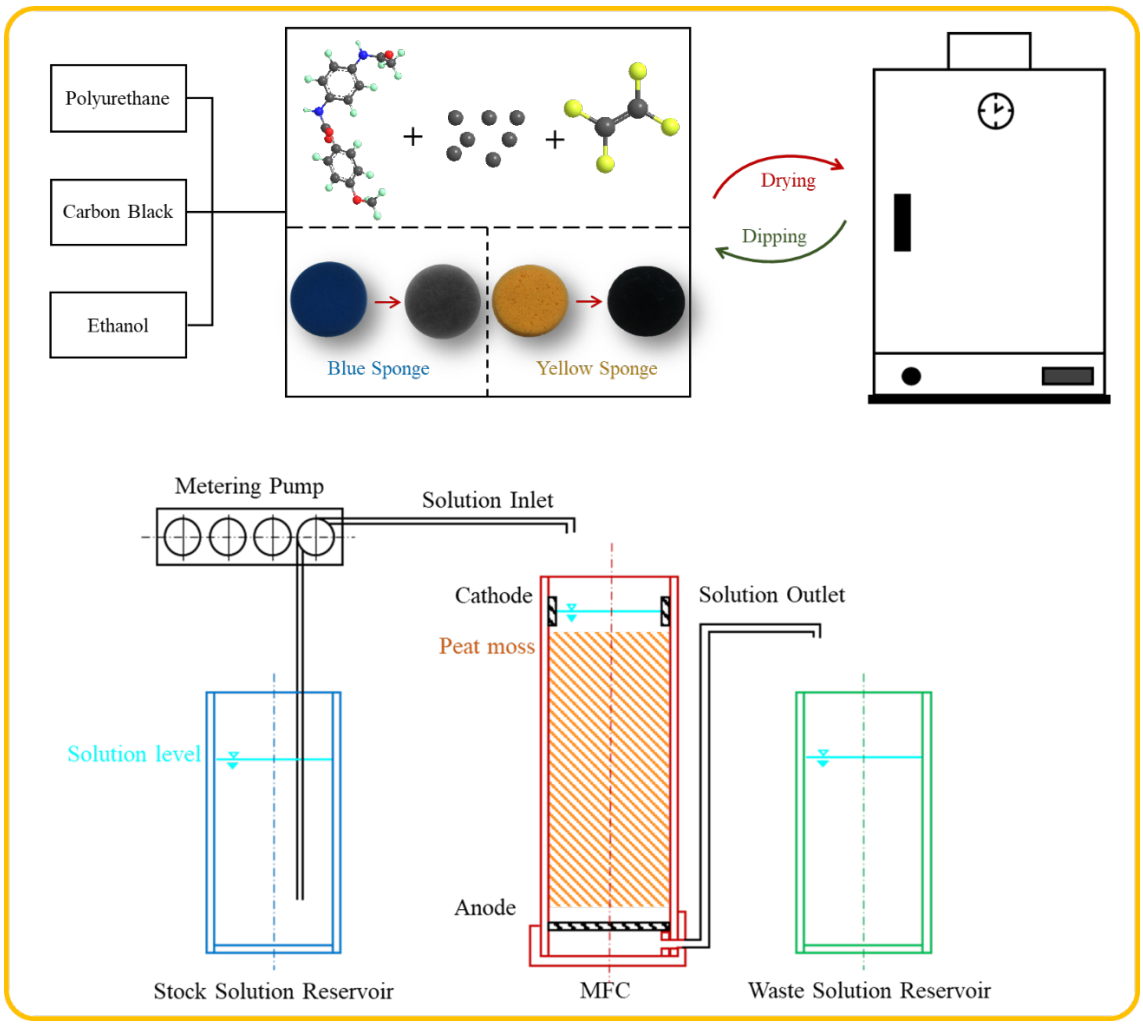

Figure 5.2. The processing of cathode fabrication and the schematic diagram.

5.3.3 Characterization of cathode material properties

5.3.3.1 Scanning electron microscopy

The surface morphology of electrode surfaces was explored utilizing a scanning electron microscope (SEM, TM3000, Hitachi High-Technologies Corporation., Tokyo, Japan).

5.3.3.2 Fourier transform infrared spectroscopy analysis

The FTIR analysis was conducted for Pristine Type-I, Pristine Type-II, Type-I/CB, Type-II, and carbon felt materials. The experimental data were obtained by an infrared spectrometer (Thermo Scientific, Nicolet iS5, MA, USA) with 64 scans. The resolution was 4.0 cm^{-1} and the scan range was 4000-550 cm^{-1}. The background

spectrum was scanned before analyzing each sample with an ATR diamond cell.

5.3.3.3 Mechanical property analysis

Material samples (50 mm × 10 mm) were tested on a tensile testing machine (INSTRON 4502, United States) with the tensile strength of electrodes (25 mm, 50 KN). The crosshead speed was 25 mm/min. Tensile strength (TS) and the percent elongation (EB) at the breakpoint were calculated as follows:

$$TS\ (MPa) = F/(a \times b)$$

$$EB\ (\%) = \Delta L/L_0 \times 100\%$$

where F (N) refers to the stress of film at break, a (mm) refers to film thickness, and b (mm) refers to film width; ΔL (mm) was elongated length of film, L_0 (mm) was original lengths of film.

5.3.3.4 Thermogravimetric analysis

The thermal behavior of Pristine Type-I, Pristine Type-II, Type-I/CB, Type-II/CB, and carbon felt materials was evaluated by TGA. High-purity nitrogen provided the inert atmosphere needed to perform pyrolysis at 60 mL/min. A TGA Q50 (TA Instruments, DE, USA) was utilized at 25 °C and heated up to 700 °C at a rate of 10 °C/min.

5.3.3.5 Water contact angle (WCA)

The surface wettability was tested by a static water-drop method. The WCA was tested under room temperature with 2 μL high purity water to quantify the hydrophobicity of Pristine Type-I, Pristine Type-II, Type-I/CB, Type-II/CB, and carbon felt materials according to the smartphone-based contact angle method developed by Chen et al. [505]. The tests were repeated 10 times for each sample, and the averaged WCA was calculated. A smartphone camera was used to record the images, and the ImageJ software was used to measure the WCA.

5.3.3.6 Carbon loss rate

The carbon loss rate of Type-I/CB and Type-II/CB cathode materials were tested

at room temperature (27 ± 3°C). All samples were weighed and dipped into the Kimura nutrition solution at room temperature. Then, all samples were dried in an oven (30 ± 5°C) until the constant weight. All samples were weighed on the dipping day 0, 2, 4, 6, 8, 10, 13, 16, 19, 22, and 30. The carbon loss percentage was calculated as follows:

$$\text{Loss percentage} = \frac{m_1 - m_2}{m_1}$$

where, m_1(g) was the initial weight of the cathode sample, and m_2(g) was the weight after dipping in the Kimura solution.

5.3.4 Microbial fuel cell operation

5.3.4.1 Nutrition solutions

The Kimura solution with sodium acetate and peat moss were used as the carbon source. The Kimura solution with sodium acetate solution was consisting of MgSO4 (280 µM), $(NH_4)_2SO_4$ (180 µM), $Ca(NO_3)_2$ (180 µM), KNO_3 (90 µM), KH_2PO_4 (90 µM), H_3BO_3 (3 µM), $MnCl_2$ (0.5 µM), CuSO4 (2 µM), $ZnSO_4$ (0.4 µM), $(NH_4)_6Mo_7O_{24}$ (1 µM), and CH_3COONa (10 µM) prepared as described by Ueno et al. [506] with some modification. 2 mM NaOH was used to adjust the pH of nutrient solution.

5.3.4.2 Microbial fuel cell design

Three single-chamber air cathode MFCs: carbon cloth (CC) anode, carbon felt cathode MFC (CC-CF-MFC), CC anode Type-I/CB cathode (CC-I-MFC), and CC anode Type-II/CB cathode MFC (CC-II-MFC) were constructed using polyvinyl chloride (PVC) water pipe (diameter: 100 mm, length: 250 mm, reactor volume: 1.96 L). The detailed MFC setup is shown in Figure 3.2.

Peat moss was utilized as the support matrix and filled with 3/5 of the volume in all MFCs. The anode electrode (CC, 100 mm, 60 mm) was placed horizontally at the bottom of MFC under peat moss matrix. The floating air-breathing cathode electrode (100 mm, 50 mm) was placed at the surface of the peat matrix. The insulated

stainless-steel wires (thickness: 0.45 mm) were used as the current collectors. The distance between the anode and cathode electrode was 150 mm connected by insulated stainless steel wires with conductive cement. An outlet port, 6.35 mm in diameter by 90 mm in length, near the bottom to export waste solution in the beaker (1L capacity). The MFC was inoculated with 5 mL of anaerobic sludge with about 40-50 g/L volatile suspended solids (Lassonde Inc., Rougemont, QC, Canada) with 5 mL phosphate buffer (K_2HPO_4: 2 g, $Na_2HPO_4 \cdot 7H_2O$: 2.55 g, $NaH_2PO_4 \cdot H_2O$: 0.55 g). A programmable peristaltic pump (15 W capacity) was used to pump the Kimura B solution (hydraulic retention time: 1 h). The MFCs were operating under a continuous mode with the flow rate of 5 mL/h.

Initially, all MFCs were run under an open circuit. Then, the polarization test (P-test) was done (day 2, day 6, and day 26) to calculate the external resistance (R_{ext}), which was carried out according to a method described elsewhere [507]. Briefly, disconnect the R_{ext} of MFC for 30 min to measure open-circuit voltage (OCV). Thereafter, reconnected and progressively decreased the R_{ext} (5 mins intervals) in descending order of 50 kΩ, 25 kΩ, 10 kΩ, 5 kΩ, 2 kΩ, 1 kΩ, 500 Ω, and 100 Ω and then in ascending order. After reading the OCV of the last resistance, the P-test was completed. During normal operation, the output voltage measurement of each MFC was logged at intervals of 1 min using a data acquisition system (34,970A, Agilent Technologies, Santa Clara, California, USA) controlled by BenchLink Data Logger software (Version 3.04, Agilent Technologies, Santa Clara, California, USA). A Vee Pro 8.0 automated software (Agilent Technologies, Santa Clara, California, USA) was used for obtaining the data used to calculate the internal resistance (R_{int}) during the polarization test.

5.3.4.3 Cyclic voltammetry test

The traditional three-electrode electrochemical cell was used to examine the direct electrode reaction of bacterial cells in all MFCs. The three-electrode electrochemical cell consists of an MFC setup with Ag/AgCl reference electrode (diameter 0.381 mm), a functional generator (PI-8127, PASCO, Oakville, Canada),

and a data acquisition system (34,970A, Agilent Technologies, Santa Clara, California, USA). Measurements were carried out at the scanning rate of 5 mV/s under room temperature. All experiments were repeated three times.

5.3.4.4 Chemical oxygen demand test

According to the Standard Methods (APHA 1995), the closed reflux colorimetric method with a spectrophotometer (MiltonRoy, Model Spectronic 21D) was used to examine the COD of all MFCs.

5.3.5 Statistical analysis

The SPSS software (SPSS Inc., Ver. 18, Chicago, IL, USA) was used to analyze experimental data. The analysis of variance (ANOVA) was performed using Duncan multiple range test to separate the means and to establish significance (α= 0.05).

5.4. RESULTS AND DISCUSSION

5.4.1 Characterization of cathode materials

The morphologies of all Pristine Type-I and Pristine Type-II materials (**Figure 5.3.(a) & (d)**), Type-I/CB, Type-II/CB, and carbon felt cathode materials (**Figure 5.3.(b), (c), (e), (f), (g), & (h)**) are seen clearly in SEM images. It can be noticed that bare Pristine Type-1 (**Figure 5.3.(a)**) and Pristine Type-II materials (**Figure 5.3.(d)**) made up of polyurethane exhibited an open 3D hierarchical microporous structure with continuously large specific surfaces. Compared with Pristine Type-II material, Pristine Type-I material displayed a tighter pore structure with a smaller size and rougher surface. These microporous structures and rough surfaces were conducive to increasing carbon black loading capacity. Xu et al. [508] proved that the rougher structure could help material electrodes to have better conductivity and capacitance.

By the simple dip-drying method, the insulated Type-I/CB and Type-II/CB cathode materials gained conductive electricity ability. **Figure 5.3.(b) & (e)** observation confirmed carbon black was well attached to both Type-I/CB and Type-II/CB materials. Compared with **Figure 5.3.(a) & (d)**, the small size of carbon black

powder enabled it to fill macropores of the materials with the help of a PTFE binder. Carbon black-PTFE composites were agglomerated and connected with another carbon black as a bulk. This result indicates a continuous carbon black coating layer, which could offer good conductivity for the entire 3D matrix.

Further, Type-I/CB material showed a tighter structure than Type-II/CB material, which resulted in lower ohmic resistance (**Table 3.1.**). Carbon felt textile exhibited a layered structure with uniform microfibers (**Figure 5.3.(g)**). However, the layered independent fiber structure could interrupt contact between the carbon felt textile fibers, causing uneven spacing between fibers and low electrical conductivity [495]. Moreover, different from carbon felt textiles with limited thickness, materials are isotropic and can be processed into any shape to accommodate various device configurations [495].

Figure 5.3.(c), (f), & (h) showed the SEM results of Type-I/CB, Type-II/CB, and carbon felt cathode materials after 130 days of operation in MFCs, which revealed the biofilm covering the cathode materials. Yang et al. [509] noticed that the single-chamber air-cathode MFCs usually grow the biofilm on the air-cathode surface because of membraneless between the anode and cathode compartments. Compared with Type-I/CB (**Figure 5.3.(c)**), Tye-II/CB and carbon felt cathode materials (**Figure 5.3.(f) & (h)**) demonstrated more obvious biofilm growth. This may be due to the Type-I/CB cathode material not being suitable for microbial attachment with a smoother and tighter surface (**Figure 5.3.(c)**) than Type-II/CB and carbon felt cathode materials (**Figure 5.3.(e) & (g)**). Different from Type-II/CB cathode material, where the biofilm covers the surface of the material, carbon felt showed an opened 3D structure, where the biofilm covers the surface of the single fibers and leads to higher internal resistance. This phenomenon was consistent with the results of the P-test. Biofilms have been considered as the diffusion barriers for the transport of mass ion to the cathode interface, thus influence the transport of H^+/OH^- and the electrode surface overall reaction rate [510].

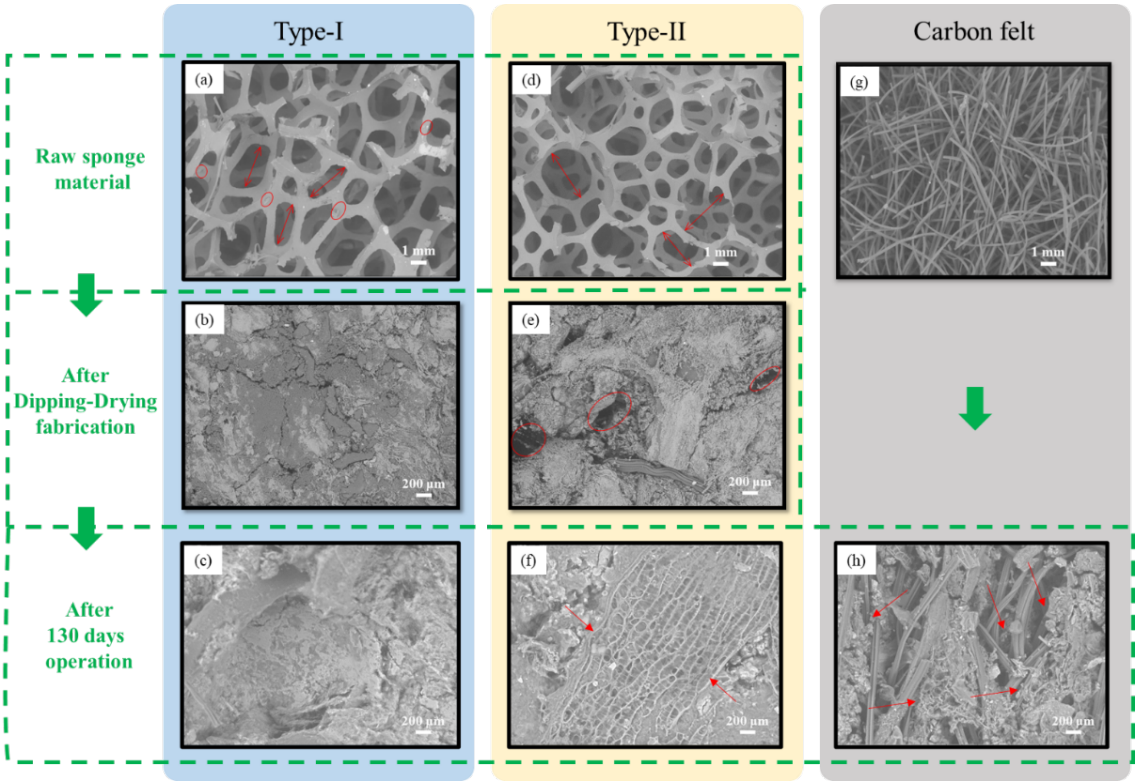

Figure 5.3. The ×500 magnify SEM images of (a) Pristine Type-I material, (b) Type-I/CB cathode material, (c) Type-I/CB cathode material after 130 days running in MFC, (d) Pristine Type-II material, (e), Type-II/CB cathode material, (f) Type-II/CB cathode material after 130 days running in MFC, (g) carbon felt material, (h) carbon felt cathode material after 130 days running in MFC.

5.4.2 Fourier transform infrared spectroscopy analysis

FT-IR spectroscopy is a practical method for gaining organic material qualitative information [511]. As shown in **Figure 5.4.(a)** carbon felt did not present apparent peaks because of this simple C/C-composed material with very few oxygens functional groups, which was similar to the results reported by Wang et al. [512]. Similar spectral fingerprints were observed between the Pristine Type-I and Pristine Type-II, presenting several functional groups such as the N-H stretching at 3304 cm^{-1}, the C-H stretch of CH_3, CH_2, and CH at 2950-2850 cm^{-1}, the C=O carbonyl stretching of urethane and at 1736 cm^{-1}, the C=C stretching at 1535 cm^{-1}, as well as the vibration of ring C-O-C at around 1224 cm^{-1} [513]. Compared to the Pristine Type-I and Pristine Type-II, Type-I/CB and Type-II/CB did not form covalent bonds after combining the

carbon black and PTFE. Therefore, around similar major peaks in all the Type-I/CB and Type-II/CB cathode materials, the different absorptions show that all compound interactions were more likely due to physical response [514]. Besides, the Type-I/CB and Type-II/CB cathode materials showed more intensive spectral absorptions than Pristine Type-I and Pristine Type-II materials. This indicated the more vital molecular forces of functional groups after the combinations of carbon black by PTFE. Besides, compared with Type-II cathode materials, Type-I/CB cathode material displayed more intensive wavebands, demonstrating that the size and number of pores of sponge materials could affect the combination properties with carbon black and PTFE.

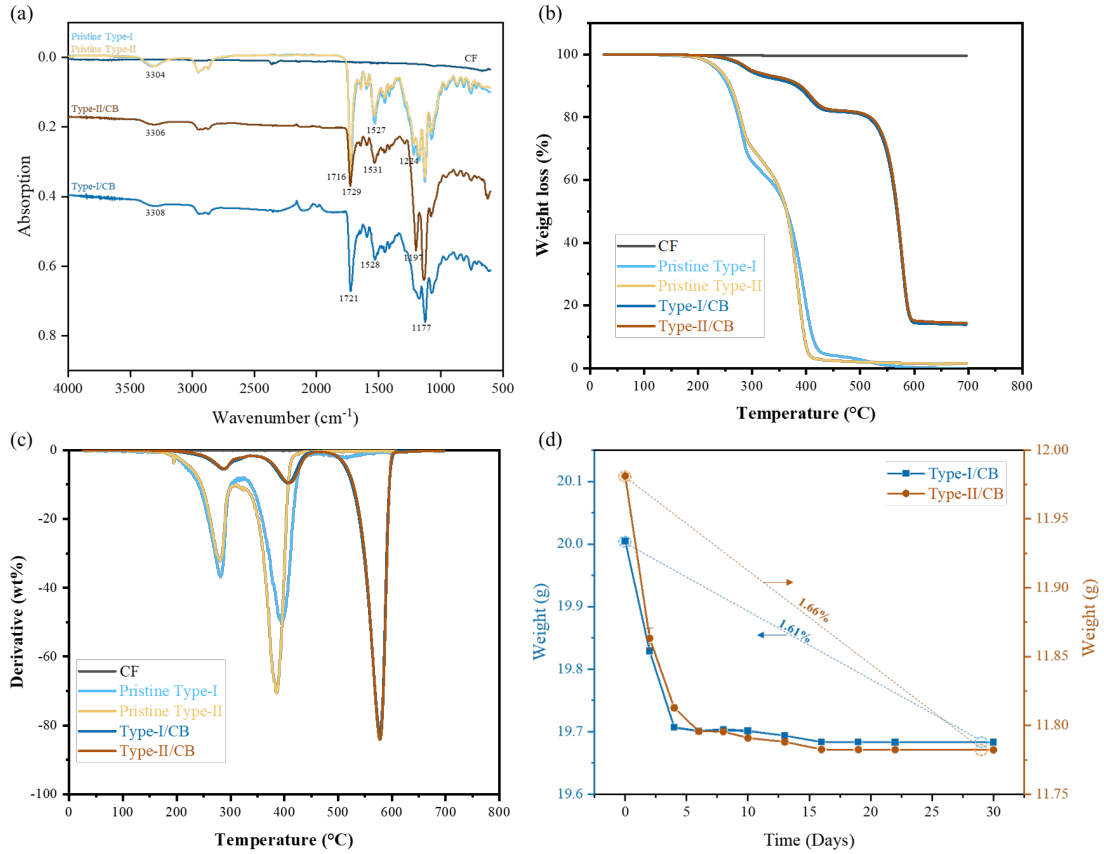

Figure 5.4. The (a) FTIR spectrum, (b) TGA curve, (c) DSC curve, (d) carbon loss rate of carbon felt, Pristine Type-I, Pristine Type-II, Type-I/CB, and Type-II/CB materials.

5.4.3 Mechanical properties

TS and EB are two valuable parameters used to describe material mechanical properties. TS represents the cohesion property between polymer chains, and the EB

indicates the flexibility and extensibility of material before material fracture [515]. All results are shown in **Table 5.2.** Compared with Pristine Type-I, Pristine Type II, Type-I/CB, and Type II/CB, the carbon felt material showed significantly low TS and EB values of 0.09 ± 0.05 MPa and 12.46 ± 6.04% ($p< 0.05$), respectively. This is due to the carbon felt being a C/C composite material; the overall load-bearing performance of the composite structure is determined by the fiber and matrix connect interface [516]. In particular, the stress transfer from the matrix to the fiber is determined by the interface bonding quality [517, 518]. As shown in **Figure 5.3.(g)**, carbon felt fibers displayed a random direction pathway, and the layered independent fiber structure could interrupt contact between the carbon felt textile fibers, causing uneven spacing between fibers, then resulting in a poor mechanical property. Pristine Type-I and Pristine Type-II were all polyurethane materials with the same molecular structure; therefore, they had similar EB before and after treatment ($p > 0.05$). However, Pristine Type-I materials presented a significantly high TS than Pristine Type-II materials before and after treatment ($p < 0.05$). This was caused by the pore-stress concentration effects. As described before, Pristine Type-I showed a tighter and more uniform pore structure than Pristine Type-II materials. Due to small pore sizes, the interaction between crack and pore limit the pore-stress concentrations effects, which lead to a high TS [519]. Besides, Type-I/CB and Type II/CB cathode materials showed slightly higher mechanical properties than pristine materials ($p > 0.05$). This means combining carbon black and PTFE will not change the chemical structure of polyurethane materials, which gave consistent results with the FTIR approach. The higher mechanical properties of Type-I/CB and Type II/CB cathode than carbon felt also demonstrated that the polyurethane-based cathode materials have more application value in large-scale MFCs.

Table 5.2. The mechanical properties and water contact angle of all sample materials.

	Carbon felt	Type-I	Type-II	Type-I /CB	Type-II/CB
TS (MPa)	0.09 ± 0.05^{c}	0.32 ± 0.03^{a}	0.17 ± 0.02^{b}	0.34 ± 0.04^{a}	0.19 ± 0.01^{b}
EB (%)	12.46 ± 6.04^{b}	125.37 ± 5.14^{a}	128.57 ± 6.65^{a}	131.83 ± 6.47^{a}	132.87 ± 5.21^{a}
WCA (°)	150.98 ± 0.35^{a}	131.36 ± 0.67^{b}	114.36 ± 0.28^{c}	67.62 ± 0.81^{d}	77.18 ± 0.27^{e}

Notes: Different letters in the same row indicate significant differences ($p < 0.05$)

5.4.4 Water contact angle analysis

In the floating air cathode MFC, surface wettability is one of the critical parameters, especially the floating air-cathode, which has a complex three-phase interface: air (oxygen), water (protons), and solid (electricity) [520]. According to Chai et al. [521], the better cathode material surface hydrophilic property favors the electron transfer between electrolyte surface and electrode surface, thereby accelerating oxygen reduction reaction (ORR) kinetics. Therefore, the floating air cathode should have a specific ability of surface wettability to provide more surface-active area for the ORR [522]. The WCA of different solid surfaces are as follows: θ<5°, super-hydrophilic; 5°<θ<90°, hydrophilic; 90°<θ<150°, hydrophobic; and θ>150°, superhydrophobic. As shown in **Table 5.2.** the carbon felt shows the highest WCA value, slightly higher than 150°. The Pristine Type-I and Pristine Type-II materials present a WCA value of 131.36 ± 0.67° and 114.47 ± 0.27°, respectively. These results indicated that the Pristine Type-I and Pristine Type-II materials are hydrophobic but could provide a higher surface-active area with water and oxygen surface than carbon felt. Besides, the WCA of Type-I/CB and Type-II/CB materials were 67.63 ± 0.81° and 77.17 ± 0.27°, respectively. The surface wettability of a solid is associated with the surface chemical composition and morphology. Therefore, we proved that the carbon black could alter the surface characterization of the sponge materials, which is consistent with the results of the SEM and FTIR test (Figure 3.3 & 3.4.), enhancing the hydrophilic characteristics of cathodes. Meanwhile, Type-I/CB displayed a significantly low WCA value than Type-II/CB material ($p < 0.05$), thus, we speculated that the Type-I/CB cathode material has a higher electron transfer ability than the Type-II/CB cathode material.

5.4.5 Thermogravimetric analysis

The thermal stability and degradation mechanism of the Pristine Type-I, Pristine Type-II, Type-I/CB, Type-II/CB, and carbon felt were measured by the TGA and

derivative thermogravimetric (DTG). The initial temperature was defined as the temperature at which the weight loss at 5 wt% [523]. **Figure 5.4.(b) & (c)** indicate that the carbon felt is stable over the whole tested temperature range (0-700 °C). The Pristine Type-I and Pristine Type-II materials show a similar TGA and DTG thermograms trend, which indicates a process of two-stage thermal degradation. The first stage of thermal degradation temperature for Pristine Type-I and Pristine Type-II materials occurred in the range of 240-306 °C with a significant weight loss of 30.48% and 24.17%, respectively. This phenomenon was corresponding to physically absorbed water release and toluene diisocyanate liberation, which is caused by urethane depolymerization and urea groups bisubstitution [524]. These results are consistent with the results obtained by the FTIR (**Figure 5.4.(a)**). The second stage is the main pyrolysis region of Pristine Type-I and Pristine Type-II materials, which occurred in 326-440 °C with a weight loss of 55.69% and 61.78%, respectively. This is due to the decarboxylation reactions and dehydration, producing combustible gases (e.g., ketones, ethers, and aldehydes) [523].

Different from Pristine Type-I and Pristine Type-II materials, there are three similar degradation steps in Type I/CB and Type-II/CB cathode materials. The third step weight loss of Type-I/CB and Type-II/CB cathode materials, occurs in the temperature range 494-627 °C, which approaches the thermo-oxidation of carbon black [525-527]. This demonstrates that the polyurethane phase was decomposed, and the main component is carbon black which rules the overall decomposition of the material. Besides, incorporating carbon black into the Pristine Type-I and Pristine Type-II networks demonstrates a higher initial degradation temperature with stronger thermal stability. Therefore, a retarded weight loss rate and an improved char yield in the higher temperature area of Type-I/CB and Type-II/CB cathode materials were obtained. This is primarily because of the high thermal stability and blocking effect of nanosized carbon black-based coating, which took part in the homogeneous hybrid network formation [523]. The higher char production for Type-I/CB and Type-II/CB cathode materials suggested that less volatiles were released from the nanocomposites during heating process, and the reduced volatiles release rate implied the flame

retardance of the nanocomposites was enhanced [528, 529].

5.4.6 Carbon loss rate analysis

The results of the carbon loss from Type-I/CB and Type-II/CB cathode materials are displayed in **Figure 5.4.(d)** During the first 4 days of dipping into the Kimura solution, both Type-I/CB and Type-II/CB cathode materials show a high loss rate of carbon mass of 1.49% and 1.41%. After day 16, the Type-I/CB and Type-II/CB cathode materials showed a stable weight value. Compared with Type-II/CB material, Type-I/CB material exhibited a higher weight value, which may be due to the tight and rough structure that could enhance the surface adhesion of carbon black [530]. Furthermore, after 30 days of testing, the carbon loss rate of Type-I/CB and Type-II/CB cathode materials were only 1.61% and 1.66%, which have no obvious difference from the initial weight value. This result indicated the good carbon black adhesive stability when the Type-I/CB and Type-II/CB materials were air-floating cathodes.

5.4.7 Performance at startup

In the beginning, all MFCs were run under open-circuit mode (OCM), and continuous monitoring was started after 10 days. The initial polarization curves and PD curves of the P-test of all MFCs are shown in **Figure 5.5.(a)-(c)**. CC-I-MFC showed the highest open-circuit voltage (603.78 mV) with a maximum PD of 1397 mW/m^3 normalized by the anode volume at the current density of 2314.80 mA/m^3. Thus, CC-I-MFC has a higher capacity to accumulate charge under P-test open circuit mode [531]. Based on the P-test, the R_{int} of CC-CF-MFC, CC-I-MFC, and CC-II-MFC were about 8180 Ω, 2757 Ω, and 2272 Ω, respectively. Then, the MFCs were started with the fixed R_{ext} of 7000 Ω, 2700 Ω, and 2170 Ω. Under the closed-circuit mode, strong fluctuations appeared before monitoring day 26 on all MFCs due to the poor connections (**Figure 5.6.**).

Further, the last P-test was performed on monitoring day 26 (**Figure 5.5.(d)-(f)**). The MFC with Type-I/CB material cathode showed the lowest slope, indicating that

the polarization of CC-I-MFC was the lowest, the extracellular electron transfer rate was accelerated, and the R_{int} was reduced [498]. The maximum PD of CC-CF-MFC was 92.28 mW/m^3, 4 times lower than CC-I-MFC (436.44 mW/m^3) and CC-II-MFC (439.76 mW/m^3). The R_{int} of CC-CF-MFC and CC-I-MFC was slightly decreased to 5532 Ω and 2250 Ω, respectively. However, it was increased by 2 times (4721 Ω) for CC-II-MFC (**Figure 5.6.(c)**). A stable trend of voltage was noticed after the introduction of 5510 Ω, 2670 Ω, and 4930 Ω R_{ext} for CC-CF-MFC, CC-I-MFC, and CC-II-MFC, respectively (**Figure 5.6.(a)-(c)**). The voltage of CC-CF-MFC reached the maximum value of around 71.56 mV. However, beyond day 40, the output voltage of CC-I-MFC and CC-II-MFC continued to increase. CC-I-MFC keeps showing higher value than CC-II-MFC. This behavior was attributable to the R_{int} from polarization tests, where CC-I-MFC consistently displayed the lowest R_{int}, followed by CC-II-MFC and CC-CF-MFC (**Figure 5.6.(a)-(c)**) similar to the results reported by Adekunle et al. [277]. Besides, the cathode biofilm shown in SEM results (**Figure 5.3.**) also increases the R_{int} of MFCs, which subsequently decreased the generation of electricity [532, 533].

In this work, to improve and stabilize output power, the R_{ext} of MFCs was adjusted according to the estimated R_{int} determined from the polarization test. However, because of the R_{int} changes, significant variations were observed until the last P-test in all MFCs over time. This could mean the R_{ext} optimization method is not appropriate for MFCs. The R_{int} may not change as quickly as in MFCs with more soluble organic matter to fit too frequently changing R_{int} [534]. Therefore, a fixed R_{ext} value is suggested, which should be similar to the initial R_{int}. Otherwise, it could result in unstable performance.

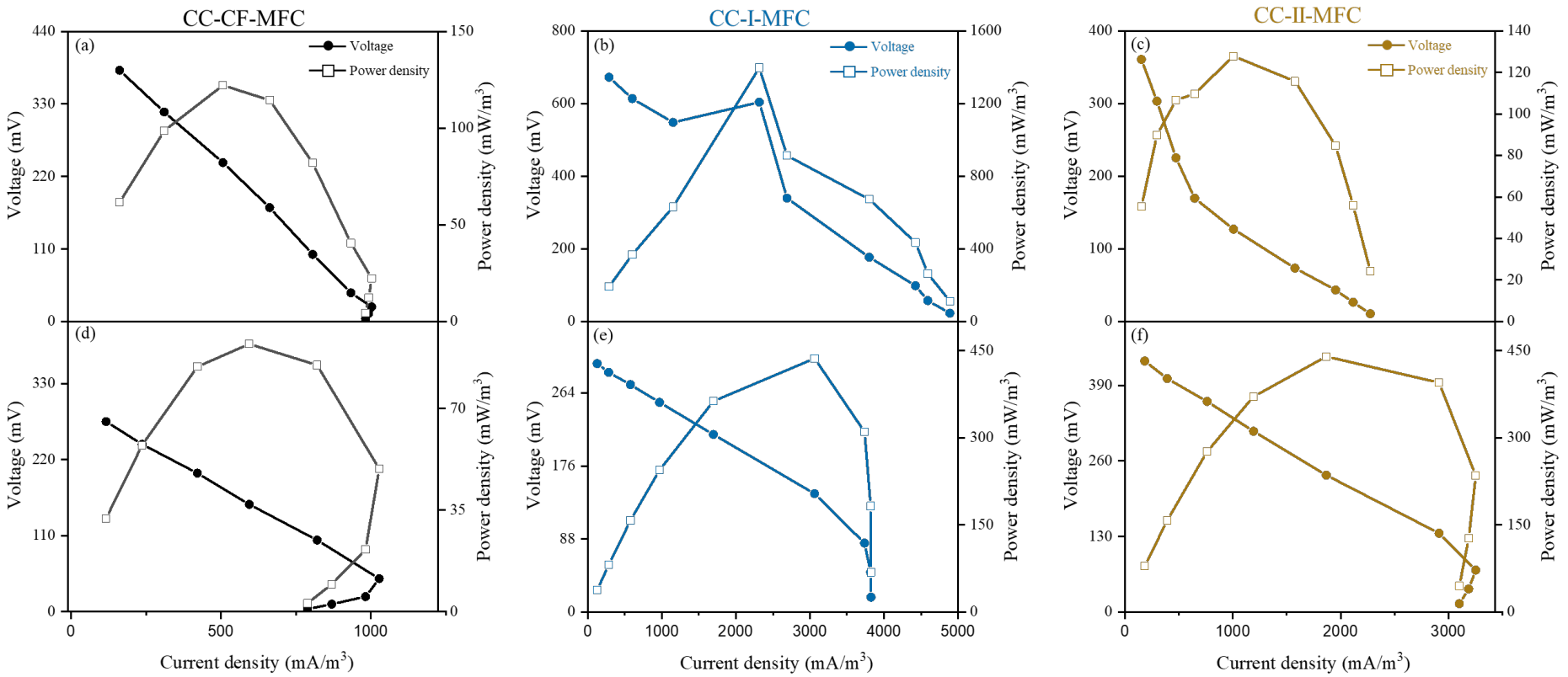

Figure 5.5. Polarization curves of (a) CC-CF-MFC, (b) CC-I-MFC, (C) CC-II-MFC on monitoring day 1, and (d) CC-CF-MFC, (e) CC-I-MFC, (f) CC-II-MFC on monitoring day 26.

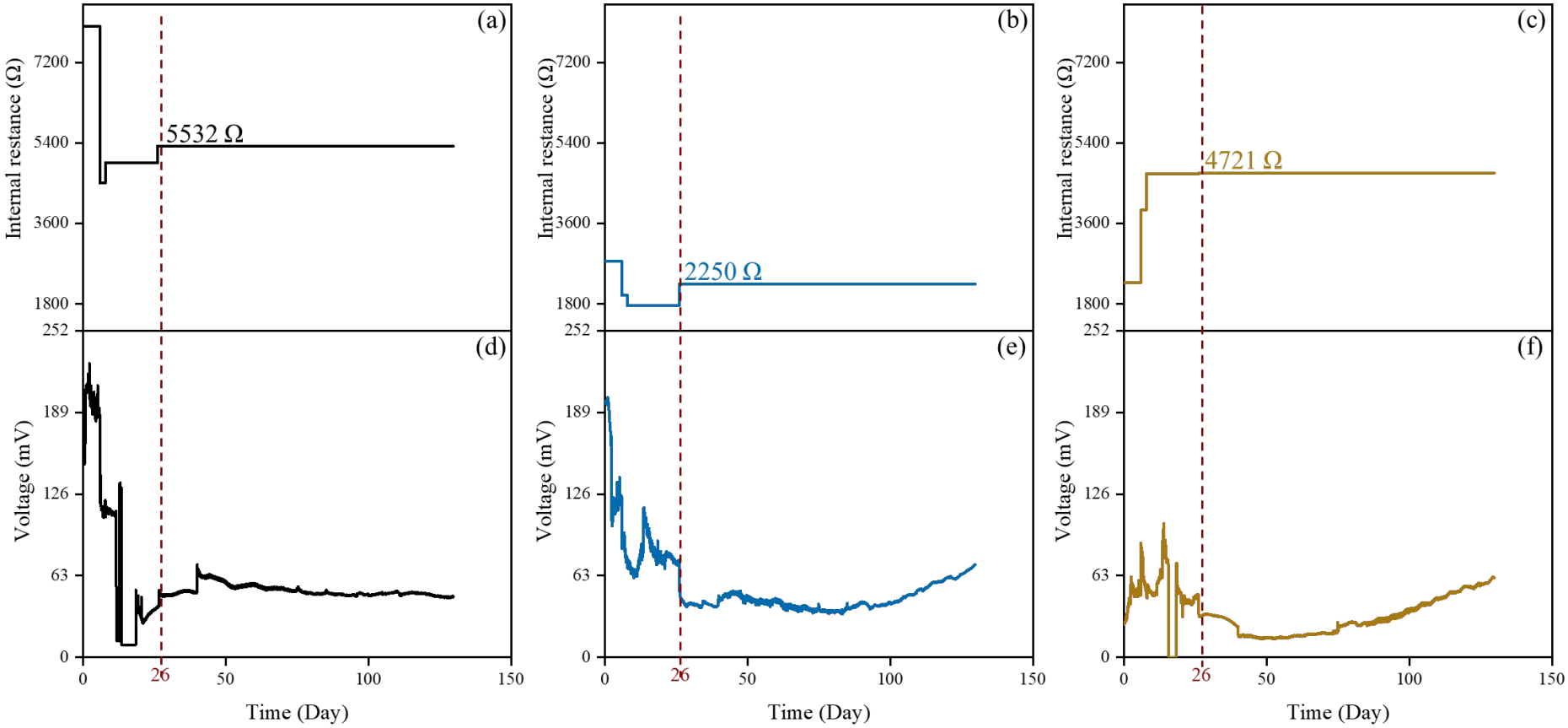

Figure 5.6. The internal resistance of (a) CC-CF-MFC, (b) CC-I-MFC, (c) CC-II-MFC and the voltage curves of (d) CC-CF-MFC, (e) CC-I-MFC, (f) CC-II-MFC.

5.4.8 Power production of microbial fuel cells

As shown in **Figure 5.7.** the PD curve exhibits three distinct regions of all MFCs throughout the study. During the first 26 monitoring days, the PD of all MFCs was unstable. In addition to the bad wire connection between the anode and cathode electrodes, this was most likely due to the immature anodic biofilm. Besides, periodic changes in R_{ext} (**Figure 5.6.(a)-(c)**) and pH (**Figure 5.7.**) can also lead to fluctuations in power outputs [531]. Monitoring day 40 from the start is noteworthy. After about 40 days of monitoring, all MFCs turn into a stationary trend. These stable output voltages mean the maturation of anodic biofilm [535]. CC-CF-MFC registered its maximum PD of 20.05 mW/m^3 at a monitoring day of 40. Then followed by a gradual declining trend until monitoring day at 130. At the end of the monitoring day, the highest value of PD was gained in CC-I-MFC at 92.58 mW/m^3, followed by CC-II-MFC at 35.63 mW/m^3. It was clear that MFC with a floating air-cathode had higher PD than MFC with a normal cathode when coordinated with the same anode electrode material. This might have resulted from the oxygen intrusion into the MFCs. Khudzari et al [27] proved that oxygen could flow into the anode chamber via a porous air-cathode. The presence of oxygen could consume electrons through chemical and biological oxygen reduction processes, leading to increased anode potential, resulting in lower cell voltage and energy output. In comparison to the carbon felt cathode, the floating air-cathode displayed a tighter microstructure in the SEM test (**Figure 5.3.**). Hence, CC-CF-MFC was more likely affected by oxygen diffusion. Besides, as shown in SEM results, more biofilms grown on Type-II/CB and carbon felt cathode materials, which may consume part of the available oxygen through aerobic respiration, thereby reducing the cell voltage [510]. Compared with CC-II-MFC, CC-I-MFC showed 4.6 times higher PD, therefore, it proved that the Type-I/CB cathode material has a higher electron transfer ability than the Type-II/CB cathode material. This result is consistent with the WCA test. Further, the PD of floating air-cathode MFCs keeps increasing at the end of the experiment demonstrating floating air-cathode are more suitable for long-time MFC operation.

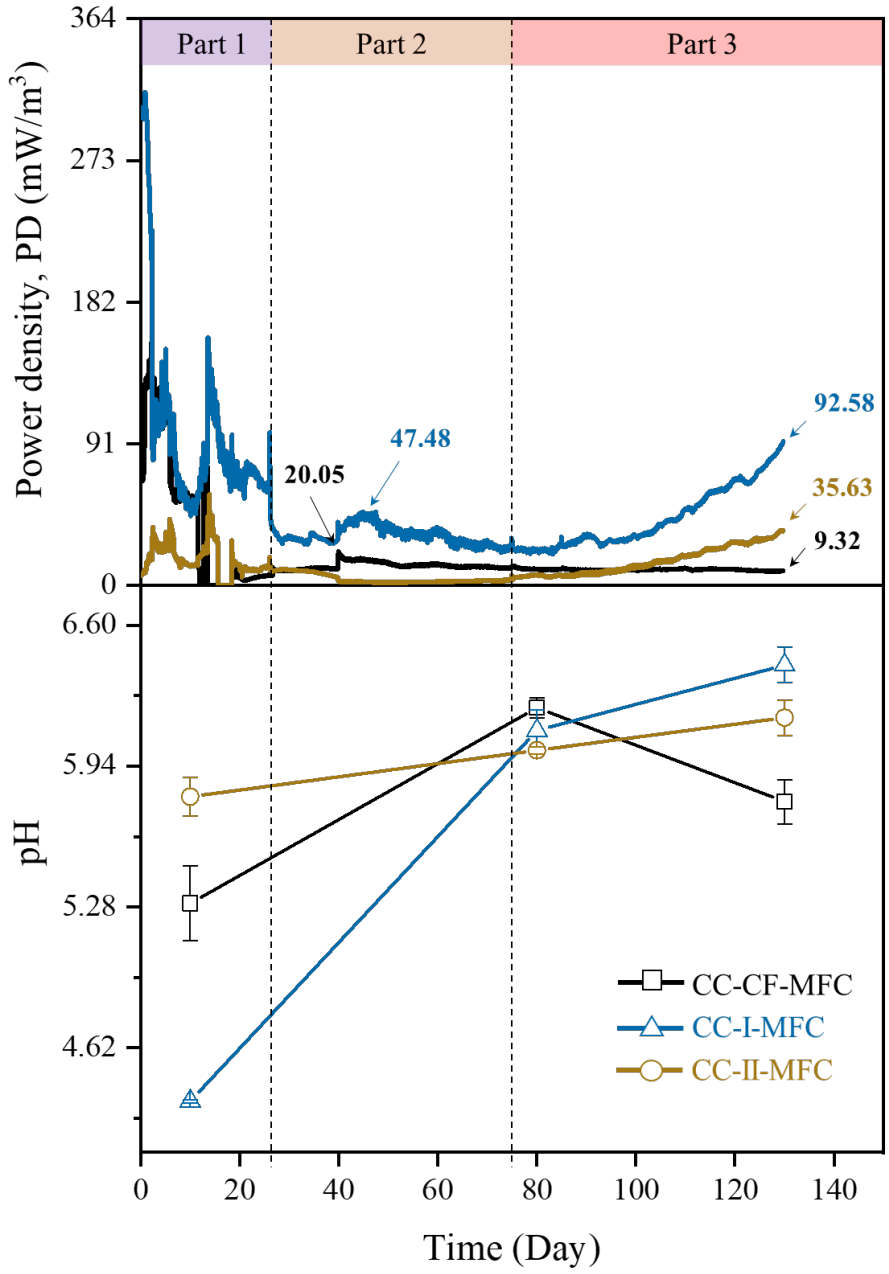

Figure 5.7. Changes in power density and pH measured in CC-CF-MFC, CC-I-MFC, and CC-II-MFC.

5.4.9 Electrochemical analyses

The electrochemical performance of the three cathode surfaces was evaluated by CV at the experiment completion. As demonstrated in **Figure 5.8.(a)** all the cathode samples exhibited several asymmetrical redox peaks. This result suggested the generation of electro-activated compounds during the electricity production process.

The anodic oxidation peak of these three electrodes was carbon felt (0.000097 mA) > Type-I/CB (0.000045 mA) > Type-II/CB (-0.000004 mA). The reduction reaction of these three electrodes was Type-II/CB (-0.000136 mA) > Type-I/CB (-0.000017 mA) > carbon felt (-0.000038 mA). A higher peak current indicates a higher electrocatalytic value [536]. Thus, the carbon felt electrode was the best in the anodic oxidation reaction but the worst in the reduction reaction; Type-II/CB cathode was the best in the cathodic reduction reaction but the worst in the oxidation reaction. Therefore, the Type-I/CB cathode electrode performs better overall oxidation-reduction.

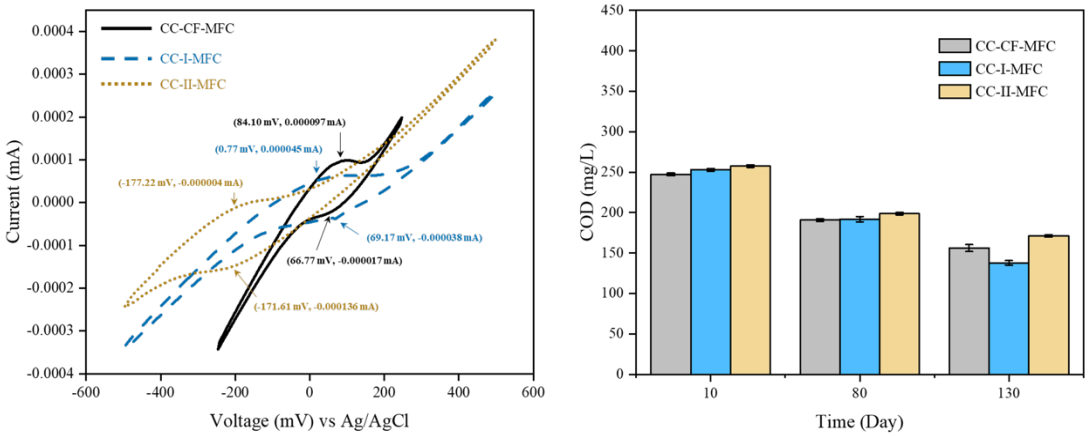

Figure 5.8. (a) CV of carbon felt, Type-I/CB, and Type-II/CB cathode materials at a scan rate of 5mV/s; (b) COD concentration from the CC-CF-MFC, CC-I-MFC, and CC-II-MFC.

5.4.10 Performance in chemical oxygen demand removal

The COD removal levels of all MFCs with all cathode electrodes were also tested. The influent COD was 288.21 ± 1.62. During the cycle of electricity generation, a decrease in the COD trend of all MFCs was observed. After 10 days of monitoring, the COD concentrations in the CC-CF-MFC, CC-I-MFC, and CC-II-MFC effluent were 247.11 ± 1.63, 252.85 ± 1.63, and 257.45 ± 1.63 mg/L, respectively (**Figure 5.8(b)**). By day 50, the COD was decreased to 190.79 ± 1.62, 191.94 ± 3.25, and 198.84 ± 1.63 mg/L in CC-CF-MFC, CC-I-MFC, and CC-II-MFC,

respectively. At the end of the electricity generation cycle, a marked decrease occurred in CC-I-MFC. Notably, the COD decreased from 252.85 ± 1.63 mg/L to 137.92 ± 2.82 mg/L, resulting in the highest COD removal of 45.45%, followed by CC-CF-MFC at 36.74% and CC-II-MFC 33.48%. Clearly, the Type-I electrode is most effective at COD removal. Thus, MFC equipped with Type-I floating air-cathodes was more efficient in increasing mass transfer rate, thereby facilitating the conversion of organic/inorganic carbon into electricity. However, Type-II/CB and Type-I/CB electrodes showed a different COD removal ability in this study. U. Abbasi et al. [537] reported that COD removal efficiency is directly proportional to the amount of voltage generated. As mentioned in the power density and SEM test, Type-I/CB has the higher PD due to its tighter pore structure, smaller size, and a rougher surface than Type-II/CB. Therefore, the microstructure has a crucial influence on COD removal rate.

5.4.11 Cost of assessment of floating air-cathode

The cost of Type-I floating air-cathode was calculated according to the current North American market. The cost of carbon felt cathode is \$0.02/cm^2. The price of Type-I material, carbon black, and PTFE are \$0.04/cm^2, \$1/g, and \$0.74/mL, respectively. For one Type-I cathode, 2.4 g/cm^2 carbon black and 16 mL/cm^2 PTFE will be utilized. Thus, the estimated cost of a Type-I cathode will be \$0.006/cm^2. For future studies, stainless-steel mesh could be used to improve the electrical conductivity of Type-I cathode. The price of stainless-steel mesh is 0.013/cm^2. Hence, the cost of Type-I could be 0.019/cm^2. This is still less compared with carbon felt cathode (0.019/cm^2 < 0.02/cm^2).

5.5. CONCLUSION

In this study, two kinds of inexpensive 3D air-floating cathodes were made by commercially available material through the simple dip-drying method. The SEM results showed that PTFE was utilized as a binder with carbon black successfully coating on the sponge matrix. Although the ideal 3D cathode should be free of organic

binder, PTFE in the cathode could introduce oxygen transfer and limit electrode water losses [538]. PTFE has chemical stability and hydrophobic nature and can form a porous microstructure network in the electrodes, significantly enhancing the active area and mass transport in the electrodes [539, 540]. Electricity was constantly monitored for 130 days from CC-CF-MFC, CC-I-MFC, and CC-II-MFC. Compared with carbon felt cathode material, floating air-cathodes show tighter and more continuous microstructure, which results in 4.52 (CC-I-MFC *vs.* CC-CF-MFC) and 3.82 times (CC-II-MFC *vs.* CC-CF-MFC) higher maximum PD. According to previous studies, 3D sponge anode performs better due to its specific surface area and higher affinity for living bacterial cells, which allows sufficient substrate exchange to support the growth of internal bacterial biofilms [541]. However, in our study, when 3D sponge utilized as cathode in MFCs, the biofilms on cathode electrode surface have been considered as the diffusion barriers for the transport of mass ion to the cathode interface, which has negative effects of MFCs [510]. Also, biofilms grown on the cathode surface may consume part of the available oxygen by respiration progress, causing low voltage [510].

During the CV test, the carbon felt electrode exhibited the best result in anodic oxidation but the worst in the reduction reaction. Type-II/CB cathode showed the best effect in the cathodic reduction reaction but the worst in the anodic oxidation. Whereas Type-I/CB cathode electrode offers the best overall oxidation-reduction performance. Further, CC-I-MFC is most effective at COD removal of 1.24 and 1.36 times higher than CC-II-MFC and CC-CF-MFC, respectively. The essential estimated cost of a Type-I/CB cathode will be \$0.006/cm^2 less than a carbon felt cathode. Therefore, the air-floating cathodes investigated in this study demonstrated the potential application in MFCs. The Type-I/CB cathode electrode is an efficient and cost-effective cathode material for the MFC setups. Further studies could use stainless-steel mesh on both sides of cathode to enhance the wire connection between the electrodes and the electrical conductivity of Type-I/CB floating air-cathode.

CONNECTING TEXT

This Chapter V explored carbon cloth and carbon felt anodes, as well as the new low-cost 3D air floating cathode to improve the efficiency of hydroponic MFC. The results showed that the carbon cloth anode and Type-I/CB cathode microbial fuel cell (CC-II-MFC) had the best overall performance for 130 days running. Type-I/CB cathode has the lowest cost compared with carbon cloth and Type/II cathode. Therefore, carbon cloth anode and Type-I/CB cathode will be used in the following H-PMFC studies.

The potential application of PMFCs to decrease CH_4 in rice plants has been summarized in the literature review. However, no study has reported the effects of H-PMFC on rice CH_4 emission. Chapter VI investigated the influence of bioelectricity production on CH_4 emission from H-PMFC cultivated by rice plants. The impact of H-PMFC and potted rice plants on the CH_4 production, plant growth, and plant biomass production were also be compared.

CHAPTER VI

THE ROLE OF HYDROPONIC MICROBIAL FUEL CELL IN THE REDUCTION OF METHANE EMISSION FROM RICE PLANTS

6.1 ABSTRACT

In this study, to achieve low-carbon agriculture, we built an innovative flow-through hydroponic microbial fuel cell (H-MFC) to decrease rice plants' methane (CH_4) emissions. A single-chamber H-MFC equipped air-floating cathode design was modified for the hydroponic cultivation of Hayayuki rice plants (*Oryza sativa L.*). For comparison purposes, two hydroponic plant microbial fuel cell (H-PMFCs) seeded with rice (PMFC-A, PMFC-B), two H-MFCs with no plant (NPMFC-A, NPMFC-B), and two potted rice plants (Control-A, Control-B) were tested. Then, the output power density (PD), effluent COD, rice plant biomass yield, and methane flux emission were evaluated. PMFC showed the highest power density 504.39 mW/m^3 (PD_{max}), which is 4.88 times higher than NPMFC. The higher PD_{max} observed in the PMFCs can be attributed to an increased hotpot of microbes' activity in the rhizodeposition zone, leading to increased (1.45 times higher) average COD concentration in PMFCs when compared to NPMFCs. The average CH_4 emission flux in the Control (2.03 ± 5.21 $mg/m^2/h$) was 1.97 times higher than PMFC (1.03 ± 0.05 $mg/m^2/h$). These results showed that integrating MFC technology could decrease CH_4 emissions from rice plants in hydroponic systems. In addition, the rice plants grown in PMFC and Control have similar shoot heights (58.9±1.85 cm *vs.* 59±1.75 cm) and root weight (0.1964±0.0047 *vs.* 0.1777±0.0078). The integration of H-MFC has no significant influence on the biomass production of rice plants.

Keywords: cleaner bioelectricity production; hydroponic microbial fuel cell; low-carbon agriculture; methane control

6.2 INTRODUCTION

For the sustainable development of the earth, green growth, clean energy, and environmentally friendly concept gain lots of attention around the world. However, traditional agriculture, such as rice crops, has brought severe environmental damage due to greenhouse gas emissions, which is a considerable threat to sustainable agriculture. Compared to wheat and maize, the global warming potential of rice crops is 467% and 169%, respectively [4]. Rice cultivation is a primary source of vital and long-lasting greenhouse gases, primarily CH_4. The rice fields account for 30% of global agricultural CH_4 emissions [5]. Annually, 1×10^{14} g of CH_4 is released by rice plants, accounting for 1/5 of the total amount of produced CH_4 around the world [542]. However, CH_4 has 28 times higher global warming potential than CO_2 [2]. Therefore, this indicates the essential need for conventional agriculture to switch toward clean energy agriculture.

Facultative anaerobic archaea are the primary bacteria that could produce CH_4 in the rhizodeposition (e.g., exudates, secretions, lysates, etc. [15, 16]) around plants' roots [543]. The rhizodeposition can account for more than 50% of total CH_4 production [544]. The rice paddy field CH_4 production is around 0~60 mg $CH_4/m^2/h$ [545-547], corresponding to an electrical current of 0~804 mA/m^2 [24]. However, the rice paddy field emission of low concentration of CH_4, and a substantial portion of it is immediately consumed by methanotrophs before being released into the air [548]. Therefore, it cannot be used to serve as capturable energy.

Microbial fuel cell (MFC) is a renewable developing technology that can utilize living microbes as electrode catalysts to produce electricity [18] and capture the latent energy in CH_4 from rice paddy fields [549]. According to research in 2008, a variant of MFCs built with a growing plant - Plant MFC (PMFC) could generate up to 120 mA/m^2 [16]. This current value is well within the same order of magnitude as CH_4 emission from the paddy field. Previous studies have shown that PMFCs could reduce rice paddy CH_4 by up to 50% [24, 25]. However, most of those studies sampled the CH_4 from portable containers [24, 26]; only two directly measured CH_4 gas from rice

plants [27, 28]. Besides, these studies mainly focused on the influence of plants on MFCs; only Khudzari et al. [550] discussed the effect of MFCs on plant growth. However, they grew rice plants in solid MFCs, far from the natural environment where rice plants grow.

Furthermore, to solve the shortage of soil, hydroponics is gaining more and more attention. In up-to-date literature reports, no study has investigated the performance of such a system in growing modern agriculture - hydroponics.

Hydroponic agriculture has gained wide recognition due to its ability to increase plants by exposing plant roots to nutritious liquid, eliminating the reliance on the soil medium [23]. The advantages of hydroponic systems include: addressing the water and soil scarcity problems; enhancing the productivity of various crop species; without seasonal restrictions; having a wide range of nutrient sources promising the nutrition supply, etc. [29, 49].

In this study, we proposed a hydroponic-MFC system (H-MFC) and investigated the influence of bioelectricity production on CH_4 emission from hydroponic rice cultivation. This work analyzed CH_4 production levels, rice plant growth, and plant biomass production data in Control and experimental units. We also investigated the performance of the H-MFC operating in such conditions. This research is the first to investigate and report the impact of coupling MFC to rice plants growing hydroponic systems and their overall effect on CH_4 emission. The MFC-hydroponic agriculture system could provide a promising method to achieve the energy-clean and low-carbon agriculture of a sustainable and new smart city.

6.3 MATERIALS AND METHODS

The duration of the experiment was 130 days. In the Post-Harvest Engineering Laboratory at Macdonald Campus, McGill University (Sainte-Anne-de-Bellevue, Québec, Canada), the photoperiod was 12 hours light (26±2 °C) and 12 hours darkness (23±2 °C) which 1000 W LED Plant Grow Light controlled (TOLYS) at room temperature.

6.3.1 Analytical methods and stock solutions

Chemical oxygen demand (COD) was measured according to the Standard Methods (APHA 1995) with a spectrophotometer (MiltonRoy, Model Spectronic 21D).

The nutrient solution of all H-MFCs and rice plants was made according to the Kimura B solution with some modifications. $MgSO_4$ (280 µM), $(NH_4)_2SO_4$ (180 µM), $Ca(NO_3)_2$ (180 µM), KNO_3 (90 µM), KH_2PO_4 (90 µM), H_3BO_3 (3 µM), $MnCyl_2$ (0.5 µM), CuSO4 (2 µM), $ZnSO_4$ (0.4 µM), $(NH_4)_6Mo_7O_{24}$ (1 µM) $EDTANa_2Fe(III)$ (10 µM) [551]. 2 mM NaOH was used to adjust the pH of nutrient solution.

6.3.2 Hydroponic-microbial fuel cell design

All H-MFCs were constructed using polyvinyl chloride (PVC) water pipe, 100 mm in diameter by 250 mm in length. Cocopeat moss was utilized as the support matrix and filled 3/5 of the volume in H-MFCs. A carbon cloth anode (CC, 100 mm × 60 mm) was placed horizontally at a depth of 150 mm under the cocopeat matrix, and a round floating air-cathode (100 mm × 50 mm) was placed on the surface of the cocopeat matrix. The insulated stainless-steel wires (0.45 mm thickness) were used as the current collectors and connected with the electrodes using conductive cement. An outlet port, 6.35 mm in diameter by 90 mm in length, near the bottom to export waste solution in the beaker (1 L capacity). A submersible pump (15 W capacity, 5 mL/h flow rate) for pumping Kimura B solution [506].

An airtight headspace was placed on the top of the setups with a sampling port positioned halfway to trap gases for the CH_4 test. A small electric blower on the headspace was used for air mixing. The detailed MFC and airtight headspace setups are shown in **Figure 6.1.(a).**

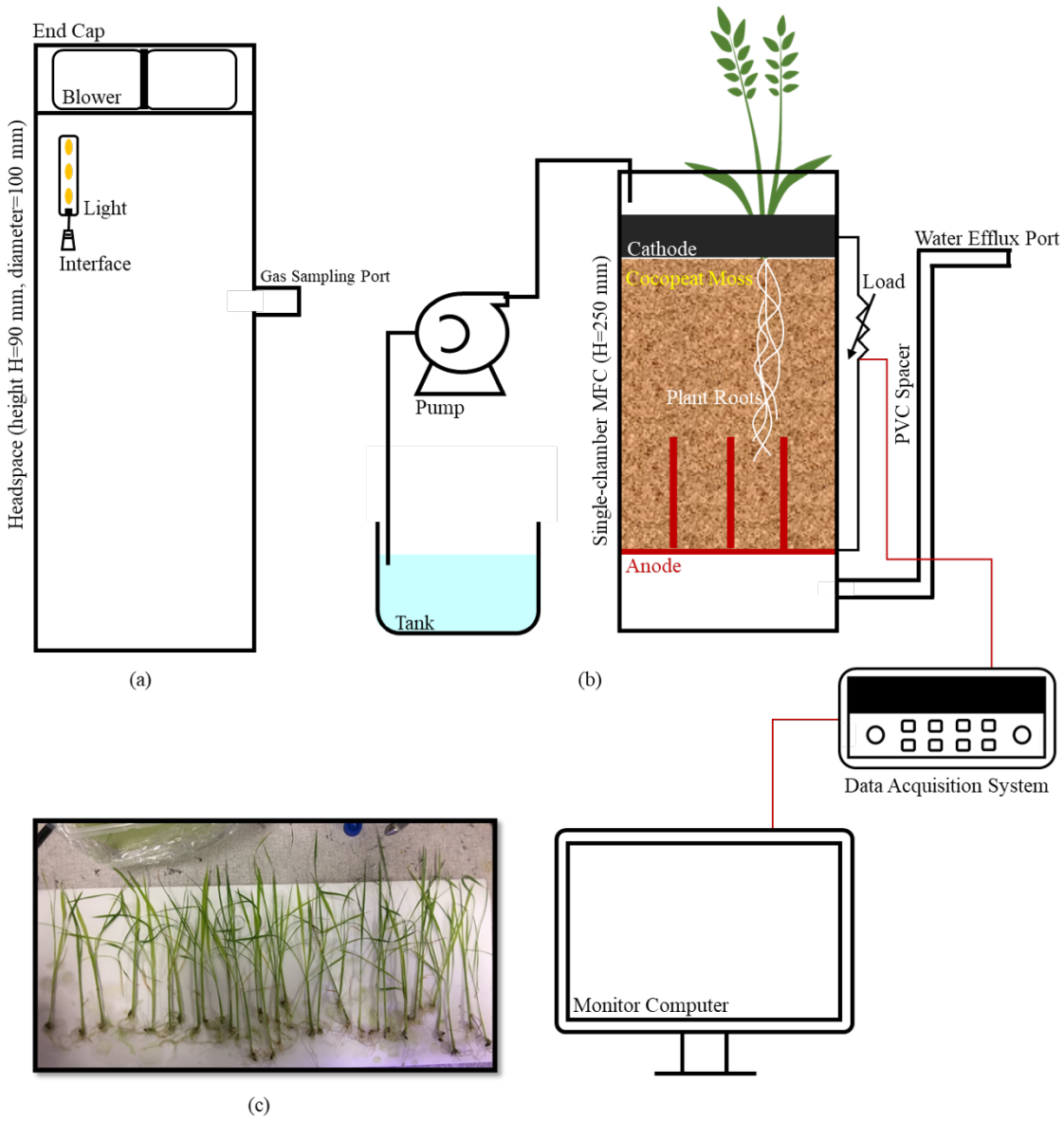

Figure 6.1. The schematic diagram of (a) airtight headspace for methane collection; (b) H-MFC setups; (c) 3-leaf stage rice plants.

6.3.3 Experimental design and H-MFC operation

Two H-MFCs without rice plants (named MFC-A, MFC-B) and two H-MFCs with rice plants (named PMFC-A, PMFC-B) were used to study the effect of rice plants on the bioelectricity production of H-MFCs. Two potted rice plants (Control-A, Control-B) and the mentioned two PMFCs were used to study the influence of flow H-MFC on CH_4 emission from hydroponic cultivation of rice plants.

Initially, the external resistance (R_{ext}) used in the closed-circuit H-MFCs ranged

between 1000-2000 Ω. The internal resistance (R_{int}) of each H-MFC was calculated by periodic polarization test (P-test) to optimize power production. The P-test was carried out according to a method described elsewhere [507]. Briefly, open-circuit voltage (OCV) was measured by disconnecting the R_{ext} from the H-MFC for 30 min. Thereafter, the R_{ext} is reconnected and progressively decreased (5 min interval) in a descending order (50 kΩ, 25 kΩ, 10 kΩ, 5 kΩ, 2 kΩ, 1 kΩ, 500 Ω, and 100 Ω), and then in ascending order. 30 min later, by reading the final OCV, the P-test was finished. The P-test was performed on day 3, 9, 15, 22, 29, 36, 57,75, and 99 of the tests. Then calculated current (I, mA) and power (P, mW) to plot polarization (voltage *vs.* current) and power (output power *vs.* current) figures. The slope of the linear part of the current-voltage polarization curve corresponding to ohmic losses was used to estimate the total R_{int}. During regular operation, the output voltage measurement of each H-MFC was logged (1 min interval) by a data acquisition system (34,970A, Agilent Technologies, Santa Clara, California, USA) controlled by BenchLink Data Logger software (Version 3.04, Agilent Technologies, Santa Clara, California, USA). A Vee Pro 8.0 (Agilent Technologies, Santa Clara, California, USA) automated software was used for obtaining the data used to calculate the R_{int} during the P-test.

6.3.4 Rice plants cultivation and characterization

6.3.4.1 Rice plant cultivation

Oryza sativa L. cultivar Hayayuki was used in this study. Hayayuki is a cold-tolerant as well as short-grained brown rice [552]. The seeds of Hayayuki were obtained from LA SOCIÉTÉ DES PLANTES (Quebec, Canada). Before germination, the seeds were soaked in distilled water for 48 hours. Then, all seeds were germinated in the plate and transplanted at the 3-leaf stage (**Figure 6.1.(b) & (c)**).

6.3.4.2 Measurement of methane

CH_4 production from H-MFCs and Control group potted rice plants were quantified by the static chamber method [27]. All of them were sealed by a headspace

chamber according to the dark photoperiod for 12 hours under room temperature. Firstly, turn on the internal blower to thoroughly mix the air in the headspace. Then a 2.5 mL gas sample was extracted through the sampling port, and all samples were done in triplicate. The concentration of CH_4 (parts per million, ppm) was measured by an HP 5890A gas chromatograph (Hewlett Packard, Palo Alto, California, USA) equipped with a Porapak-N column (120 mm ×3mm, 149-177 microns) and a thermal conductivity detector. The helium was used as the carrier gas. The injector temperature was 210 °C. The detector and analysis temperatures were 210 °C and 45 °C, respectively. The CH_4 emission flux (F, mg/m^2/h) was calculated following equation (6.1) [553, 554]:

$$F = H \times (M_W/M_V) \times [273.2/(273.2 + T)] \times (\Delta C/\Delta t) \quad 6.1$$

Where H is the chamber height, m. M_w is the CH_4 mole mass, 16.123×10^{-3} mg. M_v is the CH_4 mole volume, 22.41×10^{-3} m^3. T is the chamber air temperature, 23 °C. $\Delta C/\Delta t$ is the change in the CH_4 between the initial and final measurement per unit of time (12 h), ppm. The CH_4 measurement was performed on the day.

6.3.4.3 Measurement of plant growth parameters

The height of the plants was measured by a measuring tape as an indicator of rice growth. The nutrition solution pH was measured by a pH meter (AB150, Fisher Scientific, Canada).

At the end of the experiment, the whole rice plants were harvested. The plants were soaked in the sodium hexametaphosphate solution to facilitate the separation of peat moss from the roots [27]. Cut the roots from the shoots, then separately place them in the paper bag to dry. Under 50 °C, after 48 h drying in the hot air oven, the dry matter content of the shoots and roots were weighed.

6.3.5 Statistical analysis

The experimental data were analyzed by analysis of variance (ANOVA) of the SPSS software (SPSS Inc., Ver. 18, Chicago, IL, USA). The Duncan multiple range tests were applied to separate the means and to establish significance, which was accepted at $p < 0.05$.

6.4 RESULTS AND DISCUSSION

6.4.1 The performance of setup and adjustment of R_{ext}

At the start of the experiment, all H-MFCs were operating under open-circuit mode. All H-MFCs voltage kept showing positive values. Khudzari et al. [531] recommended temporarily running MFCs under an open circuit to compensate for anodophilic activity caused by carbon consumption, which could also help harvest more electrical energy. One week later, the circuit condition was switched from open to closed circuit by connecting 1180 Ω resistors. A marked decrease was noticed for all H-MFCs after R_{ext} was connected. Menicucci et al. [555] reported that the decline in output value was more significant when the R_{ext} was less than 3000 Ω. This was attributed to the limitations imposed on the electrode reaction kinetics at the current-limiting electrode [555]. From day 22 to day 40, the output voltage increased significantly with the increase in R_{ext} for PMFCs and NPMFCs. A similar phenomenon was also reported by Ghangrekar and Shinde [556]. This makes the R_{ext} regulate anode potentials [557]. The anode potential became more negative and steady with the higher $R_{ext.}$ [558], which resulted in a higher voltage value. While low anode potential cannot afford enough energy for electron transfer and cell maintenance [559]. Hence, the optimal value of R_{ext} was close to the $R_{int,}$ as shown in **Figure 6.2.** where the output voltage is more stable.

In this study, a total of nine P-test were done to adjust the R_{ext} close to its R_{int}. However, too frequent adjustment causes an unstable performance for PMFCs and NPMFCs (**Figure 6.2.**). Helder et al. also found a similar phenomenon [560]. Therefore, the fixed R_{ext} value is more appropriate for PMFCs and NPMFCs.

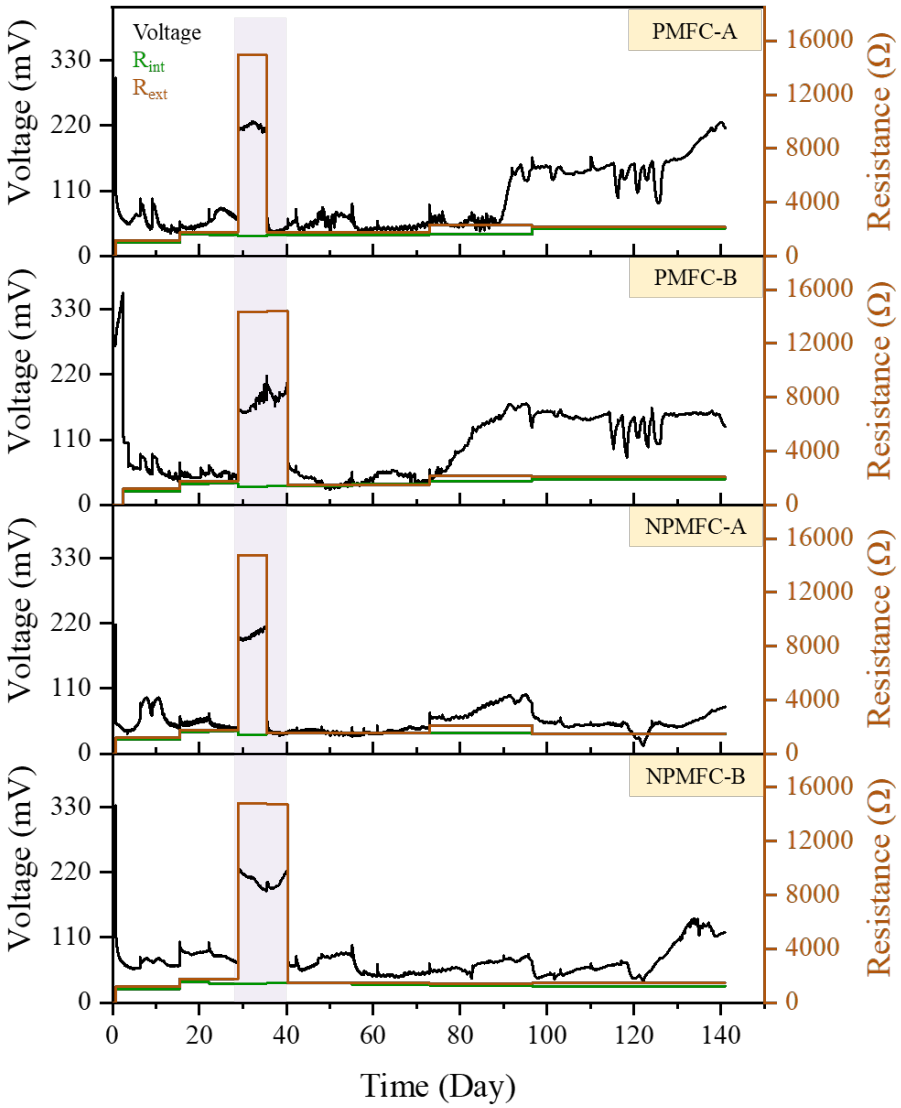

Figure 6.2. The curve of output voltage and external resistance of all H-MFCs.

6.4.2 Polarization tests

The P-test was used to estimate the maximum H-MFC power by estimating the R_{int} and adjusted R_{ext} values. P-test was performed at day 3, 9, 15, 22, 29, 36, 57,75, and 99. As shown in **Figure 6.3.** the changes in the R_{int} of PMFCs (966-2051 Ω) were higher than NPMFCs (1014-1557 Ω), and the day 36 is worth noting. Before day 36, the R_{int} of all H-MFCs has similar R_{int} values and trends. From day 36 to day 99, the R_{int} of PMFCs increased from 1598 Ω to 2051 Ω of PMFC-A, from 1385 Ω to 1913 Ω of PMFC-B. However, NPMFCs showed an opposite trend, which decreased from 1511 Ω to 1460 Ω of NPMFC-A, from 1488 Ω to 1201 Ω of NPMFC-B. In the NPMFCs, In the MFCs, the R_{int} is decided by the anode resistance, cathode resistance,

electrolyte resistance, and membrane resistance [36]. Therefore, the R_{int} tested by P-test can be written as follow:

$$R_{int} = R_{anode} + R_{cathode} + R_{membrane} + R_{electrolyte} \quad 6.2$$

Anode resistance is mainly decided by the size of the anode and the activity of the exoelectrogenic bacteria, as well as both the anode biofilm and planktonic bacteria in bulk solution contribute to the power production of MFCs in the mixed bacterial culture environment [561]. $R_{electrolyte}$ is proportional to the electrode spacing while inversely proportional to the cross-sectional area of the MFC reactor and the concentration of charge transfer electrolyte; therefore, according to Fan et al., the internal resistance equation of single chamber MFC is as follows [562]:

$$R_{int} = r_{anode}/S_{anode} + r_{cathode}/S_{cathode} + aL/(S_r \times C_{electrolyte}) \quad 6.3$$

where $r_{anode/cathode}$ and $S_{anode/cathode}$ are the area-specific resistance and the projected areas of anode/cathode, respectively; a is a constant; L is electrode spacing; S_r is the cross-sectional area of the reactor; $C_{electrolyte}$ is the concentration of charge transfer electrolyte.

In this study, PMFCs and NPMFCs utilized the same size and material of anode, cathode, and chambers. Fan et al. [562] found that when the MFCs are equipped with the anode and cathode with the same size and material, the anode only accounted for 5.4% of the R_{int}, while the cathode and the electrolyte each contributed 47.3%. Thus, $C_{electrolyte}$ is an important factor in MFCs' internal resistance. Due to plants' consumption of ions in the nutrient solution, the $C_{electrolyte}$ of PMFC was lower than $C_{electrolyte}$ of NPMFC. Therefore, according to eq (6.3), the R_{int} of PMFC is higher than NPMFC. With the plants growing in PMFCs, rice plants' ability to absorb nutrients was enhanced, leading to low $C_{electrolyte}$, resulting in the improvement of the R_{int} trend of PMFCs.

The highest PD value during the P-test was noticed on NPMFC-B 707.92 mW/m^3 (Day-9). Besides, at the end of P-test, the overall average PD_{max} of PMFCs (349.50 mW/m^3) was higher than NPMFCs (306.86 mW/m^3). It was observed that when PD_{max} was inversely related to R_{int} for PMFCs. However, on the last P-test, the PD_{max} was increased with the R_{int} increase. Similar results were also reported by

Timmers et al. [563], who found that the polarization had a distinct hysteresis; the increased R_{int} makes it challenging to interpret the maximum power output of the PMFC. Besides, the microbes' hotspots that occurred in the rhizosphere could enhance microbial activity and exudation [564]. The intensity of microbes turnover processes in their hotspots in the rhizodeposition zone is at least one order of magnitude higher than the normal soil [564]. Therefore, we assumed that the hotspots of microbial activity in PMFCs also have a key impact on the PD_{max} during P-test.

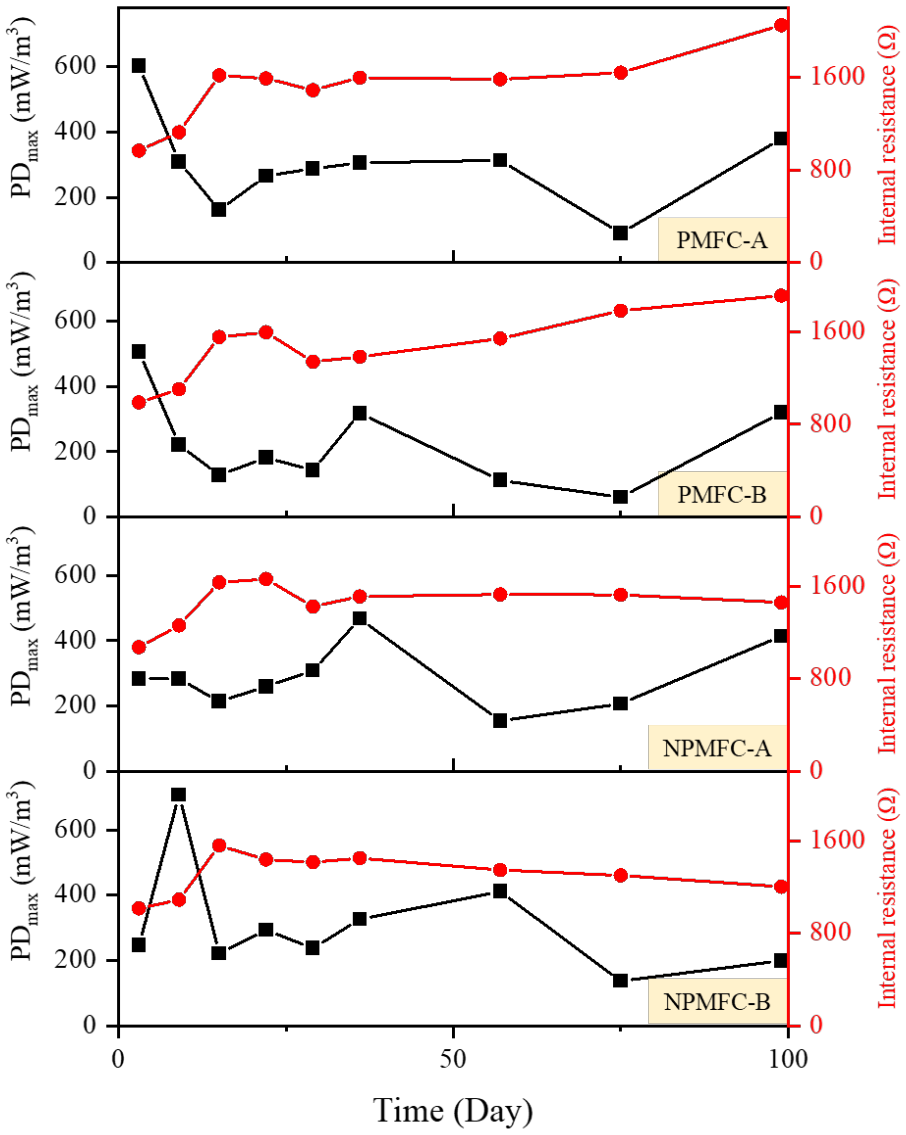

Figure 6.3. A comparison between internal resistance and maximum power density from polarization test.

6.4.3 Power production of rice PMFCs and MFCs

Figure 6.4. shows the power density (PD) during 141 days of all H-MFCs. The PD curve exhibits three distinct regions. Initially, the PD of all H-MFCs fluctuated. Except for the poor connection between anode and cathode electrodes, the immature anodic biofilm and periodic changes of R_{ext} (**Figure 6.2.**) also influenced PD [531]. About 55 days later, the PD of all H-MFCs turned into a stationary trend, which marked the maturation of anodic biofilm [535]. The PD between PMFCs and NPMFCs has no significant difference during Part A and Part B periods. After monitoring day 74, an exponentially increasing trend was observed for PMFCs. The highest PD_{max} was achieved by PMFC-A at 504.39 mW/m^3, followed by PMFC-B at 290.63 mW/m^3, NPMFC-B at 285.16 mW/m^3, and NPMFC-A at 103.30 mW/m^3 (Figure 4.4.). This difference was attributed to the rhizodeposition and microbes' hotspots [564, 565]. However, the rhizodeposition decreases when the plants get older [18]. Therefore, declining trends were noticed for PMFC-A and PMFC-B near the end of the experiment.

The O_2 has main influence on MFC performance. Generally, O_2 could be transported from the atmosphere via a well-developed aerenchyma system to the plant root area, inhibits methanogens, reducing CH_4 emission [566]. Besides, in the cathode chamber of PMFC, under aerobic conditions, with the participation of incoming electrons and hydrogen ions, cathode will occur the reduction of molecular oxygen and water formation as follows [567]:

$$O_2 + 4e^- + 4H^+ \rightarrow 2H_2O \qquad 6.4$$

The oxic conditions in MFCs lead to the consumption of electrons through chemical/biological oxygen reduction, then reducing the number of available electrons for electrical generation [568]. Therefore, the PMFC and MFC generally have similar power output due to the oxygen release from the plant root system [27]. However, in this study, the average PD_{max} of PMFCs was higher than MFCs (364.98 *vs.* 164.93 mW/m^3) (**Figure 6.4.**). This is because the rhizosphere around plant roots could produce organic matter to anode microbes and the flowing nutrition solution

removes excess O_2 from the anode chamber.

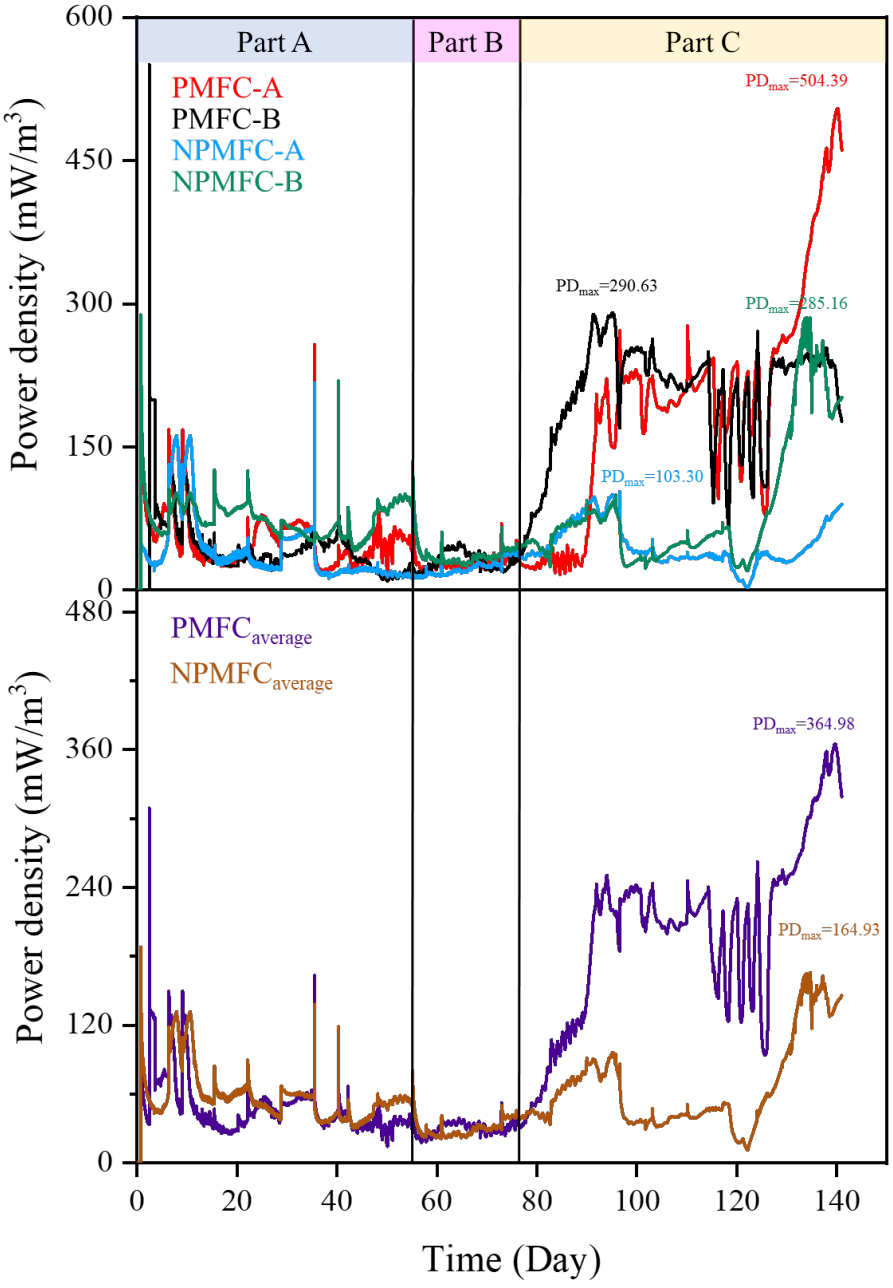

Figure 6.4. The performance of all H-MFCs in terms of power density.

6.4.4 Relationship between chemical oxygen demand and output voltage

The COD concentration in the outlet nutrition solution of MFCs could represent the number of reduced organics [16]. As the microbial substrates, the reduced organics form the source of electrical energy in the whole setup [16]. **Figure 6.5.** shows the relationship between the COD concentration and output voltage. For 141 days, the

COD concentration in all H-MFCs kept decreasing until day 55, and NPMFC-A showed a maximum COD of 37 mg/L. After day 55, COD concentration remained fairly constant in both NPMFCs but increased in PMFCs to reach a maximum at around day 100. Then the COD values decreased slowly till the end of the experiment.

The output voltage showed a similar trend as COD concentration increased with the COD concentration increase. The average COD concentration in the PMFCs was 1.45 times higher than the COD concentration in NPMFCs. Moreover, after day 90, the output voltage of PMFCs exhibited more fluctuations than NPMFCs. This indicated that rhizodeposits worked as COD concentration increased in PMFCs [569]. Rhizodeposits provide C and N to help microbial growth and affect the anode potential [569]. As described before, the anode potential could affect the output voltage. However, the amount and specific action of rhizodeposits are related to the physiological state of individual roots and changes with the root life cycle [570]. Thus, the fluctuations in the amount and action of rhizodeposits resulted in changes in output voltage (**Figure 6.3.**), especially from day 92 to day 130.

The positive relationship between COD and output voltage indicates that the COD derived from rice plants acts as the electron donor for electricity generation in PMFCs. The output voltage significantly increased during the active growth period of plants, suggesting that the excreted compounds, sloughed-off cells, mucilage, etc., could make up the anodic substrate [16]. Further, a slight increase was also noticed for NPMFCs. This may be causing the need for periodic replacement R_{ext}. As mentioned before, R_{ext} influences the anode potential, which may alter the anode metabolic activities, while the microbial species could provide different mechanisms for the organic matter utilization [571].

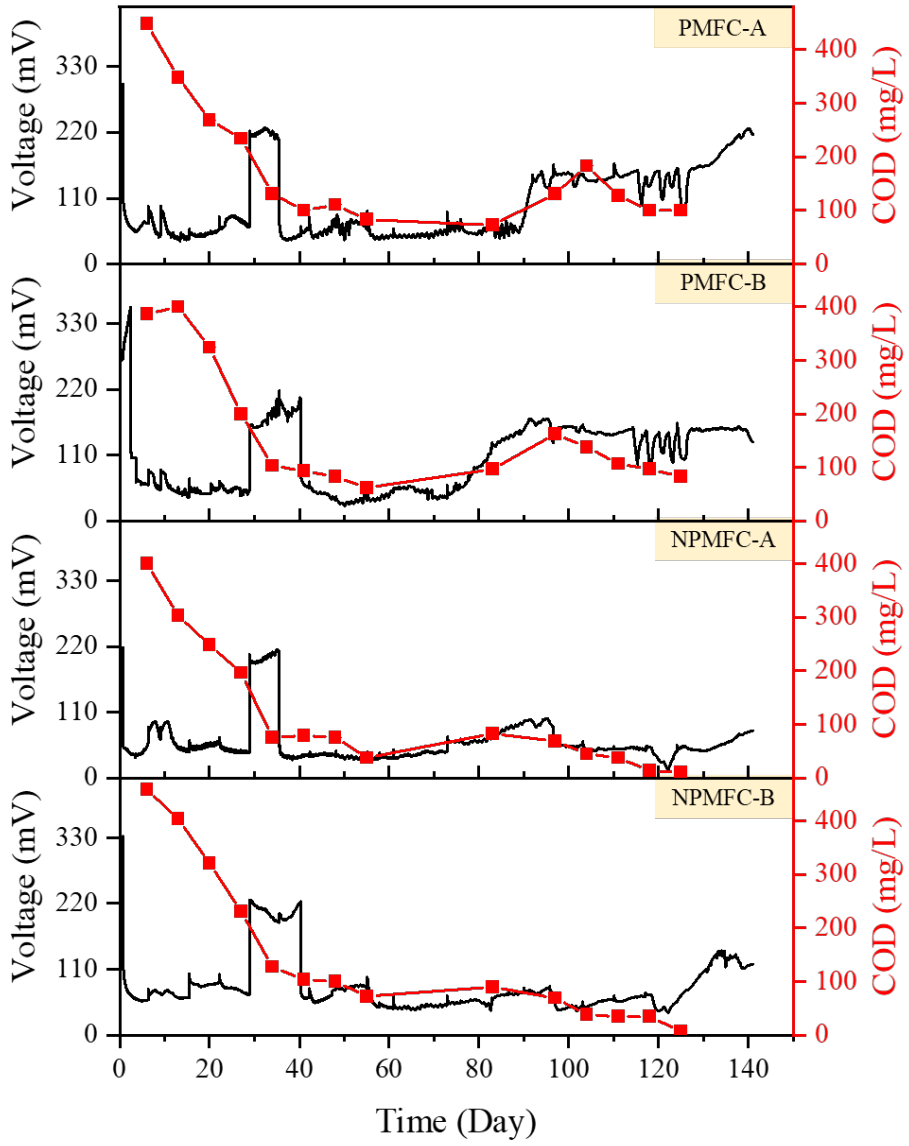

Figure 6.5. The curve of output voltage and COD concentration of all H-MFCs.

6.4.5 Methane flux emission

Figure 6.6. displays (a) the current generation of PMFCs, and (b) the progression of CH_4 production from Control and PMFCs as a function of operation time. From day 100-110 to day 110-120, the CH_4 emission flux of potted rice plants sharply increased, and then it continued its gradual increase until the end of the experiment. This phenomenon is attributed to the physiological changes in rice plants [572]. During the entire vegetation period, the CH_4 from rice plants (90%) travels up from the soil to the atmosphere by the plant aerenchyma [573]. The emission rate of CH_4 in rice plants generally peaks towards the end of the tillering stage, then

decreases as the growing season ends [26]. For the entire duration of the experiment, the CH_4 flux from Control was significantly higher than the PMFCs, especially after days 100-110. From **Table 6.1.** the CH_4 emission $flux_{avg/plant}$ of the Control was almost two times higher than PMFC (2.0254±5.2061 mg/m^2/h *vs.* 1.0281±0.0480 mg/m^2/h). These results indicated that the PMFCs could effectively reduce CH_4 emissions. The possible reason for this phenomenon is that in the MFCs, the electrogens present in the anaerobic environment can oxidize organic matter to generate current. The electrogens on anodes may compete with methanogens for carbon substrates, thereby suppressing methanogenesis [24] (**Figure 6.7.**). Previous studies have reported that anodic installation around rhizosphere could alter the microbiome structure by stimulating the growth of exoelectrogenic bacteria, particularly *Geobacter* species, and inhibits the growth of competing methanogens [574, 575]. When the anode is introduced into the waterlogged rhizosphere, the composition of methanogens will be affecting results in a delayed methanogenesis [576, 577]. Besides, Rozendal et al., [284] found that the anodic oxidation of organic matter causes a decrease in pH during the current generation, while methanogenic metabolism will be prevented by the decrease in pH [578].

As shown in **Figure 6.6.(a)**, current production decreased during the first 40 days of the experiment. Then, the current remained fairly constant at about 0.03 mA till day 80 in PMFC-B and day 90 in PMFC-A. A rapid increase followed the above result to about 0.07 mA in both PMFCs, and the current remained around that value till the end of the experiment in PMFC-B. PMFC-A's current increased to 0.10 mA during the last ten days. In PMFC-B, it was observed that the increase in current production from day 80 to day 90 was associated with a decrease in CH_4 emission flux from 1.88 to 1.46 mg/m^2/h (**Figure 6.6.(b)**), followed by a slight decrease in current production between day 90 and day 110. During that time, the CH_4 emission flux in PMFC-B increased from 1.46 to 2.14 mg/m^2/h. Similar trends were also noticed for PMFC-A. Jung and Regan [579] reported similar trends where CH_4 emission lessened in their MFCs as the output voltage increased. Rizzo et al. [200] found that the transport processes with a higher current could limit CH_4 emission.

Kouzuma et al. [577] indicated that the syntrophic interactions between exoelectrogenic bacteria and fermentative bacteria could facilitate electricity generation in rhizosphere MFCs by promoting the growth of specific types of electricity-producing bacteria. Ishii et al. [580] reported that the electrogenesis is ecologically superior to methanogenesis. Therefore, we can conclude that the electro-biochemical reactions taking place in PMFCs can help in the reduction of CH_4 emissions.

Table 6.1. The average power density, average rice plant biomass production and average CH_4 emission flux over 141 days.

	Shoot height$_{avg/plant}$ (cm)	**Shoot weight$_{avg/plant}$ (g dry mass)**	**Root weight$_{avg/plant}$ (g dry mass)**	**CH_4 emission flux$_{avg/plant}$ (mg/m^2/h)**
PMFC	58.9±1.85^a	0.1964±0.0047^a	0.1133±0.0047^a	1.0281±0.0480^a
NPMFC	--	--	--	--
Control	59±1.75^a	0.1777±0.0078^b	0.1102±.00047^a	2.0254±5.2061^b

Notes: Different letters in the same row indicate significant differences ($p < 0.05$)

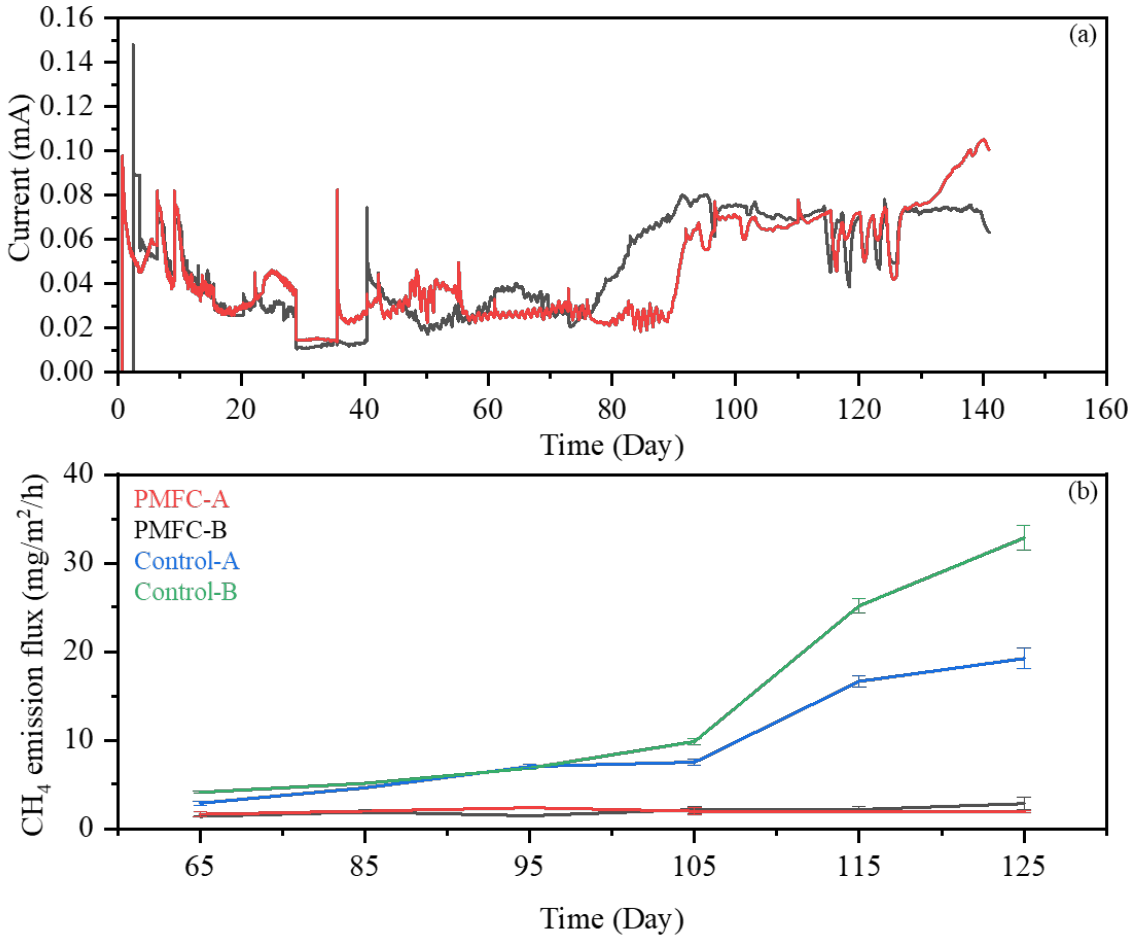

Figure 6.6. (a) The current generation of PMFCs, and (b) the CH_4 emission flux from PMFCs and Controls.

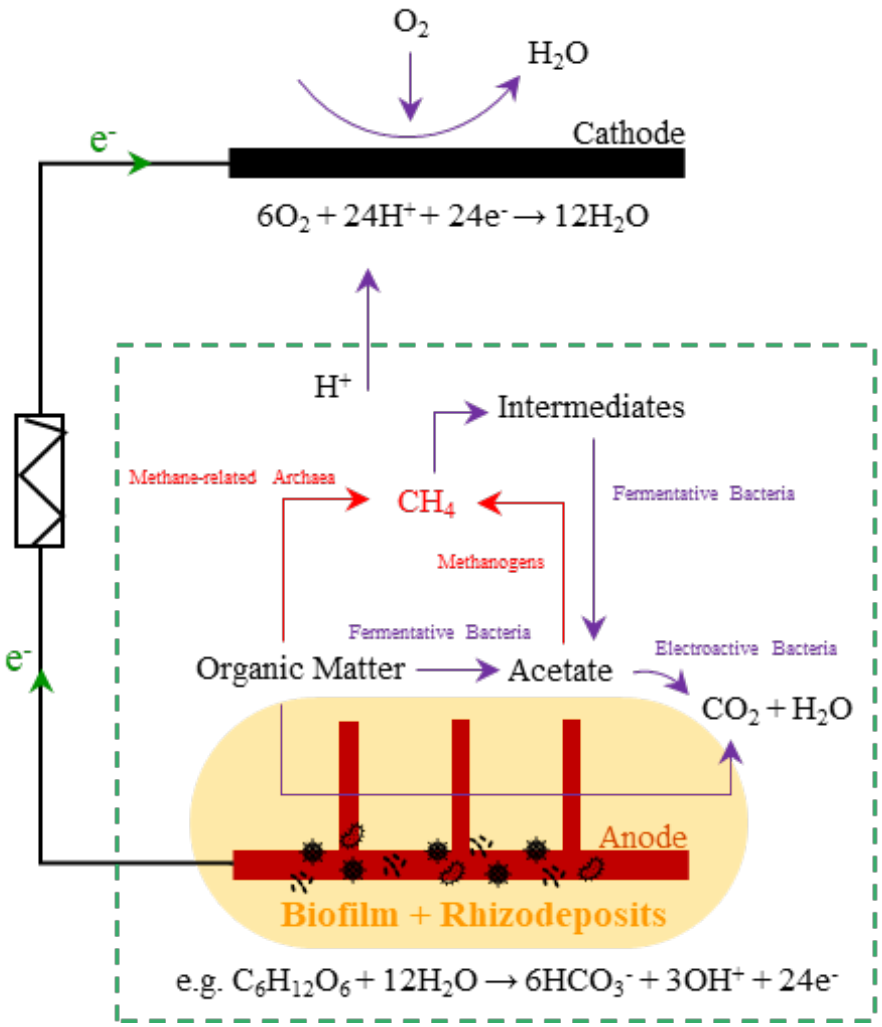

Figure 6.7. Schematic of CH_4 reaction mechanisms in H-PMFC.

6.4.6 Rice growth and biomass yield

During the early stage of the research, the growth of the Controls rice plants and PMFCs was good, and the height of the shoot gradually increased over time (**Figure 6.8.**). 106 days after the startup of the study, the shoot growth slowed in all Controls and PMFCs. At the end of the experiment, PMFC-B (60.75 cm) and Control-B (60.75 cm) showed the highest shoots, followed by Control-A (57.25 cm) and PMFC-A (57.05 cm). The difference, however, was not significant ($p \leq 0.05$). Besides, Table 4.1. showed that the plants with H-MFCs did not significantly affect plant biomass yield; the $shoot_{avg}$/plant of PMFCs was 0.1964 ± 0.0047 g dry mass similar to potted Controls 0.1777 ± 0.0078 g dry mass. These results indicated that the PMFC technology could produce bioelectricity without reducing crop yields [27].

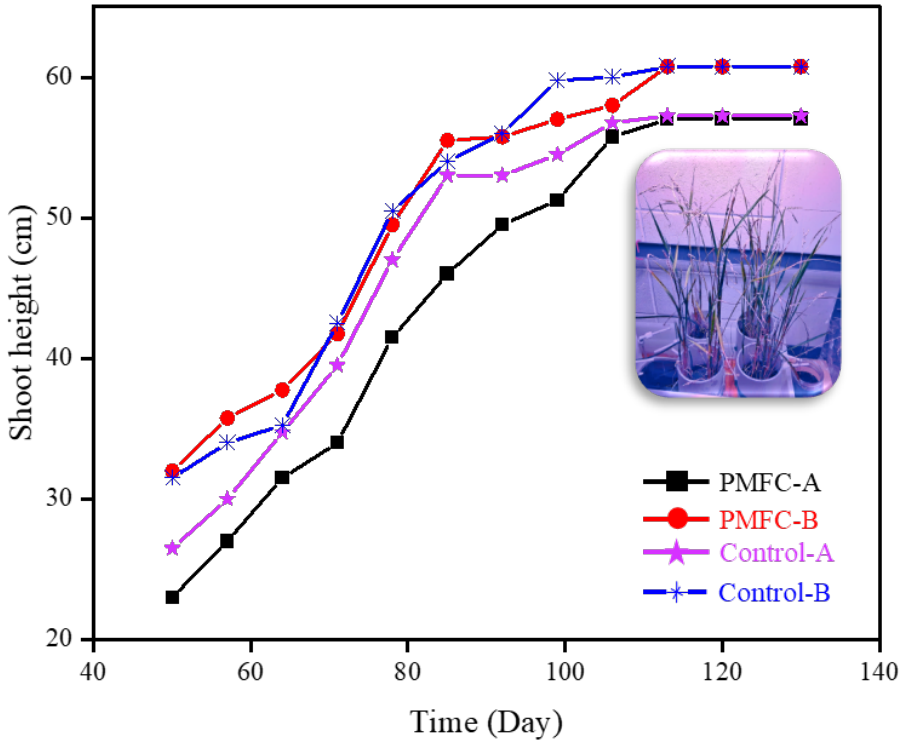

Figure 6.8. The height of the rice shoots of all PMFCs and Controls

6.5 CONCLUSION

In this study, two flow NPMFCs (NPMFC-A and NPMFC-B), two flow PMFCs (PMFC-A and PMFC-B), and two potted rice plants (Control-A and Control-B) were utilized to test the influence of flow H-MFC on CH_4 emission from hydroponically cultivated rice plants. During 141 days of monitoring, PMFC-A showed the highest PD of 504.39 mW/m^3, which was 1.7 times higher than PMFC-B, 1.77 times higher than NPMFC-A, and 4.88 times higher than NPMFC-B. Further, with the help of hotspots of microbes in the rhizodeposition zone, PMFCs displayed higher R_{int} and PD_{max} than the NPMFCs during P-test. The average COD concentration in PMFCs was 1.4 times higher than NPMFCs. The output voltage and COD concentration exhibited a positive relationship, indicating that the COD derived from plants' root secretions could act as the electron donor for electricity generation in PMFCs. However, the root life cycle affected the specific action of rhizodeposits, which caused the fluctuation in bioelectricity production. Operating the flow PMFC while harvesting its electricity does not seem to hinder the growth of hydroponic rice plants.

The average shoot height of PMFCs was 59.00 cm, almost the same as Controls (58.90 cm). The average shoot dry weight of PMFCs was 0.1964 ± 0.0047 g dry mass, similar to potted plants' 0.1777 ± 0.0078 g dry mass. For the entire duration of the experiment, the CH_4 flux from the PMFCs was about 2 times lower than Controls, especially after days 100-110. The current production from PMFCs showed a negative relationship with CH_4 emission flux, which indicated that the bioelectricity generation influences the CH_4 emission from the hydroponic cultivation of rice plants. In brief, our study has demonstrated the synergy effect between H-MFCs and the hydroponic cultivation of rice plants. With the help of H-MFC, the CH_4 emission could be reduced without a decrease in the biomass yield of hydroponic rice plants. The bioelectricity generation and lifetime of PMFCs were also improved by rice plant roots' rhizodeposition and hotspots of microbes' activity. Future PMFC studies could focus on the mechanism of microbe activity hotspots to enhance the performance of PMFCs.

CONNECTING TEXT

This Chapter VI investigated the influence of bioelectricity production on CH_4 emission from H-PMFCs. The results showed that operating the flow H-PMFC while harvesting its electricity does not seem to hinder the growth of hydroponic rice plants. The current production from PMFCs showed a negative relationship with CH_4 emission flux, which indicated that the bioelectricity generation has an influence on the CH_4 emission from the hydroponic cultivation of rice plants. With the help of MFC, the CH_4 emission could be reduced without decreasing biomass yield of hydroponic rice plants.

Rice is often exposed to Fe deficiency because of its cultivation under waterlogged conditions, where Fe is not readily available for plant uptake. In BES, metal ions affect not only biocatalysts but also electrolyte conductivity and internal resistance of the system. Although some research reported the effects of Fe on rice plants or MFC systems, there has been no study to investigate the influence of Fe on H-PMFC systems. Therefore, Chapter V studied the effect of concentration and forms of Fe chelate fertilization on methane emission and electricity generation from H-PMFC. The best forms and concentration ratio of chelated Fe ions, which can maximize the highest electricity production with reduced methane emission in H-PMFC, were also explored.

CHAPTER VII

FE FERTILIZATION FORM AND CONCENTRATION: THE INFLUENCE ON BIOELECTRICITY AND METHANE PRODUCTION FROM HYDROPONIC MICROBIAL FUEL CELLS

7.1 ABSTRACT

This study aimed to evaluate the effect of iron form (Fe^{2+} and Fe^{3+}) and concentration (0 μM, 7.5 μM, and 15 μM) on the biomass production, bioelectricity generation, and methane (CH_4) emissions of hydroponic plant microbial fuel cells (H-PMFCs). Rice plants (*Oryza sativa L.*) were grown in H-PMFCs. During the 90 days of operation, the highest power density (PD_{max}) was observed in Group 7.5-15 of 949.17 Mw/m^3, 4.56 times higher than Group 0-0. When adding single-form iron (Fe^{2+} or Fe^{3+}), the PD_{max} of H-PMFCs was positively correlated with iron concentration. Further, the H-PMFC feed with Fe^{3+} showed higher power output than the feed with Fe^{2+}. Furthermore, the CH_4 emission test indicated that the addition of iron in rice H-PMFCs can decrease the emission of CH_4 in two ways: (i) iron electron acceptors directly inhibit methanogens; (ii) iron electron acceptor enhances the electricity production ability of MFC to inhibit CH_4 production. In comparison with Group 0-0, Group 7.5-15 reduced 65% CH_4 emissions from H-PMFC. Therefore, adding 7.5 μM Fe^{2+} and 15 μM Fe^{3+} showed great potential to enhance the performance of H-PMFCs on biomass production, bioelectricity generation, and CH_4 emission inhibition.

Keywords: ferrous iron, ferric iron, plant microbial fuel cell, methane emission

7.2 INTRODUCTION

Global energy demand is increasing rapidly with the increase in human population and technology development [581]. As a result, a corresponding increase in the use of conventional and non-renewable energy has led to an increase in environmental and human health problems. The resulting increase in greenhouse gas (GHG) emissions from fossil fuels and land in the atmosphere has contributed to global warming in the last few decades [582]. A staple food in several cultures and continents, the cultivation of rice is a primary source of vital and long-lasting greenhouse gases. Compared to wheat and maize, the global warming potentials of the rice crop are 467% and 169%, respectively [4]. Around 30% of global agricultural methane (CH_4) is emitted from rice fields [5]. On a 100-year time horizon, CH_4 comprises a large share of farm emissions with relative global warming potentials 298 times higher than CO_2 [2].

Plant microbial fuel cells (PMFCs) have been demonstrated to alleviate the greenhouse emissions from rice cultivation [583, 584]. PMFC is considered a promising alternative green energy technology that can convert solar energy into bioelectricity with the help of microbes found in the rhizosphere zone of plants, reducing GHG production in the process. [18]. Other advantages of the technology include continuous generation of energy and no adverse effect on plant health [18, 585]. Nevertheless, some optimization of the technology is needed for practical applications. Optimization of both the electrochemical components [586], as well as the plants, is needed for better integration and long-term performance.

Iron (Fe) is of great importance to plant growth and health as the redox-active metal which is involved in various biochemical activities (e.g., respiration, chlorophyll synthesis, pathogen defense, generation and scavenging of reactive oxygen species, nitrogen assimilation, photosynthesis, etc.) [587]. It is also a key cofactor for enzymes, acting as a proton acceptor and donor [588]. Chen et al. [589] found that the addition of 10 μM EDTANa2Fe(II) and 10 μM EDDHAFe(III) showed

the highest biomass production of rice plants. Both Fe deficiency and toxicity can adversely affect plants. Strategy I and Strategy II are the primary mechanisms for Fe uptake in rice plants [590, 591] (**Figure 7.1.**). During Strategy I, Fe^{3+} is reduced to Fe^{2+} by ferric chelate reductase; then, the free Fe^{2+} is chelated by nicotinamide and transported into the cell by ferroprotein. During Strategy II, the root system secretes the secondary metabolite magnetic acid to chelate Fe^{3+}, then ferroprotein transports Fe^{3+} into plant cells [592]. Therefore, both Fe^{2+} and Fe^{3+} are very important to plant health.

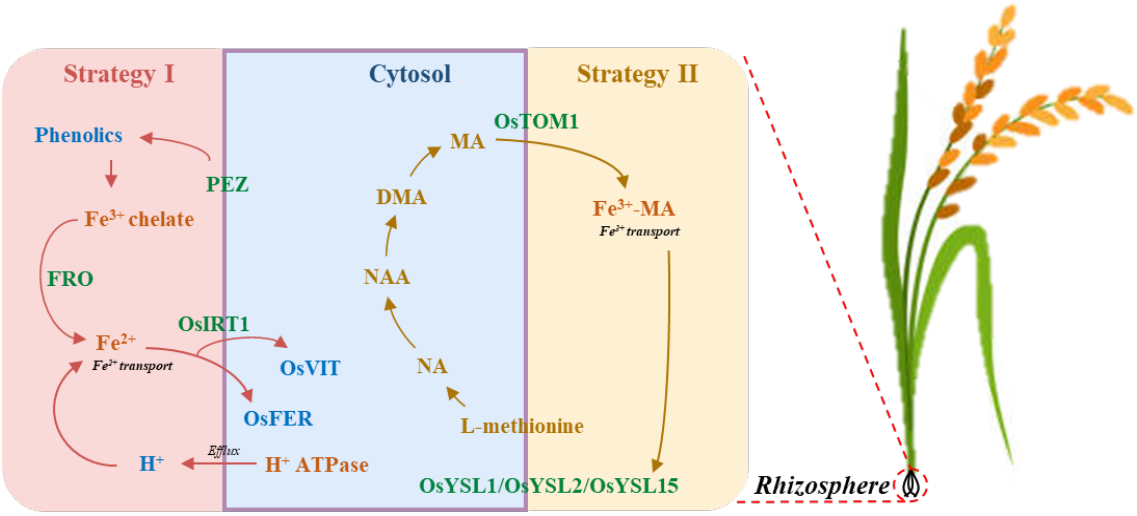

Figure 7.1. Mechanism of iron transport in rice.

The Influence of Fe^{3+}/Fe^{2+} on the electrochemical performance or anode biofilm formation of MFCs has been reported [593, 594]. Iron-chelated materials as cathode catalysts in MFC enhance the oxygen reduction reaction (ORR) in MFCs, resulting in higher electrochemical activity [595]. Wang et al. [596] found that Fe^{3+} supplements accelerate the rapid enrichment of anodophilic consortium in MFCs. The exogenous Fe^{3+} plays a crucial role in flavin secretion and biofilm formation in MFCs [597]. The electrically conductive magnetite derived from Fe^{3+} facilitates direct interspecies electron transfer [598]. Besides, in MFCs, Fe^{3+} could be reduced into Fe^{2+} at the cathode surface [599], then Fe^{2+} reoxidation and precipitation as oxi(hydroxi)des [600]. However, no study has investigated the influence of Fe^{2+} and Fe^{3+} on PMFCs, especially the CH_4 production from hydroponic PMFCs (H-PMFCs).

This work investigates the electrochemical performance, CH_4 emission, and biomass production of H-PMFCs with different concentrations and ratios of Fe^{2+} and Fe^{3+}. Orthogonal array experimental design is used to optimize the contribution of Fe^{2+} and Fe^{3+} on H-PMFCs performance. This study is the first to investigate and report the influence of Fe chelates fertilization form and concentration on H-PMFCs systems; our work provides a more effective method to improve the performance of H-PMFCs.

7.3 MATERIALS AND METHODS

7.3.1 Analytical methods and stock solutions

The experiment was 90 days and conducted in the Automated Research Greenhouse (McGill University, Sainte-Anne-de-Bellevue, Québec, Canada). A Priva Maximizer (Priva North America, Ontario, Canada) was used to control the temperature (day: 12 hours light, 26 ± 2 °C; night: 12 hours darkness, 23 ± 2 °C)

Kimura B solution with some modification was used as the nutrient solution of all H-PMFCs [589]. $MgSO_4$ (280 μM), $(NH_4)_2SO_4$ (180 μM), $Ca(NO_3)_2$ (180 μM), KNO_3 (90 μM), KH_2PO_4 (90 μM), H_3BO_3 (3 μM), $MnCl_2$ (0.5 μM), $CuSO_4$ (2 μM), $ZnSO_4$ (0.4 μM), $(NH_4)_6Mo_7O_{24}$ (1 μM), $FeSO_4/Fe_2(SO_4)_3$ (0, 7.5, or 15 μM) [551]. The different concentrations and forms of Fe are shown in **Table 7.1.** 0.1 μM NaOH was used to adjust the PH of the nutrient solution.

Table 7.1. H-PMFCs with difference of Fe concentration and forms.

Group	Fe(II) (μM)	Fe(III) (μM)
0-0	0	0
0-7.5	0	7.5
0-15	0	15
7.5-0	7.5	0
7.5-7.5	7.5	7.5
7.5-15	7.5	15
15-0	15	0
15-7.5	15	7.5
15-15	15	15

7.3.2 H-PMFCs design

Polyvinyl chloride (PVC) water pipes were used to construct H-PMFCs. Cocopeat moss was utilized as the support matrix. A carbon cloth anode was placed horizontally under the cocopeat matrix, and a round floating air-cathode was placed on the surface of the cocopeat matrix. The distance between the anode and cathode was 150 mm. The insulated stainless-steel wires were used as the current collectors and connected with the electrodes by conductive cement. An outlet port near the bottom to export waste solution in the beaker. A programmable metering pump was used to pump the Kimura B solution [506].

Airtight headspace was used to trap gases for the CH_4 test. A small electric blower on the top of the headspace was used for air mixing. More details about H-PMFC and airtight headspace configuration are shown in **Table 7.2. & Figure 7.2**.

Table 7.2. The material specifications of H-PMFCs.

Materials	Size
Polyvinyl chloride	Diameter:100 mm; Length 250 mm; Volume :1.96 L
Cocopeat moss	3/5 of the volume in flow H-PMFCs
Carbon cloth	Diameter:100 mm; Thickness: 5 mm
Floating air-cathode	Diameter:100 mm; Thickness: 10 mm
Insulated stainless-steel wires	Thickness: 0.5 mm; < 5 Ω/m
Outlet port tube	Diameter: 10 mm; Length: 90 mm
Wastewater beaker	1L capacity
Pump	Capacity: 15 W; fLow rate: 5 mL/h
Airtight headspace	Height: 900 mm; Diameter: 101 mm)

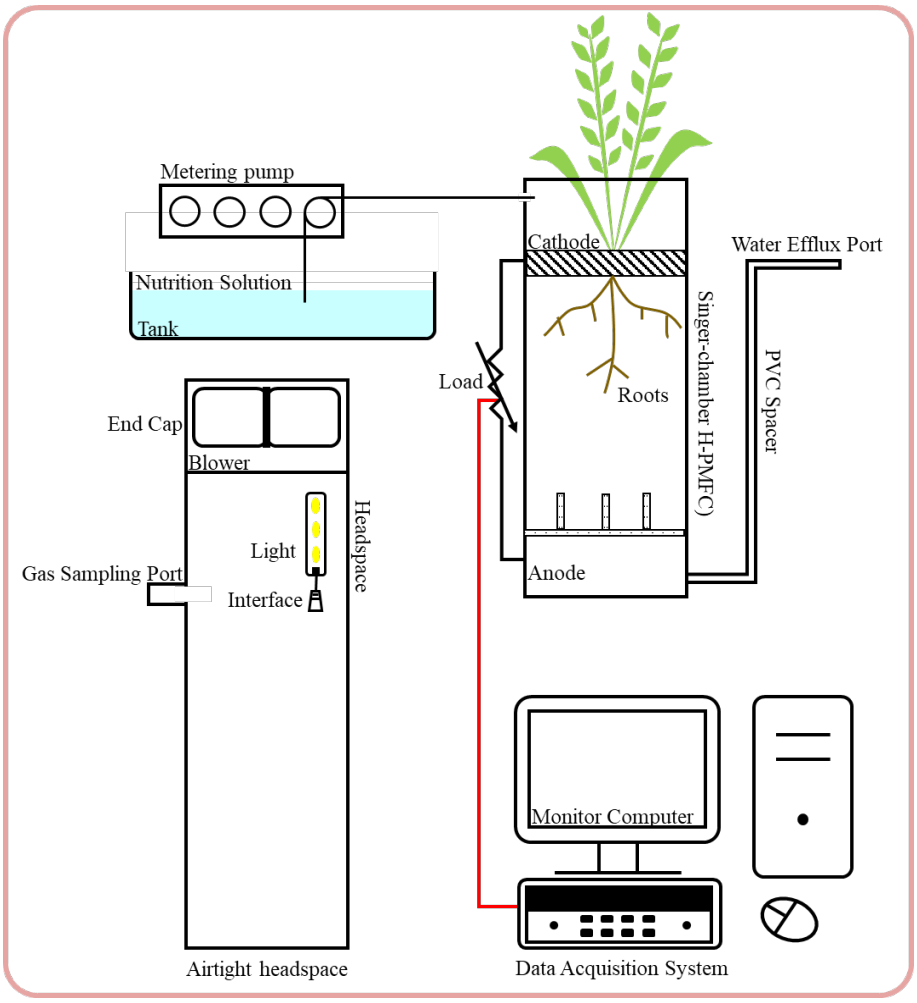

Figure 7.2. The schematic diagram of H-PMFC and methane collection arrangement in airtight headspace.

7.3.3 Floating air-cathode fabrication

The dip-dry method was used to make the floating air-cathodes. The commercially available blue polyurethane sponge of 5 pores/mm (diameter: 8 cm, projected surface area: 50.27 cm^2, thickness: 1.0 cm) was used as the cathode electrode support. The conductive layer and catalyst were carbon black (CB, Vulcan XC 72R, 50 nm, Fuel Cell Earth Co., Ltd). Polytetrafluoroethylene (PTFE, 60 wt% dispersion in H_2O, Sigma-Aldrich Co., Ltd) was used as the binder. The CB/PTFE with the ratio of 6:1 dispersed in ethanol (ethanol: PTFE = 1:15) under ultrasonication (30 min) to form a uniform suspension was setup. The sponge was dipped into the suspension and dried in the oven at 80 °C until the resistance of the sponge was stable

[504].

7.3.4 Experimental design and H-PMFC operation

The external resistance (R_{ext}) in the closed-circuit H-PMFCs ranged between 1000-2000 Ω. The internal resistance (R_{int}) of each H-PMFC was calculated by periodic polarization test (P-test) to optimize power production. The P-test was conducted by varying the R_{ext} from 10,000 to 50 Ω [507]. The P-test was performed on day 2 and 45 of the tests period. The current (I, mA) and power (48P, mW) were calculated by plotting polarization (voltage *vs.* current) and power (output power *vs.* current) figures. The output voltage measurement of each H-MFC was logged (1 min interval) by a data acquisition system (34,970A, Agilent Technologies, Santa Clara, California, USA).

7.3.5 Rice plants cultivation and characterization

7.3.5.1 Rice plant cultivation

Oryza sativa L. cultivar Indian Rani paddy rice was used in this study. The seeds of Indian rain paddy rice were obtained from Rani Foods (United States). Before germination, the seeds were soaked in distilled water for 48 hours. Then, all seeds were germinated on the plate and transplanted at the 3-leaf stage.

7.3.5.2 Measurement of methane

CH_4 generation from H-PMFCs was tested by the static chamber method [27]. The headspace chamber sealed all the H-PMFCs at room temperature for 12 h. Before gas sampling, the internal blower was turned on to thoroughly mix the air inside the headspace. Then, a 2.5 mL gas sample was extracted through the sampling port. All samples were done in triplicate. The concentration of CH_4 was measured by the HP 5890A gas chromatograph (Hewlett Packard, Palo Alto, California, USA), equipped with a Porapak-N column (120 mm × 3mm, 149-177 microns) and a thermal conductivity detector. Helium was used as the carrier gas. The analysis was performed

at a constant oven temperature of 45 °C. The injector and detector temperatures were 210 °C. The concentrations of CH_4 were given in units of parts per million (ppm). The CH_4 emission flux (F, mg/m^2/h) was calculated following Eq.(1) [553, 554]:

$$F = H \times (M_W/M_V) \times [273.2/(273.2 + T)] \times (\Delta C/\Delta t) \quad (7.1)$$

where, H is the chamber height, m; M_w is the CH_4 mole mass, 16.123×10^{-3} mg; M_v is the CH_4 mole volume, 22.41×10^{-3} m^3; T is the chamber air temperature, 23 °C; $\Delta C/\Delta t$ is the change in the CH_4 between the initial and final measurement per unit of time (12 h), ppm.

7.3.5.3 Measurement of plant growth parameters

A measuring tape measured the height of the highest three leaves of each plant as an indicator of rice growth. The nutrition solution PH was measured by a PH meter (AB150, Fisher Scientific, Canada).

At the end of the experiment, the whole rice plants were harvested. The plants were soaked in the sodium hexametaphosphate solution to facilitate the separation of peat moss from the roots [27]. The roots were cut from the shoots, then separately placed in the paper bag to dry. After 48 h drying in the hot air oven at 50 °C, the dry matter content of the shoots and roots were weighed.

7.3.6 Statistical analysis

The experimental data was analyzed by analysis of variance (ANOVA) of the SPSS software (SPSS Inc., Ver. 18, Chicago, IL, USA). The Duncan multiple range test was applied to separate the means and to establish significance, which was accepted at $p < 0.05$.

7.4 RESULTS AND DISCUSSION

7.4.1 Effect of iron concentration and Fe^{2+}/Fe^{3+} ratio on plant growth

Figure 7.3. shows the height of rice shoots from 90 experiment days in H-PMFCs. During the early period (day 30-46), the height of shoots on all rice plants

gradually increased. After 1.5 months of the H-PMFC operation, the shoot growth slowed in all H-PMFCs; similar results were also reported by Khudzari et al. [27]. After day 46, Group 0-7.5 and Group 0-15 exhibited lower plant shoot height in comparison with Group 0-0, which indicated that without Fe^{2+}, the exist of Fe^{3+} in H-PMFCs would inhibit the growth of rice plants. Giri et al. [601] reported that Fe^{3+} does not sufficiently meet plant needs, leading to iron deficiency and stunted growth. Although Fe^{3+} can be reduced into Fe^{2+} at the surface of the cathode in H-PMFCs [599], Fe^{2+} will be re-oxidized and precipitated as oxi(hydroxi)des [600]. Besides, in comparison with Group 0-0, the shorter plant shoot was also observed in Group 15-0, Group 15-7.5, and Group 15-15. This might have resulted result from the Fe^{2+} toxicity to the rice plants, generally occurring at 10-500 mg/L Fe^{2+} concentration [602]. However, although 7.5 μM is higher than 10 mg/L, Group 7.5-0, Group 7.5-7.5, and Group 7.5-15 showed higher shoots than Group 0-0. This may be attributed to the fact that Fe^{2+} could be recovered in H-PMFCs by oxidizing to insoluble $Fe(OH)_3$, then reduced the toxic effects of Fe^{2+} [603]. This phenomenon indicates that H-PMFC could regulate the concentration of iron in the plant nutrient solution and lowers the toxic effect of Fe^{2+} when the Fe^{2+} concentration is $\leq$ 7.5 μM.

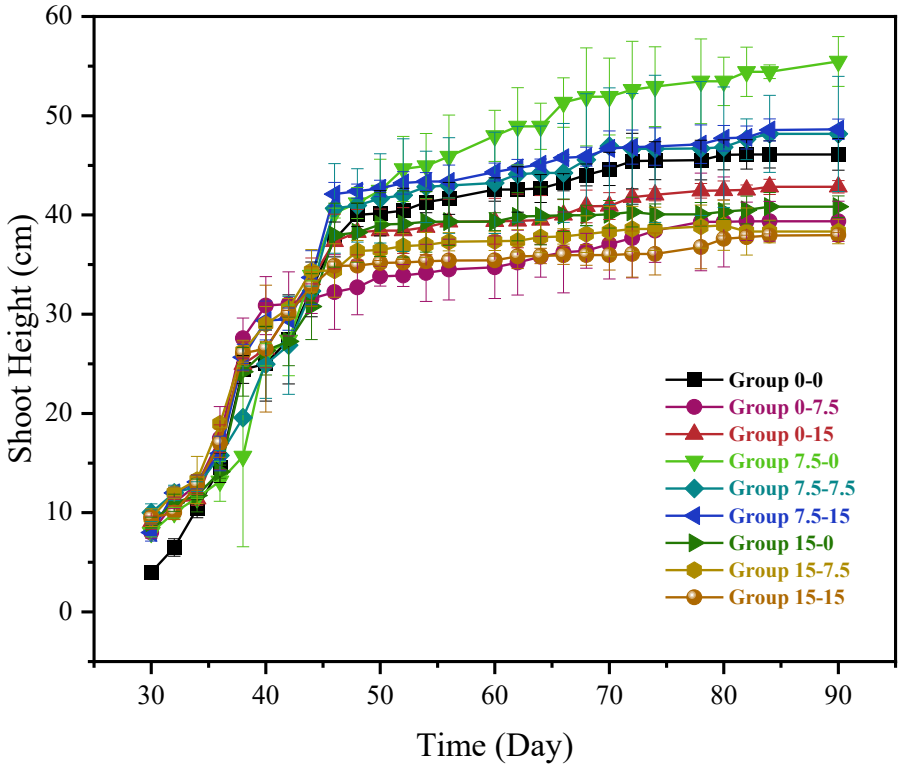

Figure 7.3. The height of the rice shoots of all H-PMFCs.

7.4.2 Effect of iron concentration and Fe^{2+}/Fe^{3+} ratio on plant biomass production

The results of univariate variance analysis for the plant $height_{avg/plant}$ (shoot + root) and plant $weight_{avg/plant}$ (shoot + root) values of experiments are demonstrated in **Table 7.3.** The interaction effect of Fe^{2+}-Fe^{3+} in H-PMFCs for both plant $height_{avg/plant}$ and plant $weight_{avg/plant}$ were significant ($p < 0.001$), especially for plant $weight_{avg/plant}$ ($1.00 > 0.66$). When the concentration of Fe^{2+} was 7.5 or 15 μM, the concentration of Fe^{3+} significantly affected plant $height_{avg/plant}$ ($p < 0.05$). When the concentration of Fe^{3+} was 0, 7.5 or 15 μM, the concentration of Fe^{2+} had a significant effect on plant $height_{avg/plant}$ ($p< 0.001$), especially when Fe^{3+} was 15 μM ($0.91 > 0.86 > 0.67$). Besides, when the concentration of Fe^{2+} was 0, 7.5, or 15 μM), the concentration of Fe3+ significantly affected plant $weight_{avg/plant}$ ($p < 0.001$). When the concentration of Fe^{3+} was 0, 7.5, or 15 μM, the concentration of Fe^{2+} significantly affected plant $weight_{avg/plant}$ ($p< 0.001$).

Table 7.4. shows the rice plant biomass production at the end of the study. In

comparison with Group 0-0, Group 15-0, Group 15-7.5, and Group 15-15 exhibited significantly lower plant $height_{avg/plant}$ and plant $weight_{avg/plant}$ ($p < 0.05$). This because of the Fe^{2+} toxicity to the rice plants. Besides, previous studies proved that high Fe^{2+} concentrations would lead to an imbalance in nutrient uptake by significantly reducing the uptake of other nutrients (e.g., Zn, K, Mn, P, Ca, Mg, etc.), thereby reducing the biomass production of rice plants [604, 605].

We observed that Group 7.5-15 has the highest plant $length_{avg/plant}$ (89.67 ± 1.17 cm) and plant $weight_{avg/plant}$ (14.91 ± 0.02 g dry mass). Therefore, when the concentration of Fe^{2+}-Fe^{3+} was 7.5-15 in H-PMFCs, the rice plants have the best biomass production from H-PMFCs.

Table 7.3. Results of univariate variance analysis for the average plant biomass production and average CH_4 emission flux value during the experiment.

Plant length$_{avg/plant}$ (shoot & root)									
Iron concentration (μM)	Fe^{2+} simple effect			Fe^{3+} simple effect			Fe^{2+}-Fe^{3+} interaction effect		
	F	*p*	Partial η^2	*F*	*p*	Partial η^2	*F*	*p*	Partial η^2
0	2.57	0.10	0.22	55.06	< 0.001	0.86	8.71	< 0.001	0.66
7.5	28.41	<0.001	0.76	18.12	< 0.001	0.67			
15	4.10	0.03	0.22	99.44	< 0.001	0.91			
Plant weight$_{avg/plant}$ (shoot & root)									
Iron concentration (μM)	Fe^{2+} simple effect			Fe^{3+} simple effect			Fe^{2+}-Fe^{3+} interaction effect		
	F	*p*	Partial η^2	*F*	*p*	Partial η^2	*F*	*p*	Partial η^2
0	60062.92	< 0.001	1.00	18795.33	< 0.001	1.00	52427.89	<0.001	1.00
7.5	62197.93	<0.001	1.00	146633.80	<0.001	1.00	--	--	--
15	16296.70	<0.001	1.00	251840.01	<0.001	1.00	--	--	--

CH_4 emission									
Iron concentration (μM)	Fe^{2+} simple effect			Fe^{3+} simple effect			Fe^{2+}-Fe^{3+} interaction effect		
	F	*p*	Partial η^2	*F*	*p*	Partial η^2	*F*	*p*	Partial η^2
0	783.57	<0.001	0.99	301.48	< 0.001	0.97	77.93	< 0.001	0.95
7.5	600.56	<0.001	0.99	84.34	0.005	0.90			
15	390.70	<0.001	0.98	137.86	< 0.001	0.94			

Table 7.4. The average plant biomass production and average CH_4 emission flux during the experiment.

	Plant length$_{avg/plant}$ (cm)	**Plant weight$_{avg/plant}$ (g dry mass)**	**CH_4 emission flux$_{sum\ 50\ days}$ (g/m^2)**
0-0	69.19 ± 2.60 ^{c}	10.09 ± 0.01 ^{d}	122.57 ± 1.25 ^{a}
0-7.5	65.10 ± 2.97 $^{c`de}$	5.65 ± 0.00 ^{g}	85.89 ±1.14 ^{e}
0-15	69.23 ± 2.37 ^{c}	6.65 ± 0.01 ^{f}	66.84 ± 0.27 ^{f}
7.5-0	86.97 ± 4.97 ^{a}	10.25 ± 0.03 ^{c}	92.43 ± 0.93 ^{b}
7.5-7.5	74.87 ± 0.64 ^{b}	11.87 ± 0.02 ^{b}	72.58 ± 1.33 ^{e}
7.5-15	89.67 ± 1.17 ^{a}	14.91 ± 0.02 ^{a}	43.15 ± 2.00 ^{h}
15-0	66.93 ± 1.90 ^{cd}	7.92 ± 0.02 ^{e}	91.85 ± 1.68 ^{c}
15-7.5	63.10 ± 0.79 ^{de}	5.49 ± 0.02 ^{h}	90.46 ± 3.21 ^{d}
15-15	61.03 ± 2.68 ^{e}	6.66 ± 0.02 ^{f}	56.54 ± 2.22 ^{g}

Notes: Different letters in the same row indicate significant differences ($p < 0.05$)

7.4.3 Effect of iron concentration Fe^{2+}/Fe^{3+} ratio on R_{int} and P_{max}

At the beginning of the experiment, all H-PMFCs were running under an open circuit for two days. The previous study found that operating MFCs under open-circuit conditions helped compensate for carbon consumption led by the anodophilic activity and sustain the long-term energy generation to harvest more electrical energy [27, 606].

The P-test was conducted on day 2 and day 45. The effect of iron concentration on R_{int} and PD_{max} from polarization tests on all H-PMFCs is demonstrated in **Figure 7.4.(a) & (b)**. After 45 days of running, the R_{int} of all H-PMFCs showed an increasing trend, which is in accordance with our previous study [585] (**Figure 7.4.(a)**). Group 0-0 has the lowest R_{int} on both day 2 and 45 (880 Ω & 1024 Ω). This might be attributed to the lower concentration of charge-transfer electrolyte in Group 0-0 compared to

iron-containing groups. Fan et al. [607] reported that when MFCs equipped with the same size and material anode and cathode, the concentration of the charge transfer electrolyte is inversely proportional to R_{int}.

According to the thermodynamics second law and the Nernst eq, the voltage consists of the anode potential and cathode potential:

$$\Delta E = E_{cathde} - E_{anthode} \tag{7.2}$$

The anode potential ($E_{anthode}$) is decided by microbial activity, and the cathode potential ($E_{cathode}$) could be analyzed by Nernst eq:

$$E_{M^{n+}/M} = E° + \frac{RT}{nF} ln \frac{a_{M^{n+}}}{a_M} \tag{7.3}$$

where, $E°$ is standard electrode potential, R is molar gas constant, 8.314 J/mol/K; F is Faraday's constant, 96,485 C/mol; $\overline{a_{M^{n+}}}$ and a_M are the activities of the oxidized M^{n+} and reduced M species.

The possible cathode-reaction are as follows:

$$Fe^{3+} + e^- \rightleftharpoons Fe^{2+} \tag{7.4}$$

$$Fe^{2+} + 2H_2O \rightarrow Fe(OH)_2 \downarrow + 2H^+ \tag{7.5}$$

$$6O_2 + 24H^+ + 24e^- \rightarrow 12H_2O \tag{7.6}$$

$$2Fe^{2+} + 2H^+ + H_2O_2 \rightarrow Fe^{3+} + 2H_2O \text{ (biologically)} \tag{7.7}$$

The redox potential of Fe^{3+} is +0.77 V *vs.* NHE, pure oxygen is 1.23 V *vs.* NHE, and reaction (7.7) is +850 to 950 mV *vs.* NHE [608, 609]. The addition of iron in MFCs could promote the growth of anode microbes [596], and Fe^{3+}/Fe^{2+} electron pairs around the anode act as an electron mediator to promote the transfer of electrons to the cathode [610].

When the addition of Fe^{2+} was 7.5, with the concentration of Fe^{3+} increased, the R_{int} showed a decreasing trend ($R_{int\ Group\ 7.5\text{-}0} > R_{int\ Group 7.5\text{-}7.5} > R_{int\ Group\ 7.5\text{-}15}$), a similar phenomenon also noticed for Group 0-7.5 and Group 0-15 (1150 Ω > 1113 Ω), as well as Group 15-7.5 and Group 15-15 (1298 Ω > 1070 Ω). This decreasing trend of R_{int} is possible because a higher Fe concentration inhibits anodically electrogenic microorganism activity and increase E_{anode} [611], leading to a decrease in ΔE (equation (7.2)). Yoon et al. [471] reported that the potential of MFCs (E) correlates positively

with R_{int}. However, the R_{int} of Group 15-7.5 (1298 Ω) and Group 15-15 (1070 Ω) was higher than Group 15-0 (1031 Ω). This may be attributed to the H^+ and Fe^{3+}/Fe^{2+} electron pairs concentration near the cathode electrode surface having a positive influence on the cathode electrode potential when the concentration of Fe^{2+} was 15 µM [608] (equation (7.3)-(7.7)).

In comparison with day 2, the PD_{max} of all H-PMFCs decreased sharply, which was attributed to the R_{int} of H-PMFCs (**Figure 7.4.(b)**). Our previous study noticed that for H-PMFC, the PD_{max} is inversely related to R_{int}, the increasing R_{int} resulted in a decline of PD_{max} [585]. The highest PD_{max} value was found in Group 7.5-15 on day 45 (58.36 mW/m^3). This is because the PMFCs can obtain more carbon sources from plant rhizodeposition, which vary over growth stages and plant health [612]. Besides, the microbes' hotpots around the rhizosphere could improve the activity and exudation of microbes [564]. As mentioned earlier, Group 7.5-15 exhibited the highest biomass production capacity; therefore, rice plants grown in H-PMFC with Fe^{2+}-Fe^{3+} concentrations of 7.5-15 µM had the highest carbon source production capacity.

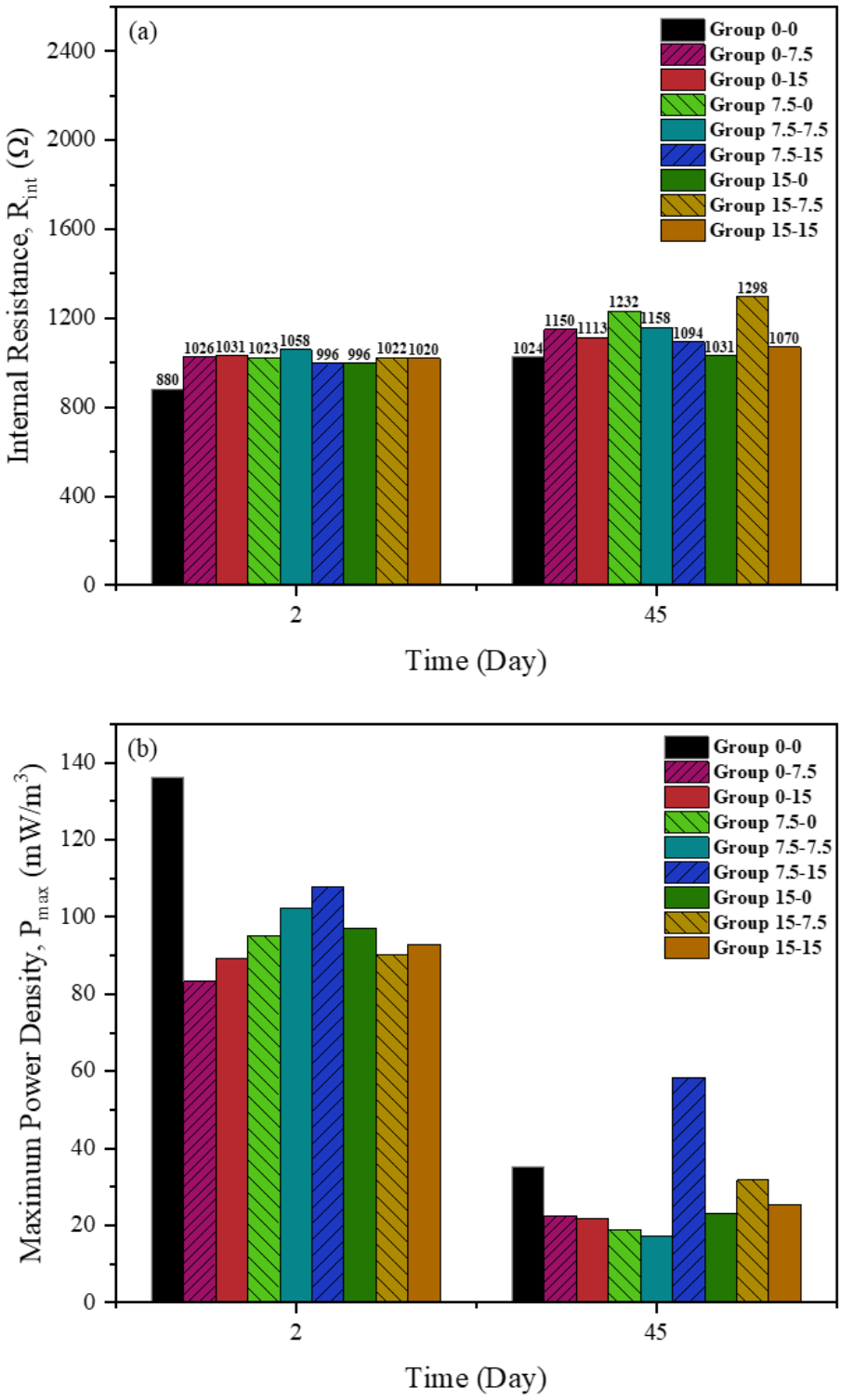

Figure 7.4. The (a) internal resistance and (b) maximum power density from polarization tests conducted on day 2 and day 45 of all H-PMFCs.

7.4.4 Effect of iron concentration and ratio on electricity-generation of H-PMFCs

Figure 7.5.(a)-(d) exhibits the power density (PD) performance of all H-PMFCs over 90 experiment days. The first peaks for all H-PMFCs were observed at the beginning of the experiment (day 10~20), which were attributable to the abundance of carbon sources in the cocopeat moss and nutrition solution [27]. Besides, a declining trend was noticed for all H-PMFCs at the end of the study, which was associated with decreased rhizodeposition. Nitisoravut et al. [18] reported that when plants age, rhizodeposition production also decreases. Group 0-0 reached its maximum PD (PD_{max}) of 208.02 mW/m^3 at day 10 after being connected with external resistance (R_{ext}), followed by a decline in PD_{max}. Khudzari et al. also noticed a similar phenomenon [27], which indicated that Group 0-0 consumed the most easily degradable organic materials. Despite the PD of Group 0-0 showing an upward trend after day 77 due to the rhizodeposition and microbes' hotspots, the PD_{max} between day 77~90 was still lower than day 10 (183.04 mW/m^3 *vs.* 208.02 mW/m^3). Besides, Group 0-0 showed the lowest PD over the experiment among all H-PMFCs (**Figure 7.5.(a)-(d)**), which may be the result of the Fe deficiency of Group 0-0. Researchers demonstrated that due to the low phytosiderophore production, rice plants are highly susceptible to Fe deficiency [613], which resulted in decreased abundance of photosynthetic proteins [614], reduced electron transport chain components [615], and inhibited root elongation [616].

In **Figure 7.5.(a)** Group15-0 shows the highest PD_{max} of 397.84 mW/m^3, followed by Group 7.5-0 (327.36 mW/m^3) and Group 0-0 (208.02 mW/m^3). Thus, when the F^{3+} concentration was 0 μM, the PD_{max} of H-PMFCs increased with the Fe^{2+} concentration increased. A similar trend was also noticed in **Figure 7.5.(b)**, Group 0-15 exhibits the highest PD_{max} of 626.51 mW/m^3, followed by Group 0-7.5 of 534.85 mW/m^3. It can be seen that H-PMFCs feed with the Fe^{3+} has higher power output than feed with the Fe^{2+}. We hypothesize that the difference in PD was associated with oxygen reaction in H-PMFCs around the cathode. A large amount of available energy

is required to establish the overpotential to drive oxygen reduction in MFCs [599]. Ter Heijne et al. [599] proved that during the conversion of Fe^{3+} to Fe^{2+} (equation (7.4)) around the cathode in MFCs, the electron transfer reaction considerably reduced the cathodic overpotential around the cathode. Therefore, H-PMFC feed with Fe^{3+} showed higher power generation ability than feed with Fe^{2+}.

When the Fe^{2+} concentration was constant (7.5 or 15 μM) (**Figure 7.5.(c) & (d)**), the increase of Fe^{3+} concentration showed a positive fluence on the power output of H-PMFCs. In **Figure 7.5.(c)** Group 7.5-15 has the highest PD_{max} of 949.17 $mW/m^{3,}$ followed by Group 7.5-7.5 (479.40 mW/m^3) and Group 7.5-0. **Figure 7.5.(d)** Group 15-15 shows the highest PD_{max} of 573.45 mW/m^3, followed by Group 15-7.5 (540.25 mW/m^3) and Group 15-0. Group 7.5-15 is noteworthy, demonstrating the highest PD_{max} among all H-PMFCs. This difference might be attributed to the growth of rice plants in Grouup 7.5-15, which exhibited the best biomass yield ability and carbon source generation capacity.

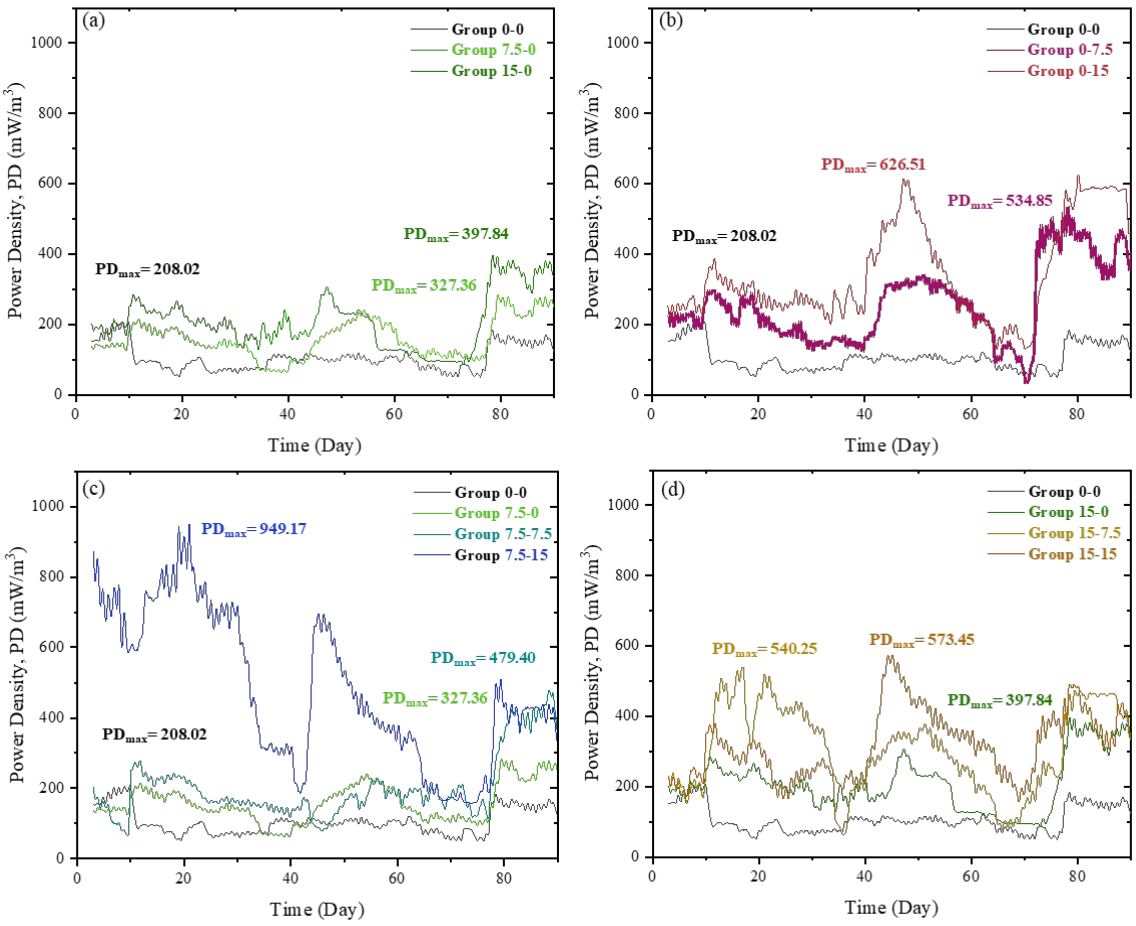

Figure 7.5. The performance of (a) Group 0-0, Group 7.5-0, and Group 15-0; (b) Group 0-0, Group 0-7.5, and Group 0-15; (c) Group 0-0, Group 7.5-0, Group 7.5-7.5, and Group 7.5-15; (d) Group 0-0, Group 15-0, Group 15-7.5, and Group 15-15 in terms of power density.

7.4.5 Effect of iron concentration Fe^{2+}/Fe^{3+} ratio on methane flux emissions

The results of univariate variance analysis for the CH_4 emission from H-PMFCs are displayed in **Table 7.3**. The interaction effect of Fe^{2+}-Fe^{3+} in H-PMFCs for CH_4 emission was significant ($p < 0.001$). From the results of the simple effect of Fe^{2+} and Fe^{3+}, when the concentration of Fe^{2+} was 0, 7.5, or 15 µM, the concentration of Fe^{3+} has a significant impact on CH_4 emission ($p < 0.01$); when the concentration of Fe^{3+} was 0, 7.5 or 15 µM, the concentration of Fe^{2+} had a significant effect on CH_4 emission ($p< 0.001$). Besides, the simple impact of Fe^{2+} was higher than Fe^{3+} ($0.99 > 0.97$).

In **Table 7.4.** Group 0-0 shows the highest CH_4 production over 50 days of operation (122.57 ± 1.25 g/m^2). This phenomenon suggests that feeding iron into rice PMFCs helps to reduce CH_4 emissions. Some studies found that iron oxides could facilitate CH_4 oxidation by iron-reducing bacteria, and adding Fe^{3+} can decrease the abundance of methanogens through toxic effects [617, 618]. Besides, Hanke et al. [619] pointed out that Fe^{3+} can inhibit CH_4 production from the paddy field by reducing to Fe^{2+}, which may also promote metabolism. Hu et al. [620] found that adding Fe^{2+} leads to lower microbial activity and biomass, decreasing CH_4 emission. The amount of CH_4 emission from Group 0-7.5, Group 0-15, Group 7.5-0, and Group 15-0 were 85.89 ±1.14 g/m^2, 66.84 ± 0.27 g/m^2, 92.43 ± 0.93 g/m^2, and 91.85 ± 1.68 g/m^2, respectively. This result indicates that Fe^{3+} has a higher inhibitory effect on CH_4 emission, proportional to its concentration. Besides, it also shows that when the concentration of Fe^{3+} was 0 µM, the CH_4 production decreased with the increasing Fe^{2+} concentration. The lowest CH_4 emission was found in Group 7.5-15 of 43.15 ± 2.00 g/m^2, followed by Group 15-15 of 56.54 ± 2.22 g/m^2. It can be noticed that Fe^{2+} and Fe^{3+}- in H-PMFCs have a synergistic effect on CH_4 suppression. However, this synergistic effect was weakened when Fe^{2+} concentration increased to 15 µM. This may be because when adding enough Fe^{2+}, equation (7.4) tended to move in the left direction, inhibiting the reduction from Fe^{3+} to Fe^{2+} [620].

Figure 7.6. exhibits the current and CH_4 emission flux trend of all H-PMFCs from monitoring day 40 to 90. It was observed that the decrease in the CH_4 emission rate was associated with the increase in the current generation. A similar trend was also reported by Jung and Regan [579]. Rizzo et al. [200] also found that the higher current transport process can limit CH_4 emission. This is probably related to the syntrophic interactions between exoelectrogenic and fermentative bacteria. These syntrophic interactions can improve the electricity production in the rhizosphere of H-PMFCs [577]. Therefore, we can conclude that iron addition in rice H-PMFCs can reduce CH_4 emission in two ways: (i) iron electron acceptors directly inhibiting methanogens; (ii) iron electron acceptors promoting the electricity production of MFC to inhibit CH_4 production.

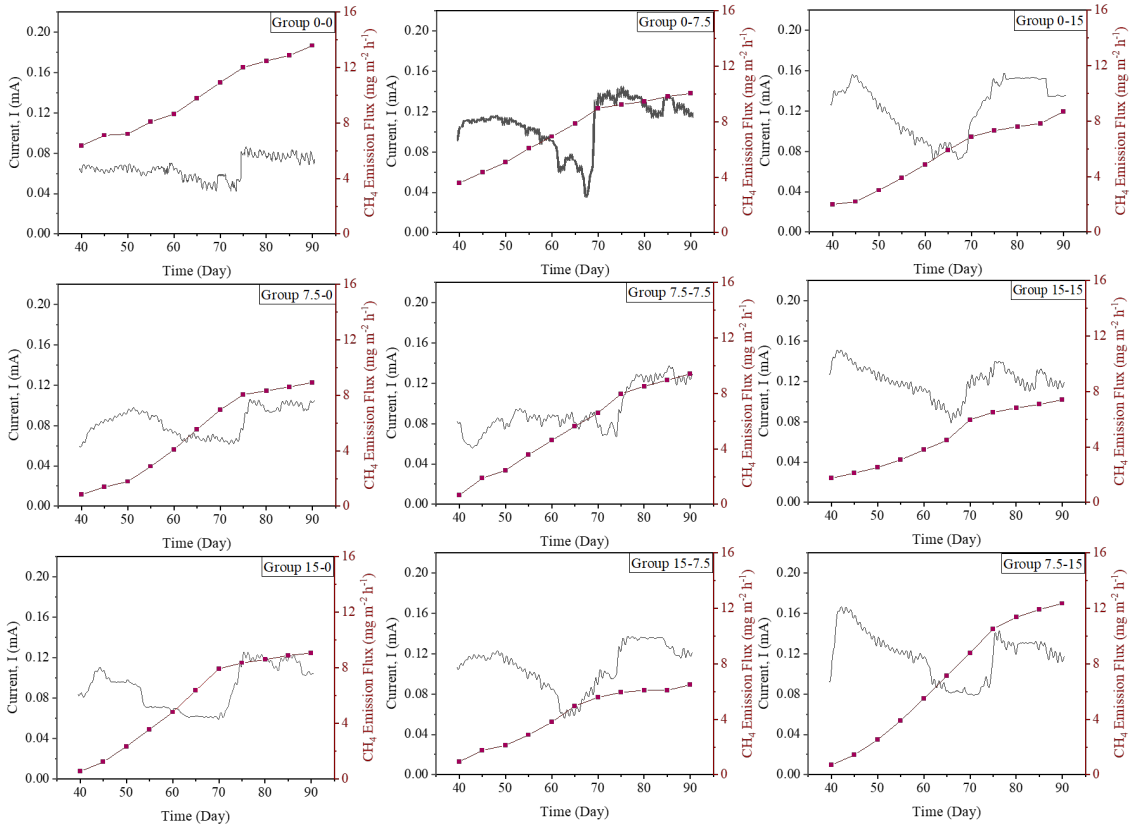

Figure 7.6. The current generation and CH_4 emission flux trend of all H-PMFCs for 50 days.

7.5 CONCLUSION

In the present study, nine H-PMFCs were utilized to test the influence of different forms and concentrations of iron on rice plants' growth, MFC electricity generation, and CH_4 emission from hydroponically cultivated rice plants. During the 90 days of monitoring, Group 7.5-0 shows the highest shoots of 55.47 ± 2.50 cm, which is 1.14 times higher than Group 7.5-15. Nonetheless, Group 7.5-15 shows the highest overall biomass production, including plant $length_{avg/plant}$ (89.67 ± 1.17 cm) and plant $weight_{avg/plant}$ (14.91 ± 0.02 g dry mass), which were 1.03 times and 1.45 times higher than Group 7.5-0, as well as 1.30 times and 1.48 times higher than Group 0-0. These results indicate that when the Fe^{2+} was 7.5 µM and Fe^{3+} was 15 µM, H-PMFCs can regulate its concentration in the nutrient solution and lower the influence of Fe^{2+} toxicity on rice plants. Besides, the iron at appropriate concentrations

facilitated the electricity generation of H-PMFCs. H-PMFCs supplemented with 7.5 μM Fe^{2+} and 15 μM Fe^{3+} obtained the highest PD_{max} of 949.17 mW/m^{3+}, 4.56 times higher than Group 0-0. For the CH_4 test, Group 7.5-15 exhibited the lowest CH_4 emission flux of 43.15 g/m^2, 2.84 times lower than Group 0-0. Therefore, we found that H-PMFCs can decrease the CH_4 generation in two ways with the addition of iron: (i) iron electron acceptors directly inhibiting methanogens; (ii) iron electron acceptor enhancing the electricity production ability of MFC to inhibit CH_4 production.

In brief, our work has demonstrated the potential application of adding Fe^{2+} and Fe^{3+} into H-PMFCs to enhance plant biomass yield and bioelectricity generation, as well as reducing CH_4 emissions. However, the influence of iron on microbial community diversity in hydroponic rice H-PMFCs is still unclear. Further studies can focus on investigating the effects of different forms and concentrations of iron on H-PMFC microbial species.

CONNECTING TEXT

This Chapter VII evaluated the influence of iron fertilization on biomass production, bioelectricity generation, and CH_4 emissions of H-PMFCs. The highest biomass and bioelectricity were observed in Group 7.5-15 (Plant $length_{avg/plant}$: 89.67 ± 1.17 cm; Plant $weight_{avg/plant}$ 14.91 ± 0.02 g dry mass; PD_{max}: 949.17 mW/m^3). The CH_4 test showed that the addition of iron fertilizer in H-PMFCs can decrease the emission of CH_4 in two ways: (i) iron electron acceptors directly inhibiting methanogens; (ii) iron electron acceptor enhancing the electricity production ability of MFC to inhibit CH_4 production. In comparison with Group 0-0, Group 7.5-15 reduced 65% CH_4 emissions from H-PMFC. Therefore, the addition of 7.5 μM Fe^{2+} and 15 μM Fe^{3+} showed great potential to enhance the performance of H-PMFCs.

In Chapter VIII, to explore an H-PMFC system to address the needs of future smart agriculture applications, the possibility of controlling biomass production, bioelectricity generation, and CH_4 emissions from hydroponic rice plants (Oryza sativa L.) under different R_{ext}/R_{int} ratios were tested.

CHAPTER VIII

EXTERNAL RESISTANCE AS A POTENTIAL TOOL FOR BIOELECTRICITY AND METHANE EMISSION CONTROL FROM RICE PLANTS IN HYDROPONIC MICROBIAL FUEL CELL

8.1. ABSTRACT

Recently, hydroponic plant microbial fuel cell (H-PMFC) was incorporated into rice plants to decrease methane (CH_4) production while generating bioelectricity. However, no information is available about the effect of the external/internal resistance (R_{ext}/R_{int}) ratio on the performance of H-PMFCs during rice plant growth. To study the possibility of controlling biomass production, bioelectricity generation, and CH_4 emissions from hydroponic rice plants (Oryza sativa L.) under different R_{ext}/R_{int} ratios, three H-PMFCs (H-PMFC-A: $R_{ext} < R_{int}$; H-PMFC-B: $R_{ext} = R_{int}$; H-PMFC-C: $R_{ext} > R_{int}$) were built. Results showed that H-PMFC-B ($R_{ext} = R_{int}$) has the highest biomass yield. H-PMFC-C ($R_{ext} > R_{int}$) displayed the highest average power density (PD), which was 4.77 and 1.23 times higher than H-PMFC-A and H-PMFC-B over 131 days of operation. The maximum PD was obtained from H-PMFC-C of 536.79 mW/m^3 when R_{ext}/R_{int} = 150%. The highest current with the lowest CH_4 was noted for H-PMFC-A (0.14 mA and 453.52 ± 0.28 $g/m^2/h$). The CH_4 emission exhibits an inverse trend with current production, decreasing with the R_{ext}/R_{int} decreased from 50% to 5%. The total CH_4 emission flux in H-PMFC-A was 1.42 and 2.07 times lower than H-PMFC-B and H-PMFC-C, respectively. Furthermore, the COD removal rate in H-PMFCs negatively correlates with R_{ext}/R_{int}, and the R_{ext} does not affect the COD removal rate when $50\% \leq R_{ext}/R_{int} \leq 150\%$. The above results indicated that the performance of H-PMFCs can be controlled by changing R_{ext}/R_{int}

ratio according to actual needs. If the goal is to achieve higher biomass production, then $R_{ext} = R_{int}$; to obtain the highest PD_{max}, then $R_{ext} > R_{int}$; to get the highest current and lowest CH_4 generation, then $R_{ext} < R_{int.}$

Keywords: bioelectricity generation control; hydroponic rice plants; methane emission control; plant microbial fuel cell

8.2. INTRODUCTION

As one of the main crops, rice dominates food production and consumption worldwide, accounting for over 21% of the human caloric requirements and up to 76% calorific intake of Southeast Asian inhabitants [621]. However, paddy rice contributes about 11% of anthropogenic methane (CH_4) emissions [622, 623]. Based on yield, rice cultivation has more than three times the global warming potential (GWP) of greenhouse gas emissions than wheat/maize and twenty-five times the GWP of CO_2 [576, 624]. The global rice production demand increases as the population grows [625]. Therefore, the elevated CH_4 concentrations in the atmosphere (global average of about 1875 ppb) raise concerns in relation to global warming [626].

The anaerobic decomposition of organic matter is the leading cause of methane formation. Firstly, bacteria degrade organic polymers into monomers. Then, monomers are converted to various organic acids. Thirdly, formed acetate, CO_2, and H_2 are transformed into CH_4 by methanogens [578]. Under waterlogged conditions, about 90% of CH_4 exchange with the rhizosphere occurs via plants' aerenchyma [12]. Thus, a promising method to reduce CH_4 emissions is to prevent CH_4 formation around the rhizosphere, e.g., introduce alternative electron acceptors. In recent years, microbial fuel cell (MFC) has gained lots of attention in producing renewable electrical energy from the degradation of various organic matters by living microorganisms [627]. Plant microbial fuel cell (PMFC) is an MFC-derivate device that generates electricity by degrading root deposits using anode bacteria. PMFCs have biocontrol and bioprocess structures and can be seen as a kind of biosystem that could convert solar energy into bioelectricity. The integral component of PMFCs consists of living plants, anode, cathode, supporting matrix, and external resistance (R_{ext}) [628]. $R_{ext,}$ also called circuit load, dissipates the electrical energy and controls the characteristic outputs of PMFCs [629]. R_{ext} affects the performance of PMFCs by controlling the flow of electrons from anode to cathode. Theoretically, the high R_{ext} results in high cell voltages and low current, and vice versa. The microbial diversity

and metabolism also changes when different R_{ext} was applied to MFCs [559]. Besides, Zhang et al. [630] demonstrated that the CH_4 emission from constructed wetland-MFC (CW-MFC) was significantly reduced after connecting R_{ext}. In MFC studies to date, the effect of R_{ext} has been adequately characterized. The lower R_{ext} leads to a higher power output and a thinner biofilm [631-633]. The higher R_{ext} result in s higher CH_4 emissions [634, 635]. However, all mentioned studies only consider the effects of R_{ext}, they ignore internal resistance (R_{int}) which will keep changing during the MFC operation, especially PMFC due to the growth of plant roots.

R_{ext} control could be a simple and promising operation tool for MFC-in corporation in agricultural processes as it is likely to affect CH_4 emission level, biomass production and bioelectricity generation from rice hydroponic PMFCs (H-PMFCs). Therefore, this study evaluates the possibility mentioned above. To achieve this goal, three H-PMFCs (H-PMFC-A: $R_{ext} < R_{int}$, $R_{ext}/R_{int} <1$; H-PMFC-B: $R_{ext} = R_{int}$, H-PMFC-C: $R_{ext} > R_{int}$ $R_{ext}/R_{int} >100\%$) were constructed with different R_{ext}/R_{int} ratio. To the best of our knowledge, this is the first report to explore the control of CH_4 emission from H-PMFC with rice plants by investigating the ratio of R_{ext}/R_{int}. Our work provides a promising outlook on how low-carbon agriculture may be achieved through the incorporation of MFCs in cultivating high greenhouse gas emitting plants.

8.3. MATERIALS AND METHODS

This study was carried out over 131 days and conducted in the Post-Harvest Engineering Laboratory, McGill University (Sainte-Anne-de-Bellevue, Québec, Canada). A 1000 W LED Plant Grow Light (TOLYS) was used to control the photoperiod (12 hours light and 12 hours darkness) at room temperature (light: 26 ± 2◦C; darkness: 23 ± 2◦C).

8.3.1. H-PMFCs design and construction

Membrane-less air floating cathode H-PMFCs were built using polyvinyl

chloride (PVC) water pipes - the H-PMFC design used in our earlier study [636]. Briefly, cocopeat moss with sodium acetate was utilized as the support matrix and carbon sources. Under the cocopeat moss matrix, a carbon cloth anode was placed horizontally. On the surface of the cocopeat moss matrix, a round floating air-cathode was placed (150 mm from the anode). The anode and cathode electrodes were connected by insulated stainless-steel wires used as the current collectors. An outlet port near the bottom to export waste solution in the beaker. Kimura B solution with some modification was used as the nutrient solution of all H-PMFCs [551]. 0.1 mM NaOH was used to adjust the pH of the nutrient solution. A programmable metering pump was used to pump the Kimura B solution [506].

Airtight headspace was used to trap gases for the CH_4 test. A small electric blower on the top of the headspace was used for air mixing. More details about H-PMFC and airtight headspace are exhibited in **Table 8.1. & Figure 8.1.**

Table 8.1. The material specifications of all H-PMFCs.

Materials	Size
Polyvinyl chloride	Diameter:100 mm; Length 250 mm; Volume :1.96 L
Cocopeat moss matrix	3/5 of the volume in flow H-PMFCs
Carbon cloth	Diameter:100 mm; Thickness: 5 mm
Floating air-cathode	Diameter:100 mm; Thickness: 10 mm
Insulated stainless-steel wires	Thickness: 0.5 mm; < 5 Ω/m
Outlet port tube	Diameter: 10 mm; Length: 90 mm
Wastewater beaker	1L capacity
Pump	Capacity: 15 W; Flow rate: 5 mL/h
Airtight headspace	Height: 900 mm; Diameter: 101 mm)

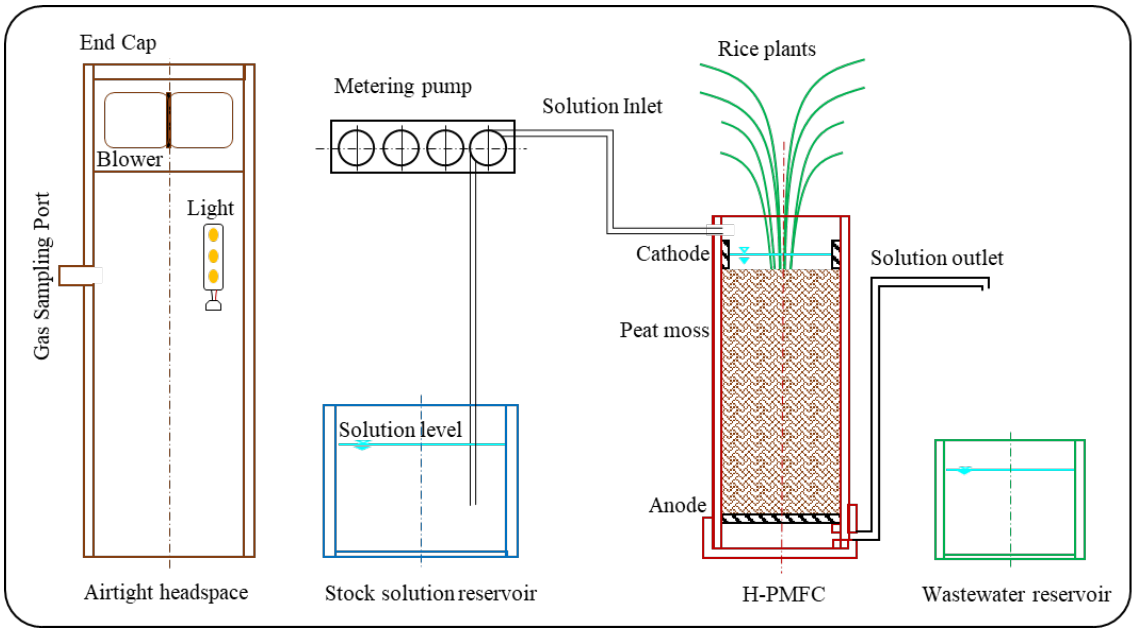

Figure 8.1. The schematic diagram of H-PMFCs.

8.3.2. Experimental design

Three H-PMFCs (H-PMFC-A: $R_{ext} < R_{int}$; H-PMFC-B: $R_{ext} = R_{int}$; H-PMFC-C: $R_{ext} > R_{int}$), were set as shown in **Table 8.2**. All H-PMFCs were started in open-circuit (OC) mode, then switched to close-circuit (CC) mode. Two polarization tests (P-tests) were performed under OC conditions (OC-1 and OC-2), and four P-tests were performed under CC conditions (CC-1, CC-2, CC3, and CC-4).

Table 8.2. The R_{ext}/R_{int} ratio design of all H-PMFCs.

	H-PMFC-A	H-PMFC-B	H-PMFC-C
OC-1	--	--	--
OC-2	--	--	--
CC-1	$R_{ext}/R_{int} = 50\%$	$R_{ext}/R_{int} = 100\%$	$R_{ext}/R_{int} = 150\%$
CC-2	$R_{ext}/R_{int} = 10\%$	$R_{ext}/R_{int} = 100\%$	$R_{ext}/R_{int} = 500\%$
CC-3	$R_{ext}/R_{int} = 9\%$	$R_{ext}/R_{int} = 100\%$	$R_{ext}/R_{int} = 1000\%$
CC-4	$R_{ext}/R_{int} = 5\%$	$R_{ext}/R_{int} = 100\%$	$R_{ext}/R_{int} = 2000\%$

*OC, open circuit; CC, close-circuit. The number represents the times to do the P-test under open circuit or close-circuit

8.3.3. Rice plants cultivation

Oryza sativa L. cultivar Indian Rani paddy rice was used in this study. The seeds of Indian rain paddy rice were obtained from Rani Foods (United States). Before germination, the seeds were soaked in distilled water for 48 hours. Then, all seeds were germinated on the plate and transplanted at the 3-leaf stage.

8.3.4. Measurement of plant growth parameters and biomass

A measuring tape was used for measuring the height of the highest three leaves of each plant as an indicator of rice growth. The nutrition solution pH was measured by a pH meter (AB150, Fisher Scientific, Canada).

At the end of the experiment, the whole rice plants were harvested. The plants were soaked in the sodium hexametaphosphate solution to facilitate the separation of peat moss from the roots [27]. The roots were cut from the shoots, then separately placed in a paper bag to dry. After 48 h drying in the hot air oven at 50 °C, the dry matter content of the shoots and roots were weighed.

8.3.5. Operation of the H-PMFCs

The external resistance (R_{ext}) in the closed-circuit H-PMFCs was decided by the ratio of R_{ext}/R_{int}. The internal resistance (R_{int}) of each H-PMFC was calculated by periodic polarization test (P-test) to optimize power production. The P-test was conducted by varying the R_{ext} from 50,000 to 50 Ω [507]. The P-test was performed on days 1, 43, 40, 84, 108, and 121 of the experiment. The current and power were calculated by plotting polarization (voltage *vs.* current) and power (output power *vs.* current) figures. A data acquisition system (34,970A, Agilent Technologies, Santa Clara, California, USA) was utilized to log the output voltage measurement of each H-PMFC at one-minute intervals.

8.3.6. Measurement of methane

CH_4 generation from H-PMFCs was tested by the static chamber method [27].

The headspace chamber sealed all the H-PMFCs at room temperature for 12 h. Before gas sampling, the internal blower was turned on to mix the air inside the headspace thoroughly. Then, a 2.5 mL gas sample was extracted through the sampling port. All samples were done in triplicate. The concentration of CH_4 was measured by the HP 5890A gas chromatograph (Hewlett Packard, Palo Alto, California, USA), equipped with a Porapak-N column (120 mm × 3mm, 149-177 microns) and a thermal conductivity detector. Helium was used as the carrier gas. The analysis was performed at a constant oven temperature of 45 °C. The injector and detector temperatures were at 210 °C. The concentrations of CH_4 were given in units of parts per million (ppm). The CH_4 emission flux (F, mg/m^2/h) was calculated as follows [553, 554]:

$$F = H \times (M_W/M_V) \times [273.2/(273.2 + T)] \times (\Delta C/\Delta t) \quad (8.1)$$

where, H is the chamber height, m; M_w is the CH_4 mole mass, 16.123×10^{-3} mg; M_v is the CH_4 mole volume, 22.41×10^{-3} m^3; T is the chamber air temperature, 23 °C; $\Delta C/\Delta t$ is the change in the CH_4 between the initial and final measurement per unit of time (12 h), ppm.

8.3.7. Chemical oxygen demand removal rate test

The closed reflux colorimetric method with a spectrophotometer (MiltonRoy, Model Spectronic 21D) was utilized to measure the chemical oxygen demand (COD) of all H-PMFCs. The R_{COD} removal rate in H-PMFCs can be calculated as follows:

$$R_{COD} = V \cdot \Delta COD \quad (8.2)$$

where, V is the liquid volume of the reservoir and ΔCOD is the amount of removed COD within a specified time.

8.3.8. Statistical analysis

The experimental data was analyzed by analysis of variance (ANOVA) of the SPSS software (SPSS Inc., Ver. 18, Chicago, IL, USA). The univariate variance analysis was performed according to the Bonferroni test for average plant biomass

production and average CH_4 emission study. The Duncan multiple range test was applied to analyze the difference between the means and to establish significance, a p < 0055 indicates statistical significance.

8.4. RESULTS AND DISCUSSION

8.4.1. Effects of R_{ext} on plant growth and biomass production

Plants can affect the redox potential of MFCs by enhancing the surface area of electrodes for the growth of microorganism biofilm and releasing oxygen to the rhizosphere area by photosynthesis [637]. **Figure 8.2.(a)** illustrates the shoot height changes over time of all rice plants during the experiment in H-PMFCs. The rice plants were transplanted in H-PMFCs on day 22. It can be seen that the shoot height of all rice plants increased with time. The growth of the rice plants increased gradually during the first 5 weeks (OC-1&2). Then, the development of the rice plant shoots slowed in all H-PMFCs (OC-2 to CC-4). The final size of all rice plants was 42.40 ± 1.46 cm for H-PMFC-A, 43.27 ± 1.07 for H-PMFC-B, and 43.03 ± 1.93 cm for H-PMFC-C. The differences, however, were not statistically significant ($p > 0.05$). Besides, in **Figure 8.2 (b)**, the shoot height of rice plants in H-PMFCs had no significant difference among CC-1 to CC-4 ($p > 0.05$). Thus, the changing of R_{ext} has no significant effect on the shoot height growth of the rice plants.

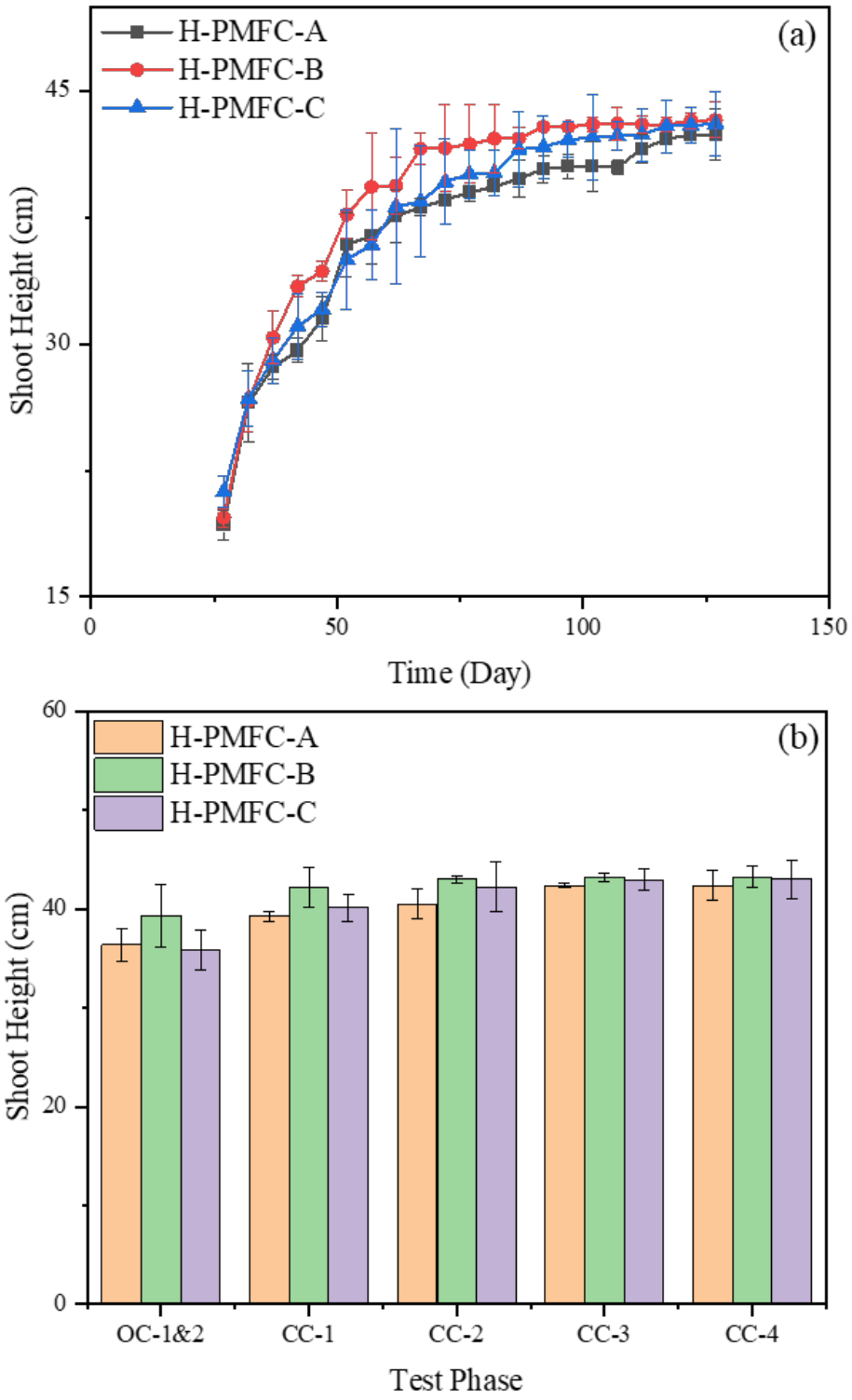

Figure 8.2. (a) The plant shoot height changes over the time of all H-PMFCs; (b) the plant shoot height changes over the test phase of all H-PMFCs for 131 days experiment.

Table 8.3. shows the biomass production of all rice plants from H-PMFCs at the

end of the experiment. H-PMFC-B exhibited the highest shoot height (43.27 ± 1.07 cm), shoot mass (7.67 ± 0.01 g dry mass), root height (42.60 ± 0.54 cm), and root mass (4.37 ± 0.02 g dry mass). Of note, the shoot mass, root height, and root mass of H-PMFC-B were significantly higher than H-PMFC-A and H-PMFC-C ($p < 0.05$).

Overall, the R_{ext}/R_{int} ratio does not significantly influence plant shoot height growth, unlike for biomass production (significant) with the highest production recorded when R_{ext} equals R_{int}.

Table 8.3. The plant biomass production and total CH_4 emission flux during the experiment.

	Shoot height$_{avg/plant}$ (cm)	**Shoot mass$_{avg/plant}$ (g dry mass)**	**Root length$_{avg/plant}$ (cm)**	**Root mass$_{avg/plant}$ (g dry mass)**	**CH_4 emission flux$_{sum\ 50\ days}$ ($g/m^2/h$)**
H-PMFC-A	42.40 ± 1.46 [a]	7.38 ± 0.02 [b]	29.23 ± 0.95 [c]	3.48 ± 0.01 [c]	453.52 ± 0.28 [c]
H-PMFC-B	43.27 ± 1.07 [a]	7.67 ± 0.01 [a]	42.60 ± 0.54 [a]	4.37 ± 0.02 [a]	645.64 ± 0.16 [b]
H-PMFC-C	43.03 ± 1.93 [a]	6.37 ± 0.02 [c]	32.77 ± 0.25 [b]	4.03 ± 0.02 [b]	983.18 ± 0.26 [a]

Notes: Different letters in the same row indicate significant differences ($p < 0.05$)

8.4.2. Polarization tests analysis

The P-test was utilized to estimate the maximum H-PMFCs power by the value of R_{int} and adjusted R_{ext}, performed on days 0, 43, 40, 84, 108, and 121. **Figure 8.3.** shows the R_{int} and PD_{max} values gained in the P-test. All H-PMFCs were operating under the open circuit (OC) until day 60. Running PMFCs temporarily under OC can compensate for carbon consumption by anodophilic activity and help maintain long-term energy generation [531]. R_{int} of all H-PMFCs exhibited an opposite trend in comparison with PD_{max} (**Figure 8.3.(a)**), which is consistent with previous experiment results. The PD_{max} inversely related to R_{int}, the increasing R_{int} resulted in a decline of PD_{max} in H-PMFC [550, 636].

In **Figure 8.3.(b)**, under the OC mode, the PD_{max} value of all H-PMFCs displayed a similar trend, which was decreased first and then increased at day 60. The highest PD_{max} during the P-test was observed in H-PMFC-C of 92.22 mW/m^3 on day 1. This may be attributed to the growth rates of the plants in H-PMFCs. The plant rhizodeposition varies over the growth stages and plant health, which can provide extra carbon sources to H-PMFCs [612]. As shown in **Figure 8.2.** H-PMFC-C has the highest plant shoot, which can provide more extra carbon sources. Under close-circuit (CC) mode, the PD_{max} of all H-PMFCs decreased, and H-PMFC-A and H-PMFC-B showed similar PD_{max} (11.09 mW/m^3 and 11.13 mW/m^3), which are significantly higher than H-PMFC-C (6.36 mW/m^3) ($p < 0.05$) on day 121. Helder et al. [638] found that more roots lead to lower R_{int} and higher electricity generation. However, in **Table 8.3.** H-PMFC-C has a higher root length and mass value than H-PMFC-A. Thus, we hypothesize that when R_{ext} is higher than R_{int}, it will inhibit power generation from H-PMFCs regardless of internal factors such as root length, as shown in this study.

Further, H-PMFCs operated under OC mode showed higher PD_{max} value than CC, which suggests energy accumulation within the anodic biofilm of H-PMFC under OC mode. Logan [639] reported that the anode potential becomes more negative under OC

mode. Due to the respiratory enzymes and electron carriers holding electrons being oxidized, the anode potential increases when the circuit is reconnected with a load, resulting in higher power output. However, Jauharah et al. [27] noticed that the PD_{max} in CC PMFC was two times higher than OC PMFC from the P-test. Similarly, Larrosa-Guerrero et al. [640] found that the PD_{max} value of CC MFC was 4 times higher than OC MFC. They proposed that CC MFCs contained more electroactive organisms than OC MFCs. The differences between the data noted above were the plants and organic matter matrix in PMFCs, and only our study was under a hydroponic situation. Therefore, the effect of various plant growth with different conditions on the PD_{max} of H-PMFCs under different operating modes needs further investigation.

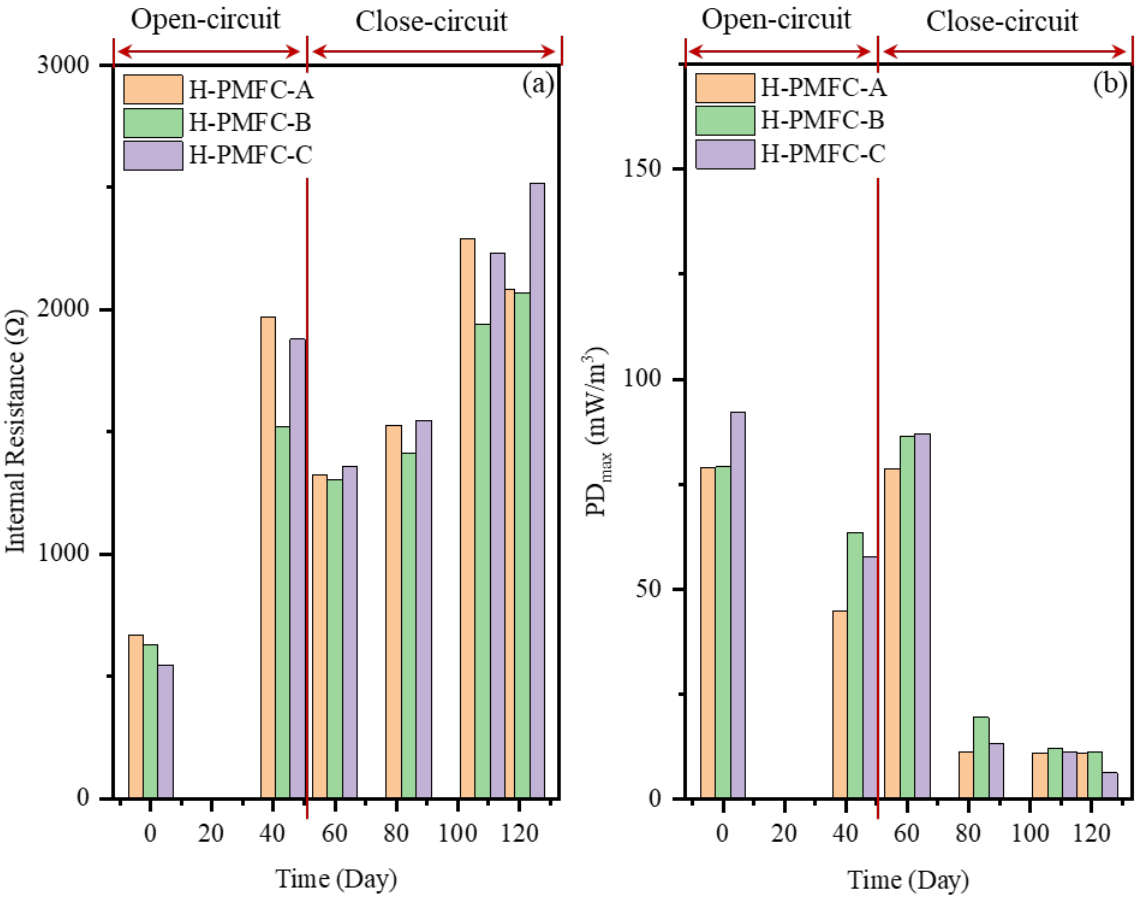

Figure 8.3. The (a) internal resistance and (b) maximum power density from polarization tests performed on day 1, 43, 40, 84, 108, and 121 of all H-PMFCs.

8.4.3. Effects of R_{ext} on electricity generation by the H-PMFC

Figure 8.4.(a) & (b) shows the voltage and power density changes of all H-PMFCs in 131 days. H-PMFC-A, H-PMFC-B, and H-PMFC-C had similar voltage trends in OC (**Figure 8.4.(a)**). The larger peaks noticed under the OC mode might be associated with the abundance of carbon sources in the peat moss. Besides, H-PMFC-A showed the highest voltage of 854.93 mV, followed by H-PMFC-C (840.11 mV) and H-PMFC-B (835.88 mV) ($p < 0.05$) under OC mode.

H-PMFC-A, H-PMFC-B, and H-PMFC-C demonstrated remarkable differences under CC mode. A marked decline was exhibited for all H-PMFCs when turned into CC mode (**Figure 8.4.(a)**); this was associated with the electrode reaction kinetics restriction by the current-limiting electrode [641]. In CC mode, H-PMFC-A demonstrated a decreasing trend of output voltage with the R_{ext}/R_{int} decreasing from 50% to 5%. H-PMFC-B showed a stable voltage performance. The voltage of H-PMFC-C keeps increasing with the R_{ext}/R_{int} rising from 50% to 2000%.

Theoretically, the maximum power of MFC is gained when $R_{ext} = R_{int}$; therefore, when the $R_{ext} > R_{int}$ or $R_{ext} < R_{int}$, the changes in voltage will be noticed and losses in power density are expected [642, 643]. However, in our study, the H-PMFC-B (189.14 ± 0.06 mW/m^2) presented an average PD 19% lower than H-PMFC-C (232.94 ± 0.13 mW/m^2) under CC mode ($p < 0.05$) (**Figure 8.4.(a) & (b)**). Suzuki et al. [644] observed a relatively high PD in the MFC when R_{ext} was 1000 Ω compared to R_{int} 10 Ω. Similarly, Cano et al. [645] found that the average PD improved 29% when R_{ext} was 300 Ω (R_{int} was 10.1 Ω). Zhang et al. [558] reported that the anode potential was more negative and steadier with higher R_{ext}, which lead to a higher voltage. However, low anode potential cannot afford enough energy for electron transfer and cell maintenance [559]. Thus, the PD of H-PMFC-C exhibited a decreasing trend from CC-3 stage to CC-4 stage in Figure 6.4.(b).

Despite the H-PMFC-C having the highest average PD value (232.94 ± 0.13 mW/m^2) than H-PMFC-B (189.14 ± 0.06 mW/m^2) and H-PMFC-A (48.81 ± 0.09 mW/m^3) ($p < 0.05$), H-PMFC-B exhibited the highest PD_{max} from CC-2 to CC-4 stage

(**Figure 8.4. (b)**). The results found that an increased R_{ext}/R_{int} ratio could enhance the power density of H-PMFCs but should be within a limitation of 50%.

The stage CC-3 is noteworthy. An increasing trend of PD was observed for all H-PMFCs. The highest PD_{max} was achieved by H-PMFC-B (397.02 mW/m^3), followed by H-PMFC-C (256.68 mW/m^3), and H-PMFC-A (84.64 mW/m^3). This interesting phenomenon was associated with the rhizodeposition and microbes' hotspots of rice plants, which can offer extra carbon sources and help MFC sustain the power production [564, 646]. Furthermore, all H-PMFCs showed a decreasing trend from stage CC-3 to stage CC-4, especially in H-PMFC-B, which was decreased by 81%. We speculate this towards to the plants getting older and hence oxygen release from the plant roots. As summarized in Table 6.3. H-PMFC-B exhibits the longest root length and mass. However, the oxygen release from roots could create oxic conditions at the anode, which consumed electrons through biological/chemical oxygen reduction and reduced the available electrons for electricity generation [568].

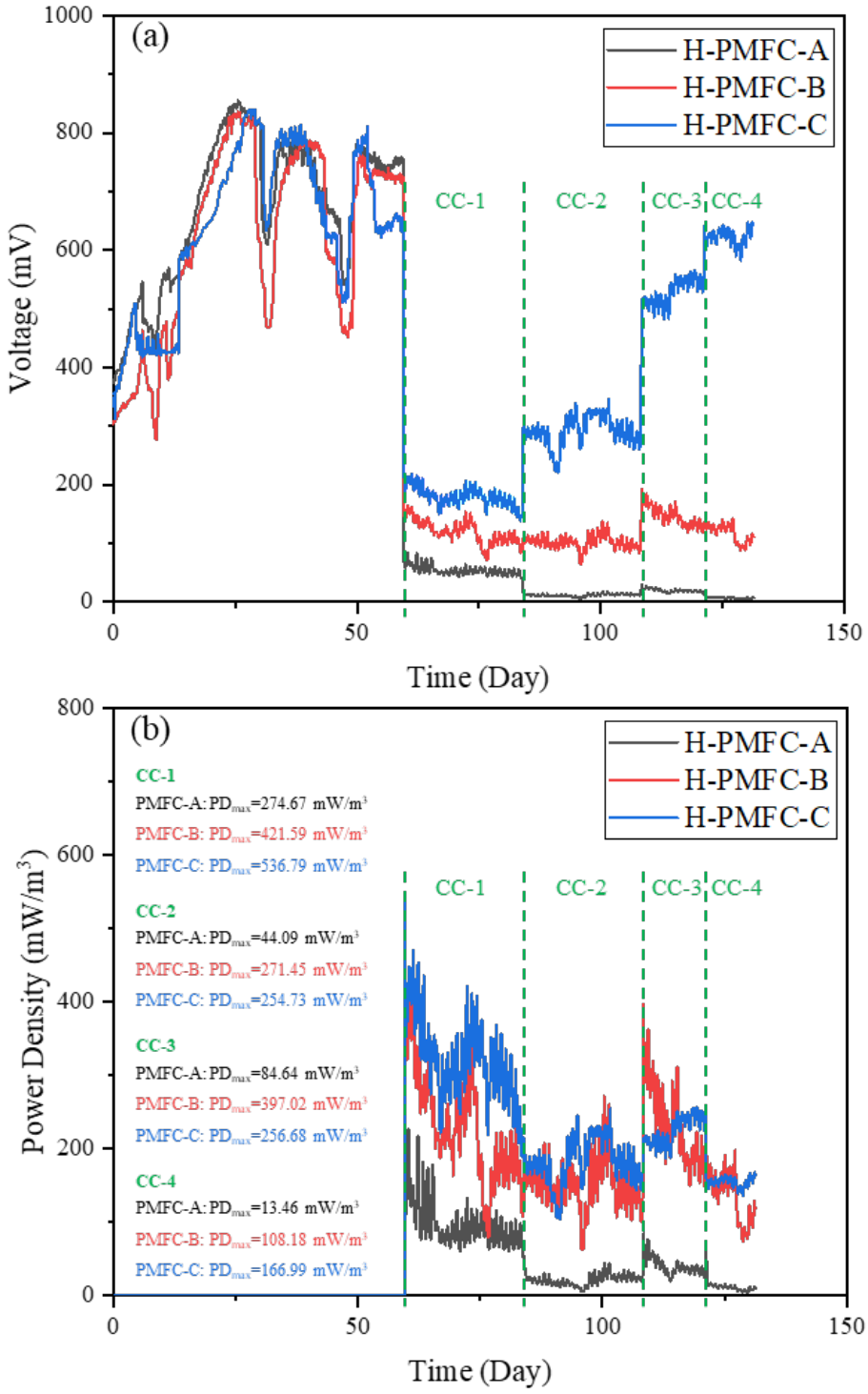

Figure 8.4. The performance of all H-PMFCs in (a) voltage and (b) power density for 131 days experiment.

8.4.4. Effects of R_{ext} on methane flux emissions

Figure 8.5. shows the relationship between the current generation and CH_4

emission. During the 131 days of operation, H-PMFC-A showed the highest current production, followed by H-PMFC-B and H-PMFC-C. At the end of the experiment, H-PMFC-C showed the highest CH_4 emission flux of 983.18 ± 0.26 g/m^2/h, which was 1.8 times higher than H-PMFC-B and 2.2 times higher than H-PMFC-A (**Table 8.2**). These results displayed that the CH_4 emission exhibits an inverse trend with current production in all H-PMFCs. Previous studies found that the current output from PMFCs depends on the metabolism of the microorganism, while the anode acts as the electron acceptor for electrochemically active bacteria [647, 648]. Therefore, the competition between methanogens and the electrogens on the anode in H-PMFCs for carbon substrates suppresses methanogenesis [576].

Compared with H-PMFC-B, the CH_4 emission from H-PMFC-A keeps decreasing with the R_{ext}/R_{int} decreasing from 50% to 5%. (**Figure 8.5.**). Similar results were also reported by Liu et al. [197], who found the plant-mediated CH_4 decreased gradually with the decrease of R_{ext}. This may be because of the R_{ext} variation which can affect the methanogens' activity and diversity by altering the potential of the H-PMFC anode [204]. Rismani-Yazdi et al. [204] reported that the redox potential in MFCs determines the methanogenesis process. Lower R_{ext} leads to less negative anode potential, thus reducing methanogens' diversity [197]. Besides, the decreased R_{ext} led to the decline in the cathode potential of H-PMFCs. The lower redox potential could be unfavorable for methanotrophic activity/CH_4 oxidation, thereby resulting in the decrease of CH_4 emission [649].

The above results suggest that setting the value of R_{ext} lower than R_{int} is an optimal choice for ensuring both higher current output and less methane emission from the H-PMFCs.

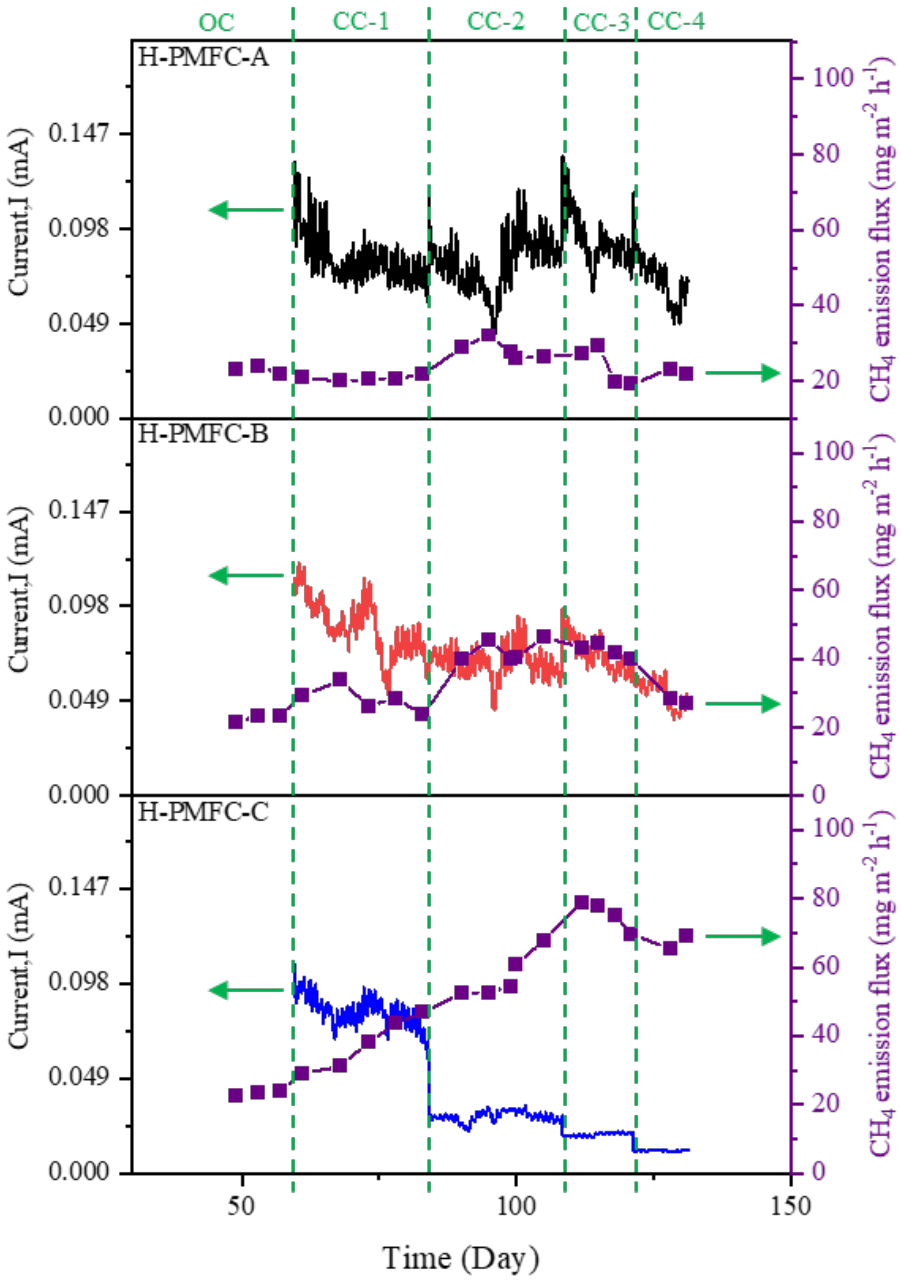

Figure 8.5. The current generation and CH_4 emission flux trend of all H-PMFCs for 131 days experiment.

8.4.5. Effects of R_{ext} on chemical oxygen demand removal rate performance

The effect of R_{ext} on the COD removal performance of all H-PMFCs is exhibited in **Figure 8.6.** Compared with the OC operation stage, all H-PMFCs showed a significantly higher COD removal rate ($p < 0.05$). This is attributed to the generation of current in H-PMFCs; with the installation of R_{ext}, electroactive bacteria need to drive the current flow by consuming organic matter, which shows in the COD

removal rate [571]. H-PMFC-B showed a similar COD removal rate among CC-1 to CC-4 stage ($p > 0.05$). Besides, H-PMFC-A (34.62 ± 0.67 %), H-PMFC-B (32.51 ± 0.41 %), and H-PMFC-C (36.55 ± 0.53 %) have no significant difference ($p > 0.05$) in the CC-1 stage. This result indicated that the R_{ext} does not affect the COD removal rate when $50\% \leq R_{ext}/R_{int} \leq 150\%$.

H-PMFC-A showed an increasing COD removal rate from CC-1 to CC-4 stage, with the value of R_{ext}/R_{int} decreasing from 50% to 5%. However, H-PMFC-C showed the opposite trend. Thus, it was confirmed that the COD removal rate in H-PMFCs negatively correlates with R_{ext} as demonstrated in several studies [571, 650]. This tendency may be attributed to the anode potential that can regulate the bacterial activity in H-PMFCs. During carbon source oxidation, the microbe available Gibbs free energy is proportional to the electron transfer number and the potential difference between anode and substrate redox potential [651]. Thus, the lower R_{ext} leads to the higher anode potential and the greater current, while the bacteria can obtain more energy per unit of time to perform its metabolic activity [642].

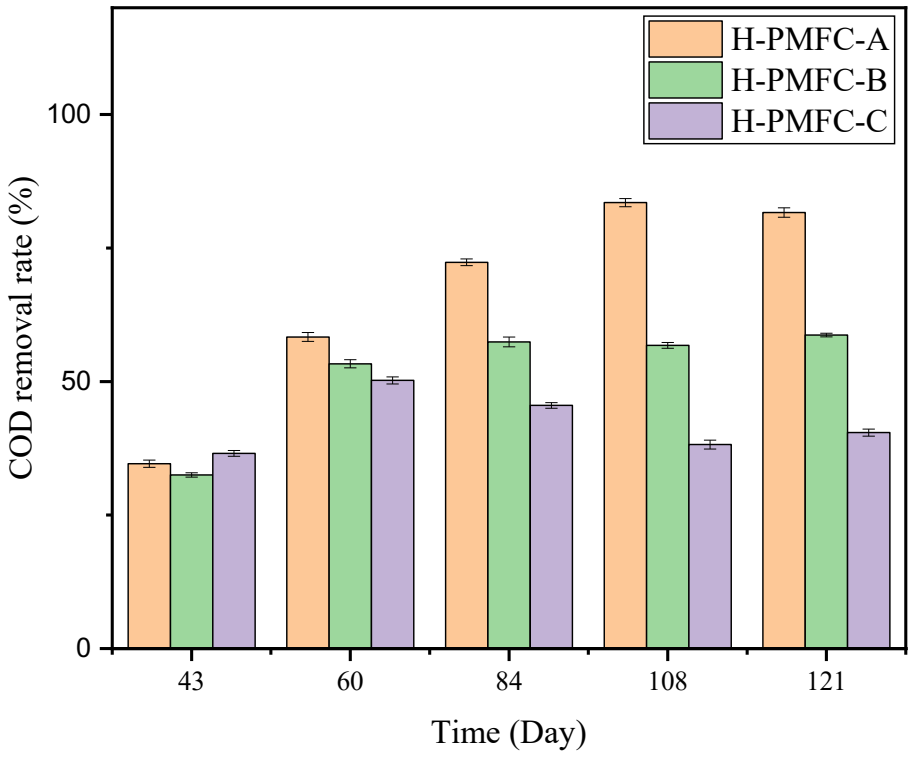

Figure 8.6. The COD removal rate of all H-PMFCs for 131 days experiment.

8.5. CONCLUSION

In the present work, we explored the possibility of utilizing R_{ext} control to optimize the performance of hydroponic H-PMFCs cultivated rice plants. As shown in this work, the R_{ext}/R_{int} ratios of H-PMFCs do not significantly influence the rice plant height growth ($p > 0.05$) but can significantly affect biomass production. H-PMFC-C showed the highest average PD, which was 4.77 higher than H-PMFC-A and 1.23 times than H-PMFC-B over 131 days of operation. Additionally, increasing the R_{ext}/R_{int} ratio within the 50% limit could improve PD. H-PMFC-A exhibited the highest current generation of 0.14 mA (R_{ext}/R_{int} = 9%) in comparison with H-PMFC-B (0.12 mA) and H-PMFC-C (0.11 mA). The CH_4 emission exhibits an inverse trend with its current production, decreasing with the R_{ext}/R_{int} ratio decrease from 50% to 5%. Finally, the COD removal rate in H-PMFCs negatively correlates with R_{ext}/R_{int}. Therefore, the biomass, bioelectricity, and CH_4 production from H-PMFCs of rice plants can be controlled by changing R_{ext}/R_{int} ratio. Further studies regarding the effect of plant species and plant growth progress on H-PMFC performance need to be performed.

CHAPTER IX

GENERAL SUMMARY, SCIENTIFIC CONTRIBUTIONS TO KNOWLEDGE, AND RECOMMENDATIONS FOR FUTURE RESEARCH

9.1. GENERAL SUMMARY AND CONCLUSION

This thesis's main emphasis was to explore the potential application of BES for sustainable agriculture. We developed a H-PMFC system to evaluate the effect of H-PMFC on CH_4 emission, biomass production, and bioelectricity generation from rice plants. Firstly, 3D floating air-cathode was fabricated to lower the configuration budget and improve the performance of H-PMFCs. We also explored the background level of CH_4 emission in a rice cultivation hydroponic system and characterized plant health. Furthermore, different concentrations and forms of iron fertilization in rice H-PMFCs were investigated to optimize the electrochemical components. Finally, we explored the potential application to control CH_4 emission, biomass production, and bioelectricity generation by the ratio of external and internal resistance of H-PMFCs.

The literature review (Chapter II) summarized the agriculture impacts on global warming, especially the CH_4 emission from rice paddy. The mechanism of CH_4 emission from rice paddy and the main strategies are also reviewed. However, these existing methods have many problems, such as requiring specific soil for plants, needing abundant water sources, causing environmental problems, or increasing the overall cost. Thus, we discussed the potential application of bioelectrochemical technology and hydroponic systems. Hydroponic is a sustainable agriculture alternative that emphasizes the effectiveness and efficiency of land and time. We first

systematically i) overviewed the main problems hindering hydroponic agricultural developments; then ii) conceptualized and discussed the potential solutions of the bioelectrochemical systems (BES) to resolve the identified issues, and finally iii) provided our perspectives for the future developmental trends of hydroponic-BES. In the literature, we found that BES can save energy, treatment wastewater, and monitoring of nutrient composition of hydroponic agriculture, and has huge potential application to solve the problem of gas emissions from hydroponic systems. Therefore, based on the discussion of hydroponic-BES, we proposed hydroponic-plant microbial fuel cell (H-PMFC) systems. Until now, there has been no study paying attention to H-PMFCs.

9.1.1. The novel 3D floating air-cathode fabrication

In the MFC, cathode reactions have a more severe impact on the MFC performances for bioelectric generation due to the irreversible responses and processes. Also, the cathode accounts for the main part of high cost and low power density problems due to its components' high value and slow oxygen reduction kinetics at a neutral medium.

Therefore, Chapter III developed effective and economical 3D floating air-cathodes using a simple dip-drying method in carbon black, ethanol, and PTFE solution. Although sponge materials have been used as electrode materials in MFCs, the previous studies only focused on the anode of MFCs. The influence of different pore sizes of 3D sponge-based floating air-cathode in MFC was first investigated. According to the several advanced characterizations of the traditional carbon felt cathode by scanning electron microscopy, Fourier transforms infrared spectroscopy, thermogravimetric analysis, mechanical property analysis, water contact angle, carbon loss rate, power density, cyclic voltammogram, and chemical oxygen demand, the 3D floating air-cathodes (3 pores/mm) showed cost-effectieness and higher performance efficcency for electricity production during the MFC operation. Consequently, this effective and economical 3D floating air-cathode open a new opportunity for scaling

up simple, inexpensive, high-performance MFCs for energy production.

9.1.2. Hydroponic microbial fuel cells design

The original work of Chapter IV proposed a hydroponic-microbial fuel cell (H-MFC) agriculture system fixed with an air-floating cathode from Chapter III, which could reduce CH_4 emissions by converting CH_4 to fuel energy and produce bioelectricity during rice cultivation. The main results showed up to 50% reduction of CH_4 emissions from rice plants in comparison with the control group, and the maximum power density was 504.39 mW/m^3. Besides, the H-PMFC system had no significant effect on biomass production. This work allows CH_4 emission reduction and control in rice paddy fields. It provides a potential method to achieve low-carbon agriculture as well as produce cleaner energy for a sustainable and new smart city in the future. To improve the H-PMFC system's performance, the system's optimization is still needed.

9.1.3. Iron fertilization concentration and its effect on optimization challenges

In this study, we found the need for iron fertilization concentration level and its effect on the biomass production, CH_4 emission, and bioelectricity generation of H-PMFC systems. Although Group 7.5-0 shows the highest shoot height of 55.47 ± 2.50 cm, Group 7.5-15 exhibits the most increased overall biomass production (plant $length_{avg/plant}$: 89.67 ± 1.17; plant $weight_{avg/plant}$:14.91 ± 0.02 g dry mass). Besides, H-PMFCs supplemented with 7.5 μM Fe^{2+} and 15 μM Fe^{3+} obtained the highest PD_{max} of 949.17 mW/m^3 with the lowest CH_4 emission flux of 43.15 g/m^2, 2.84 times lower than Group 0-0. These phenomena indicated that H-PMFCs could regulate the iron concentration in the nutrient solution, lower the influence of Fe^{2+} toxicity on rice plants, and facilitate electricity generation when the Fe^{2+} was 7.5 μM and Fe^{3+} was 15 μM. We also found that H-PMFCs can decrease the CH_4 generation in two ways with the addition of iron: (i) iron electron acceptors directly inhibit methanogens; (ii) iron electron acceptor enhances the electricity production ability of MFC to inhibit CH_4

production.

9.1.4. The control of R_{ext}/R_{int} ratio for H-PMFC

In Chapter VIII, we explored the possibility of utilizing R_{ext}/R_{int} control ratio to optimize the performance of hydroponic H-PMFCs cultivated rice plants. The H-PMFC system was built based on the results of Chapter VII. The results showed that the R_{ext}/R_{int} ratios of H-PMFCs have no significant influence on the rice plant height growth ($p > 0.05$) but can affect biomass production significantly ($p < 0.05$). The highest biomass production was obtained by H-PMFC-B when $R_{ext} = R_{int}$, the highest power density was obtained in H-PMFC-C (536.79 mW/m^3) when $R_{ext}/R_{int} = 150\%$, and the highest current was obtained in H-PMFC-A (o.14 mA) when $R_{ext}/R_{int} = 9\%$. The CH_4 emission exhibits an inverse trend with its current production, decreasing with the R_{ext}/R_{int} ratio decrease from 50% to 5%. Thus, our results indicated that the ratio of Rext/Rint can control the performance of H-PMFCs according to the actual needs.

9.2. CONTRIBUTION TO KNOWLEDGE

This thesis investigated the potential application of H-PMFC systems on biomass production, CH_4 emission, and bioelectricity generation from rice plants. The following are important contributions to knowledge:

i. This study made an inexpensive and high-performance 3D floating air-cathode of hydroponic MFCs. The sponge 3D floating air-cathodes were fabricated by a simple dip-drying method, which can be used in hydroponic MFC systems. This study proved that the pore size of the 3D cathode played a crucial role in 3D floating air-cathode properties. The 3D floating air-cathode are inexpensive since the cost of sponge materials is low and the fabrication method is easy. The floating ability and soft texture of the sponge can be made into any shape to fit the various sizes of hydroponic MFCs.
ii. The background level of CH_4 emission in the rice cultivation hydroponic system

was explored. The H-PMFC agriculture system proposed could reduce CH4 emissions by converting CH_4 to fuel energy and product bioelectricity during rice cultivation. This study found that up to 50% of CH_4 decrease from rice plants without affecting the biomass production.

iii. This thesis demonstrated for the first time that the concentration and forms of iron fertilizer affect the performance of H-PMFCs. The results showed when Fe^{2+} is 7.5 μM and Fe^{3+} is 15 μM, the H-PMFC has the best overall performance.

iv. Our study indicated that the addition of iron in rice H-PMFCs could decrease the emission of CH_4 in two ways: (i) iron electron acceptors directly inhibit methanogens; (ii) iron electron acceptor enhances the electricity production ability of MFC to inhibit CH_4 production.

v. The research on the ratio of R_{ext}/R_{int} shows the possibility of controlling the performance of H-PMFCs, including biomass production, CH_4 emission, and bioelectricity generation.

vi. This work allows CH_4 emission reduction and its control in rice paddy fields' application. It provides a potential method to achieve low-carbon agriculture as well as produce cleaner energy for a sustainable and new smart city in the future.

9.3. RECOMMENDATIONS FOR FUTURE WORK

H-PMFC system for rice CH_4 control is an emerging field of study. Limitations of our work include that we did not analyze microbial species, did not have rice field applications, did not optimize anode materials, etc. From the insights obtained from our thesis work, the following recommendations for further research are presented below:

i. To further enhance the performance of H-PMFCs, future studies could use stainless-steel mesh on both sides of the cathode to improve the wire connection between the electrodes and the electrical conductivity of Type-I/CB floating air-cathode in H-PMFCs.

ii. Further studies could optimize other H-PMFC structural components such as reactor design, substrate choice, catalyst, enzyme coating, and bacteria species to

improve efficiency and lower the overall cost.

iii. Both plant roots' rhizodeposition and hotspots of microbes' activity could improve the bioelectricity generation and lifetime of H-PMFCs. Most of the research focused on the rhizodeposition of plant roots. Thus, future PMFC studies could focus on the mechanism of microbe activity hotspots to enhance the performance of PMFCs.

iv. Our thesis studied the influence of iron on the performance of H-PMFC (biomass production, CH4 emission, and bioelectricity generation). However, the effect of iron on microbial community diversity in hydroponic rice H-PMFCs is still unclear. Further studies can focus on investigating the impact of different forms and concentrations of iron on H-PMFC microbial species.

v. Our study only focused on the H-PMFC cultivated by rice plants; further studies regarding the effect of plant species and plant growth progress on H-PMFC performance need to be performed in the future.

vi. Exploring model systems for H-PMFC to optimize the overall system performance. Modeling could simplify the complex H-PMFC system and related mechanisms into a simpler form to better understand and represent the whole system.

REFERENCES

[1] Roberts L. 9 Billion? Science. 2011;333:540-3.

[2] Stocker T. Close Climate Change 2013: The Physical Science Basis. Contribution of Working Group I to the Fifth Assessment Report of the Intergovernmental Panel on Climate Change. 2013.

[3] Gupta K, Kumar R, Baruah KK, Hazarika S, Karmakar S, Bordoloi N. Greenhouse gas emission from rice fields: a review from Indian context. Environmental Science and Pollution Research. 2021:1-22.

[4] Linquist BA, Adviento-Borbe MA, Pittelkow CM, van Kessel C, van Groenigen KJ. Fertilizer management practices and greenhouse gas emissions from rice systems: a quantitative review and analysis. Field Crops Research. 2012;135:10-21.

[5] Hussain S, Peng S, Fahad S, Khaliq A, Huang J, Cui K, et al. Rice management interventions to mitigate greenhouse gas emissions: a review. Environmental Science and Pollution Research. 2015;22:3342-60.

[6] Pittelkow CM, Adviento-Borbe MA, Hill JE, Six J, van Kessel C, Linquist BA. Yield-scaled global warming potential of annual nitrous oxide and methane emissions from continuously flooded rice in response to nitrogen input. Agriculture, Ecosystems & Environment. 2013;177:10-20.

[7] Menon S, Denman KL, Brasseur G, Chidthaisong A, Ciais P, Cox PM, et al. Couplings between changes in the climate system and biogeochemistry. Lawrence Berkeley National Lab.(LBNL), Berkeley, CA (United States); 2007.

[8] Gagnon B, Ziadi N, Rochette P, Chantigny MH, Angers DA. Fertilizer source influenced nitrous oxide emissions from a clay soil under corn. Soil Science Society of America Journal. 2011;75:595-604.

[9] Ge Z, Li J, Xiao L, Tong Y, He Z. Recovery of electrical energy in microbial fuel cells: brief review. Environmental Science & Technology Letters. 2013;1:137-41.

[10] Logan BE, Hamelers B, Rozendal R, Schröder U, Keller J, Freguia S, et al.

Microbial fuel cells: methodology and technology. Environmental science & technology. 2006;40:5181-92.

[11] Du Z, Li H, Gu T. A state of the art review on microbial fuel cells: a promising technology for wastewater treatment and bioenergy. Biotechnol Adv. 2007;25:464-82.

[12] Aulakh M, Wassmann R, Rennenberg H, Fink. Pattern and amount of aerenchyma relate to variable methane transport capacity of different rice cultivars. Plant Biology. 2000;2:182-94.

[13] Bazhin N. Theory of methane emission from wetlands. Energy & Environmental Science. 2010;3:1057-72.

[14] Moore JC, McCann K, de Ruiter PC. Soil rhizosphere food webs, their stability, and implications for soil processes in ecosystems. The Rhizosphere: Elsevier; 2007. p. 101-25.

[15] Strik DP, Hamelers H, Snel JF, Buisman CJ. Green electricity production with living plants and bacteria in a fuel cell. International Journal of Energy Research. 2008;32:870-6.

[16] Schamphelaire LD, Bossche LVd, Dang HS, Höfte M, Boon N, Rabaey K, et al. Microbial fuel cells generating electricity from rhizodeposits of rice plants. Environmental Science & Technology. 2008;42:3053-8.

[17] Powell RJ, White R, Hill RT. Merging metabolism and power: development of a novel photobioelectric device driven by photosynthesis and respiration. PloS one. 2014;9:e86518.

[18] Nitisoravut R, Regmi R. Plant microbial fuel cells: A promising biosystems engineering. Renewable and Sustainable Energy Reviews. 2017;76:81-9.

[19] Eisenhut M, Bräutigam A, Timm S, Florian A, Tohge T, Fernie AR, et al. Photorespiration is crucial for dynamic response of photosynthetic metabolism and stomatal movement to altered CO2 availability. Molecular plant. 2017;10:47-61.

[20] da Rosa AC. Diversity and function of the microbial community on anodes of sediment microbial fuel cells fueled by root exudates. Doctor Dissertation of

Philipps-Universitit. 2010.

[21] Ramankutty N, Mehrabi Z, Waha K, Jarvis L, Kremen C, Herrero M, et al. Trends in global agricultural land use: implications for environmental health and food security. Annual Review of Plant Biology. 2018;69:789-815.

[22] Barbosa GL, Gadelha FDA, Kublik N, Proctor A, Reichelm L, Weissinger E, et al. Comparison of land, water, and energy requirements of lettuce grown using hydroponic vs. conventional agricultural methods. International journal of environmental research and public health. 2015;12:6879-91.

[23] dos Santos JD, Lopes da Silva AL, da Luz Costa J, Scheidt GN, Novak AC, Sydney EB, et al. Development of a vinasse nutritive solution for hydroponics. Journal of Environmental Management. 2013;114:8-12.

[24] Arends JB, Speeckaert J, Blondeel E, De Vrieze J, Boeckx P, Verstraete W, et al. Greenhouse gas emissions from rice microcosms amended with a plant microbial fuel cell. Applied microbiology and biotechnology. 2014;98:3205-17.

[25] Friedman ES, McPhillips LE, Werner JJ, Poole AC, Ley RE, Walter MT, et al. Methane emission in a specific riparian-zone sediment decreased with bioelectrochemical manipulation and corresponded to the microbial community dynamics. Frontiers in microbiology. 2016;6:1523.

[26] Deng H, Cai L, Jiang Y, Zhong W. Application of microbial fuel cells in reducing methane emission from rice paddy. Huan jing ke xue= Huanjing kexue. 2016;37:359-65.

[27] Khudzari JM, Gariépy Y, Kurian J, Tartakovsky B, Raghavan GV. Effects of biochar anodes in rice plant microbial fuel cells on the production of bioelectricity, biomass, and methane. Biochemical engineering journal. 2019;141:190-9.

[28] Kaku N, Yonezawa N, Kodama Y, Watanabe K. Plant/microbe cooperation for electricity generation in a rice paddy field. Appl Microbiol Biotechnol. 2008;79:43-9.

[29] Rahimnejad M, Ghoreyshi AA, Najafpour G, Jafary T. Power generation from organic substrate in batch and continuous flow microbial fuel cell operations.

Applied Energy. 2011;88:3999-4004.

[30] Parry M, Parry ML, Canziani O, Palutikof J, Van der Linden P, Hanson C. Climate change 2007-impacts, adaptation and vulnerability: Working group II contribution to the fourth assessment report of the IPCC: Cambridge University Press; 2007.

[31] Palut MPJ, Canziani OF. Contribution of working group II to the fourth assessment report of the intergovernmental panel on climate change. 2007.

[32] Verge X, De Kimpe C, Desjardins R. Agricultural production, greenhouse gas emissions and mitigation potential. Agricultural and forest meteorology. 2007;142:255-69.

[33] Rodhe H. A comparison of the contribution of various gases to the greenhouse effect. Science. 1990;248:1217-9.

[34] Nations U. World population prospects 2017. United Nations New York; 2017.

[35] Bruinsma J. World agriculture: towards 2015/2030: an FAO perspective: Earthscan; 2003.

[36] Wollenberg EK. The mitigation pillar of Climate-Smart Agriculture (CSA): targets and options. Agriculture for Development. 2017.

[37] Burney JA, Davis SJ, Lobell DB. Greenhouse gas mitigation by agricultural intensification. Proceedings of the national Academy of Sciences. 2010;107:12052-7.

[38] Tilman D, Balzer C, Hill J, Befort BL. Global food demand and the sustainable intensification of agriculture. Proceedings of the national academy of sciences. 2011;108:20260-4.

[39] Sass R. Short summary chapter for methane. Global Emission and Controls from Rice Fields and Other Agricultural and Industrial Sources. 1994.

[40] Le Mer J, Roger P. Production, oxidation, emission and consumption of methane by soils: a review. European journal of soil biology. 2001;37:25-50.

[41] Conrad R, Klose M. How specific is the inhibition by methyl fluoride of acetoclastic methanogenesis in anoxic rice field soil? FEMS Microbiology Ecology. 1999;30:47-56.

[42] Conrad R, Klose M. Anaerobic conversion of carbon dioxide to methane, acetate and propionate on washed rice roots. FEMS microbiology ecology. 1999;30:147-55.

[43] Roy R, Conrad R. Effect of methanogenic precursors (acetate, hydrogen, propionate) on the suppression of methane production by nitrate in anoxic rice field soil. FEMS Microbiology Ecology. 1999;28:49-61.

[44] Schütz H, Holzapfel-Pschorn A, Conrad R, Rennenberg H, Seiler W. A 3-year continuous record on the influence of daytime, season, and fertilizer treatment on methane emission rates from an Italian rice paddy. Journal of Geophysical Research: Atmospheres. 1989;94:16405-16.

[45] Van Der Gon HD, Neue H-U. Oxidation of methane in the rhizosphere of rice plants. Biology and Fertility of Soils. 1996;22:359-66.

[46] Lin BB. Resilience in agriculture through crop diversification: adaptive management for environmental change. BioScience. 2011;61:183-93.

[47] Rijsberman FR. Water scarcity: fact or fiction? Agricultural water management. 2006;80:5-22.

[48] Sardare MD, Admane SV. A review on plant without soil-hydroponics. International Journal of Research in Engineering and Technology. 2013;2:299-304.

[49] Jones Jr JB. Hydroponics: a practical guide for the soilless grower: CRC press; 2016.

[50] Martinez-Mate MA, Martin-Gorriz B, Martínez-Alvarez V, Soto-García M, Maestre-Valero JF. Hydroponic system and desalinated seawater as an alternative farm-productive proposal in water scarcity areas: Energy and greenhouse gas emissions analysis of lettuce production in southeast Spain. Journal of Cleaner Production. 2018;172:1298-310.

[51] Carmassi G, Incrocci L, Maggini R, Malorgio F, Tognoni F, Pardossi A. Modeling Salinity Build-Up in Recirculating Nutrient Solution Culture. Journal of Plant Nutrition. 2005;28:431-45.

[52] Grewal HS, Maheshwari B, Parks SE. Water and nutrient use efficiency of a low-

cost hydroponic greenhouse for a cucumber crop: An Australian case study. Agricultural Water Management. 2011;98:841-6.

[53] Modu F, Adam A, Aliyu F, Mabu A, Musa M. A Survey of Smart Hydroponic Systems.

[54] Ke W, Xiong Z. Difference of Growth, Copper Accumulation and Mineral Element Uptake in Two Elsholtzia Haichowensis Populations under Copper and Mineral Nutrition Stress. 2008 2nd International Conference on Bioinformatics and Biomedical Engineering2008. p. 4704-8.

[55] Wang H, Wang Y, Yang Y. Effects of exogenous phenolic acids on roots of poplar hydroponic cuttings. 2011 International Conference on Remote Sensing, Environment and Transportation Engineering2011. p. 8245-9.

[56] Suzui N, Kawachi N, Yamaguchi M, Ishioka NS, Fujimaki S. A monitoring system of radioactive tracers in hydroponic solution for research on plant physiology. 2009 1st International Conference on Advancements in Nuclear Instrumentation, Measurement Methods and their Applications2009. p. 1-3.

[57] Liu MY, Xi XY, Wang SF, Xu Y, Song WL. Research on differences of component and quantity of organic acids in the root exudates among the three green manures. World Automation Congress 20122012. p. 1-4.

[58] Hussain A, Iqbal K, Aziem S, Mahato P, Negi A. A review on the science of growing crops without soil (soilless culture)-a novel alternative for growing crops. International Journal of Agriculture and Crop Sciences. 2014;7:833.

[59] Valentinuzzi F. Youry Pii Y, Vigani G, Lehmann M, Cesco S, Mimmo T (2015) Phosphorus and iron deficiencies induce a metabolic reprogramming and affect the exudation traits of the woody plant Fragaria× ananassa. J Exp Bot.66:6483-95.

[60] Sambo P, Nicoletto C, Giro A, Pii Y, Valentinuzzi F, Mimmo T, et al. Hydroponic solutions for soilless production systems: issues and opportunities in a smart agriculture perspective. Frontiers in Plant Science. 2019;10:923.

[61] Hoang AT, Nižetić S, Ng KH, Papadopoulos AM, Le AT, Kumar S, et al. Microbial fuel cells for bioelectricity production from waste as sustainable

prospect of future energy sector. Chemosphere. 2022;287:132285.

[62] Zhang X, Li X, Zhao X, Li Y. Factors affecting the efficiency of a bioelectrochemical system: a review. RSC advances. 2019;9:19748-61.

[63] Ivase TJP, Nyakuma BB, Oladokun O, Abu PT, Hassan MN. Review of the principal mechanisms, prospects, and challenges of bioelectrochemical systems. Environmental Progress & Sustainable Energy. 2020;39:13298.

[64] Patil SB, Basavarajappa PS, Ganganagappa N, Jyothi M, Raghu A, Reddy KR. Recent advances in non-metals-doped TiO2 nanostructured photocatalysts for visible-light driven hydrogen production, CO2 reduction and air purification. International Journal of Hydrogen Energy. 2019;44:13022-39.

[65] Sirohi R, Pandey AK, Ranganathan P, Singh S, Udayan A, Awasthi MK, et al. Design and applications of photobioreactors-A review. Bioresource technology. 2022:126858.

[66] Kumar R, Singh L, Zularisam AW, Hai FI. Microbial fuel cell is emerging as a versatile technology: a review on its possible applications, challenges and strategies to improve the performances. International Journal of Energy Research. 2018;42:369-94.

[67] Li S, Chen G, Anandhi A. Applications of emerging bioelectrochemical technologies in agricultural systems: a current review. Energies. 2018;11:2951.

[68] Hadiyanto H, Christwardana M, Pratiwi WZ, Purwanto P, Sudarno S, Haryani K, et al. Response surface optimization of microalgae microbial fuel cell (MMFC) enhanced by yeast immobilization for bioelectricity production. Chemosphere. 2022;287:132275.

[69] Yan W, Xiao Y, Yan W, Ding R, Wang S, Zhao F. The effect of bioelectrochemical systems on antibiotics removal and antibiotic resistance genes: a review. Chemical Engineering Journal. 2019;358:1421-37.

[70] Cecconet D, Sabba F, Devecseri M, Callegari A, Capodaglio AG. In situ groundwater remediation with bioelectrochemical systems: a critical review and future perspectives. Environment international. 2020;137:105550.

[71] Al-Sahari M, Al-Gheethi A, Mohamed RMSR, Noman E, Naushad M, Rizuan

MB, et al. Green approach and strategies for wastewater treatment using bioelectrochemical systems: A critical review of fundamental concepts, applications, mechanism, and future trends. Chemosphere. 2021;285:131373.

[72] Das S, Das S, Das I, Ghangrekar M. Application of bioelectrochemical systems for carbon dioxide sequestration and concomitant valuable recovery: A review. Materials Science for Energy Technologies. 2019;2:687-96.

[73] Zou S, He Z. Efficiently "pumping out" value-added resources from wastewater by bioelectrochemical systems: A review from energy perspectives. Water research. 2018;131:62-73.

[74] Gul MM, Ahmad KS. Bioelectrochemical systems: sustainable bio-energy powerhouses. Biosensors and Bioelectronics. 2019;142:111576.

[75] Logan BE, Rossi R, Ragab A, Saikaly PE. Electroactive microorganisms in bioelectrochemical systems. Nature Reviews Microbiology. 2019;17:307-19.

[76] Gadkari S, Gu S, Sadhukhan J. Towards automated design of bioelectrochemical systems: A comprehensive review of mathematical models. Chemical Engineering Journal. 2018;343:303-16.

[77] Fernando EY, Keshavarz T, Kyazze G. The use of bioelectrochemical systems in environmental remediation of xenobiotics: a review. Journal of Chemical Technology & Biotechnology. 2019;94:2070-80.

[78] Wang H, Xing L, Zhang H, Gui C, Jin S, Lin H, et al. Key factors to enhance soil remediation by bioelectrochemical systems (BESs): A review. Chemical Engineering Journal. 2021;419:129600.

[79] Barbosa SG, Peixoto L, Alves JI, Alves MM. Bioelectrochemical systems (BESs) towards conversion of carbon monoxide/syngas: A mini-review. Renewable and Sustainable Energy Reviews. 2021;135:110358.

[80] Zhao Q, An J, Wang X, Li N. In-situ hydrogen peroxide synthesis with environmental applications in bioelectrochemical systems: a state-of-the-art review. International Journal of Hydrogen Energy. 2021;46:3204-19.

[81] Kabutey FT, Zhao Q, Wei L, Ding J, Antwi P, Quashie FK, et al. An overview of plant microbial fuel cells (PMFCs): Configurations and applications. Renewable

and Sustainable Energy Reviews. 2019;110:402-14.

[82] Maddalwar S, Nayak KK, Kumar M, Singh L. Plant microbial fuel cell: Opportunities, challenges, and prospects. Bioresource Technology. 2021;341:125772.

[83] Apollon W, Luna-Maldonado AI, Kamaraj S-K, Vidales-Contreras JA, Rodríguez-Fuentes H, Gómez-Leyva JF, et al. Progress and recent trends in photosynthetic assisted microbial fuel cells: a review. Biomass and Bioenergy. 2021;148:106028.

[84] Wang W, Zhang Y, Li M, Wei X, Wang Y, Liu L, et al. Operation mechanism of constructed wetland-microbial fuel cells for wastewater treatment and electricity generation: A review. Bioresource Technology. 2020;314:123808.

[85] Yadav RK, Chiranjeevi P, Sukrampal, Patil SA. Integrated drip hydroponics-microbial fuel cell system for wastewater treatment and resource recovery. Bioresource Technology Reports. 2020;9:100392.

[86] Goddek S, Joyce A, Kotzen B, Burnell GM. Aquaponics Food Production Systems: Combined Aquaculture and Hydroponic Production Technologies for the Future: Springer Nature; 2019.

[87] Kozai T. Smart plant factory: Springer; 2018.

[88] Sharma N, Acharya S, Kumar K, Singh N, Chaurasia O. Hydroponics as an advanced technique for vegetable production: An overview. Journal of Soil and Water Conservation. 2018;17:364-71.

[89] Khan FAA. A review on hydroponic greenhouse cultivation for sustainable agriculture. International Journal of Agriculture Environment and Food Sciences. 2018;2:59-66.

[90] Maharana L, Koul D. The emergence of Hydroponics. Yojana (June). 2011;55:39-40.

[91] Lakhiar IA, Gao J, Syed TN, Chandio FA, Tunio MH, Ahmad F, et al. Overview of the aeroponic agriculture–An emerging technology for global food security. International Journal of Agricultural and Biological Engineering. 2020;13:1-10.

[92] Singh S, Singh B. Hydroponics–A technique for cultivation of vegetables and

medicinal plants‖. Proceedings of 4th Global conference on Horticulture for Food, Nutrition and Livelihood Options Bhubaneshwar, Odisha, India2012. p. 220.

[93] Hayden AL. Aeroponic and hydroponic systems for medicinal herb, rhizome, and root crops. HortScience. 2006;41:536-8.

[94] Liu Y, Guo R, Zhang S, Sun Y, Wang F. Uptake and translocation of nano/microplastics by rice seedlings: Evidence from a hydroponic experiment. Journal of Hazardous Materials. 2022;421:126700.

[95] Urbina MA, Correa F, Aburto F, Ferrio JP. Adsorption of polyethylene microbeads and physiological effects on hydroponic maize. Science of the Total Environment. 2020;741:140216.

[96] Yurina NA, Koshchaev AG, Osepchuk DV, Maksim EA, Danilova AA, Shumeiko D. Artificial ecological system–Hydroponics: The wheat grains germination rate. International Journal of Engineering and Advanced Technology. 2019;9:4957-60.

[97] Portero A FJ, Quimbiamba C JV, Hidalgo O AG, Vargas C RS. Economic Assessment of Hydroponic Greenhouse Automation: A Case Study of Oat Farming. The International Conference on Advances in Emerging Trends and Technologies: Springer; 2020. p. 139-50.

[98] Lebreton A, Labbé C, De Ronne M, Xue A, Marchand G, Bélanger R. Development of a simple hydroponic assay to study vertical and horizontal resistance of soybean and pathotypes of Phytophthora sojae. Plant disease. 2018;102:114-23.

[99] Contreras P J, Tunque Q M, Cordero F A. Performance of hydroponics of peas with barley and wheat in the production of germinates. Revista de Investigaciones Veterinarias del Perú (RIVEP). 2015;26:9-19.

[100] Yang T, Kim H-J. Comparisons of nitrogen and phosphorus mass balance for tomato-, basil-, and lettuce-based aquaponic and hydroponic systems. Journal of Cleaner Production. 2020;274:122619.

[101] Aji GK, Hatou K, Morimoto T. Modeling the dynamic response of plant growth to root zone temperature in hydroponic chili pepper plant using neural networks.

Agriculture. 2020;10:234.

[102] CHAUDHARY J, PATEL S. Isolation of Pythium aphanidermatum from Soil by Bait Technique and Prove Pathogenicity on Brinjal under Different Conditions. Advances.388.

[103] Latique S, Chernane H, Mansori M, El Kaoua M. Seaweed liquid fertilizer effect on physiological and biochemical parameters of bean plant (Phaesolus vulgaris variety Paulista) under hydroponic system. European Scientific Journal. 2013;9.

[104] Khan RI, Hafiz IA, Shafique M, Ahmad T, Ahmed I, Qureshi AA. Effect of pre-harvest foliar application of amino acids and seaweed (Ascophylum nodosum) extract on growth, yield, and storage life of different bell pepper (Capsicum annuum L.) cultivars grown under hydroponic conditions. Journal of Plant Nutrition. 2018;41:2309-19.

[105] Sagardoy R, Morales F, López-Millán AF, Abadía A, Abadía J. Effects of zinc toxicity on sugar beet (Beta vulgaris L.) plants grown in hydroponics. Plant Biology. 2009;11:339-50.

[106] Asadi A, Kafi M, Nabati J, Goldani M. Effect of different light sources in in vitro on growth, morphology and minituber production of potato (Solanum tuberosum L.) in hydroponic conditions. Iranian Journal of Horticultural Science. 2018;48.

[107] Singh H, Dunn B, Payton M, Brandenberger L. Fertilizer and cultivar selection of lettuce, basil, and swiss chard for hydroponic production. HortTechnology. 2019;29:50-6.

[108] Lomonte C, Sgherri C, Baker AJ, Kolev SD, Navari-Izzo F. Antioxidative response of Atriplex codonocarpa to mercury. Environmental and experimental botany. 2010;69:9-16.

[109] LIRA RMD, SILVA ÊFD, SILVA AOD, MEDEIROS PRFD, SILVA GFD, SOARES HRE. Watercress and chinese cabbage in a hydroponic system using groundwater. Revista Caatinga. 2020;32:1038-47.

[110] Soares HR, Silva ÊFdF, Silva GFd, Cruz AFdS, Santos JA, Rolim MM. Salinity

and flow rates of nutrient solution on cauliflower biometrics in NFT hydroponic system. Revista Brasileira de Engenharia Agrícola e Ambiental. 2020;24:258-65.

[111] Pramanik M, Nagai M, Asao T, Matsui Y. Effects of temperature and photoperiod on phytotoxic root exudates of cucumber (Cucumis sativus) in hydroponic culture. Journal of Chemical Ecology. 2000;26:1953-67.

[112] Pascual MP, Lorenzo GA, Gabriel AG. Vertical farming using hydroponic system: Toward a sustainable onion production in Nueva Ecija, Philippines. Open Journal of Ecology. 2018;8:25.

[113] Sakamoto M, Komatsu Y, Suzuki T. Nutrient Deficiency Affects the Growth and Nitrate Concentration of Hydroponic Radish. Horticulturae. 2021;7:525.

[114] Gao W, He D, Ji F, Zhang S, Zheng J. Effects of daily light integral and LED spectrum on growth and nutritional quality of hydroponic spinach. Agronomy. 2020;10:1082.

[115] Zheng J, He D, Ji F. Effects of light intensity and photoperiod on runner plant propagation of hydroponic strawberry transplants under LED lighting. International Journal of Agricultural and Biological Engineering. 2019;12:26-31.

[116] Jun HJ, Jo IH. Changes of Nutrient Contents of Circulating Solution in Three Different New Hydroponics for Oriental Melons. Journal of Bio-Environment Control. 2002;11:168-74.

[117] Dominguez JJA, Inoue C, Chien M-F. Hydroponic approach to assess rhizodegradation by sudangrass (Sorghum x drummondii) reveals pH-and plant age-dependent variability in bacterial degradation of polycyclic aromatic hydrocarbons (PAHs). Journal of hazardous materials. 2020;387:121695.

[118] Zhao Z, Zhang W, Liu Y, Li S, Yao W, Sun X, et al. De novo hydroponics system efficiency for the cuttings of alfalfa (Medicago sativa L.). Physiology and Molecular Biology of Plants. 2021;27:1413-21.

[119] Abd Elsallam ME, El-Moslamy SH, Abd El-Al A, Zahran HF. Scaling-up production of cost-effective and eco-friendly bio-fertilizer and its application on Barley green fodder via IoT hydroponic system. Journal of Genetic Engineering and Biotechnology. 2021;19:1-12.

[120] Xie Y, Luo H, Hu L, Sun X, Lou Y, Fu J. Classification of genetic variation for cadmium tolerance in Bermudagrass [Cynodon dactylon (L.) Pers.] using physiological traits and molecular markers. Ecotoxicology. 2014;23:1030-43.

[121] Hassan MM, Haleem N, Baig MA, Jamal Y. Phytoaccumulation of heavy metals from municipal solid waste leachate using different grasses under hydroponic condition. Scientific Reports. 2020;10:1-8.

[122] Bardiya-Bhurat K, Sharma S, Mishra Y, Patankar C. Tagetes erecta (marigold), a phytoremediant for Ni-and Pb-contaminated area: a hydroponic analysis and factors involved. Rendiconti Lincei. 2017;28:673-8.

[123] Alvarado-Camarillo D, Valdez-Aguilar LA, Castillo-González AM, Trejo-Téllez LI, Martínez-Amador SY. Biomass, nitrogen and potassium dynamics in hydroponic rose production. Acta Agriculturae Scandinavica, Section B—Soil & Plant Science. 2018;68:719-26.

[124] Medina L. Study of the effect of some mineral deficiencies on greenhouse carnations (Dianthus caryophyllus) in hydroponic culture. IV International Symposium on Carnation Culture 3071991. p. 203-12.

[125] Bharti A, Prasanna R, Kumar G, Kumar A, Nain L. Co-cultivation of cyanobacteria for raising nursery of chrysanthemum using a hydroponic system. Journal of Applied Phycology. 2019;31:3625-35.

[126] Martins JB, Santos JA, Silva FJd, Silva GFd, Medeiros SdS. Production of parsley in hydroponic conditions under isosmotic brackish nutrient solutions. Ciência e Agrotecnologia. 2019;43.

[127] Bovi O, Zullo M, Perecin M, Granja N, Carmello Q, Robaina C, et al. Hydroponic cultivation of mint and vetiver with spirostane analogues of brassinosteroids. International Symposium on Growing Media and Hydroponics 6442001. p. 55-9.

[128] Silva MGd, Oliveira IdS, Soares TM, Gheyi HR, Santana GdO, Pinho JdS. Growth, production and water consumption of coriander in hydroponic system using brackish waters. Revista Brasileira de Engenharia Agrícola e Ambiental. 2018;22:547-52.

[129] Yeritsyan N, Economakis C. Effect of nutrient solution's iron concentration on growth and essential oil content of oregano plants grown in solution culture. International Conference on Medicinal and Aromatic Plants Possibilities and Limitations of Medicinal and Aromatic Plant 5762001. p. 277-83.

[130] Salighehdar F, Safari A, Nalousi AM, Avestan S. The effect of different ratios of peat and perlite on quantitative and qualitative characteristics of Aloe vera grown in hydroponic system. Journal of Science and Technology of Greenhouse Culture. 2016;7.

[131] Sundar P, Jyothi K, Sundar C. Indoor Hydroponics: A Potential Solution to Reuse Domestic Rinse Water. Biosciences Biotechnology Research Asia. 2021;18:373-83.

[132] Adler P, Harper J, Takeda F, Summerfelt S. Economic analysis of an aquaponic system for the integrated production of rainbow trout and plants. 2000.

[133] Benli H. A performance comparison between a horizontal source and a vertical source heat pump systems for a greenhouse heating in the mild climate Elazığ, Turkey. Appl Therm Eng. 2013;50:197-206.

[134] Patil S, Kadam U, Mane M, Mahale D, Dekale J. Hydroponic nutrient solution: A review. Journal of Pharmacognosy and Phytochemistry. 2020;9:2095-9.

[135] Xydis GA, Liaros S, Botsis K. Energy demand analysis via small scale hydroponic systems in suburban areas – An integrated energy-food nexus solution. Sci Total Environ. 2017;593-594:610-7.

[136] Vourdoubas J. Overview of heating greenhouses with renewable energy sources a case study in Crete-Greece. Journal of Agriculture and Environmental Sciences. 2015;4:70-6.

[137] Freese B, Clemmer S, Nogee A. Coal power in a warming world: A sensible transition to cleaner energy options: Union of Concerned Scientists; 2008.

[138] Denier van der Gon HAC, Kropff MJ, van Breemen N, Wassmann R, Lantin RS, Aduna E, et al. Optimizing grain yields reduces CH₄ emissions from rice paddy fields. Proceedings of the National Academy of Sciences. 2002;99:12021.

[139] Camilia E-D, ZAGHLOUL A, Fikry A. Utilization of rice straw as a low-cost natural by-product in agriculture. International Journal of Environmental Pollution and Environmental Modelling. 2018;1:91-102.

[140] Lehtomäki A. Biogas production from energy crops and crop residues: University of Jyväskylä; 2006.

[141] Paul BK, Ali MA, Saha KK, Khan MB. Effect of standing water levels on methane gas emission and yield performance of transplanted Aman rice (Oryza sativa L. cv. BRRI dhan51). Archives of Agriculture and Environmental Science. 2020;5:299-305.

[142] Akhtar H, Lupascu M, Sukri RS. Interactions between microtopography, root exudate analogues and temperature determine CO2 and CH4 production rates in fire-degraded tropical peat. Soil Biology and Biochemistry. 2022:108646.

[143] Lyu Z, Shao N, Akinyemi T, Whitman WB. Methanogenesis. Current Biology. 2018;28:R727-R32.

[144] Singh H, Batish DR, Kohli R. Autotoxicity: concept, organisms, and ecological significance. Critical Reviews in Plant Sciences. 1999;18:757-72.

[145] Hosseinzadeh S, Verheust Y, Bonarrigo G, Van Hulle S. Closed hydroponic systems: operational parameters, root exudates occurrence and related water treatment. Reviews in Environmental Science and Bio/Technology. 2017;16:59-79.

[146] Zhao Y, Wu L, Chu L, Yang Y, Li Z, Azeem S, et al. Interaction of Pseudostellaria heterophylla with Fusarium oxysporum f. sp. heterophylla mediated by its root exudates in a consecutive monoculture system. Scientific reports. 2015;5:1-7.

[147] Yu JQ, Matsui Y. Extraction and identification of phytotoxic substances accumulated in nutrient solution for the hydroponic culture of tomato. Soil Science and Plant Nutrition. 1993;39:691-700.

[148] Singh HP, Batish DR, Kohli RK. Autotoxicity: Concept, Organisms, and Ecological Significance. Critical Reviews in Plant Sciences. 1999;18:757-72.

[149] Mondal MF, Asaduzzaman M, Tanaka H, Asao T. Effects of amino acids on the

growth and flowering of Eustoma grandiflorum under autotoxicity in closed hydroponic culture. Scientia Horticulturae. 2015;192:453-9.

[150] Curl EA, Truelove B. The rhizosphere: Springer Science & Business Media; 2012.

[151] Mimmo T, Hann S, Jaitz L, Cesco S, Gessa CE, Puschenreiter M. Time and substrate dependent exudation of carboxylates by Lupinus albus L. and Brassica napus L. Plant Physiol Biochem. 2011;49:1272-8.

[152] Blum U, Gerig TM. Relationships between phenolic acid concentrations, transpiration, water utilization, leaf area expansion, and uptake of phenolic acids: nutrient culture studies. Journal of Chemical Ecology. 2005;31:1907-32.

[153] Asaduzzaman M, Asao T. Autotoxicity in strawberry under recycled hydroponics and its mitigation methods. The Horticulture Journal. 2020;89:124-37.

[154] Talukder MR, Asaduzzaman M, Tanaka H, Asao T. Electro-degradation of culture solution improves growth, yield and quality of strawberry plants grown in closed hydroponics. Scientia Horticulturae. 2019;243:243-51.

[155] Valentinuzzi F, Pii Y, Vigani G, Lehmann M, Cesco S, Mimmo T. Phosphorus and iron deficiencies induce a metabolic reprogramming and affect the exudation traits of the woody plant Fragaria×ananassa. J Exp Bot. 2015;66:6483-95.

[156] Richa A, Touil S, Fizir M, Martinez V. Recent advances and perspectives in the treatment of hydroponic wastewater: a review. Reviews in Environmental Science and Bio/Technology. 2020:1-22.

[157] Mohammed S. Tomorrow's Agriculture:" NFT Hydroponics"-Grow Within Your Budget: Springer; 2018.

[158] Steiner AA. A universal method for preparing nutrient solutions of a certain desired composition. Plant and Soil. 1961;15:134-54.

[159] Asao T. Hydroponics: A Standard Methodology for Plant Biological Researches: BoD–Books on Demand; 2012.

[160] Suazo-López F, Zepeda-Bautista R, Sánchez-Del Castillo F, Martínez-Hernández JJ, Virgen-Vargas J, Tijerina-Chávez L. Growth and yield of tomato

(Solanum lycopersicum L.) as affected by hydroponics, greenhouse and irrigation regimes. Annual Research & Review in Biology. 2014:4246-58.

[161] Sonneveld C, Voogt W. Plant nutrition in future greenhouse production. Plant nutrition of greenhouse crops: Springer; 2009. p. 393-403.

[162] Signore A, Serio F, Santamaria P. A targeted management of the nutrient solution in a soilless tomato crop according to plant needs. Frontiers in Plant Science. 2016;7:391.

[163] DeKorne JB. The hydroponic hot house: Low-cost, high-yield greenhouse gardening: Loompanics Unlimited; 1992.

[164] Silkova OG, Leonova IN, Krasilova NM, Dubovets NI. Preferential elimination of chromosome 5R of rye in the progeny of 5R5D dimonosomics. Russian Journal of Genetics. 2011;47:942.

[165] Park C-J, Kim K-H, Yoo K-Y, Ok Y-S, Yang J-E. Recycling of hydroponic waste solution for red pepper (Capsicum annum L.) growth. Korean Journal of Environmental Agriculture. 2005;24:24-8.

[166] Saxena P, Bassi A. Removal of nutrients from hydroponic greenhouse effluent by alkali precipitation and algae cultivation method. Journal of Chemical Technology & Biotechnology. 2013;88:858-63.

[167] Richa A, Touil S, Fizir M, Martinez V. Recent advances and perspectives in the treatment of hydroponic wastewater: a review. Reviews in Environmental Science and Bio/Technology. 2020;19:945-66.

[168] Kumar RR, Cho JY. Reuse of hydroponic waste solution. Environmental Science and Pollution Research. 2014;21:9569-77.

[169] Mielcarek A, Rodziewicz J, Janczukowicz W, Dobrowolski A. Analysis of Wastewater Generated in Greenhouse Soilless Tomato Cultivation in Central Europe. Water. 2019;11.

[170] Rufí-Salís M, Petit-Boix A, Villalba G, Sanjuan-Delmás D, Parada F, Ercilla-Montserrat M, et al. Recirculating water and nutrients in urban agriculture: An opportunity towards environmental sustainability and water use efficiency? Journal of Cleaner Production. 2020;261:121213.

[171] Lopez-Galvez F, Allende A, Pedrero-Salcedo F, Alarcon JJ, Gil MI. Safety assessment of greenhouse hydroponic tomatoes irrigated with reclaimed and surface water. International journal of food microbiology. 2014;191:97-102.

[172] Hochmuth R, Lamb E, McAvoy E, Olczyk T, Lamberts M, Tyson R. Greenhouse vegetables in Florida's mild winter climate-2004 update. VII International Symposium on Protected Cultivation in Mild Winter Climates: Production, Pest Management and Global Competition 6592004. p. 37-40.

[173] R.A. A, J.W. B. Greenhouse engineering. 3rd rev., August 1994. NRAES (USA) Greenhouse series no 33. 1994.

[174] Kozai T, Niu G, Takagaki M. Plant factory: an indoor vertical farming system for efficient quality food production: Academic press; 2019.

[175] Higashide T, Kasahara Y, Ibuki T, Sumikawa O. Development of closed, energy-saving hydroponics for sloping land. International Conference on Sustainable Greenhouse Systems-Greensys2004 6912004. p. 243-8.

[176] KHAN FAJIJoAE, Sciences F. A review on hydroponic greenhouse cultivation for sustainable agriculture. 2018;2:59-66.

[177] He F, Ma CJC, Agriculture Ei. Modeling greenhouse air humidity by means of artificial neural network and principal component analysis. 2010;71:S19-S23.

[178] Santoro C, Arbizzani C, Erable B, Ieropoulos I. Microbial fuel cells: From fundamentals to applications. A review. J Power Sources. 2017;356:225-44.

[179] Brastad KS, He Z. Water softening using microbial desalination cell technology. Desalination. 2013;309:32-7.

[180] Wang H, Ren ZJ. A comprehensive review of microbial electrochemical systems as a platform technology. Biotechnol Adv. 2013;31:1796-807.

[181] Le Goff A, Holzinger M, Cosnier S. Recent progress in oxygen-reducing laccase biocathodes for enzymatic biofuel cells. Cellular and Molecular Life Sciences. 2015;72:941-52.

[182] Kim Y, Logan BE. Microbial Reverse Electrodialysis Cells for Synergistically Enhanced Power Production. Environmental Science & Technology. 2011;45:5834-9.

[183] Nam J-Y, Cusick RD, Kim Y, Logan BE. Hydrogen Generation in Microbial Reverse-Electrodialysis Electrolysis Cells Using a Heat-Regenerated Salt Solution. Environmental Science & Technology. 2012;46:5240-6.

[184] Zhu X, Hatzell MC, Logan BE. Microbial Reverse-Electrodialysis Electrolysis and Chemical-Production Cell for H2 Production and CO2 Sequestration. Environmental Science & Technology Letters. 2014;1:231-5.

[185] Fischer F. Photoelectrode, photovoltaic and photosynthetic microbial fuel cells. Renewable and Sustainable Energy Reviews. 2018;90:16-27.

[186] Pagnoncelli KC, Pereira AR, Sedenho GC, Bertaglia T, Crespilho FN. Ethanol generation, oxidation and energy production in a cooperative bioelectrochemical system. Bioelectrochemistry. 2018;122:11-25.

[187] Jafary T, Daud WRW, Ghasemi M, Kim BH, Md Jahim J, Ismail M, et al. Biocathode in microbial electrolysis cell; present status and future prospects. Renewable and Sustainable Energy Reviews. 2015;47:23-33.

[188] Xiao L, Young EB, Berges JA, He Z. Integrated Photo-Bioelectrochemical System for Contaminants Removal and Bioenergy Production. Environmental Science & Technology. 2012;46:11459-66.

[189] Yuan L, Yang X, Liang P, Wang L, Huang Z-H, Wei J, et al. Capacitive deionization coupled with microbial fuel cells to desalinate low-concentration salt water. Bioresour Technol. 2012;110:735-8.

[190] Esen M, Yuksel T. Experimental evaluation of using various renewable energy sources for heating a greenhouse. Energy and Buildings. 2013;65:340-51.

[191] Strik DPBTB, Timmers RA, Helder M, Steinbusch KJJ, Hamelers HVM, Buisman CJN. Microbial solar cells: applying photosynthetic and electrochemically active organisms. Trends Biotechnol. 2011;29:41-9.

[192] Zafar Z, Ayaz K, Nasir M, Yousaf S, Sharafat I, Ali N. Electrochemical performance of biocathode microbial fuel cells using petroleum-contaminated soil and hot water spring. International Journal of Environmental Science and Technology. 2019;16:1487-500.

[193] Wang S, Adekunle A, Tartakovsky B, Raghavan V. Synthesizing developments in

the usage of solid organic matter in microbial fuel cells: A review. Chemical Engineering Journal Advances. 2021;8:100140.

[194] Gul H, Raza W, Lee J, Azam M, Ashraf M, Kim K-H. Progress in microbial fuel cell technology for wastewater treatment and energy harvesting. Chemosphere. 2021;281:130828.

[195] Yamashita T, Hayashi T, Iwasaki H, Awatsu M, Yokoyama H. Ultra-low-power energy harvester for microbial fuel cells and its application to environmental sensing and long-range wireless data transmission. Journal of Power Sources. 2019;430:1-11.

[196] Prasad J, Tripathi RK. Voltage control of sediment microbial fuel cell to power the AC load. Journal of Power Sources. 2020;450:227721.

[197] Liu S, Feng X, Li X. Bioelectrochemical approach for control of methane emission from wetlands. Bioresource Technology. 2017;241:812-20.

[198] Zhang K, Wu X, Luo H, Li X, Chen W, Chen J, et al. CH4 control and associated microbial process from constructed wetland (CW) by microbial fuel cells (MFC). Journal of Environmental Management. 2020;260:110071.

[199] Md Khudzari J, Gariépy Y, Kurian J, Tartakovsky B, Raghavan GSV. Effects of biochar anodes in rice plant microbial fuel cells on the production of bioelectricity, biomass, and methane. Biochem Eng J. 2019;141:190-9.

[200] Rizzo A, Boano F, Revelli R, Ridolfi L. Can microbial fuel cells be an effective mitigation strategy for methane emissions from paddy fields? Ecological engineering. 2013;60:167-71.

[201] Moreno R, San-Martín MI, Escapa A, Morán A. Domestic wastewater treatment in parallel with methane production in a microbial electrolysis cell. Renewable Energy. 2016;93:442-8.

[202] Ishii S, rsquo, ichi, Hotta Y, Watanabe K. Methanogenesis <I>versus</I> Electrogenesis: Morphological and Phylogenetic Comparisons of Microbial Communities. Bioscience, Biotechnology, and Biochemistry. 2008;72:286-94.

[203] Xu H, Song H-L, Singh RP, Yang Y-L, Xu J-Y, Yang X-L. Simultaneous reduction of antibiotics leakage and methane emission from constructed wetland by integrating microbial fuel cell. Bioresour Technol. 2021;320:124285.

[204] Rismani-Yazdi H, Carver SM, Christy AD, Yu Z, Bibby K, Peccia J, et al. Suppression of methanogenesis in cellulose-fed microbial fuel cells in relation to performance, metabolite formation, and microbial population. Bioresour Technol. 2013;129:281-8.

[205] Wu S-S, Hernández M, Deng Y-C, Han C, Hong X, Xu J, et al. The voltage signals of microbial fuel cell-based sensors positively correlated with methane emission flux in paddy fields of China. FEMS Microbiol Ecol. 2019;95.

[206] Xiao B, Han Y, Liu X, Liu J. Relationship of methane and electricity production in two-chamber microbial fuel cell using sewage sludge as substrate. Int J Hydrogen Energy. 2014;39:16419-25.

[207] Cattani M, Maccarana L, Rossi G, Tagliapietra F, Schiavon S, Bailoni L. Dose-response and inclusion effects of pure natural extracts and synthetic compounds on in vitro methane production. Animal Feed Science and Technology. 2016;218:100-9.

[208] Su L, Jia W, Hou C, Lei Y. Review: Microbial biosensors. Biosens Bioelectron. 2011;26:1788-99.

[209] Chouler J, Di Lorenzo M. Water quality monitoring in developing countries; can microbial fuel cells be the answer? Biosensors. 2015;5:450-70.

[210] Peixoto L, Min B, Martins G, Brito AG, Kroff P, Parpot P, et al. In situ microbial fuel cell-based biosensor for organic carbon. Bioelectrochemistry. 2011;81:99-103.

[211] Feng Y, Harper Jr WF. Biosensing with microbial fuel cells and artificial neural networks: laboratory and field investigations. Journal of environmental management. 2013;130:369-74.

[212] Wang X, Gao N, Zhou Q. Concentration responses of toxicity sensor with Shewanella oneidensis MR-1 growing in bioelectrochemical systems. Biosensors and Bioelectronics. 2013;43:264-7.

[213] Naik S, Jujjavarapu SE. Self-powered and reusable microbial fuel cell biosensor for toxicity detection in heavy metal polluted water. Journal of Environmental Chemical Engineering. 2021;9:105318.

[214] Prévoteau A, Clauwaert P, Kerckhof F-M, Rabaey K. Oxygen-reducing microbial cathodes monitoring toxic shocks in tap water. Biosensors and Bioelectronics.

2019;132:115-21.

[215] Jin X, Li X, Zhao N, Angelidaki I, Zhang Y. Bio-electrolytic sensor for rapid monitoring of volatile fatty acids in anaerobic digestion process. Water Res. 2017;111:74-80.

[216] Jin X, Li X, Zhao N, Angelidaki I, Zhang YJWr. Bio-electrolytic sensor for rapid monitoring of volatile fatty acids in anaerobic digestion process. 2017;111:74-80.

[217] Koffi NDJ, Okabe S. Bioelectrochemical anoxic ammonium nitrogen removal by an MFC driven single chamber microbial electrolysis cell. Chemosphere. 2021;274:129715.

[218] Adekunle A, Gomez Vidales A, Woodward L, Tartakovsky B. Microbial fuel cell soft sensor for real-time toxicity detection and monitoring. Environmental Science and Pollution Research. 2021;28:12792-802.

[219] Brunelli D, Tosato P, Rossi M. Flora health wireless monitoring with plant-microbial fuel cell. Procedia Engineering. 2016;168:1646-50.

[220] Atci E, Babauta JT, Sultana ST, Beyenal H. Microbiosensor for the detection of acetate in electrode-respiring biofilms. Biosens Bioelectron. 2016;81:517-23.

[221] Zhao L, He L, Chen S, Zou L, Zhou K, Ao X, et al. Microbial BOD sensors based on Zr (IV)-loaded collagen fiber. Enzyme Microb Technol. 2017;98:52-7.

[222] Mohyudin S, Farooq R, Jubeen F, Rasheed T, Fatima M, Sher F. Microbial fuel cells a state-of-the-art technology for wastewater treatment and bioelectricity generation. Environmental Research. 2022;204:112387.

[223] Nguyen HD, Babel S. Insights on microbial fuel cells for sustainable biological nitrogen removal from wastewater: A review. Environmental Research. 2022;204:112095.

[224] Katuri KP, Ali M, Saikaly PE. The role of microbial electrolysis cell in urban wastewater treatment: integration options, challenges, and prospects. Current opinion in biotechnology. 2019;57:101-10.

[225] Kondaveeti S, Choi KS, Kakarla R, Min B. Microalgae Scenedesmus obliquus as renewable biomass feedstock for electricity generation in microbial fuel cells (MFCs). Frontiers of Environmental Science & Engineering. 2014;8:784-91.

[226] Velasquez-Orta SB, Curtis TP, Logan BE. Energy from algae using microbial fuel cells. Biotechnol Bioeng. 2009;103:1068-76.

[227] Wang H, Lu L, Cui F, Liu D, Zhao Z, Xu Y. Simultaneous bioelectrochemical degradation of algae sludge and energy recovery in microbial fuel cells. Rsc Advances. 2012;2:7228-34.

[228] Kakarla R, Kim JR, Jeon B-H, Min B. Enhanced performance of an air–cathode microbial fuel cell with oxygen supply from an externally connected algal bioreactor. Bioresour Technol. 2015;195:210-6.

[229] Hou Q, Nie C, Pei H, Hu W, Jiang L, Yang Z. The effect of algae species on the bioelectricity and biodiesel generation through open-air cathode microbial fuel cell with kitchen waste anaerobically digested effluent as substrate. Bioresour Technol. 2016;218:902-8.

[230] Kumar R, Singh L, Zularisam A, Hai FI. Microbial fuel cell is emerging as a versatile technology: a review on its possible applications, challenges and strategies to improve the performances. International Journal of Energy Research. 2018;42:369-94.

[231] Bolognesi S, Cecconet D, Callegari A, Capodaglio AG. Combined microalgal photobioreactor/microbial fuel cell system: Performance analysis under different process conditions. Environ Res. 2021;192:110263.

[232] Wetser K, Sudirjo E, Buisman CJN, Strik DPBTB. Electricity generation by a plant microbial fuel cell with an integrated oxygen reducing biocathode. Applied Energy. 2015;137:151-7.

[233] Martinucci E, Pizza F, Perrino D, Colombo A, Trasatti SPM, Lazzarini Barnabei A, et al. Energy balance and microbial fuel cells experimentation at wastewater treatment plant Milano-Nosedo. Int J Hydrogen Energy. 2015;40:14683-9.

[234] Baawain MS, Al-Mamun A, Omidvarborna H, Al-Sabti A, Choudri BS. Public perceptions of reusing treated wastewater for urban and industrial applications: challenges and opportunities. Environment, Development and Sustainability. 2020;22:1859-71.

[235] Rahman S, Jafary T, Al-Mamun A, Baawain MS, Choudhury MR, Alhaimali H, et al. Towards upscaling microbial desalination cell technology: A comprehensive

review on current challenges and future prospects. Journal of Cleaner Production. 2021;288:125597.

[236] Saeed T, Yadav AK, Miah MJ. Landfill leachate and municipal wastewater co-treatment in microbial fuel cell integrated unsaturated and partially saturated tidal flow constructed wetlands. Journal of Water Process Engineering. 2022;46:102633.

[237] Larrosa-Guerrero A, Scott K, Head I, Mateo F, Ginesta A, Godinez C. Effect of temperature on the performance of microbial fuel cells. Fuel. 2010;89:3985-94.

[238] Kumar T, Naik S, Jujjavarappu SE. A critical review on early-warning electrochemical system on microbial fuel cell-based biosensor for on-site water quality monitoring. Chemosphere. 2021:133098.

[239] Stoll ZA, Ma Z, Trivedi CB, Spear JR, Xu P. Sacrificing power for more cost-effective treatment: A techno-economic approach for engineering microbial fuel cells. Chemosphere. 2016;161:10-8.

[240] Christwardana M, Yoshi LA. Mathematical Modeling for Determination of Correlation Between Current Density and Dissolved Oxygen in Yeast Microbial Fuel Cell-Based Biosensor. Reaktor. 2020;20:117-21.

[241] Riggio GM, Jones SL, Gibson KE. Risk of human pathogen internalization in leafy vegetables during lab-scale hydroponic cultivation. Horticulturae. 2019;5:25.

[242] Sevda S, Garlapati VK, Naha S, Sharma M, Ray SG, Sreekrishnan TR, et al. Biosensing capabilities of bioelectrochemical systems towards sustainable water streams: technological implications and future prospects. Journal of bioscience and bioengineering. 2020;129:647-56.

[243] Ahmad A, Priyadarshani M, Das S, Ghangrekar MM. Role of bioelectrochemical systems for the remediation of emerging contaminants from wastewater: A review. Journal of Basic Microbiology. 2022;62:201-22.

[244] Regmi R, Nitisoravut R, Charoenroongtavee S, Yimkhaophong W, Phanthurat O. Earthen Pot–Plant Microbial Fuel Cell Powered by Vetiver for Bioelectricity Production and Wastewater Treatment. CLEAN–Soil, Air, Water. 2018;46:1700193.

[245] Alatraktchi FAa, Zhang Y, Angelidaki I. Nanomodification of the electrodes in microbial fuel cell: impact of nanoparticle density on electricity production and

microbial community. Applied Energy. 2014;116:216-22.

[246] Gajda I, Greenman J, Ieropoulos IA. Recent advancements in real-world microbial fuel cell applications. Current opinion in electrochemistry. 2018;11:78-83.

[247] Tang RCO, Jang J-H, Lan T-H, Wu J-C, Yan W-M, Sangeetha T, et al. Review on design factors of microbial fuel cells using Buckingham's Pi Theorem. Renewable and Sustainable Energy Reviews. 2020;130:109878.

[248] Inamuddin I, Asiri AM, Lichtfouse E. Nanophotocatalysis and environmental applications: detoxification and disinfection: Springer; 2020.

[249] Sharma G, Kumar A, Lichtfouse E, Asiri AM. Nanophotocatalysis and Environmental Applications. Materials and Technology.29:83-105.

[250] Jyothi M, Nayak V, Reddy KR, Naveen S, Raghu A. Non-metal (oxygen, sulphur, nitrogen, boron and phosphorus)-doped metal oxide hybrid nanostructures as highly efficient photocatalysts for water treatment and hydrogen generation. Nanophotocatalysis and Environmental Applications: Springer; 2019. p. 83-105.

[251] Shwetharani R, Chandan H, Sakar M, Balakrishna GR, Reddy KR, Raghu AV. Photocatalytic semiconductor thin films for hydrogen production and environmental applications. International Journal of Hydrogen Energy. 2020;45:18289-308.

[252] Sampath P, Reddy KR, Reddy CV, Shetti NP, Kulkarni RV, Raghu AV. Biohydrogen production from organic waste–a review. Chemical Engineering & Technology. 2020;43:1240-8.

[253] Cai W, Lesnik KL, Wade MJ, Heidrich ES, Wang Y, Liu H. Incorporating microbial community data with machine learning techniques to predict feed substrates in microbial fuel cells. Biosensors and Bioelectronics. 2019;133:64-71.

[254] Zhang F, Li C, Yu Y, Johnson DM. Resources and Future Availability of Agricultural Biomass for Energy Use in Beijing. Energies. 2019;12:1828.

[255] Ahmed FE, Hashaikeh R, Hilal N. Solar powered desalination–Technology, energy and future outlook. Desalination. 2019;453:54-76.

[256] Lin H, He M, Jing Q, Yang W, Wang S, Liu Y, et al. Angle-shaped triboelectric nanogenerator for harvesting environmental wind energy. Nano energy. 2019;56:269-76.

[257] Schröder U. Anodic electron transfer mechanisms in microbial fuel cells and their energy efficiency. PCCP. 2007;9:2619-29.

[258] Rossi R, Cario BP, Santoro C, Yang W, Saikaly PE, Logan BE. Evaluation of electrode and solution area-based resistances enables quantitative comparisons of factors impacting microbial fuel cell performance. Environmental science & technology. 2019;53:3977-86.

[259] Mousavi MR, Ghasemi S, Sanaee Z, Nejad ZG, Mardanpour MM, Yaghmaei S, et al. Improvement of the microfluidic microbial fuel cell using a nickel nanostructured electrode and microchannel modifications. J Power Sources. 2019;437:226891.

[260] Rathour R, Patel D, Shaikh S, Desai C. Eco-electrogenic treatment of dyestuff wastewater using constructed wetland-microbial fuel cell system with an evaluation of electrode-enriched microbial community structures. Bioresour Technol. 2019;285:121349.

[261] Liu Z, Liu J, Zhang S, Su Z. Study of operational performance and electrical response on mediator-less microbial fuel cells fed with carbon-and protein-rich substrates. Biochem Eng J. 2009;45:185-91.

[262] Chae K-J, Choi M-J, Lee J-W, Kim K-Y, Kim IS. Effect of different substrates on the performance, bacterial diversity, and bacterial viability in microbial fuel cells. Bioresour Technol. 2009;100:3518-25.

[263] Pant D, Van Bogaert G, Diels L, Vanbroekhoven K. A review of the substrates used in microbial fuel cells (MFCs) for sustainable energy production. Bioresour Technol. 2010;101:1533-43.

[264] Potter MC. Electrical effects accompanying the decomposition of organic compounds. Proceedings of the Royal Society of London Series B, Containing Papers of a Biological Character. 1911;84:260-76.

[265] Cohen B. The bacterial culture as an electrical half-cell. J Bacteriol. 1931;21:18-9.

[266] Habermann W, Pommer EH. Biological fuel cells with sulphide storage capacity. Appl Microbiol Biotechnol. 1991;35:128-33.

[267] Zhao Q, Yu H, Zhang W, Kabutey FT, Jiang J, Zhang Y, et al. Microbial fuel cell with high content solid wastes as substrates: a review. Frontiers of Environmental

Science & Engineering. 2017;11:13.

[268] Catal T, Xu S, Li K, Bermek H, Liu H. Electricity generation from polyalcohols in single-chamber microbial fuel cells. Biosens Bioelectron. 2008;24:849-54.

[269] Ren Z, Ward TE, Regan JM. Electricity Production from Cellulose in a Microbial Fuel Cell Using a Defined Binary Culture. Environmental Science & Technology. 2007;41:4781-6.

[270] Sivasankar V, Mylsamy P, Omine K. Microbial Fuel Cell Technology for Bioelectricity: Springer; 2018.

[271] Sarma PJ, Mohanty K. Epipremnum aureum and Dracaena braunii as indoor plants for enhanced bio-electricity generation in a plant microbial fuel cell with electrochemically modified carbon fiber brush anode. Journal of bioscience and bioengineering. 2018;126:404-10.

[272] Tremouli A, Karydogiannis I, Pandis PK, Papadopoulou K, Argirusis C, Stathopoulos VN, et al. Bioelectricity production from fermentable household waste extract using a single chamber microbial fuel cell. Energy Procedia. 2019;161:2-9.

[273] Asai Y, Miyahara M, Kouzuma A, Watanabe K. Comparative evaluation of wastewater-treatment microbial fuel cells in terms of organics removal, waste-sludge production, and electricity generation. Bioresources and bioprocessing. 2017;4:1-8.

[274] Lu Z, Yin D, Chen P, Wang H, Yang Y, Huang G, et al. Power-generating trees: Direct bioelectricity production from plants with microbial fuel cells. Applied Energy. 2020;268:115040.

[275] Srivastava P, Abbassi R, Garaniya V, Lewis T, Yadav AK. Performance of pilot-scale horizontal subsurface flow constructed wetland coupled with a microbial fuel cell for treating wastewater. Journal of Water Process Engineering. 2020;33:100994.

[276] Yang Y, Zhao Y, Tang C, Xu L, Morgan D, Liu R. Role of macrophyte species in constructed wetland-microbial fuel cell for simultaneous wastewater treatment and bioenergy generation. Chem Eng J. 2020;392:123708.

[277] Adekunle A, Raghavan V, Tartakovsky B. Carbon source and energy harvesting optimization in solid anolyte microbial fuel cells. J Power Sources. 2017;356:324-30.

[278] Zhang X, Cheng S, Liang P, Huang X, Logan BE. Scalable air cathode microbial

fuel cells using glass fiber separators, plastic mesh supporters, and graphite fiber brush anodes. Bioresour Technol. 2011;102:372-5.

[279] Nimje VR, Chen C-C, Chen H-R, Chen C-Y, Tseng M-J, Cheng K-C, et al. A single-chamber microbial fuel cell without an air cathode. International journal of molecular sciences. 2012;13:3933-48.

[280] Catal T, Li K, Bermek H, Liu H. Electricity production from twelve monosaccharides using microbial fuel cells. J Power Sources. 2008;175:196-200.

[281] Zhang X, Miao X, Li J, Li Z. Evaluation of electricity production from Fenton oxidation pretreated sludge using a two-chamber microbial fuel cell. Chem Eng J. 2019;361:599-608.

[282] Kim BH, Chang IS, Gadd GM. Challenges in microbial fuel cell development and operation. Appl Microbiol Biotechnol. 2007;76:485.

[283] Kim JR, Cheng S, Oh S-E, Logan BE. Power generation using different cation, anion, and ultrafiltration membranes in microbial fuel cells. Environmental science & technology. 2007;41:1004-9.

[284] Rozendal RA, Hamelers HV, Buisman CJ. Effects of membrane cation transport on pH and microbial fuel cell performance. Environmental science & technology. 2006;40:5206-11.

[285] Zafar Z, Ayaz K, Nasir MH, Yousaf S, Sharafat I, Ali N. Electrochemical performance of biocathode microbial fuel cells using petroleum-contaminated soil and hot water spring. International Journal of Environmental Science and Technology. 2019;16:1487-500.

[286] Gustave W, Yuan Z-F, Sekar R, Ren Y-X, Liu J-Y, Zhang J, et al. Soil organic matter amount determines the behavior of iron and arsenic in paddy soil with microbial fuel cells. Chemosphere. 2019;237:124459.

[287] Krishnaraj RN, Berchmans S, Pal P. The three-compartment microbial fuel cell: a new sustainable approach to bioelectricity generation from lignocellulosic biomass. Cellulose. 2015;22:655-62.

[288] Hutchinson AJ, Tokash JC, Logan BE. Analysis of carbon fiber brush loading in anodes on startup and performance of microbial fuel cells. J Power Sources.

2011;196:9213-9.

[289] Roy JN, Babanova S, Garcia KE, Cornejo J, Ista LK, Atanassov P. Catalytic biofilm formation by Shewanella oneidensis MR-1 and anode characterization by expanded uncertainty. Electrochim Acta. 2014;126:3-10.

[290] Penteado ED, Fernandez-Marchante CM, Zaiat M, Gonzalez ER, Rodrigo MA. Influence of carbon electrode material on energy recovery from winery wastewater using a dual-chamber microbial fuel cell. Environ Technol. 2017;38:1333-41.

[291] Kaur R, Marwaha A, Chhabra VA, Kim K-H, Tripathi SK. Recent developments on functional nanomaterial-based electrodes for microbial fuel cells. Renewable and Sustainable Energy Reviews. 2020;119:109551.

[292] Zhao C, Gai P, Liu C, Wang X, Xu H, Zhang J, et al. Polyaniline networks grown on graphene nanoribbons-coated carbon paper with a synergistic effect for high-performance microbial fuel cells. Journal of Materials Chemistry A. 2013;1:12587-94.

[293] Sonawane JM, Patil SA, Ghosh PC, Adeloju SB. Low-cost stainless-steel wool anodes modified with polyaniline and polypyrrole for high-performance microbial fuel cells. J Power Sources. 2018;379:103-14.

[294] Rismani-Yazdi H, Carver SM, Christy AD, Tuovinen OH. Cathodic limitations in microbial fuel cells: an overview. J Power Sources. 2008;180:683-94.

[295] Logan B, Cheng S, Watson V, Estadt G. Graphite fiber brush anodes for increased power production in air-cathode microbial fuel cells. Environmental science & technology. 2007;41:3341-6.

[296] Yuan H, Hou Y, Abu-Reesh IM, Chen J, He Z. Oxygen reduction reaction catalysts used in microbial fuel cells for energy-efficient wastewater treatment: a review. Materials Horizons. 2016;3:382-401.

[297] Santoro C, Guilizzoni M, Baena JC, Pasaogullari U, Casalegno A, Li B, et al. The effects of carbon electrode surface properties on bacteria attachment and start up time of microbial fuel cells. Carbon. 2014;67:128-39.

[298] Kakarla R, Min B. Evaluation of microbial fuel cell operation using algae as an oxygen supplier: carbon paper cathode vs. carbon brush cathode. Bioprocess and biosystems engineering. 2014;37:2453-61.

[299] Mustakeem M. Electrode materials for microbial fuel cells: nanomaterial approach. 2015.

[300] Choi J, Ahn Y. Increased power generation from primary sludge in microbial fuel cells coupled with prefermentation. Bioprocess and biosystems engineering. 2014;37:2549-57.

[301] Chaudhuri SK, Lovley DR. Electricity generation by direct oxidation of glucose in mediatorless microbial fuel cells. Nat Biotechnol. 2003;21:1229-32.

[302] Zhang Y, Sun J, Hu Y, Li S, Xu Q. Bio-cathode materials evaluation in microbial fuel cells: a comparison of graphite felt, carbon paper and stainless steel mesh materials. Int J Hydrogen Energy. 2012;37:16935-42.

[303] Liu Y, Zhao Y, Li K, Wang Z, Tian P, Liu D, et al. Activated carbon derived from chitosan as air cathode catalyst for high performance in microbial fuel cells. J Power Sources. 2018;378:1-9.

[304] Wang X, Yuan C, Shao C, Zhuang S, Ye J, Li B. Enhancing oxygen reduction reaction by using metal-free nitrogen-doped carbon black as cathode catalysts in microbial fuel cells treating wastewater. Environ Res. 2020;182:109011.

[305] Türker OC, Baran T, Yakar A, Türe C, Saz Ç. Novel chitosan based smart cathode electrocatalysts for high power generation in plant based-sediment microbial fuel cells. Carbohydr Polym. 2020;239:116235.

[306] Zhen G, Lu X, Kato H, Zhao Y, Li Y-Y. Overview of pretreatment strategies for enhancing sewage sludge disintegration and subsequent anaerobic digestion: Current advances, full-scale application and future perspectives. Renewable and Sustainable Energy Reviews. 2017;69:559-77.

[307] Zhuang X, Huang Y, Song Y, Zhan H, Yin X, Wu C. The transformation pathways of nitrogen in sewage sludge during hydrothermal treatment. Bioresour Technol. 2017;245:463-70.

[308] Wang Y, Zhang H, Li B, Feng Y. Integrating sludge microbial fuel cell with inclined plate settling and membrane filtration for electricity generation, efficient sludge reduction and high wastewater quality. Chem Eng J. 2018;331:152-60.

[309] Kim JR, Min B, Logan BE. Evaluation of procedures to acclimate a microbial fuel

cell for electricity production. Appl Microbiol Biotechnol. 2005;68:23-30.

[310] Sun J, Hu Y, Bi Z, Cao Y. Improved performance of air-cathode single-chamber microbial fuel cell for wastewater treatment using microfiltration membranes and multiple sludge inoculation. J Power Sources. 2009;187:471-9.

[311] Lares M, Ncibi MC, Sillanpää M, Sillanpää M. Occurrence, identification and removal of microplastic particles and fibers in conventional activated sludge process and advanced MBR technology. Water Res. 2018;133:236-46.

[312] Nielsen PH, Frølund B, Keiding K. Changes in the composition of extracellular polymeric substances in activated sludge during anaerobic storage. Appl Microbiol Biotechnol. 1996;44:823-30.

[313] Sommers LE, Nelson DW, Yost KJ. Variable Nature of Chemical Composition of Sewage Sludges. Journal of Environmental Quality. 1976;5:303-6.

[314] Yusoff MZM, Hu A, Feng C, Maeda T, Shirai Y, Hassan MA, et al. Influence of pretreated activated sludge for electricity generation in microbial fuel cell application. Bioresour Technol. 2013;145:90-6.

[315] Ge Z, Zhang F, Grimaud J, Hurst J, He Z. Long-term investigation of microbial fuel cells treating primary sludge or digested sludge. Bioresour Technol. 2013;136:509-14.

[316] Oh S-E, Yoon JY, Gurung A, Kim D-J. Evaluation of electricity generation from ultrasonic and heat/alkaline pretreatment of different sludge types using microbial fuel cells. Bioresour Technol. 2014;165:21-6.

[317] Yang F, Ren L, Pu Y, Logan BE. Electricity generation from fermented primary sludge using single-chamber air-cathode microbial fuel cells. Bioresour Technol. 2013;128:784-7.

[318] Wang D, Zhang D, Xu Q, Liu Y, Wang Q, Ni B-J, et al. Calcium peroxide promotes hydrogen production from dark fermentation of waste activated sludge. Chem Eng J. 2019;355:22-32.

[319] Peng H, Zhang Y, Tan D, Zhao Z, Zhao H, Quan X. Roles of magnetite and granular activated carbon in improvement of anaerobic sludge digestion. Bioresour Technol. 2018;249:666-72.

[320] Pulicharla R, Brar SK, Rouissi T, Auger S, Drogui P, Verma M, et al. Degradation of chlortetracycline in wastewater sludge by ultrasonication, Fenton oxidation, and ferro-sonication. Ultrason Sonochem. 2017;34:332-42.

[321] Xiao B, Yang F, Liu J. Evaluation of electricity production from alkaline pretreated sludge using two-chamber microbial fuel cell. J Hazard Mater. 2013;254:57-63.

[322] Qiu R, Zhang B, Li J, Lv Q, Wang S, Gu Q. Enhanced vanadium (V) reduction and bioelectricity generation in microbial fuel cells with biocathode. J Power Sources. 2017;359:379-83.

[323] Zhang Y, Zhao Y-G, Guo L, Gao M. Two-stage pretreatment of excess sludge for electricity generation in microbial fuel cell. Environ Technol. 2019;40:1349-58.

[324] Zhen G, Lu X, Kobayashi T, Kumar G, Xu K. Promoted electromethanosynthesis in a two-chamber microbial electrolysis cells (MECs) containing a hybrid biocathode covered with graphite felt (GF). Chem Eng J. 2016;284:1146-55.

[325] Vicari F, Asensio Y, Fernandez-Marchante CM, Lobato J, Cañizares P, Scialdone O, et al. Influence of the initial sludge characteristics and acclimation on the long-term performance of double-compartment acetate-fed microbial fuel cells. J Electroanal Chem. 2018;825:1-7.

[326] Feng H, Jia Y, Shen D, Zhou Y, Chen T, Chen W, et al. The effect of chemical vapor deposition temperature on the performance of binder-free sewage sludge-derived anodes in microbial fuel cells. Sci Total Environ. 2018;635:45-52.

[327] Geng Y-K, Yuan L, Liu T, Li Z-H, Zheng X, Sheng G-P. Thermal/alkaline pretreatment of waste activated sludge combined with a microbial fuel cell operated at alkaline pH for efficient energy recovery. Applied Energy. 2020;275:115291.

[328] Abourached C, Lesnik KL, Liu H. Enhanced power generation and energy conversion of sewage sludge by CEA–microbial fuel cells. Bioresour Technol. 2014;166:229-34.

[329] Lv Y, Wang Y, Ren Y, Li X, Wang X, Li J. Effect of anaerobic sludge on the bioelectricity generation enhancement of bufferless single-chamber microbial fuel cells. Bioelectrochemistry. 2020;131:107387.

[330] Zhang H, Da Z, Feng Y, Wang Y, Cai L, Cui H. Enhancing the electricity generation and sludge reduction of sludge microbial fuel cell with graphene oxide and reduced graphene oxide. Journal of Cleaner Production. 2018;186:104-12.

[331] Taşkan B, Taşkan E, Hasar H. Electricity generation potential of sewage sludge in sediment microbial fuel cell using Ti–TiO2 electrode. Environmental Progress & Sustainable Energy. 2020;n/a:e13407.

[332] Xin X, Pang H, She Y, Hong J. Insights into redox mediators-resource harvest/application with power production from waste activated sludge through freezing/thawing-assisted anaerobic acidogenesis coupling microbial fuel cells. Bioresour Technol. 2020;311:123469.

[333] Xu L, Zhao Y, Doherty L, Hu Y, Hao X. Promoting the bio-cathode formation of a constructed wetland-microbial fuel cell by using powder activated carbon modified alum sludge in anode chamber. Scientific reports. 2016;6:26514.

[334] Du H, Li F. Enhancement of solid potato waste treatment by microbial fuel cell with mixed feeding of waste activated sludge. Journal of cleaner production. 2017;143:336-44.

[335] Du H, Guo J, Xu Y, Wu Y, Li F, Wu H. Enhancing microbial fuel cell (MFC) performance in treatment of solid potato waste by mixed feeding of boiled potato and waste activated sludge. Water Sci Technol. 2018;78:1054-63.

[336] Karthikeyan R, Selvam A, Cheng KY, Wong JW-C. Influence of ionic conductivity in bioelectricity production from saline domestic sewage sludge in microbial fuel cells. Bioresour Technol. 2016;200:845-52.

[337] Raad NK, Farrokhi F, Mousavi SA, Darvishi P, Mahmoudi A. Simultaneous power generation and sewage sludge stabilization using an air cathode-MFCs. Biomass Bioenergy. 2020;140:105642.

[338] Cai L, Zhang H, Feng Y, Wang Y, Yu M. Sludge decrement and electricity generation of sludge microbial fuel cell enhanced by zero valent iron. Journal of cleaner production. 2018;174:35-41.

[339] Tiwari B, Ghangrekar M. Enhancing electrogenesis by pretreatment of mixed anaerobic sludge to be used as inoculum in microbial fuel cells. Energy & Fuels.

2015;29:3518-24.

[340] John RP, Anisha G, Nampoothiri KM, Pandey A. Micro and macroalgal biomass: a renewable source for bioethanol. Bioresour Technol. 2011;102:186-93.

[341] Singh J, Gu S. Commercialization potential of microalgae for biofuels production. Renewable and sustainable energy reviews. 2010;14:2596-610.

[342] Baicha Z, Salar-García M, Ortiz-Martínez V, Hernández-Fernández F, De los Ríos A, Labjar N, et al. A critical review on microalgae as an alternative source for bioenergy production: A promising low cost substrate for microbial fuel cells. Fuel Process Technol. 2016;154:104-16.

[343] Gajda I, Greenman J, Melhuish C, Ieropoulos I. Photosynthetic cathodes for microbial fuel cells. Int J Hydrogen Energy. 2013;38:11559-64.

[344] Yang Z, Zhang L, Nie C, Hou Q, Zhang S, Pei H. Multiple anodic chambers sharing an algal raceway pond to establish a photosynthetic microbial fuel cell stack: Voltage boosting accompany wastewater treatment. Water Res. 2019;164:114955.

[345] Ndayisenga F, Yu Z, Yu Y, Lay C-H, Zhou D. Bioelectricity generation using microalgal biomass as electron donor in a bio-anode microbial fuel cell. Bioresour Technol. 2018;270:286-93.

[346] Kondaveeti S, Mohanakrishna G, Pagolu R, Kim I-W, Kalia VC, Lee J-K. Bioelectrogenesis from Raw Algal Biomass Through Microbial Fuel Cells: Effect of Acetate as Co-substrate. Indian journal of microbiology. 2019;59:22-6.

[347] Lakshmidevi R, Gandhi NN, Muthukumar K. Carbon Neutral Electricity Production from Municipal Solid Waste Landfill Leachate Using Algal-Assisted Microbial Fuel Cell. Appl Biochem Biotechnol. 2020:1-15.

[348] Mohd Zaini Makhtar M, Tajarudin HA. Electricity generation using membrane-less microbial fuel cell powered by sludge supplemented with lignocellulosic waste. International Journal of Energy Research. 2020;44:3260-5.

[349] Li S, Song X. Study on the preparation and production factors of a direct lignocellulose biomass fuel cell. J Electroanal Chem. 2018;810:55-61.

[350] Lan L, Li J, Feng Q, Zhang L, Fu Q, Zhu X, et al. Enhanced current production of the anode modified by microalgae derived nitrogen-rich biocarbon for microbial fuel

cells. Int J Hydrogen Energy. 2019.

[351] Cui Y, Rashid N, Hu N, Rehman MSU, Han J-I. Electricity generation and microalgae cultivation in microbial fuel cell using microalgae-enriched anode and bio-cathode. Energy Convers Manage. 2014;79:674-80.

[352] Christwardana M, Hadiyanto H, Motto SA, Sudarno S, Haryani K. Performance evaluation of yeast-assisted microalgal microbial fuel cells on bioremediation of cafeteria wastewater for electricity generation and microalgae biomass production. Biomass Bioenergy. 2020;139:105617.

[353] Motto SA, Christwardana M. Potency of Yeast–Microalgae Spirulina Collaboration in Microalgae-Microbial Fuel Cells for Cafeteria Wastewater Treatment. IOP Conference Series: Earth and Environmental Science: IOP Publishing; 2018. p. 012022.

[354] Mohamed SN, Hiraman PA, Muthukumar K, Jayabalan T. Bioelectricity production from kitchen wastewater using microbial fuel cell with photosynthetic algal cathode. Bioresour Technol. 2020;295:122226.

[355] Zhang Y, He Q, Xia L, Li Y, Song S. Algae cathode microbial fuel cells for cadmium removal with simultaneous electricity production using nickel foam/graphene electrode. Biochem Eng J. 2018;138:179-87.

[356] Zainal MH, Hassan OH, Ab Samad LS, Ali AMM, Yahya MZA. Energy conversion from biodegradation of non-thermal pre-treated algae biomass for microbial fuel cell. Journal of Mechanical Engineering. 2016;13:26-31.

[357] Song X, Wang W, Cao X, Wang Y, Zou L, Ge X, et al. Chlorella vulgaris on the cathode promoted the performance of sediment microbial fuel cells for electrogenesis and pollutant removal. Sci Total Environ. 2020;728:138011.

[358] Zhang Y, Zhao Y, Zhou M. A photosynthetic algal microbial fuel cell for treating swine wastewater. Environmental Science and Pollution Research. 2019;26:6182-90.

[359] Li M, Zhou M, Luo J, Tan C, Tian X, Su P, et al. Carbon dioxide sequestration accompanied by bioenergy generation using a bubbling-type photosynthetic algae microbial fuel cell. Bioresour Technol. 2019;280:95-103.

[360] Khandelwal A, Chhabra M, Yadav P. Performance evaluation of algae assisted

microbial fuel cell under outdoor conditions. Bioresour Technol. 2020;310:123418.

[361] Bazdar E, Roshandel R, Yaghmaei S, Mardanpour MM. The effect of different light intensities and light/dark regimes on the performance of photosynthetic microalgae microbial fuel cell. Bioresour Technol. 2018;261:350-60.

[362] Yang Z, Pei H, Hou Q, Jiang L, Zhang L, Nie C. Algal biofilm-assisted microbial fuel cell to enhance domestic wastewater treatment: nutrient, organics removal and bioenergy production. Chem Eng J. 2018;332:277-85.

[363] Khandelwal A, Vijay A, Dixit A, Chhabra M. Microbial fuel cell powered by lipid extracted algae: a promising system for algal lipids and power generation. Bioresour Technol. 2018;247:520-7.

[364] Yadav G, Sharma I, Ghangrekar M, Sen R. A live bio-cathode to enhance power output steered by bacteria-microalgae synergistic metabolism in microbial fuel cell. J Power Sources. 2020;449:227560.

[365] Ameran HM, Kamalruzaman NKA, Hassan OH, Yahya MZA. Bioenergy production from freeze dried chlorella vulgaris biomass via microbial fuel cell. J Therm Eng. 2016;2:1029-33.

[366] Wang D-B, Song T-S, Guo T, Zeng Q, Xie J. Electricity generation from sediment microbial fuel cells with algae-assisted cathodes. Int J Hydrogen Energy. 2014;39:13224-30.

[367] Zhao X, Zhang L, Liu D. Biomass recalcitrance. Part I: the chemical compositions and physical structures affecting the enzymatic hydrolysis of lignocellulose. Biofuels, Bioproducts and Biorefining. 2012;6:465-82.

[368] ElMekawy A, Diels L, De Wever H, Pant D. Valorization of Cereal Based Biorefinery Byproducts: Reality and Expectations. Environmental Science & Technology. 2013;47:9014-27.

[369] Rezaei F, Xing D, Wagner R, Regan JM, Richard TL, Logan BE. Simultaneous Cellulose Degradation and Electricity Production by Enterobacter cloacae in a Microbial Fuel Cell. Applied and Environmental Microbiology. 2009;75:3673.

[370] Wang X, Feng Y, Wang H, Qu Y, Yu Y, Ren N, et al. Bioaugmentation for

electricity generation from corn stover biomass using microbial fuel cells. Environmental science & technology. 2009;43:6088-93.

[371] Gregoire KP, Becker JG. Design and characterization of a microbial fuel cell for the conversion of a lignocellulosic crop residue to electricity. Bioresour Technol. 2012;119:208-15.

[372] Farmanbordar S, Karimi K, Amiri H. Municipal solid waste as a suitable substrate for butanol production as an advanced biofuel. Energy Convers Manage. 2018;157:396-408.

[373] Sindhu R, Gnansounou E, Rebello S, Binod P, Varjani S, Thakur IS, et al. Conversion of food and kitchen waste to value-added products. Journal of environmental management. 2019.

[374] Lu X, Jin W, Xue S, Wang X. Effects of waste sources on performance of anaerobic co-digestion of complex organic wastes: taking food waste as an example. Scientific reports. 2017;7:15702.

[375] Choi J, Ahn Y. Enhanced bioelectricity harvesting in microbial fuel cells treating food waste leachate produced from biohydrogen fermentation. Bioresour Technol. 2015;183:53-60.

[376] Xin X, Ma Y, Liu Y. Electric energy production from food waste: Microbial fuel cells versus anaerobic digestion. Bioresour Technol. 2018;255:281-7.

[377] Chen Y, Luo J, Yan Y, Feng L. Enhanced production of short-chain fatty acid by co-fermentation of waste activated sludge and kitchen waste under alkaline conditions and its application to microbial fuel cells. Applied Energy. 2013;102:1197-204.

[378] Bridier A, Desmond-Le Quemener E, Bureau C, Champigneux P, Renvoisé L, Audic J-M, et al. Successive bioanode regenerations to maintain efficient current production from biowaste. Bioelectrochemistry. 2015;106:133-40.

[379] Hou Q, Pei H, Hu W, Jiang L, Yu Z. Mutual facilitations of food waste treatment, microbial fuel cell bioelectricity generation and Chlorella vulgaris lipid production. Bioresour Technol. 2016;203:50-5.

[380] Asefi B, Li S-L, Moreno HA, Sanchez-Torres V, Hu A, Li J, et al. Characterization of electricity production and microbial community of food waste-fed microbial fuel

cells. Process Safety and Environmental Protection. 2019;125:83-91.

[381] Ma H, Peng C, Jia Y, Wang Q, Tu M, Gao M. Effect of fermentation stillage of food waste on bioelectricity production and microbial community structure in microbial fuel cells. Royal Society open science. 2018;5:180457.

[382] Xin X, Hong J, Liu Y. Insights into microbial community profiles associated with electric energy production in microbial fuel cells fed with food waste hydrolysate. Sci Total Environ. 2019;670:50-8.

[383] Venkata Mohan S, Chandrasekhar K. Solid phase microbial fuel cell (SMFC) for harnessing bioelectricity from composite food waste fermentation: Influence of electrode assembly and buffering capacity. Bioresour Technol. 2011;102:7077-85.

[384] Li Z, Haynes R, Sato E, Shields MS, Fujita Y, Sato C. Microbial community analysis of a single chamber microbial fuel cell using potato wastewater. Water Environ Res. 2014;86:324-30.

[385] Moqsud MA, Omine K, Yasufuku N, Bushra QS, Hyodo M, Nakata Y. Bioelectricity from kitchen and bamboo waste in a microbial fuel cell. Waste Management & Research. 2014;32:124-30.

[386] Youn S, Yeo J, Joung H, Yang Y. Energy harvesting from food waste by inoculation of vermicomposted organic matter into Microbial Fuel Cell (MFC). 2015 IEEE SENSORS: IEEE; 2015. p. 1-4.

[387] Karluvalı A, Köroğlu EO, Manav N, Çetinkaya AY, Özkaya B. Electricity generation from organic fraction of municipal solid wastes in tubular microbial fuel cell. Sep Purif Technol. 2015;156:502-11.

[388] Iigatani R, Ito T, Watanabe F, Nagamine M, Suzuki Y, Inoue K. Electricity generation from sweet potato-shochu waste using microbial fuel cells. Journal of bioscience and bioengineering. 2019;128:56-63.

[389] Moharir PV, Tembhurkar A. Comparative performance evaluation of novel polystyrene membrane with ultrex as Proton Exchange Membranes in Microbial Fuel Cell for bioelectricity production from food waste. Bioresour Technol. 2018;266:291-6.

[390] Han W, Liu Y, Xu X, He H, Chen L, Tian X, et al. A novel combination of

enzymatic hydrolysis and microbial fuel cell for electricity production from bakery waste. Bioresour Technol. 2020;297:122387.

[391] Chatzikonstantinou D, Tremouli A, Papadopoulou K, Kanellos G, Lampropoulos I, Lyberatos G. Bioelectricity production from fermentable household waste in a dual-chamber microbial fuel cell. Waste Management & Research. 2018;36:1037-42.

[392] Frattini D, Falcuccia G, Minutilloa M, Feronea C, Cioffia R, Jannellia E. On the effect of different configurations in air-cathode MFCs fed by composite food waste for energy harvesting. CHEMICAL ENGINEERING. 2016;49.

[393] Ganjar S, Syafrudin S, Irawan WW, Cagayana C, Meishinta A, Erika L. Effect of Moisture Content on Power Generation in Dual Graphene Anode Compost Solid Phase Microbial Fuel Cells (DGACSMFCs). E3S Web of Conferences: EDP Sciences; 2018. p. 05004.

[394] Florio C, Nastro RA, Flagiello F, Minutillo M, Pirozzi D, Pasquale V, et al. Biohydrogen production from solid phase-microbial fuel cell spent substrate: A preliminary study. Journal of Cleaner Production. 2019;227:506-11.

[395] Antonopoulou G, Ntaikou I, Pastore C, di Bitonto L, Bebelis S, Lyberatos G. An overall perspective for the energetic valorization of household food waste using microbial fuel cell technology of its extract, coupled with anaerobic digestion of the solid residue. Applied Energy. 2019;242:1064-73.

[396] Li H, Tian Y, Zuo W, Zhang J, Pan X, Li L, et al. Electricity generation from food wastes and characteristics of organic matters in microbial fuel cell. Bioresour Technol. 2016;205:104-10.

[397] Adekunle A, Raghavan V. Evaluation of the suitability and performance of cassava waste (peel) extracts in a microbial fuel cell for supplementary and sustainable energy production. Waste Management & Research. 2017;35:47-55.

[398] Roesch LF, Fulthorpe RR, Riva A, Casella G, Hadwin AK, Kent AD, et al. Pyrosequencing enumerates and contrasts soil microbial diversity. The ISME journal. 2007;1:283.

[399] Walker AL, Walker Jr CW. Biological fuel cell and an application as a reserve power source. J Power Sources. 2006;160:123-9.

[400] Liu X-W, Li W-W, Yu H-Q. Cathodic catalysts in bioelectrochemical systems for energy recovery from wastewater. Chem Soc Rev. 2014;43:7718-45.

[401] Li X, Wang X, Zhang Y, Ding N, Zhou Q. Opening size optimization of metal matrix in rolling-pressed activated carbon air–cathode for microbial fuel cells. Applied Energy. 2014;123:13-8.

[402] Deng H, Jiang Y, Zhou Y, Shen K, Zhong W. Using electrical signals of microbial fuel cells to detect copper stress on soil microorganisms. European Journal of Soil Science. 2015;66:369-77.

[403] Wang X, Cai Z, Zhou Q, Zhang Z, Chen C. Bioelectrochemical stimulation of petroleum hydrocarbon degradation in saline soil using U-tube microbial fuel cells. Biotechnol Bioeng. 2012;109:426-33.

[404] Simeon MI, Asoiro FU, Aliyu M, Raji OA, Freitag R. Polarization and power density trends of a soil-based microbial fuel cell treated with human urine. International Journal of Energy Research. 2020;44:5968-76.

[405] Gustave W, Yuan Z-F, Sekar R, Toppin V, Liu J-Y, Ren Y-X, et al. Relic DNA does not obscure the microbial community of paddy soil microbial fuel cells. Res Microbiol. 2019;170:97-104.

[406] Afsham N, Roshandel R, Yaghmaei S, Vajihinejad V, Sherafatmand M. Bioelectricity generation in a soil microbial fuel cell with biocathode denitrification. Energy Sources, Part A: Recovery, Utilization, and Environmental Effects. 2015;37:2092-8.

[407] Cao X, Song H-l, Yu C-y, Li X-n. Simultaneous degradation of toxic refractory organic pesticide and bioelectricity generation using a soil microbial fuel cell. Bioresour Technol. 2015;189:87-93.

[408] Cao X, Yu C, Wang H, Zhou F, Li X. Simultaneous degradation of refractory organic pesticide and bioelectricity generation in a soil microbial fuel cell with different conditions. Environ Technol. 2017;38:1043-50.

[409] Wang H, Song H, Yu R, Cao X, Fang Z, Li X. New process for copper migration by bioelectricity generation in soil microbial fuel cells. Environmental Science and Pollution Research. 2016;23:13147-54.

[410] Wolińska A, Stępniewska Z, Bielecka A, Ciepielski J. Bioelectricity production from soil using microbial fuel cells. Appl Biochem Biotechnol. 2014;173:2287-96.

[411] Li X, Wang X, Zhang Y, Cheng L, Liu J, Li F, et al. Extended petroleum hydrocarbon bioremediation in saline soil using Pt-free multianodes microbial fuel cells. Rsc Advances. 2014;4:59803-8.

[412] Yu B, Li Y, Feng L. Enhancing the performance of soil microbial fuel cells by using a bentonite-Fe and Fe3O4 modified anode. J Hazard Mater. 2019;377:70-7.

[413] Song TS, Zhang J, Hou S, Wang H, Zhang D, Li S, et al. In situ electrokinetic remediation of toxic metal-contaminated soil driven by solid phase microbial fuel cells with a wheat straw addition. Journal of Chemical Technology & Biotechnology. 2018;93:2860-7.

[414] Huang G, Zhang Y, Tang J, Du Y. Remediation of Cd Contaminated Soil in Microbial Fuel Cells: Effects of Cd Concentration and Electrode Spacing. Journal of Environmental Engineering. 2020;146:04020050.

[415] Li X, Wang X, Zhao Q, Wan L, Li Y, Zhou Q. Carbon fiber enhanced bioelectricity generation in soil microbial fuel cells. Biosens Bioelectron. 2016;85:135-41.

[416] Yu B, Tian J, Feng L. Remediation of PAH polluted soils using a soil microbial fuel cell: influence of electrode interval and role of microbial community. J Hazard Mater. 2017;336:110-8.

[417] Gustave W, Yuan Z-F, Sekar R, Chang H-C, Zhang J, Wells M, et al. Arsenic mitigation in paddy soils by using microbial fuel cells. Environ Pollut. 2018;238:647-55.

[418] Wang N, Chen Z, Li H-B, Su J-Q, Zhao F, Zhu Y-G. Bacterial community composition at anodes of microbial fuel cells for paddy soils: the effects of soil properties. Journal of Soils and Sediments. 2015;15:926-36.

[419] Habibul N, Hu Y, Sheng G-P. Microbial fuel cell driving electrokinetic remediation of toxic metal contaminated soils. J Hazard Mater. 2016;318:9-14.

[420] Nandy A, Kumar V, Khamrai M, Kundu PP. MFC with vermicompost soil: power generation with additional importance of waste management. RSC Advances.

2015;5:41300-6.

[421] Yuan H-Y, Liu P-P, Wang N, Li X-M, Zhu Y-G, Khan ST, et al. The influence of soil properties and geographical distance on the bacterial community compositions of paddy soils enriched on SMFC anodes. Journal of soils and sediments. 2018;18:517-25.

[422] Huan D, Yi-Cheng W, Zhang F, HUANG Z-C, Zheng C, Hui-Juan X, et al. Factors affecting the performance of single-chamber soil microbial fuel cells for power generation. Pedosphere. 2014;24:330-8.

[423] Jiang Y-B, Zhong W-H, Han C, Deng H. Characterization of electricity generated by soil in microbial fuel cells and the isolation of soil source exoelectrogenic bacteria. Frontiers in microbiology. 2016;7:1776.

[424] Li X, Li Y, Zhao X, Weng L, Li Y. Cation accumulation leads to the electrode aging in soil microbial fuel cells. Journal of soils and sediments. 2018;18:1003-8.

[425] Li Y, Li X, Sun Y, Zhao X, Li Y. Cathodic microbial community adaptation to the removal of chlorinated herbicide in soil microbial fuel cells. Environmental Science and Pollution Research. 2018;25:16900-12.

[426] Cheng S, Liu W. Microbial Fuel Cells and Other Bio-Electrochemical Conversion Devices. Electrochemically Enabled Sustainability: Devices, Materials and Mechanisms for Energy Conversion. 2014:55-120.

[427] Li H, Qu Y, Tian Y, Feng Y. The plant-enhanced bio-cathode: Root exudates and microbial community for nitrogen removal. Journal of Environmental Sciences. 2019;77:97-103.

[428] Guadarrama-Pérez O, Gutiérrez-Macías T, García-Sánchez L, Guadarrama-Pérez VH, Estrada-Arriaga EB. Recent advances in constructed wetland-microbial fuel cells for simultaneous bioelectricity production and wastewater treatment: A review. International Journal of Energy Research. 2019.

[429] Fang Z, Song H-L, Cang N, Li X-N. Performance of microbial fuel cell coupled constructed wetland system for decolorization of azo dye and bioelectricity generation. Bioresour Technol. 2013;144:165-71.

[430] Liu X, Liu Y, Guo X, Lu S, Wang Y, Zhang J, et al. High degree of contaminant

removal and evolution of microbial community in different electrolysis-integrated constructed wetland systems. Chem Eng J. 2020;388:124391.

[431] Doherty L, Zhao Y, Zhao X, Hu Y, Hao X, Xu L, et al. A review of a recently emerged technology: constructed wetland–microbial fuel cells. Water Res. 2015;85:38-45.

[432] Yadav A. Design and development of novel constructed wetland cum microbial fuel cell for electricity production and wastewater treatment. Proceedings of 12th International Conference on Wetland Systems for Water Pollution Control (IWA)2010.

[433] Villasenor J, Capilla P, Rodrigo M, Canizares P, Fernandez F. Operation of a horizontal subsurface flow constructed wetland–microbial fuel cell treating wastewater under different organic loading rates. Water Res. 2013;47:6731-8.

[434] Jethwa K, Bajpai S. Role of plants in constructed wetlands (CWS): A review. J Chem Pharm Sci. 2016;2:4-10.

[435] Srivastava P, Dwivedi S, Kumar N, Abbassi R, Garaniya V, Yadav AK. Performance assessment of aeration and radial oxygen loss assisted cathode based integrated constructed wetland-microbial fuel cell systems. Bioresour Technol. 2017;244:1178-82.

[436] Villaseñor Camacho J, Rodríguez Romero L, Fernández Marchante CM, Fernández Morales FJ, Rodrigo Rodrigo MA. The salinity effects on the performance of a constructed wetland-microbial fuel cell. Ecol Eng. 2017;107:1-7.

[437] Wetser K, Sudirjo E, Buisman CJ, Strik DP. Electricity generation by a plant microbial fuel cell with an integrated oxygen reducing biocathode. Applied energy. 2015;137:151-7.

[438] Sophia AC, Sreeja S. Green energy generation from plant microbial fuel cells (PMFC) using compost and a novel clay separator. Sustainable Energy Technologies and Assessments. 2017;21:59-66.

[439] Gilani SR, Yaseen A, Zaidi SRA, Zahra M, Mahmood Z. Photocurrent Generation through Plant Microbial Fuel Cell by Varying Electrode Materials. J Chem Soc Pak. 2016;38.

[440] Khudzari JM, Kurian J, Gariépy Y, Tartakovsky B, Raghavan G. Effects of salinity,

growing media, and photoperiod on bioelectricity production in plant microbial fuel cells with weeping alkaligrass. Biomass Bioenergy. 2018;109:1-9.

[441] Martinucci E, Pizza F, Perrino D, Colombo A, Trasatti S, Barnabei AL, et al. Energy balance and microbial fuel cells experimentation at wastewater treatment plant Milano-Nosedo. Int J Hydrogen Energy. 2015;40:14683-9.

[442] Ahn J-H, Jeong W-S, Choi M-Y, Kim B-Y, Song J, Weon H-Y. Phylogenetic diversity of dominant bacterial and archaeal communities in plant-microbial fuel cells using rice plants. J Microbiol Biotechnol. 2014;24:1707-18.

[443] Liu S, Song H, Wei S, Yang F, Li X. Bio-cathode materials evaluation and configuration optimization for power output of vertical subsurface flow constructed wetland—Microbial fuel cell systems. Bioresour Technol. 2014;166:575-83.

[444] Corbella C, Guivernau M, Viñas M, Puigagut J. Operational, design and microbial aspects related to power production with microbial fuel cells implemented in constructed wetlands. Water Res. 2015;84:232-42.

[445] Wang L, Zhou Y, Peng F, Zhang A, Pang Q, Lian J, et al. Intensified nitrogen removal in the tidal flow constructed wetland-microbial fuel cell: Insight into evaluation of denitrifying genes. Journal of Cleaner Production. 2020;264:121580.

[446] Di L, Li Y, Nie L, Wang S, Kong F. Influence of plant radial oxygen loss in constructed wetland combined with microbial fuel cell on nitrobenzene removal from aqueous solution. J Hazard Mater. 2020;394:122542.

[447] Zhao C, Shang D, Zou Y, Du Y, Wang Q, Xu F, et al. Changes in electricity production and microbial community evolution in constructed wetland-microbial fuel cell exposed to wastewater containing Pb(II). Sci Total Environ. 2020;732:139127.

[448] Tao M, Guan L, Jing Z, Tao Z, Wang Y, Luo H, et al. Enhanced denitrification and power generation of municipal wastewater treatment plants (WWTPs) effluents with biomass in microbial fuel cell coupled with constructed wetland. Sci Total Environ. 2020;709:136159.

[449] Yan D, Song X, Weng B, Yu Z, Bi W, Wang J. Bioelectricity generation from air-cathode microbial fuel cell connected to constructed wetland. Water Sci Technol. 2018;78:1990-6.

[450] Oon Y-L, Ong S-A, Ho L-N, Wong Y-S, Dahalan FA, Oon Y-S, et al. Constructed wetland–microbial fuel cell for azo dyes degradation and energy recovery: Influence of molecular structure, kinetics, mechanisms and degradation pathways. Sci Total Environ. 2020;720:137370.

[451] Doherty L, Zhao Y, Zhao X, Wang W. Nutrient and organics removal from swine slurry with simultaneous electricity generation in an alum sludge-based constructed wetland incorporating microbial fuel cell technology. Chem Eng J. 2015;266:74-81.

[452] Wetser K, Liu J, Buisman C, Strik D. Plant microbial fuel cell applied in wetlands: spatial, temporal and potential electricity generation of Spartina anglica salt marshes and Phragmites australis peat soils. Biomass Bioenergy. 2015;83:543-50.

[453] Liu F, Sun L, Wan J, Shen L, Yu Y, Hu L, et al. Performance of different macrophytes in the decontamination of and electricity generation from swine wastewater via an integrated constructed wetland-microbial fuel cell process. Journal of Environmental Sciences. 2020;89:252-63.

[454] Mu C, Wang L, Wang L. Performance of lab-scale microbial fuel cell coupled with unplanted constructed wetland for hexavalent chromium removal and electricity production. Environmental Science and Pollution Research. 2020:1-9.

[455] Khuman Chabungbam N, Bhowmick Gourav D, Ghangrekar Makarand M, Mitra A. Effect of Using a Ceramic Separator on the Performance of Hydroponic Constructed Wetland-Microbial Fuel Cell. Journal of Hazardous, Toxic, and Radioactive Waste. 2020;24:04020005.

[456] Oon Y-L, Ong S-A, Ho L-N, Wong Y-S, Dahalan FA, Oon Y-S, et al. Role of macrophyte and effect of supplementary aeration in up-flow constructed wetland-microbial fuel cell for simultaneous wastewater treatment and energy recovery. Bioresour Technol. 2017;224:265-75.

[457] Teoh T-P, Ong S-A, Ho L-N, Wong Y-S, Oon Y-L, Oon Y-S, et al. Up-flow constructed wetland-microbial fuel cell: Influence of floating plant, aeration and circuit connection on wastewater treatment performance and bioelectricity generation. Journal of Water Process Engineering. 2020;36:101371.

[458] Tamta P, Rani N, Yadav AK. Enhanced wastewater treatment and electricity

generation using stacked constructed wetland–microbial fuel cells. Environmental Chemistry Letters. 2020:1-9.

[459] Song H, Zhang S, Long X, Yang X, Li H, Xiang W. Optimization of bioelectricity generation in constructed wetland-coupled microbial fuel cell systems. Water. 2017;9:185.

[460] Corbella C, Garfí M, Puigagut J. Vertical redox profiles in treatment wetlands as function of hydraulic regime and macrophytes presence: Surveying the optimal scenario for microbial fuel cell implementation. Sci Total Environ. 2014;470:754-8.

[461] Cheng K, Hu J, Hou H, Liu B, Chen Q, Pan K, et al. Aerobic granular sludge inoculated microbial fuel cells for enhanced epoxy reactive diluent wastewater treatment. Bioresour Technol. 2017;229:126-33.

[462] Nguyen HT, Kakarla R, Min B. Algae cathode microbial fuel cells for electricity generation and nutrient removal from landfill leachate wastewater. Int J Hydrogen Energy. 2017;42:29433-42.

[463] Oon YL, Ong SA, Ho LN, Wong YS, Oon YS, Lehl HK, et al. Hybrid system up-flow constructed wetland integrated with microbial fuel cell for simultaneous wastewater treatment and electricity generation. Bioresour Technol. 2015;186:270-5.

[464] Li X, Wang X, Wan L, Zhang Y, Li N, Li D, et al. Enhanced biodegradation of aged petroleum hydrocarbons in soils by glucose addition in microbial fuel cells. Journal of Chemical Technology & Biotechnology. 2016;91:267-75.

[465] Ewing T, Ha PT, Beyenal H. Evaluation of long-term performance of sediment microbial fuel cells and the role of natural resources. Applied energy. 2017;192:490-7.

[466] Semenec L, Franks AE. The microbiology of microbial electrolysis cells. Microbiology Australia. 2014;35:201-6.

[467] Abbas SZ, Rafatullah M, Ismail N, Syakir MI. A review on sediment microbial fuel cells as a new source of sustainable energy and heavy metal remediation: mechanisms and future prospective. International Journal of Energy Research. 2017;41:1242-64.

[468] Gustave W, Yuan Z-F, Ren Y-X, Sekar R, Zhang J, Chen Z. Arsenic alleviation in rice by using paddy soil microbial fuel cells. Plant and Soil. 2019:1-17.

[469] Sun J-Z, Peter Kingori G, Si R-W, Zhai D-D, Liao Z-H, Sun D-Z, et al. Microbial fuel cell-based biosensors for environmental monitoring: a review. Water Sci Technol. 2015;71:801-9.

[470] Tapia NF, Rojas C, Bonilla CA, Vargas IT. A new method for sensing soil water content in green roofs using plant microbial fuel cells. Sensors. 2018;18:71.

[471] Yoon TH, Song HJ, Jung WY, Kim JE, Kim KJ, Kim HH, et al. Monitoring Plant Health Using a Plant Microbial Fuel Cell. Bull Korean Chem Soc. 2018;39:1193-7.

[472] Jia H, Yang G, Wang J, Ngo HH, Guo W, Zhang H, et al. Performance of a microbial fuel cell-based biosensor for online monitoring in an integrated system combining microbial fuel cell and upflow anaerobic sludge bed reactor. Bioresour Technol. 2016;218:286-93.

[473] Logan BE, Regan JM. Electricity-producing bacterial communities in microbial fuel cells. Trends in Microbiology. 2006;14:512-8.

[474] Zhang G, Wang K, Zhao Q, Jiao Y, Lee D-J. Effect of cathode types on long-term performance and anode bacterial communities in microbial fuel cells. Bioresour Technol. 2012;118:249-56.

[475] Yoshizawa T, Miyahara M, Kouzuma A, Watanabe K. Conversion of activated-sludge reactors to microbial fuel cells for wastewater treatment coupled to electricity generation. Journal of bioscience and bioengineering. 2014;118:533-9.

[476] Nor MHM, Mubarak MFM, Elmi HSA, Ibrahim N, Wahab MFA, Ibrahim Z. Bioelectricity generation in microbial fuel cell using natural microflora and isolated pure culture bacteria from anaerobic palm oil mill effluent sludge. Bioresour Technol. 2015;190:458-65.

[477] Islam MA, Ethiraj B, Cheng CK, Yousuf A, Khan MMR. Electrogenic and antimethanogenic properties of Bacillus cereus for enhanced power generation in anaerobic sludge-driven microbial fuel cells. Energy & Fuels. 2017;31:6132-9.

[478] Peng X, Tang T, Zhu X, Jia G, Ding Y, Chen Y, et al. Remediation of acid mine drainage using microbial fuel cell based on sludge anaerobic fermentation. Environ Technol. 2017;38:2400-9.

[479] Nandy A, Sharma M, Venkatesan SV, Taylor N, Gieg L, Thangadurai V.

Comparative Evaluation of Coated and Non-Coated Carbon Electrodes in a Microbial Fuel Cell for Treatment of Municipal Sludge. Energies. 2019;12:1034.

[480] Ruslan AR, Vadivelu VM. Nitrite pre-treatment of dewatered sludge for microbial fuel cell application. Journal of Environmental Sciences. 2019;77:148-55.

[481] Takahashi S, Miyahara M, Kouzuma A, Watanabe K. Electricity generation from rice bran in microbial fuel cells. Bioresources and bioprocessing. 2016;3:50.

[482] Vilajeliu-Pons A, Puig S, Pous N, Salcedo-Dávila I, Bañeras L, Balaguer MD, et al. Microbiome characterization of MFCs used for the treatment of swine manure. J Hazard Mater. 2015;288:60-8.

[483] Akdeniz F, Çağlar A, Güllü D. Recent energy investigations on fossil and alternative nonfossil resources in Turkey. Energy Conversion and Management. 2002;43:575-89.

[484] Kalair A, Abas N, Saleem MS, Kalair AR, Khan N. Role of energy storage systems in energy transition from fossil fuels to renewables. Energy Storage. 2021;3:e135.

[485] Kotcher J, Maibach E, Choi W-T. Fossil fuels are harming our brains: identifying key messages about the health effects of air pollution from fossil fuels. BMC public health. 2019;19:1-12.

[486] Mahmood N, Wang Z, Zhang B. The role of nuclear energy in the correction of environmental pollution: Evidence from Pakistan. Nuclear Engineering and Technology. 2020;52:1327-33.

[487] Rahimnejad M, Ghoreyshi A, Najafpour G, Younesi H, Shakeri M. A novel microbial fuel cell stack for continuous production of clean energy. International journal of hydrogen energy. 2012;37:5992-6000.

[488] Choudhury P, Uday USP, Mahata N, Tiwari ON, Ray RN, Bandyopadhyay TK, et al. Performance improvement of microbial fuel cells for waste water treatment along with value addition: a review on past achievements and recent perspectives. Renewable and Sustainable Energy Reviews. 2017;79:372-89.

[489] Wang S, Adekunle A, Tartakovsky B, Raghavan V. Synthesizing developments in the usage of solid organic matter in microbial fuel cells: A review. 2017.

[490] Munoz-Cupa C, Hu Y, Xu C, Bassi A. An overview of microbial fuel cell usage in wastewater treatment, resource recovery and energy production. Science of the Total Environment. 2021;754:142429.

[491] Gupta S, Srivastava P, Patil SA, Yadav AK. A comprehensive review on emerging constructed wetland coupled microbial fuel cell technology: potential applications and challenges. Bioresource Technology. 2021;320:124376.

[492] Lu M, Li SFY. Cathode reactions and applications in microbial fuel cells: a review. Critical reviews in environmental science and technology. 2012;42:2504-25.

[493] Cheng S, Wu J. Air-cathode preparation with activated carbon as catalyst, PTFE as binder and nickel foam as current collector for microbial fuel cells. Bioelectrochemistry. 2013;92:22-6.

[494] Fu Z, Yan L, Li K, Ge B, Pu L, Zhang X. The performance and mechanism of modified activated carbon air cathode by non-stoichiometric nano Fe3O4 in the microbial fuel cell. Biosensors and Bioelectronics. 2015;74:989-95.

[495] Xie X, Ye M, Hu L, Liu N, McDonough JR, Chen W, et al. Carbon nanotube-coated macroporous sponge for microbial fuel cell electrodes. Energy & Environmental Science. 2012;5:5265-70.

[496] Xie X, Yu G, Liu N, Bao Z, Criddle CS, Cui Y. Graphene–sponges as high-performance low-cost anodes for microbial fuel cells. Energy & Environmental Science. 2012;5:6862-6.

[497] Chabi S, Peng C, Hu D, Zhu Y. Ideal three-dimensional electrode structures for electrochemical energy storage. Advanced Materials. 2014;26:2440-5.

[498] Xu H, Wang L, Lin C, Zheng J, Wen Q, Chen Y, et al. Improved simultaneous decolorization and power generation in a microbial fuel cell with the sponge anode modified by polyaniline and chitosan. Applied Biochemistry and Biotechnology. 2020;192:698-718.

[499] Ma H, Xia T, Bian C, Sun H, Liu Z, Wu C, et al. Bacterial electroactivity and viability depends on the carbon nanotube-coated sponge anode used in a microbial fuel cell. Bioelectrochemistry. 2018;122:26-31.

[500] Wang Y, Pan X, Chen Y, Wen Q, Lin C, Zheng J, et al. A 3D porous nitrogen-

doped carbon nanotube sponge anode modified with polypyrrole and carboxymethyl cellulose for high-performance microbial fuel cells. Journal of Applied Electrochemistry. 2020;50:1281-90.

[501] Rago L, Cristiani P, Villa F, Zecchin S, Colombo A, Cavalca L, et al. Influences of dissolved oxygen concentration on biocathodic microbial communities in microbial fuel cells. Bioelectrochemistry. 2017;116:39-51.

[502] Lepage G, Albernaz FO, Perrier G, Merlin G. Characterization of a microbial fuel cell with reticulated carbon foam electrodes. Bioresource technology. 2012;124:199-207.

[503] Vergara BS. Rice plant growth and development. Rice: Volume I Production/Volume II Utilization: Springer; 1991. p. 13-22.

[504] Zhang H, Li Y, Zhang H, Li G, Zhang F. A Three-dimensional Floating Air Cathode with Dual Oxygen Supplies for Energy-efficient Production of Hydrogen Peroxide. Scientific Reports. 2019;9:1817.

[505] Chen H, Muros-Cobos JL, Amirfazli A. Contact angle measurement with a smartphone. Review of Scientific Instruments. 2018;89:035117.

[506] Ueno D, Koyama E, Kono I, Ando T, Yano M, Ma JF. Identification of a Novel Major Quantitative Trait Locus Controlling Distribution of Cd Between Roots and Shoots in Rice. Plant and Cell Physiology. 2009;50:2223-33.

[507] Mehta P, Hussain A, Tartakovsky B, Neburchilov V, Raghavan V, Wang H, et al. Electricity generation from carbon monoxide in a single chamber microbial fuel cell. Enzyme Microb Technol. 2010;46:450-5.

[508] Xu H, Wang L, Wen Q, Chen Y, Qi L, Huang J, et al. A 3D porous NCNT sponge anode modified with chitosan and Polyaniline for high-performance microbial fuel cell. Bioelectrochemistry. 2019;129:144-53.

[509] Yang W, Chata G, Zhang Y, Peng Y, Lu JE, Wang N, et al. Graphene oxide-supported zinc cobalt oxides as effective cathode catalysts for microbial fuel cell: High catalytic activity and inhibition of biofilm formation. Nano Energy. 2019;57:811-9.

[510] Yuan Y, Zhou S, Tang J. In situ investigation of cathode and local biofilm

microenvironments reveals important roles of OH–and oxygen transport in microbial fuel cells. Environmental science & technology. 2013;47:4911-7.

[511] Rajesh P, Noori MT, Ghangrekar M. Improving performance of microbial fuel cell by using polyaniline-coated carbon–felt anode. Journal of Hazardous, Toxic, and Radioactive Waste. 2020;24:04020024.

[512] Wang Y-T, Tu C-H, Lin Y-S. Application of graphene and carbon nanotubes on carbon felt electrodes for the electro-fenton system. Materials. 2019;12:1698.

[513] Badri KBH, Sien WC, Shahrom M, Hao LC, Baderuliksan NY, Norzali N. FTIR spectroscopy analysis of the prepolymerization of palm-based polyurethane. Solid State Sci Technol. 2010;18:1-8.

[514] Lan W, Wang S, Chen M, Sameen DE, Lee K, Liu Y. Developing poly (vinyl alcohol)/chitosan films incorporate with d-limonene: Study of structural, antibacterial, and fruit preservation properties. International journal of biological macromolecules. 2020;145:722-32.

[515] Silva MAd, Bierhalz ACK, Kieckbusch TG. Influence of drying conditions on physical properties of alginate films. Drying Technology. 2012;30:72-9.

[516] Budiman BA, Takahashi K, Inaba K, Kishimoto K. Evaluation of interfacial strength between fiber and matrix based on cohesive zone modeling. Composites Part A: Applied Science and Manufacturing. 2016;90:211-7.

[517] Broutman L, Agarwal BD. Effect of the interface on the mechanical properties of composite materials. Rheologica Acta. 1974;13:618-26.

[518] Okoli O, Smith G. Failure modes of fibre reinforced composites: The effects of strain rate and fibre content. Journal of Materials Science. 1998;33:5415-22.

[519] Rice R. Limitations of pore-stress concentrations on the mechanical properties of porous materials. Journal of Materials Science. 1997;32:4731-6.

[520] Logan BE. Scaling up microbial fuel cells and other bioelectrochemical systems. Applied microbiology and biotechnology. 2010;85:1665-71.

[521] Chai C, Xu H, Zhao C, Guo H, Li N, Lin X, et al. Effect of carbonization temperature of carbon felt on removal of methylene blue: carbon felt as the cathode of Electro-Fenton system. Journal of Physics: Conference Series: IOP Publishing; 2022.

p. 012034.

[522] Wang X, Zhou B, Jiang M. Dynamic contact angle effects on gas-liquid transport phenomena in proton exchange membrane fuel cell cathode with parallel design. International Journal of Energy Research. 2018;42:4439-57.

[523] Wang W, Pan H, Yu B, Pan Y, Song L, Liew KM, et al. Fabrication of carbon black coated flexible polyurethane foam for significantly improved fire safety. RSC Advances. 2015;5:55870-8.

[524] Zammarano M, Krämer RH, Harris Jr R, Ohlemiller TJ, Shields JR, Rahatekar SS, et al. Flammability reduction of flexible polyurethane foams via carbon nanofiber network formation. Polymers for Advanced Technologies. 2008;19:588-95.

[525] Scuracchio C, Waki D, Da Silva M. Thermal analysis of ground tire rubber devulcanized by microwaves. Journal of Thermal Analysis and Calorimetry. 2007;87:893-7.

[526] Shan CW, Idris MI, Ghazali MI. Study of flexible polyurethane foams reinforced with coir fibres and tyre particles. International Journal of Applied Physics and Mathematics. 2012;2:123-30.

[527] Liu Y, Zheng H, Liu M. High performance strain sensors based on chitosan/carbon black composite sponges. Materials & Design. 2018;141:276-85.

[528] Dong M, Li Q, Liu H, Liu C, Wujcik EK, Shao Q, et al. Thermoplastic polyurethane-carbon black nanocomposite coating: Fabrication and solid particle erosion resistance. Polymer. 2018;158:381-90.

[529] Liu H, Zheng S. Polyurethane networks nanoreinforced by polyhedral oligomeric silsesquioxane. Macromolecular Rapid Communications. 2005;26:196-200.

[530] Khalil HA, Firoozian P, Bakare I, Akil HM, Noor AM. Exploring biomass based carbon black as filler in epoxy composites: Flexural and thermal properties. Materials & Design. 2010;31:3419-25.

[531] Khudzari JM, Tartakovsky B, Raghavan GV. Effect of C/N ratio and salinity on power generation in compost microbial fuel cells. Waste Management. 2016;48:135-42.

[532] Cheng S, Liu H, Logan BE. Power densities using different cathode catalysts (Pt

and CoTMPP) and polymer binders (Nafion and PTFE) in single chamber microbial fuel cells. Environmental science & technology. 2006;40:364-9.

[533] Yang S, Jia B, Liu H. Effects of the Pt loading side and cathode-biofilm on the performance of a membrane-less and single-chamber microbial fuel cell. Bioresource Technology. 2009;100:1197-202.

[534] Helder M, Strik DPBTB, Hamelers HVM, Kuhn AJ, Blok C, Buisman CJN. Concurrent bio-electricity and biomass production in three Plant-Microbial Fuel Cells using Spartina anglica, Arundinella anomala and Arundo donax. Bioresour Technol. 2010;101:3541-7.

[535] Paitier A, Godain A, Lyon D, Haddour N, Vogel TM, Monier J-M. Microbial fuel cell anodic microbial population dynamics during MFC start-up. Biosens Bioelectron. 2017;92:357-63.

[536] Xu H, Wu J, Qi L, Chen Y, Wen Q, Duan T, et al. Preparation and microbial fuel cell application of sponge-structured hierarchical polyaniline-texture bioanode with an integration of electricity generation and energy storage. J Appl Electrochem. 2018;48:1285-95.

[537] Abbasi U, Jin W, Pervez A, Bhatti ZA, Tariq M, Shaheen S, et al. Anaerobic microbial fuel cell treating combined industrial wastewater: Correlation of electricity generation with pollutants. Bioresource technology. 2016;200:1-7.

[538] Cheng S, Liu H, Logan BE. Increased performance of single-chamber microbial fuel cells using an improved cathode structure. Electrochemistry communications. 2006;8:489-94.

[539] Zhang T, Zeng Y, Chen S, Ai X, Yang H. Improved performances of E. coli-catalyzed microbial fuel cells with composite graphite/PTFE anodes. Electrochemistry Communications. 2007;9:349-53.

[540] Litster S, McLean G. PEM fuel cell electrodes. Journal of power sources. 2004;130:61-76.

[541] Yuan Y, Zhou S, Liu Y, Tang J. Nanostructured macroporous bioanode based on polyaniline-modified natural loofah sponge for high-performance microbial fuel cells. Environmental science & technology. 2013;47:14525-32.

[542] Cicerone RJ, Oremland RS. Biogeochemical aspects of atmospheric methane. Global biogeochemical cycles. 1988;2:299-327.

[543] Lu Y, Wassmann R, Neue HU, Huang C. Dissolved organic carbon and methane emissions from a rice paddy fertilized with ammonium and nitrate. Wiley Online Library; 2000.

[544] Tokida T, Fumoto T, Cheng W, Matsunami T, Adachi M, Katayanagi N, et al. Effects of free-air CO 2 enrichment (FACE) and soil warming on CH 4 emission from a rice paddy field: impact assessment and stoichiometric evaluation. Biogeosciences. 2010;7:2639-53.

[545] Gogoi N, Baruah K, Gogoi B, Gupta PK. Methane emission characteristics and its relations with plant and soil parameters under irrigated rice ecosystem of northeast India. Chemosphere. 2005;59:1677-84.

[546] Singh S, Singh J, Kashyap A. Methane flux from irrigated rice fields in relation to crop growth and N-fertilization. Soil Biology and Biochemistry. 1999;31:1219-28.

[547] Xu S, Jaffé PR, Mauzerall DL. A process-based model for methane emission from flooded rice paddy systems. ecological modelling. 2007;205:475-91.

[548] Conrad R. Microbial ecology of methanogens and methanotrophs. Advances in agronomy. 2007;96:1-63.

[549] Wang S, Adekunle A, Raghavan V. Exploring the integration of bioelectrochemical systems and hydroponics: Possibilities, challenges, and innovations. Journal of Cleaner Production. 2022;366:132855.

[550] Khudzari JM, Gariépy Y, Kurian J, Tartakovsky B, Raghavan GVJBEJ. Effects of biochar anodes in rice plant microbial fuel cells on the production of bioelectricity, biomass, and methane. 2019;141:190-9.

[551] Chen Z, Tang Y-T, Zhou C, Xie S-T, Xiao S, Baker AJ, et al. Mechanisms of Fe biofortification and mitigation of Cd accumulation in rice (Oryza sativa L.) grown hydroponically with Fe chelate fertilization. Chemosphere. 2017;175:275-85.

[552] Satake T, Hayase H. Male sterility caused by cooling treatment at the young microspore stage in rice plants: V. Estimations of pollen developmental stage and the most sensitive stage to coolness. Japanese journal of crop science. 1970;39:468-73.

[553] Zhong W-H, Cai L-C, Wei Z-G, Xue H-J, Han C, Deng H. The effects of closed circuit microbial fuel cells on methane emissions from paddy soil vary with straw amount. Catena. 2017;154:33-9.

[554] Nouchi I, Hosono T, Aoki K, Minami K. Seasonal variation in methane flux from rice paddies associated with methane concentration in soil water, rice biomass and temperature, and its modelling. Plant and soil. 1994;161:195-208.

[555] Menicucci J, Beyenal H, Marsili E, Veluchamy RA, Demir G, Lewandowski Z. Procedure for determining maximum sustainable power generated by microbial fuel cells. Environmental science & technology. 2006;40:1062-8.

[556] Ghangrekar M, Shinde V. Performance of membrane-less microbial fuel cell treating wastewater and effect of electrode distance and area on electricity production. Bioresource Technology. 2007;98:2879-85.

[557] Chae K-J, Choi M-J, Kim K-Y, Ajayi F, Park W, Kim C-W, et al. Methanogenesis control by employing various environmental stress conditions in two-chambered microbial fuel cells. Bioresource technology. 2010;101:5350-7.

[558] Zhang L, Zhu X, Li J, Liao Q, Ye D. Biofilm formation and electricity generation of a microbial fuel cell started up under different external resistances. Journal of Power Sources. 2011;196:6029-35.

[559] Lyon DY, Buret F, Vogel TM, Monier J-M. Is resistance futile? Changing external resistance does not improve microbial fuel cell performance. Bioelectrochemistry. 2010;78:2-7.

[560] Helder M, Strik D, Hamelers H, Kuhn A, Blok C, Buisman C. Concurrent bio-electricity and biomass production in three Plant-Microbial Fuel Cells using Spartina anglica, Arundinella anomala and Arundo donax. Bioresource technology. 2010;101:3541-7.

[561] Rabaey K, Boon N, Höfte M, Verstraete W. Microbial phenazine production enhances electron transfer in biofuel cells. Environmental science & technology. 2005;39:3401-8.

[562] Fan Y, Sharbrough E, Liu H. Quantification of the internal resistance distribution of microbial fuel cells. Environmental science & technology. 2008;42:8101-7.

[563] Timmers RA, Strik DP, Hamelers HV, Buisman CJ. Characterization of the internal resistance of a plant microbial fuel cell. Electrochimica Acta. 2012;72:165-71.

[564] Kuzyakov Y. Priming effects: interactions between living and dead organic matter. Soil Biology and Biochemistry. 2010;42:1363-71.

[565] Timmers RA, Rothballer M, Strik DP, Engel M, Schulz S, Schloter M, et al. Microbial community structure elucidates performance of Glyceria maxima plant microbial fuel cell. Applied microbiology and biotechnology. 2012;94:537-48.

[566] Hanson R. Ecology and diversity of methylotrophic organisms. Advances in applied Microbiology. 1980;26:3-39.

[567] Kuleshova T, Ivanova A, Galushko A, Kruchinina IY, Shilova O, Udalova O, et al. Influence of the electrode systems parameters on the electricity generation and the possibility of hydrogen production in a plant-microbial fuel cell. InternatIonal Journal of Hydrogen Energy. 2022;47:24297-309.

[568] Timmers RA, Strik DP, Arampatzoglou C, Buisman CJ, Hamelers HV. Rhizosphere anode model explains high oxygen levels during operation of a Glyceria maxima PMFC. Bioresource Technology. 2012;108:60-7.

[569] Farrar J, Hawes M, Jones D, Lindow S. How roots control the flux of carbon to the rhizosphere. Ecology. 2003;84:827-37.

[570] Neumann G, Romheld V. The release of root exudates as affected by the plant's physiological status. The rhizosphere: CRC press; 2000. p. 57-110.

[571] Katuri KP, Scott K, Head IM, Picioreanu C, Curtis TP. Microbial fuel cells meet with external resistance. Bioresource technology. 2011;102:2758-66.

[572] Lancashire PD, Bleiholder H, Boom Tvd, Langelüddeke P, Stauss R, WEBER E, et al. A uniform decimal code for growth stages of crops and weeds. Annals of applied Biology. 1991;119:561-601.

[573] Butterbach-Bahl K, Papen H, Rennenberg H. Impact of gas transport through rice cultivars on methane emission from rice paddy fields. Plant, Cell & Environment. 1997;20:1175-83.

[574] De Schamphelaire L, Cabezas A, Marzorati M, Friedrich MW, Boon N, Verstraete W. Microbial community analysis of anodes from sediment microbial fuel cells

powered by rhizodeposits of living rice plants. Applied and environmental microbiology. 2010;76:2002-8.

[575] Kouzuma A, Kasai T, Nakagawa G, Yamamuro A, Abe T, Watanabe K. Comparative metagenomics of anode-associated microbiomes developed in rice paddy-field microbial fuel cells. PLoS One. 2013;8:e77443.

[576] Arends JB, Speeckaert J, Blondeel E, De Vrieze J, Boeckx P, Verstraete W, et al. Greenhouse gas emissions from rice microcosms amended with a plant microbial fuel cell. Applied Microbiology and Biotechnology. 2014;98:3205-17.

[577] Kouzuma A, Kaku N, Watanabe K. Microbial electricity generation in rice paddy fields: recent advances and perspectives in rhizosphere microbial fuel cells. Applied Microbiology and Biotechnology. 2014;98:9521-6.

[578] Appels L, Baeyens J, Degrève J, Dewil R. Principles and potential of the anaerobic digestion of waste-activated sludge. Progress in energy and combustion science. 2008;34:755-81.

[579] Jung S, Regan JM. Influence of external resistance on electrogenesis, methanogenesis, and anode prokaryotic communities in microbial fuel cells. Applied and environmental microbiology. 2011;77:564-71.

[580] ISHII Si, Hotta Y, Watanabe K. Methanogenesis versus electrogenesis: morphological and phylogenetic comparisons of microbial communities. Bioscience, biotechnology, and biochemistry. 2008;72:286-94.

[581] Nepal R, Phoumin H, Khatri A. Green technological development and deployment in the association of southeast Asian economies (ASEAN)—At crossroads or roundabout? Sustainability. 2021;13:758.

[582] Anderson TR, Hawkins E, Jones PD. CO2, the greenhouse effect and global warming: from the pioneering work of Arrhenius and Callendar to today's Earth System Models. Endeavour. 2016;40:178-87.

[583] Liu S, Xue H, Wang M, Feng X, Lee H-SJIJoHE. The role of microbial electrogenesis in regulating methane and nitrous oxide emissions from constructed wetland-microbial fuel cell. 2022;47:27279-92.

[584] Wang S, Gariepy Y, Adekunle A, Raghavan VJEA. The role of hydroponic

microbial fuel cell in the reduction of methane emission from rice plants. 2023;450:142229.

[585] Wang S, Gariepy Y, Adekunle A, Raghavan V. The role of hydroponic microbial fuel cell in the reduction of methane emission from rice plants. Electrochimica Acta. 2023:142229.

[586] Wang S, Gariepy Y, Adekunle A, Raghavan V. Effective and Economical 3D Carbon Sponge with Carbon Nanoparticles as Floating Air Cathode for Sustainable Electricity Production in Microbial Fuel Cells. Applied Biochemistry and Biotechnology. 2023.

[587] Hänsch R, Mendel RR. Physiological functions of mineral micronutrients (cu, Zn, Mn, Fe, Ni, Mo, B, cl). Current opinion in plant biology. 2009;12:259-66.

[588] Rout GR, Sahoo SJRiAS. Role of iron in plant growth and metabolism. 2015;3:1-24.

[589] Chen Z, Tang Y-T, Zhou C, Xie S-T, Xiao S, Baker AJ, et al. Mechanisms of Fe biofortification and mitigation of Cd accumulation in rice (Oryza sativa L.) grown hydroponically with Fe chelate fertilization. 2017;175:275-85.

[590] Kobayashi T, Nishizawa NK. Iron uptake, translocation, and regulation in higher plants. Annu Rev Plant Biol. 2012;63:131-52.

[591] Sikirou M, Saito K, Achigan-Dako EG, Dramé KN, Ahanchédé A, Venuprasad R. Genetic improvement of iron toxicity tolerance in rice-progress, challenges and prospects in West Africa. Plant Production Science. 2015;18:423-34.

[592] Kar S, Panda SK. Iron homeostasis in rice: Deficit and excess. Proceedings of the National Academy of Sciences, India Section B: Biological Sciences. 2020;90:227-35.

[593] Liu Q, Yang Y, Mei X, Liu B, Chen C, Xing D. Response of the microbial community structure of biofilms to ferric iron in microbial fuel cells. Science of the Total Environment. 2018;631:695-701.

[594] Hassan M, Pous N, Xie B, Colprim J, Balaguer MD, Puig S. Influence of iron species on integrated microbial fuel cell and electro-Fenton process treating landfill leachate. Chemical Engineering Journal. 2017;328:57-65.

[595] Nguyen M-T, Mecheri B, D'Epifanio A, Sciarria TP, Adani F, Licoccia S. Iron

chelates as low-cost and effective electrocatalyst for oxygen reduction reaction in microbial fuel cells. International Journal of Hydrogen Energy. 2014;39:6462-9.

[596] Wang A, Sun D, Ren N, Liu C, Liu W, Logan BE, et al. A rapid selection strategy for an anodophilic consortium for microbial fuel cells. Bioresource technology. 2010;101:5733-5.

[597] Wu D, Xing D, Lu L, Wei M, Liu B, Ren N. Ferric iron enhances electricity generation by Shewanella oneidensis MR-1 in MFCs. Bioresource technology. 2013;135:630-4.

[598] Kato S, Hashimoto K, Watanabe K. Iron-oxide minerals affect extracellular electron-transfer paths of Geobacter spp. Microbes and environments. 2013:ME12161.

[599] Ter Heijne A, Hamelers HV, De Wilde V, Rozendal RA, Buisman CJ. A bipolar membrane combined with ferric iron reduction as an efficient cathode system in microbial fuel cells. Environmental science & technology. 2006;40:5200-5.

[600] Lefebvre O, Neculita CM, Yue X, Ng HY. Bioelectrochemical treatment of acid mine drainage dominated with iron. Journal of hazardous materials. 2012;241:411-7.

[601] Giri A, Saxena RR, Verma SK, Porte S, Rawte S, Saxena RR, et al. Genetic and morphological analysis tolerance to ferrous and ferric forms of iron in rice. Journal of Agriculture and Food Research. 2022;9:100331.

[602] Green M, Etherington J. Oxidation of ferrous iron by rice (Oryza sativa L.) roots: a mechanism for waterlogging tolerance? Journal of Experimental Botany. 1977;28:678-90.

[603] Wang S, Adekunle A, Raghavan VJJoEM. Bioelectrochemical systems-based metal removal and recovery from wastewater and polluted soil: Key factors, development, and perspective. 2022;317:115333.

[604] Genon J, De Hepcee N, Duffy J, Delvaux B, Hennebert P. Iron toxicity and other chemical soil constraints to rice in highland swamps of Burundi. Plant and Soil. 1994;166:109-15.

[605] Sahrawat Ká. Iron toxicity in wetland rice and the role of other nutrients. Journal of plant nutrition. 2005;27:1471-504.

[606] Khudzari JM, Tartakovsky B, Raghavan GVJWM. Effect of C/N ratio and salinity

on power generation in compost microbial fuel cells. 2016;48:135-42.

[607] Fan Y, Sharbrough E, Liu HJEs, technology. Quantification of the internal resistance distribution of microbial fuel cells. 2008;42:8101-7.

[608] Kong X, Sun Y, Yuan Z, Li D, Li L, Li Y. Effect of cathode electron-receiver on the performance of microbial fuel cells. International journal of hydrogen energy. 2010;35:7224-7.

[609] Rohwerder T, Gehrke T, Kinzler K, Sand W. Bioleaching review part A: progress in bioleaching: fundamentals and mechanisms of bacterial metal sulfide oxidation. Applied microbiology and biotechnology. 2003;63:239-48.

[610] Ji J, Jia Y, Wu W, Bai L, Ge L, Gu Z. A layer-by-layer self-assembled Fe2O3 nanorod-based composite multilayer film on ITO anode in microbial fuel cell. Colloids and Surfaces A: Physicochemical and Engineering Aspects. 2011;390:56-61.

[611] Wei L, Han H, Shen J. Effects of temperature and ferrous sulfate concentrations on the performance of microbial fuel cell. International Journal of Hydrogen Energy. 2013;38:11110-6.

[612] Aulakh M, Wassmann R, Bueno C, Kreuzwieser J, Rennenberg H. Characterization of root exudates at different growth stages of ten rice (Oryza sativa L.) cultivars. Plant biology. 2001;3:139-48.

[613] Takahashi M, Nakanishi H, Kawasaki S, Nishizawa NK, Mori S. Enhanced tolerance of rice to low iron availability in alkaline soils using barley nicotianamine aminotransferase genes. Nature biotechnology. 2001;19:466-9.

[614] Pushnik JC, Miller G. The effects of iron and light treatments on chloroplast composition and ultrastructure in iron-deficient barley leaves. Journal of Plant Nutrition. 1982;5:311-21.

[615] Andaluz S, López-Millán A-F, De las Rivas J, Aro E-M, Abadía J, Abadía A. Proteomic profiles of thylakoid membranes and changes in response to iron deficiency. Photosynthesis Research. 2006;89:141-55.

[616] Schmidt W, Tittel J, Schikora A. Role of hormones in the induction of iron deficiency responses in Arabidopsis roots. Plant Physiology. 2000;122:1109-18.

[617] Luo D, Meng X, Zheng N, Li Y, Yao H, Chapman SJ. The anaerobic oxidation of

methane in paddy soil by ferric iron and nitrate, and the microbial communities involved. Science of the Total Environment. 2021;788:147773.

[618] Gwon HS, Khan MI, Alam MA, Das S, Kim PJ. Environmental risk assessment of steel-making slags and the potential use of LD slag in mitigating methane emissions and the grain arsenic level in rice (Oryza sativa L.). Journal of hazardous materials. 2018;353:236-43.

[619] Summers ZM, Fogarty HE, Leang C, Franks AE, Malvankar NS, Lovley DR. Direct exchange of electrons within aggregates of an evolved syntrophic coculture of anaerobic bacteria. Science. 2010;330:1413-5.

[620] Hu J, Wu H, Sun Z, Peng Q-a, Zhao J, Hu R. Ferrous iron addition decreases methane emissions induced by rice straw in flooded paddy soils. ACS Earth and Space Chemistry. 2020;4:843-53.

[621] Zhao M, Lin Y, Chen HJT, Genetics A. Improving nutritional quality of rice for human health. 2020;133:1397-413.

[622] Meinshausen M, Vogel E, Nauels A, Lorbacher K, Meinshausen N, Etheridge DM, et al. Historical greenhouse gas concentrations for climate modelling (CMIP6). Geoscientific Model Development. 2017;10:2057-116.

[623] Jackson RB, Saunois M, Bousquet P, Canadell JG, Poulter B, Stavert AR, et al. Increasing anthropogenic methane emissions arise equally from agricultural and fossil fuel sources. Environmental Research Letters. 2020;15:071002.

[624] Carlson KM, Gerber JS, Mueller ND, Herrero M, MacDonald GK, Brauman KA, et al. Greenhouse gas emissions intensity of global croplands. Nature Climate Change. 2017;7:63-8.

[625] Cassman K. Crop science research to assure food security. Crop science: progress and prospects Papers presented at the Third International Crop Science Congress, Hamburg, Germany, 17-22 August 2000: CABI Publishing Wallingford UK; 2001. p. 33-51.

[626] Tian H, Lu C, Ciais P, Michalak AM, Canadell JG, Saikawa E, et al. The terrestrial biosphere as a net source of greenhouse gases to the atmosphere. Nature. 2016;531:225-8.

[627] Schröder U. From Wastewater to Hydrogen: Biorefineries Based on Microbial Fuel-Cell Technology. ChemSusChem: Chemistry & Sustainability Energy & Materials. 2008;1:281-2.

[628] Wang S, Adekunle A, Tartakovsky B, Raghavan V. Synthesizing developments in the usage of solid organic matter in microbial fuel cells: A review. Chem Eng J Adv. 2021;8:10.1016.

[629] Rismani-Yazdi H, Christy AD, Carver SM, Yu Z, Dehority BA, Tuovinen OH. Effect of external resistance on bacterial diversity and metabolism in cellulose-fed microbial fuel cells. Bioresource technology. 2011;102:278-83.

[630] Zhang K, Wu X, Wang W, Chen J, Chen J, Luo H. Roles of external circuit and rhizosphere location in CH4 emission control in sequencing batch flow constructed wetland-microbial fuel cell. Journal of Environmental Chemical Engineering. 2021;9:106583.

[631] Aelterman P, Versichele M, Marzorati M, Boon N, Verstraete W. Loading rate and external resistance control the electricity generation of microbial fuel cells with different three-dimensional anodes. Bioresource technology. 2008;99:8895-902.

[632] Liu H, Cheng S, Logan BE. Production of electricity from acetate or butyrate using a single-chamber microbial fuel cell. Environmental science & technology. 2005;39:658-62.

[633] McLean J, Wanger G, Gorby Y, Wainstein M, McQuaid J. S. i. Ishii, O. Bretschger, H. Beyenal, and KH Nealson,“Quantification of electron transfer rates to a solid phase electron acceptor through the stages of biofilm formation from single cells to multicellular communities,”. Environmental Science and Technology. 2010;44:2721-7.

[634] Wang X, Tian Y, Liu H, Zhao X, Peng S. The influence of incorporating microbial fuel cells on greenhouse gas emissions from constructed wetlands. Science of the Total Environment. 2019;656:270-9.

[635] Jeon H-J, Choi Y-K, Kumaran RS, Kim S-H, Song K-G, Hong S-W, et al. Electrochemical control of methane emission from lake sediment using microbial fuel cells. Bulletin of the Korean Chemical Society. 2012;33:2401-4.

[636] Wang S, Gariepy Y, Adekunle A, Raghavan V. The role of hydroponic microbial

fuel cell in the reduction of methane emission from rice plants. Electrochimica Acta. 2023;450:142229.

[637] Tang X-Y, Yang Y, McBride MB, Tao R, Dai Y-N, Zhang X-M. Removal of chlorpyrifos in recirculating vertical flow constructed wetlands with five wetland plant species. Chemosphere. 2019;216:195-202.

[638] Helder M, Strik DP, Hamelers HV, Buisman CJ. The flat-plate plant-microbial fuel cell: the effect of a new design on internal resistances. Biotechnology for biofuels. 2012;5:1-11.

[639] Logan BE. Exoelectrogenic bacteria that power microbial fuel cells. Nature Reviews Microbiology. 2009;7:375-81.

[640] Larrosa-Guerrero A, Scott K, Katuri KP, Godinez C, Head IM, Curtis T. Open circuit versus closed circuit enrichment of anodic biofilms in MFC: effect on performance and anodic communities. Applied microbiology and biotechnology. 2010;87:1699-713.

[641] Menicucci J, Beyenal H, Marsili E, Veluchamy, Demir G, Lewandowski Z. Procedure for determining maximum sustainable power generated by microbial fuel cells. Environmental science & technology. 2006;40:1062-8.

[642] Aelterman P, Freguia S, Keller J, Verstraete W, Rabaey K. The anode potential regulates bacterial activity in microbial fuel cells. Applied microbiology and biotechnology. 2008;78:409-18.

[643] Buitrón G, López-Prieto I, Zúñiga IT, Vargas A. Reduction of start-up time in a microbial fuel cell through the variation of external resistance. Energy Procedia. 2017;142:694-9.

[644] Suzuki K, Kato Y, Yui A, Yamamoto S, Ando S, Rubaba O, et al. Bacterial communities adapted to higher external resistance can reduce the onset potential of anode in microbial fuel cells. Journal of bioscience and bioengineering. 2018;125:565-71.

[645] Cano V, Cano J, Nunes SC, Nolasco MA. Electricity generation influenced by nitrogen transformations in a microbial fuel cell: assessment of temperature and external resistance. Renewable and Sustainable Energy Reviews. 2021;139:110590.

[646] Timmers RA, Rothballer M, Strik DP, Engel M, Schulz S, Schloter M, et al. Microbial community structure elucidates performance of Glyceria maxima plant microbial fuel cell. Applied microbiology and biotechnology. 2012;94:537-48.

[647] Choi C-H, Kim M-A, Hong S-W, Choi Y-S, Song Y-I, Kim S-H, et al. Performance of a microbial fuel cell using a magnet attached cathode. Bulletin of the Korean Chemical Society. 2010;31:1729-31.

[648] Kim HJ, Park HS, Hyun MS, Chang IS, Kim M, Kim BH. A mediator-less microbial fuel cell using a metal reducing bacterium, Shewanella putrefaciens. Enzyme and Microbial technology. 2002;30:145-52.

[649] Chowdhury TR, Dick RP. Ecology of aerobic methanotrophs in controlling methane fluxes from wetlands. Applied soil ecology. 2013;65:8-22.

[650] Jadhav G, Ghangrekar M. Performance of microbial fuel cell subjected to variation in pH, temperature, external load and substrate concentration. Bioresource technology. 2009;100:717-23.

[651] Thauer RK, Jungermann K, Decker K. Energy conservation in chemotrophic anaerobic bacteria. Bacteriological reviews. 1977;41:100-80.